

Investigating pathogenesis and virulence of the human pathogen, *Vibrio vulnificus*.

A thesis submitted by Selina Rebecca Church to the University of Exeter as a thesis
for the degree of Doctor of Philosophy in Biological Sciences.

In April 2015

This thesis is available for Library use, on the understanding that it is copyright
material and that no quotation from this thesis may be published without proper
acknowledgment.

I certify that all material in this thesis which is not my own work has been identified
and that no material has previously been submitted for approval for the award of a
degree by this or any other University.

Signature.....

Abstract

V. vulnificus is a Gram negative opportunistic pathogen that is ubiquitous in the marine environment. Of the three main biotypes, biotype 1 is most commonly associated with human infection and is the causative agent of septicaemia, gastroenteritis and wound infection. In the United States *V. vulnificus* is the leading cause of seafood related deaths and is commonly associated with ingestion of raw or undercooked oysters. However, despite the abundant prevalence of this bacterium in the environment, the number of severe human infections is low. This has led to the hypothesis that not all strains of this pathogen are equal in virulence, with some strains better adapted to causing human disease than others.

Therefore the current study tested a panel of 10 *V. vulnificus* strains in several phenotypic experiments that assayed the strains for known virulence factors, with the aim of identifying a marker for strains hazardous to human health. However, not one assay correlated with either virulence potential of the strains, as determined by an *in vivo* mouse model of virulence, or source of isolation.

As the study hypothesised that the varying virulence potentials displayed by the strains may be due to genetic differences, whole genome sequencing (WGS) was performed. Bioinformatic comparison of the strains demonstrated many genetic differences between the strains. However, in unison with the WGS comparison, WGS gene annotation was also performed. This identified the presence of two previously undescribed type 6 secretion systems (T6SS). Therefore the current study continued investigation into the T6SSs.

The two T6SSs identified were termed T6SS1 and T6SS2. T6SS2 was found in all sequenced isolates, whereas T6SS1 was only present in a sub-set of strains. As T6SS1 shared synteny with the previously described T6SS in *V. cholerae*, T6SS1 was chosen for further investigation. During this study T6SS1 was shown to be functional and displayed thermoregulation. Further investigation into T6SS1 by construction and characterising of a T6SS1 mutant, demonstrated that T6SS1 contained anti-prokaryotic properties.

Declaration

Unless otherwise stated, the results and data presented in this thesis were solely the work of Selina Rebecca Church.

All gDNA preparations were carried out by S.R. Church, however quantification and preparation of extracted gDNA for whole genome sequencing was performed by Exeter Sequencing Services, University of Exeter.

All bioinformatic analyses presented in this thesis were performed in consultation with Dr. Thomas Lux.

Acknowledgements

Firstly I'd like to thank my supervisors, Dr. Stephen Michell and Dr. Craig Baker-Austin. Steve, thank you for all your belief and encouragement during this Ph.D., your guidance and help with molecular techniques has been invaluable; the teaching and support you have provided along the way has been instrumental in my development as a scientist. Thank-you also to Craig, you were always on hand to answer my questions and offer helpful discussions about *V. vulnificus*. I am also extremely thankful for the many opportunities you gave to me to present my work at CEFAS.

Thank you also to Dr. Thomas Lux, I am absolutely indebted to you for all your help. Your bioinformatic knowledge is second to none, and you have been an absolute legend in helping me. I cannot thank you enough for your time, patience, support and helpful discussions with my never ending bioinformatic tasks and ideas. Thank you. Thank you also to Dr. Stefan Pukatzki for the Hcp antibody and *V. cholerae* strains.

To the 4th floor team, thank you all for listening to my regular T6SS rants or jubilations. In particular I would like to thank Dr. Monika Bokori-Brown, your wealth of scientific knowledge has been invaluable, as have the much needed coffee breaks and scientific discussions, thank you. Thank you also to Dr. Claudia Hemsley for my never ending requests of antibiotic resistant plasmids. Thank you also to the members of "Journal Club" for providing the much needed nights outs, drinks and dinners. Especially thank you to Dr. Yvonne Lau and Vanessa Francis, so much to say, so little space, thank you both for being amazing friends.

Thanks are also extended to my wonderful friends Lucie, Angela, Dave and Ashley.

My upmost thanks however goes to my family. Mum and Dad, thank you for being such incredible parents. You have always believed in me, supported me and encouraged me. It is without a doubt that the morals and values which you have instilled in me have helped and guided me through this Ph.D. process. Analeez, I thank you for always making me smile. To my beloved Sam, thank you for reminding me of what is important in life. Thank you for always drying my tears of frustration and offering so much love and support. Your encouragement and understanding has been truly amazing, nothing short of an absolute legend.

This thesis is dedicated to my parents, thank you for helping me fulfil my dream.

Contents

Abstract.....	i
Declaration.....	ii
Acknowledgements.....	iii
List of Figures and Tables	x
List of abbreviations	xv
Chapter 1 Introduction to <i>Vibrio vulnificus</i>	1
1.1 An overview of <i>Vibrio vulnificus</i>	2
1.2 Typing of <i>V. vulnificus</i> isolates	2
1.3 Epidemiology	5
1.4 Clinical presentation and infectivity	6
1.5 Diagnosis and treatment	8
1.6 The viable but non culturable state of <i>V. vulnificus</i>	8
1.7 Regulation and quorum sensing	10
1.8 Virulence mechanisms of <i>V. vulnificus</i>	12
1.8.1 Evasion of host defenses by <i>V. vulnificus</i>	12
1.8.2 Iron uptake mechanisms of <i>V. vulnificus</i>	14
1.8.3 Motility and attachment.....	15
1.8.4 Bacterial endotoxin	17
1.8.5 Bacterial exotoxins.....	18
1.8.6 Gram negative secretion systems.....	23
1.9 Study objective.....	26
Chapter 2 Phenotypic characterisation of <i>V. vulnificus</i> isolates	27
2.1 Introduction and aim	28
2.2 Results	29
2.2.1 Confirmation of <i>V. vulnificus</i> strains.....	29
2.2.2 Growth characteristics of clinical and environmental <i>V. vulnificus</i> isolates.....	30
2.2.3 Imaging of capsule on clinical and environmental <i>V. vulnificus</i> isolates ...	33
2.2.4 Protease production by clinical and environmental <i>V. vulnificus</i> isolates..	37
2.2.5 Comparison of motility between clinical and environmental <i>V. vulnificus</i> isolates	41
2.2.6 LDH release from CaCo-2 cells infected with clinical and environmental <i>V. vulnificus</i> isolates.....	44
2.3 Discussion.....	47

2.4 Conclusion	52
Chapter 3 Bioinformatic analysis of <i>V. vulnificus</i> strains	55
3.1 Introduction and aim	56
3.2 Results	56
3.2.1 Preparation and sequencing of genomic DNA (gDNA)	56
3.2.2 Assembly of <i>V. vulnificus</i> raw sequencing reads	57
3.2.3 Bioinformatic genotyping of <i>V. vulnificus</i> strains	59
3.2.4 Phylogenetic tree construction for <i>V. vulnificus</i> strains from clinical and environmental origin	61
3.2.5 WGS comparison of <i>V. vulnificus</i> strains	65
3.2.6 Gene annotation of WGS data.....	68
3.2.7 Bioinformatic analysis of the T6SS gene clusters in sequenced <i>V. vulnificus</i> strains	69
3.3 Discussion.....	75
3.4 Conclusion	79
Chapter 4 The type 6 Secretion System (T6SS)	81
4.1 History of the T6SS.....	82
4.1.1 The T6SS discovery	82
4.1.2 Naming of T6SS components	82
4.2 The T6SS structure.....	84
4.2.1 The phage related complex	84
4.2.2 The membrane associated complex, anchoring the T6SS	85
4.3 Anti-eukaryotic properties of the T6SS	86
4.4 An introduction to anti-prokaryotic T6SS effectors and immunity proteins	88
4.5 The differing classes of anti-prokaryotic T6SS toxins	89
4.5.1 Cell wall targeting effectors.....	90
4.5.2 Cell membrane targeting effectors.....	91
4.5.3 DNA targeting effectors.....	92
4.6 The role of the T6SS in bacterial communities.....	92
4.7 Monitoring T6SS functionality	93
4.8 Monitoring T6SS killing <i>in vitro</i>	93
Chapter 5 Phenotypic characteristics of T6SS1 from <i>V. vulnificus</i> 106-2A	97
5.1 Introduction and aim	98
5.2 Results	98

5.2.1 The T6SS1 is functional in <i>V. vulnificus</i> 106-2A.	98
5.2.2 Production and confirmation of $\Delta icmF1$ and $\Delta icmF2$ mutants in <i>V. vulnificus</i> 106-2A	100
5.2.3 A $\Delta T6SS1$ mutant of <i>V. vulnificus</i> is deficient for Hcp secretion	107
5.2.4. The hypothesised role of T6SS1 in <i>V. vulnificus</i> 106-2A	108
5.2.5 Growth characteristics of <i>V. vulnificus</i> 106-2A wild-type, 106-2A $\Delta T6SS1$, 106-2A $\Delta T6SS2$, <i>V. vulnificus</i> 99-743 and <i>V. fluvialis</i>	109
5.2.6 T6SS1 positive <i>V. vulnificus</i> 106-2A can target T6SS1 negative <i>V. vulnificus</i> 99-743.....	110
5.3 Discussion.....	113
5.4 Conclusion	119
Chapter 6 The inter-species targeting abilities of <i>V. vulnificus</i> T6SS1	121
6.1 Introduction and aim	122
6.2 Results	122
6.2.1 <i>V. vulnificus</i> can utilise T6SS1 to target an alternative <i>Vibrio</i> species	122
6.2.2 <i>V. fluvialis</i> NCTC 11327 can target <i>V. vulnificus</i> 106-2A $\Delta T6SS1$ at 37°C	126
6.2.3 WGS sequencing of <i>V. fluvialis</i> NCTC 11327	129
6.2.4 The T6SS1 of <i>V. vulnificus</i> 106-2A is involved in killing non- <i>Vibrio</i> species	130
6.2.5 <i>V. vulnificus</i> contains alternative mechanisms for attacking <i>B. thailandensis</i> other than T6SS1.....	131
6.2.9 The effects of <i>V. vulnificus</i> T6SS2 on <i>Galleria mellonella</i>	134
6.3 Discussion.....	135
6.4 Conclusion	138
Chapter 7 Complementation of T6SS1 in <i>V. vulnificus</i> 106-2A	140
7.1 Introduction and aim	141
7.2 Results	141
7.2.1 Construction of a complementing plasmid, pSRC14.....	141
7.2.2 Complementation of $\Delta T6SS1$ with pSRC14.....	144
7.2.3 Optimisation of Hcp secretion by 106-2A $\Delta T6SS1::pSRC14$	145
7.2.4 Analysis of <i>icmF</i> transcription from T6SS1	150
7.2.5 <i>V. vulnificus</i> 106-2A $\Delta T6SS1$ pBAD24: <i>icmF</i> is unable to restore the killing phenotype associated with T6SS1.....	152
7.3 Discussion.....	153

7.4 Conclusion	156
7.5 Concluding summary and future work.....	156
Chapter 8 Materials and Methods	160
8.1 Bacterial strains and mammalian cell lines	161
8.1.1 Bacterial strains	161
8.1.2 Mammalian cell lines	162
8.2 Media	162
8.3 Routine culturing of bacterial strains	164
8.3.1 Culturing of <i>V. vulnificus</i> cells	164
8.3.2 Culturing of other <i>Vibrio</i> species and <i>Burkholderia thailandensis</i>	164
8.3.3 Culturing of <i>E. coli</i> cells.....	164
8.4 Routine culturing of mammalian cells	165
8.4.1 Routine culturing of CaCo-2 cells	165
8.4.2 Passaging of CaCo-2 cells.....	165
8.5 <i>In vitro</i> phenotypic assays.....	165
8.5.1 <i>V. vulnificus</i> growth curves	165
8.5.2 Capsule colony morphology.....	165
8.5.3 India ink staining of capsule.....	166
8.5.4 Azocasein protease assay	166
8.5.5 Motility assay	166
8.5.6 LDH cytotoxicity assay.....	166
8.5.7 <i>G. mellonella</i> infection assay	167
8.5.8 Co-culture killing assays	168
8.5.9 Qualitative co-culture killing assay.....	168
8.5.10 Plasmid stability testing.....	168
8.6 Molecular genetics	169
8.6.1 gDNA extraction.....	169
8.6.2 Plasmid extraction	169
8.6.3 PCR for fragments less than 1000bps	169
8.6.4 PCR for fragments greater than 1000bps	169
8.6.5 Agarose gel electrophoresis	170
8.6.6 DNA gel purification	170
8.6.7 Restriction digestion	170

8.6.8 Ligation	170
8.6.9 A-tailing of PCR fragments	170
8.6.10 Reverse transcription PCR (RT-PCR)	171
8.6.11 Production of chemically competent <i>E. coli</i>	171
8.6.12 Heat shock transformations	171
8.6.13 Tri-parental conjugation of plasmids into <i>Vibrio</i> strains.....	172
8.6.14 Generation of deletion constructs in <i>V. vulnificus</i>	172
8.7 Primers and plasmids	173
8.7.1 Primers	173
8.7.2 Plasmids	175
8.8 Preparation of protein samples	176
8.8.1 Culture filtrate and cell lysate preparations	176
8.8.2 Quantification of proteins	177
8.8.3 SDS-PAGE	177
8.8.4 Western blotting.....	177
8.9 Bioinformatic methods.....	178
8.9.1 Whole genome sequencing	178
8.9.2 Assembling and annotating scaffolds	178
8.9.3 Generating phylogenetic trees	178
8.9.4 WGS comparison to identify gaps in the alignment between the query sequences and the reference genome	178
8.9.5 WGS comparison between Δ T6SS1 mutant and wild-type strain	179
References.....	180
Appendix	198

List of Figures and Tables

Chapter 1

Table 1.1	Biochemical properties of the three <i>V. vulnificus</i> biotypes.....	3
Figure 1.1	Secretion systems in <i>V. vulnificus</i>	26

Chapter 2

Figure 2.1	Virulence groupings of <i>V. vulnificus</i> isolates in an iron dextran treated mouse model.....	29
Figure 2.2	PCR confirmation of <i>vvhA</i> positive <i>V. vulnificus</i> isolates.....	30
Figure 2.3	Growth characteristic of clinical and environmental <i>V. vulnificus</i> isolates.....	31
Figure 2.4	Scatter plot of <i>V. vulnificus</i> doubling time versus virulence groupings of the strains.....	32
Figure 2.5	Capsule colony morphology of <i>V. vulnificus</i> strain on 2% NaCl LB agar plates.....	35
Figure 2.6	Capsule imaging using India ink staining of <i>V. vulnificus</i> isolates from clinical and environmental origin.....	37
Figure 2.7	Total extracellular protease production from clinical and environmental <i>V. vulnificus</i> isolates.....	39
Figure 2.8	Scatter graph of total protease production for <i>V. vulnificus</i> strains versus virulence grouping.....	40
Figure 2.9	Motility of <i>V. vulnificus</i> clinical and environmental isolates.....	42
Figure 2.10	Motility of <i>V. vulnificus</i> isolates plotted against virulence groupings...	43
Figure 2.11	LDH cytotoxicity assay on <i>V. vulnificus</i> clinical and environmental isolates following incubation with CaCo-2 cells.....	45
Figure 2.12	LDH release plotted against virulence grouping of each <i>V. vulnificus</i> strain.....	47

Chapter 3

Table 3.1	Statistics on assembly of raw sequencing reads using a5 pipeline.....	52
Table 3.2	<i>V. vulnificus</i> strain information.....	60

Table 3.3	Alignment rate of <i>V. vulnificus</i> strains against the plasmid of YJ016...68
Table 3.4:	Prevalence of T6SS1 and T6SS among the 10 <i>V. vulnificus</i> strains analysed.....75
Figure 3.1	Primer binding sites of <i>vcg</i> genotyping primers, P1 and P2.....59
Figure 3.2	Sequence alignment of the <i>vcg</i> primer binding sites.....60
Figure 3.3:	Phylogenetic tree constructed from chromosomes 1 and 2 for <i>V. vulnificus</i>62
Figure 3.4	Chromosome 1 constructed phylogenetic tree.....63
Figure 3.5	Phylogenetic tree constructed based on SNP analysis for chromosome 2.....63
Figure 3.6	Circos visualisation of assembled scaffolds from <i>V. vulnificus</i> isolates compared to the reference strain, YJ016.....66
Figure 3.7	The core T6SS proteins and accessory proteins.....70
Figure 3.8	Genetic organisation of the <i>V. vulnificus</i> T6SS1.....71
Figure 3.9	The genetic arrangement of <i>V. vulnificus</i> T6SS2.....72
Figure 3.10	Schematic diagram showing the prevalence of the T6SSs among hyper and lesser <i>V. vulnificus</i> strains.....74
Figure 3.11	Phylogenetic tree generated for <i>V. vulnificus</i> strains based on MLST analysis.....75

Chapter 4

Table 4.1	The 13 core proteins required for a functional T6SS.....83
Figure 4.1	Schematic diagram of the T6SS in its contracted form.....84
Figure 4.2	Schematic diagram of the anti-eukaryotic properties of the T6SS from <i>V. cholerae</i>87
Figure 4.3	Schematic diagram representing T6SS effector transport.....90

Chapter 5

Figure 5.1	Western blot images demonstrating expression and secretion of Hcp.....10 0
Figure 5.2	Construction of suicide vector pSRC11.....101

Figure 5.3	Schematic representation of the integration of a suicide vector into the <i>V. vulnificus</i> genome.....	102
Figure 5.4	Schematic representation of the 2 nd homologous cross-over event...	103
Figure 5.5	Gel electrophoresis image of PCR to confirm an <i>icmF</i> mutant in <i>V. vulnificus</i> 106-2A T6SS1.....	104
Figure 5.6	WGS comparison of <i>V. vulnificus</i> 106-2A and <i>V. vulnificus</i> 106-2A Δ T6SS1.....	106
Figure 5.7	Assessment of Hcp secretion from <i>V. vulnificus</i> 106-2A wild-type and <i>V. vulnificus</i> 106-2A Δ T6SS1.....	108
Figure 5.8	Growth curves <i>Vibrio</i> strains.....	110
Figure 5.9	Miles and Misra TCBS agar serial dilution plate.....	111
Figure 5.10	The T6SS1 of <i>V. vulnificus</i> 106-2A can be utilised to target the T6SS1 negative <i>V. vulnificus</i> strain, 99-743.....	112
Figure 5.11	The T6SS1 of <i>V. vulnificus</i> 106-2A can target a T6SS1 negative <i>V. vulnificus</i> strain.....	112
Figure 5.12	T6SS1 of <i>V. vulnificus</i> is involved with intra-species targeting.....	118
<u>Chapter 6</u>		
Figure 6.1	<i>V. vulnificus</i> 106-2A is able to utilise T6SS1 to target <i>V. fluvialis</i> during co-culture.....	124
Figure 6.2	<i>V. vulnificus</i> 106-2A can target <i>V. fluvialis</i> in a T6SS1 dependent manner.....	124
Figure 6.3	Plasmid maps for pSCRhaB3 and pBHR-RFP.....	126
Figure 6.4	Genetically engineered antibiotic resistant strains demonstrate that the T6SS1 of <i>V. vulnificus</i> 106-2A can target <i>V. fluvialis</i> NCTC 11327 at 30°C.....	127
Figure 6.5	Co-culture killing assay using genetically engineered antibiotic resistant prey and attacker strains.....	127
Figure 6.6	Survival of <i>V. vulnificus</i> strains when enumerated on either TCBS agar plates or antibiotic selection plates, following co-culture with <i>V. fluvialis</i>	129
Figure 6.7	The gene organisation of the 2 T6SSs from <i>V. fluvialis</i> NCTC 11327.....	130

Figure 6.8	The T6SS1 from <i>V. vulnificus</i> 106-2A is able to target <i>B. thailandensis</i> E264 during a co-culture assay.....	132
Figure 6.9	T6SS1 from <i>V. vulnificus</i> 106-2A is able to target <i>B. thailandensis</i> ...	133
Figure 6.10	Co-culture killing assay with <i>V. vulnificus</i> and <i>B. thailandensis</i> with a 24 hour incubation period.....	134
Figure 6.11	Co-culture killing assay with <i>V. vulnificus</i> and <i>B. thailandensis</i> with a 24 hour incubation period.....	134
Figure 6.12	<i>Galleria mellonella</i> infection study using <i>V. vulnificus</i> 106-2A wild-type and Δ T6SS1 and Δ T6SS2 mutants incubated at 37°C.....	136

Chapter 7

Figure 7.1	Construction of the complement plasmid, pSRC14.....	143
Figure 7.2	Gel electrophoresis image of the digestion profile for pSRC14 using <i>Sma</i> I and <i>Sph</i> I.....	144
Figure 7.3	Gel electrophoresis image of a PCR carried out on <i>V. vulnificus</i> 106-2A Δ T6SS1 clones containing pSRC14.....	145
Figure 7.4	Western blot using anti-Hcp antibody to detect Hcp secretion in a <i>icmF</i> complemented strain of Δ T6SS1.....	146
Figure 7.5	Western blot using anti-Hcp antibody to detect optimised Hcp secretion in an <i>icmF</i> complemented strain of Δ T6SS1.....	147
Figure 7.6	Western blot using anti-Hcp antibody to detect Hcp secretion.....	148
Figure 7.7	Gel electrophoresis image of a PCR carried out on <i>V. vulnificus</i> 106-2A Δ T6SS1 pBAD24.....	150
Figure 7.8	Western blot using anti-Hcp antibody to detect Hcp secretion in <i>V. vulnificus</i> 106-2A Δ T6SS1::pBAD24.....	150
Figure 7.9	Gel electrophoresis image of RT-PCR on cDNA using the MutScreen primers.....	151
Figure 7.10	Monitoring wild-type <i>icmF</i> expression.....	152
Figure 7.11	Qualitative killing assay to monitor T6SS1 associated killing.....	154

Chapter 8

Table 8.1	Bacterial strains used in this study.....	162
Table 8.2	Mammalian cell line used in this study.....	163

Table 8.3	Growth media for bacterial and mammalian cells used in this study.	164
Table 8.4	Primers used in this study.....	174
Table 8.5	Plasmids used in this study.....	176

Appendix

Appendix A1	Statistical 2-way ANOVA analysis of <i>V. vulnificus</i> growth curve Data.....	199
Appendix A2	Ponceau S stain for Western blot images demonstrating expression and secretion of Hcp.....	205
Appendix A3	Gene sequence of <i>icmF</i> gene from <i>V. vulnificus</i> 106-2A T6SS1.....	206
Appendix A4	<i>icmF</i> gene sequence from <i>V. vulnificus</i> 106-2A T6SS2.....	210
Appendix A5	Gel electrophoresis image of PCR to confirm an <i>icmF</i> mutant in <i>V. vulnificus</i> 106-2A T6SS1 and <i>V. vulnificus</i> 106-2A T6SS2.....	215
Appendix A6	Statistical two-way ANOVA analysis of data from <i>V. vulnificus</i> 106-2A, 99-743, Δ T6SS1 mutant, Δ T6SS2 mutant and <i>V. fluvialis</i> NCTC 11327 grown in LB at 30°C.....	216
Appendix A7	Stability of the plasmid pBHR-RFP in <i>V. fluvialis</i>	220
Appendix A8	Preliminary challenge of <i>G. mellonella</i> with <i>V. vulnificus</i> 106-2A wild- type Δ T6SS1 and Δ T6SS2 mutants.....	220
Appendix A9	Western blot using anti-Hcp antibody to detect Hcp secretion in 106-2A Δ T6SS1::pSRC14.....	221

List of abbreviations

a5	Andrew and aaron's awesome assembly pipeline
AIDS	Acquired immune deficiency syndrome
ANOVA	Analysis of variance
ATP	Adenosine triphosphate
BCA	bicinchoninic acid
BLAST	Basic local alignment search tool
Bp	Base pairs
Bps	Base pairs
CaCo-2	Colorectal adenocarcinoma cells
cDNA	Complementary DNA
CEFAS	Centre for Environment, Fisheries and Aquaculture Science
Cfu	Colony forming units
CHO	Chinese hamster ovary cell line
COG	Cluster of orthologous group
CPS	Capsular polysaccharide
DNA	deoxyribonucleic acid
dNTP	deoxynucleotide triphosphate
g	Gram
x g	Gravitational force
GC	Guanine and cytosine content
GSP	General secretory pathway
Hcp/ <i>hcp</i>	Haemolysin co-regulated protein
HSI-I	Hcp secretion island-I
HSI-II	Hcp secretion island-II
HSI-III	Hcp secretion island-III
IcmF/ <i>icmF</i>	Intracellular multiplication factor

hr/hrs	Hour/hours
kDa	Kilodaltons
LB	Luria-Bertani
LDH	Lactate dehydrogenase
λ	Lambda
LD ₅₀	Lethal dose ₅₀
L	Litres
LDL	Low density lipoprotein
LPS	Lipopolysaccharide
μ g	microgram
μ l	microliter
μ M	micromolar
M	Molar
MB	Mega base
mg	Milligram
mL	Millilitre
mm	millimetres
mM	Millimolar
MLST	Multi locus sequence typing
mRNA	messenger RNA
NaCl	Sodium chloride
ng	nanogram
nm	Nanometre
NGS	Next generation sequencing
OD ₅₉₀	Optical density (measured at 590nm)
OD ₄₅₀	Optical density (measured at 450nm)
OMV	Outer membrane vesicles

PAMPs	Pathogen associated molecular patterns
PBS	Phosphate buffered saline
PCR	Polymerase chain reaction
ppt	Parts per thousand
QS	Quorum sensing
RAPD-PCR	random amplified polymorphic DNA polymerase chain reaction
RT-PCR	Reverse transcription-polymerase chain reaction
Rhs	Recombination hot spot
RNA	Ribonucleic acid
rpm	revolutions per minute
SDS-PAGE	Sodium dodecyl sulphate polyacrylamide gel electrophoresis
Sec	Secretory pathway
SNP	Single nucleotide polymorphism
TAE	Tris-acetate EDTA
Tae	Type six secretion system amidase effector
Tai	Type six secretion system amidase immunity
Tat	Twin arginine transport
TCA	Trichloroacetic acid
TCBS	Thiosulfate citrate bile salts sucrose agar
Tge	Type six secretion system glycoside effectors
Tle	Type six secretion system lipase effector
Tli	Type six secretion system lipase immunity
T1SS	Type 1 secretion system
T2SS	Type 2 secretion system
T3SS	Type 3 secretion system
T4SS	Type 4 secretion system
T5SS	Type 5 secretion system

T6SS	Type 6 secretion system
Tse	Type six effector
Tsi	Type six secretion system immunity protein
Tss	Type six secretion
V	Volts
VBNC	Viable but non culturable
vcf	Variant call format
vcg	Virulence correlated gene
VgrG/ <i>vgrG</i>	Valine-glycine repeat protein G
v/v	Volume per volume
w/v	Weight per volume
WGS	Whole genome sequencing

Chapter 1 Introduction to *Vibrio vulnificus*

1.1 An overview of *Vibrio vulnificus*

V. vulnificus was first reported by the Centre of Disease Control in 1975 [1], described as “similar but not identical to *Vibrio parahaemolyticus* and *Vibrio alginolyticus*”, it was initially named lactose positive (L+) *Vibrio* [2], however this was later changed to *Benecka vulnifuca* [3]. It was later reported in 1979 that, due to the lack of use of the term *Benecka vulnifuca* by microbiologists, the organism should be referred to as *V. vulnificus*, the naming nomenclature now commonly used today [4].

V. vulnificus is a Gram negative bacterium which is naturally part of the marine microflora and is ubiquitous in aquatic and estuarine environments [5]. As the original naming nomenclature of *V. vulnificus* would suggest, this micro-organism is able to ferment lactose and like many other *Vibrios*, it is a halophilic, facultative anaerobe [6-8]. Morphologically it is a rod shaped organism, between 1.5-3.0 µm in length and ~1.0 µm in diameter [9], with a single polar flagellum. Genetically, *V. vulnificus* strains are inherently diverse [10, 11]; they harbour two chromosomes, which on average total ~5MB with a 46-48% GC content. A select number of strains contain an additional plasmid, such as the reference strain YJ016 [12].

In addition to their genetic diversity, *V. vulnificus* isolates have been shown to vary tremendously in their pathogenicity potential [13], and as such, disease symptoms associated with this organism can include gastroenteritis, septicaemia and wound infections [14]. Unlike other species of the *Vibrio* genus, the disease symptoms associated with *V. vulnificus* are often rapid and fulminating, this has led to *V. vulnificus* being considered as one of the most fatal human pathogens [15-18]. In the United States *V. vulnificus* is the leading cause of seafood related deaths [13, 19], with a mortality rate that often exceeds 50%, and can rise to 100% if left untreated for longer than 72 hours [20].

1.2 Typing of *V. vulnificus* isolates

Historically there have been several approaches to sub-categorise *V. vulnificus* strains further than the species level. One such approach is biotyping, and there are currently three main biotypes of *V. vulnificus*. Biotype groups are based on characteristics that include; host range, serological characteristics and biochemical features [10, 21-25]. Biotype 1 is mainly associated with human infection [7],

whereas biotype 2 is associated with disease in eels and occasionally causes human disease [26]. Biotype 3 is the most recently identified biotype and has been shown to be a hybrid of both biotypes 1 and 2 [14, 27]. Table 1.1 details the difference in biochemical properties between the three main biotypes [27].

Table 1.1 Biochemical properties of the three *V. vulnificus* biotypes

Biochemical test	Biotype		
	1	2	3
Oxidase	+	+	+
Arginine dihydrolase	-	-	-
Lysine decarboxylase	+	+	+
Sucrose fermentation	-	-	-
Ornithine decarboxylase	+	-	+
Indole production	+	-	+
D-mannitol fermentation	+	-	-
D-sorbitol fermentation	-	+	-
Citrate (Simmon's)	+	+	-
Salicin fermentation	+	+	-
Cellobiose fermentation	+	+	-
Lactose fermentation	+	+	-
o-nitrophenyl- β -D-galactopyranoside	+	+	-

The literature documents that *V. vulnificus* biotype1 strains, those that predominantly account for human infections, display high intra-species diversity, as well as

dramatically different virulence potentials [8, 10, 28, 29]. Therefore, several research groups have attempted to group *V. vulnificus* biotype 1 strains genotypically, with the aim of distinguishing hyper and lesser virulent strains. Currently, the most commonly referred to genotyping protocol for this approach is the “vcg” or “virulence correlated gene” typing method. The *vcg* typing system was developed as a way to distinguish between clinical and environmental isolates [30], as it was suggested that clinical and environmental isolates vary genetically [21]. This was proposed following a comparison of clinical and environmental isolates by Random Amplified Polymorphic DNA PCR (RAPD-PCR). This study found that all of the clinical strains tested produced a 200bp band that was generally, but not exclusively, absent from environmental isolates [21]. Analysis of this region at the DNA level identified that *V. vulnificus* strains could be divided into two groups, C-types and E-types. Therefore a PCR based method was established that could readily distinguish between the C-types and E-types [21]. Clinical isolates were grouped as C-type and reported to be “a strong indicator of potential virulence”, whereas environmental isolates were grouped as E-type [30].

Alternative genotyping methods for *V. vulnificus* isolates also include analysing polymorphisms in the 16S ribosomal RNA. Analysis of the 16S ribosomal RNA led to the identification of two groups of *V. vulnificus* isolates, type A and type B. Type A generally formed clusters of environmental isolates, whereas type B formed clusters of clinical isolates [25, 29]. Alternatively, Bisharat *et al.*, [31] used Multi-Locus Sequence Typing (MLST) using housekeeping genes to type *V. vulnificus* isolates. The MLST typing method grouped *V. vulnificus* isolates into clusters, cluster one which was mainly made up of environmental isolates and cluster two which was predominantly made up of clinical isolates [31]. Similarly, Cohen *et al.*, [32] published work on MLST using housekeeping genes to group *V. vulnificus* strains. The analysis again produced two groups which were termed lineages, lineage one was mainly made up of clinical isolates, whereas lineage two mostly consisted of environmental isolates [32].

An additional published typing method for *V. vulnificus* is the *pilF* typing system. This system is based on the finding there is a difference in the DNA sequence of the *pilF* gene between pathogenic and non-pathogenic strains [33]. Due to this finding a PCR

method was developed to distinguish between *V. vulnificus* strains that are hazardous to human health, from those that are not. Pathogenic strains are reported to produce a PCR band that is 338bps in length, whereas non-pathogenic strains are PCR negative and do not produce a band [33]. The *pilF* PCR method was later followed up with a real-time PCR method to distinguish between hyper and lesser virulent strains [7]. The real-time PCR method was reported to be highly sensitive and accurate [7]. However, the real-time PCR *pilF* typing method, like many of the typing methods mentioned earlier, is limited in that it is unable to distinguish pathogenic from non-pathogenic strains with 100% accuracy. Often there will be pathogenic strains that will cluster with non-pathogenic strains and vice versa [7, 10, 13, 30].

Therefore, in order to validate the genotyping methods developed for *V. vulnificus*, a research group analysed 69 biotype 1 *V. vulnificus* strains in an iron overloaded mouse model of infection, and reported the virulence of each strain *in vivo* [13]. The strains were grouped from one to five according to virulence, whereby group one was the least virulent and group five the most virulent. Virulence was evaluated for each strain based on the following markers of disease; skin infection, liver infection, body temperature and death. The study then identified whether the current genotyping methods for *V. vulnificus* could accurately predict virulence. The study found that although there was a correlation between genotype and virulence, none of the genotyping methods tested were able to accurately predict virulence for the strains [13], and concluded that further investigation was needed into *V. vulnificus* virulence to identify genetic markers of human disease.

1.3 Epidemiology

V. vulnificus is mainly isolated from marine environments such as estuarine water, fish and shellfish [7, 34, 35]. This, coupled with the common practice in many cultures to eat shellfish such as oysters raw, means *V. vulnificus* infection is often associated with the ingestion of raw oysters [36, 37]. Therefore from a food security angle it is of interest to be able to distinguish hyper virulent *V. vulnificus* strains from lesser virulent strains, particularly as *V. vulnificus* infection has a mortality rate often exceeding 50% [14, 36].

A retrospective study between 1988 and 1996 in the US demonstrated that out of 422 *V. vulnificus* infections 45% were wound infections, 43% were primary septicaemia and a small 5% portion were gastroenteritis, the remaining 7% were unidentified exposure routes [37, 38]. The majority of *V. vulnificus* infections occur during the warmer months of May to October and only sporadic cases during the colder months of November to March [36, 37]. This has been linked to the fact that this pathogen's growth displays a seasonal pattern, whereby there is an increase in the ability to isolate and culture the organism during the warmer months [39-41]. As *V. vulnificus* environmental growth is linked to temperature, it is believed that climate change may cause an increase in *V. vulnificus* infections [42, 43]. For example, The Baltic Sea was originally thought to be an unfavourable environment for *V. vulnificus*, however due to climate change causing an increase in surface sea water temperature, the originally cooler Baltic Sea has now been demonstrated as a region from which *V. vulnificus* can be isolated [44].

In addition to the Baltic Sea Region, *V. vulnificus* has also been isolated from several other European countries including, Spain [45], Turkey [46], Belgium [47], Israel [27], Greece [48], Denmark [49], Sweden [50] and the Netherlands [51]. As well as Europe, *V. vulnificus* has also been isolated from Asian regions such as Malaysia [52], Nepal [53], Korea [54] and Taiwan [35]. In the US, the bacterium is predominantly isolated from the Gulf of Mexico and neighbouring states as well as North East America and the Northern Pacific Coast [38, 55]. It is also found in regions such as California [56] and Florida [57].

As demonstrated, *V. vulnificus* can be isolated from a range of countries throughout the world and it is believed that temperature is a major factor regarding *V. vulnificus* environmental concentrations [6]. In addition to temperature, several reports also suggest that salinity levels are an important parameter for the isolation of the bacterium. It has been found that optimum environmental salinity concentrations for isolation of this bacterium, are between 5-10 ppt [41].

1.4 Clinical presentation and infectivity

V. vulnificus is known to be a fatal pathogen often causing fulminating systemic disease symptoms, yet the infectious dose for humans is currently undetermined [38]. Clinical presentation is often dependent on the route of infection, ingestion for

example can lead to gastroenteritis, diarrhoea, vomiting and nausea. [58, 59]. In severe cases, gastroenteritis will develop into primary septicaemia a condition in which the mortality rate can exceed 50% [43]. *V. vulnificus* can also enter humans via wound infection, this occurs when open wounds come into contact with contaminated fish or water [38, 60]. Characteristic symptoms of wound infection include oedema, necrosis and swelling. Secondary cutaneous lesions can occur and large blistered regions may present along with cellulitis and pain. The mortality rate associated with wound infection is ~25% [7, 58, 60]. [61, 62]. It is also not uncommon for wound infection patients to require amputation of infected sites [14]. As with ingestion of the bacterium, wound infection can also lead to life threatening septicaemia [14, 63]. Both wound infection and primary septicemia can present with fever and chills, and occasionally hypotension [64, 65].

As well as the possible link of environmental temperatures affecting *V. vulnificus* infection rate [42], the immune state of a patient has also been shown to play a significant role in the disease outcome [36, 59]. For example, patients suffering from liver disease are at particular risk of dying from infection [20, 38, 66]. On average, 80% of fatal *V. vulnificus* infections occur in individuals who have chronic liver disease [14, 38, 67]. Chronic liver diseases can include, cirrhosis, hepatitis and alcoholic liver disease [20, 43]. In addition to patients suffering with chronic liver problems, individuals who have high iron serum levels or weakened immune systems, such as AIDS and chemotherapy patients are also at risk of infection [12, 36, 68, 69]. Males are most at risk of infection with the majority of cases occurring in males over the age of 40 [43]. One possible link to account for the small number of females contracting the infection is that oestrogen has been shown to be protective against the effects of the bacterium's lipopolysaccharide (LPS) [70]. However, the exact reason why more males contract *V. vulnificus* infection has not been fully elucidated.

As *V. vulnificus* has an extremely high mortality rate and ubiquitous prevalence in the environment, it would be expected that the number of fatal human infections would be high. Conversely, the literature reports that the number of severe infections each year is exceptionally low [13, 21]. For example, the number of "considered at risk" individuals consuming raw oysters in Florida is around 70,000, yet there are only on

average five to ten *V. vulnificus* infections a year in this region [38, 71]. This trend of low infection compared to the availability of the bacterium in the environment is typical in all areas where *V. vulnificus* has been isolated [14]. Why there are so few fatal infections, despite the high mortality rate and natural prevalence of this pathogen, has been a question which has perplexed scientists for many years [13, 21].

1.5 Diagnosis and treatment

When *V. vulnificus* infection is suspected, the general procedure is to perform bacterial culture on wound, blood or stool samples with the use of thiosulfate–citrate–bile–salts–sucrose (TCBS) agar to isolate the bacterium [72]. Additionally it is advised that a Gram stain should be performed to identify characteristic comma shaped cells [20, 59, 73]. Although TCBS agar is a selective agar for *Vibrio* growth, care should be taken when isolating *V. vulnificus* as although the majority (~85%) of *V. vulnificus* strains will appear green on TCBS agar, there are a subset (~15%) of strains that will appear yellow [74]. This is due to the ability of these latter strains to ferment sucrose in the TCBS agar, causing a pH shift that generates yellow colonies [74].

Antibiotic therapy for *V. vulnificus* infection should be administered promptly, as speed of diagnosis and treatment is directly linked to prognosis. For example, a delay in medication by up to 72 hours can increase mortality from 50% to 100% [59, 75]. Although *V. vulnificus* is susceptible to a range of antimicrobials *in vitro*, the recommended treatment is doxycycline, 100 mg intravenously or orally twice a day plus ceftazidime, 2 g intravenously every eight hours or ciprofloxacin, 750 mg orally or 400 mg intravenously twice a day [36]. In addition to antibiotics, severely infected patients may require amputation of affected limbs to prevent systemic spread of the pathogen [20, 59].

1.6 The viable but non culturable state of *V. vulnificus*

As exemplified in the previous section, cultivation of a bacterial pathogen is a fundamental step in diagnostic microbiology [76]. In 1982 however, it was shown that bacterial cells could enter a state whereby they were non-culturable on standard laboratory media, yet bacterial staining methods demonstrated that the cells were still alive [76, 77]. As the cells were not dead, but had entered a non-culturable

stage, this novel microbiological phenomenon was termed viable but non culturable (VBNC) [77].

The VBNC state of bacterial cells is thought to be triggered by an extreme change in their environmental surroundings [76]. Examples of some known VBNC triggers are; changes in temperature [78], osmolality [79], nutrient starvation [80] and chlorination [81]. When cells enter a VBNC state they undergo various changes which can include, changes to their cellular morphologies, an increase or decrease in metabolism and alterations to their cell wall and membrane compositions [76]. Unlike dead cells however, VBNC cells are metabolically active, transcribe genes, utilise nutrients and carry out respiration [82, 83].

V. vulnificus is known to enter a VBNC state [18]; which is reported to aid the bacterium in withstanding environmental stresses such as temperature shifts [84]. For example, a decrease in temperature to 5°C can induce *V. vulnificus* cells to become VBNC [85]. During this period the cells undergo cellular membrane changes and reduced amino acid transport [85, 86]. As previously mentioned, the ability to culture *V. vulnificus* cells from the environment during the winter months is greatly reduced. It is believed that this is due to the pathogen's ability to become VBNC. Accordingly the effect of temperature on the ability to culture *V. vulnificus* from the environment has been demonstrated experimentally [87, 88]. This was done by placing chambers filled with VBNC cells into estuarine water during August to November, when the water temperature was above 5°C. When the cells were taken out again and plated onto laboratory media, the cells were culturable, demonstrating the resuscitation ability of temperature on the VBNC cells. However, when laboratory culturable cells of *V. vulnificus* were placed into estuarine water that was below 15°C, when the cells were taken out again, the cells were no longer culturable on standard laboratory media, further demonstrating the effects of environmental temperatures in inducing the VBNC state of *V. vulnificus* [89].

In addition to warm temperatures resuscitating VBNC cells, the quorum sensing auto-inducer molecule, AI-2, has also been shown to play a crucial role [90]. This was demonstrated by adding the cell free supernatant from culturable *V. vulnificus* cells, to VBNC cells, causing the VBNC population to be resuscitated and become culturable. The molecule AI-2 was shown to be the important factor, as cell free

supernatants from *V. vulnificus* cells that were unable to secrete AI-2, failed to resuscitate VBNC cells [90].

To assess the virulence of VBNC *V. vulnificus* cells, iron over loaded mice were challenged with a VBNC population. The results showed that even after entering a VBNC state, *V. vulnificus* remains virulent, and able to cause disease [91].

1.7 Regulation and quorum sensing

Bacteria have many regulatory systems which aid in the coordinate expression of genes in response to environmental stimuli [92]. Iron for example is important for the survival and virulence of many different bacterial species [93], therefore the ability for bacteria to respond to environmental changes in iron is important [94]. It has been suggested that the shift from a high to low iron environment may signal to bacteria that they have entered a mammalian host [95, 96]. This is demonstrated in enterohaemorrhagic *E. coli*, whereby under low iron conditions virulence factors such as the expression of the shiga-like toxin is upregulated [97, 98]. The regulation of virulence genes in response to iron has been shown to be controlled by the *fur* gene, whereby when sufficient iron levels are reached, the *fur* gene is activated causing a down-regulation of gene expression for certain genes [99].

An early study looking for the presence of the *fur* gene in *V. vulnificus* identified *fur* homologues by Southern hybridisation. Construction of a *fur* mutant in *V. vulnificus* demonstrated that outer membrane proteins such as HupA and VuuA are iron regulated and were over-expressed in a *fur* mutant strain [99-101]. Studies have also shown that *fur* is regulated by the Sigma S factor, RpoS. This was shown by comparing the proteomic secretome of wild-type *V. vulnificus* with the secretome of *V. vulnificus* containing a mutation in the *rpoS* gene [102]. It was found that the Fur protein was significantly down regulated in an *rpoS* mutant. As well as *rpoS* regulation, the study found that Fur can also regulate its own expression under iron-limited conditions [102]. It was later shown experimentally using a transcriptional fusion that *fur* contains an upstream region, this upstream region was shown to bind Fur during iron limited conditions to control expression [103]. Fur is also known to act on virulence genes in *V. vulnificus* such as the haemolysin/cytolysin encoded by *vvhA*. A study found that Fur effected the expression of *vvhA* by causing a decrease in levels of VvhA as well as repressing the expression of *vvpE* [104]. Following on

from the identification that Fur can control the expression of *vvpE*, it was found that Fur can control the expression of SmcR [105]. SmcR (homologous to LuxR) is a quorum sensing regulator which can control the expression of virulence factors in *V. vulnificus* [106].

Quorum sensing (QS) is the ability for bacterial populations to sense environmental surroundings using signalling molecules [107]. Bacterial cells are able to use signalling molecules known as auto-inducers to modulate the cells within the bacterial population. This can affect activities such as motility, biofilm formation, extracellular secretion, luminescence, virulence and secondary metabolites [107, 108]. Studies have found that *V. vulnificus* produces the quorum sensing molecules, acylated homoserine lactones and the auto-inducer, AI-2 [109, 110]. It has been shown experimentally that the AI-2 molecule of *V. vulnificus* is able to stimulate the quorum sensing system two in *V. harveyi* [111]. The AI-2 synthase gene *luxS* is believed to be involved with coordinating the expression of virulence factors in *V. vulnificus*, as a *luxS* mutant has been shown to be attenuated both *in vivo* and *in vitro*. For example, the *luxS* mutant was less lethal in a mouse model of infection, as well as displaying attenuation towards HeLa cells in tissue culture. It was also noted that the *luxS* mutant displayed a decrease in the production of extracellular protease including VvpE) compared to the wild-type strain. Conversely, the *luxS* mutant produced an increase in the haemolysin/cytolysin compared to the wild-type strain [111].

An alternative study also demonstrated that a *luxS* mutant showed a weak attenuation towards a macrophage cell line, like-wise a mutation in *smcR* also produced a weakly cytotoxic effect towards macrophages, compared to the wild-type strain [112]. A study using *luxS* and *smcR* mutants have shown that macrophages activated with these mutants displaying differing gene expression profiles compared to macrophages activated with a wild-type strain. Differential expression was seen in genes involved with removal of toxins, cytokine production and the complement pathway. The authors concluded that *V. vulnificus* quorum sensing may therefore be involved in pathogenesis and survival of the bacterium by changing the expression profiles of host immunity genes [113].

1.8 Virulence mechanisms of *V. vulnificus*

1.8.1 Evasion of host defenses by *V. vulnificus*

V. vulnificus disease symptoms are generally dependent on the route of infection, which can either be through ingestion or wound infection [59, 60, 114]. Once inside the human host, *V. vulnificus* will be required to evade host immune defences in order to survive [12, 14, 92]. Depending on the route of infection, the bacterium may experience the acidic conditions of the stomach. Therefore in order to continue its journey through the body, the bacterium will be required to neutralise the acidic conditions in the stomach [12, 92]. Likewise, arrival of the bacterium in the bloodstream does not guarantee survival for *V. vulnificus* cells, as the bacterium will meet macrophages, and will therefore be required to evade phagocytosis. To overcome the host's immune system and establish an infection, *V. vulnificus* has evolved several virulence factors to aid in the disease process. Many of these virulence factors are outlined in more detail below.

1.8.1.1 Acid neutralisation

As *V. vulnificus* is an acid-sensitive bacterium [115], it is imperative that the organism is able to neutralise gastric acids [116]. Neutralisation of acidic conditions is achieved by the synthesis of cytoplasmic amino acid decarboxylases [92]. The *cadBA* operon of *V. vulnificus* encodes a lysine/cadaverine antiporter and a lysine decarboxylase, which both aid in countering acidification by the synthesis and excretion of cadaverine [117]. Mutagenesis studies demonstrated that lysine decarboxylase encoded by the *cadA* gene plays an important role in acid tolerance, as a *cadA* mutant is more sensitive to acidic conditions than the wild-type strain. In order for the *cadBA* operon to be induced and provide cells with the ability to withstand acidic conditions, prior exposure of the cells to a low pH is required. This was an important finding for *V. vulnificus*, as previous food safety practice involved exposing seafood to acidic conditions. This was done to suppress bacterial growth, however the method could have potentially been prepping *V. vulnificus* cells to withstand human host defenses [116].

Initial work on understanding the mechanism by which the bacterium survives acidic conditions was followed up by understanding the regulation and activation of the

cadBA operon. Activation of the *cadBA* operon in *V. vulnificus* was found to be activated by CadC, *cadC* activity is pH dependent as it is not expressed at neutral pH. Mutagenesis studies in the *aphB* gene demonstrated that *cadC* is activated by *aphB*, which causes an increase in cellular levels of CadC [117]. This ultimately leads to the production of lysine/cadaverine antiport and lysine decarboxylase, both of which are able to neutralise acid [118].

1.8.1.2 Capsule

It is well documented in the literature that capsule is involved in protecting bacteria from the host immune system and concealing pathogen associated molecular patterns (PAMPS), such as outer membrane proteins [119]. The capsular polysaccharide of *V. vulnificus* is described as one of the main virulence factors of this extracellular pathogen [12, 120, 121]. Mutagenesis studies have demonstrated the importance of the capsule as strains with mutations in capsule genes or genes involved in the expression of capsule are attenuated in animal models of infection [121, 122].

It is documented in the literature that *V. vulnificus* cells display two differing colony morphologies, designated opaque and translucent [123], due to the surface expression of capsule [120]. Opaque morphologies represent encapsulated strains expressing capsular polysaccharide (CPS), whereas translucent colonies represent non-encapsulated strains, or cells expressing decreased amounts of CPS [123]. The bacterium can vary between opaque and translucent, with single strains capable of expressing both colony types on one streak plate [38, 121, 124]. In a study by Simpson *et al.*, (1987) 38 *V. vulnificus* strains were examined for their colony morphology. They found that all strains produced either a mixture of opaque and translucent or translucent only colony types [124]. Mouse models of infection demonstrate that encapsulated strains show an increase in virulence and display resistance to serum activity, whereas translucent strains are reduced in virulence and sensitive to serum killing [121, 125]. The transition from an opaque to translucent colony morphology is based on phase variation in the group-1 CPS cluster. Phase variation is reported to be a consequence of multiple genetic alterations in the CPS operon [126].

Although capsules have long been used successfully in vaccines against pathogenic bacteria [127], the production of a capsule based vaccine is unlikely for *V. vulnificus*, due to the significant heterogeneity of the capsule between strains [12].

1.8.2 Iron uptake mechanisms of *V. vulnificus*

Many organisms require iron for a variety of cellular process, therefore the ability of pathogenic bacteria to scavenge iron from their host is important [9]. Iron in human hosts is generally unavailable to invading bacteria, as it is bound to transferrin [92]. Therefore pathogenic bacteria have evolved mechanisms to overcome this challenge. This is achieved by producing iron chelators known as siderophores, which are able to bind iron and return it to the bacterial cell. *V. vulnificus* has been shown to produce two types of siderophores, vulnibactin and hydroxymate-type [128].

The transport of siderophores across bacterial membranes is generally driven by the TonB system, in an energy dependent process [129]. Many pathogenic *Vibrios* have been shown to contain two TonB systems [129], TonB1 and TonB2. Both TonB1 and TonB2 are present in *V. vulnificus* and have been shown to be involved in the uptake of exogenous iron-bound siderophores [130]. In addition to the uptake of *V. vulnificus* siderophores, the TonB1 and TonB2 systems of *V. vulnificus* are also able to uptake siderophores which have been produced by other bacteria [130].

Unlike many other pathogenic *Vibrios*, *V. vulnificus* has been shown to encode an additional TonB system, TonB3 [9]. TonB3 is induced when *V. vulnificus* is grown in human serum and in minimal media containing glycerol. The leucine responsive protein and the cyclic AMP receptor protein, have been identified as factors that affect the regulation of the TonB3 system [131]. These are two global regulators that are able to regulate the TonB3 system in response to different environmental signals. Although the regulation of the TonB3 system has been elucidated for *V. vulnificus*, a direct role in virulence for this third system has yet to be established [131].

As previously mentioned, *V. vulnificus* produces two types of siderophores, vulnibactin and hydroxymate-type [128]. In addition to siderophores, it was suggested that *V. vulnificus* could also scavenge iron from the human host, through

the use of the metalloprotease, VvpE. It was believed that the proteolytic ability of VvpE could cleave heme proteins from host transferrins and lactoferrins [132, 133]. The ability of VvpE to aid in the accumulation of iron was demonstrated experimentally by the addition of exogenous VvpE to *V. vulnificus* cultures, demonstrating that the metalloprotease could digest heme proteins [133].

However, it was later shown by two different research groups, that the siderophore vulnibactin, is required for the uptake of iron from the human host, and not VvpE [132, 134]. This was demonstrated through the use of mutagenesis studies which showed that a deletion to either *venB* or *vuuA*, removed the ability of *V. vulnificus* to accumulate iron [132]. *venB* encodes for an enzyme required for vulnibactin synthesis, whereas *vuuA* encodes a vulnibactin receptor protein. A deletion to the *vvpE* gene however, did not affect vulnibactin production or the assimilation of iron. These results therefore suggest that vulnibactin is required for the assimilation of iron, whereas VvpE is not [132]. Recent work understanding how vulnibactin is secreted from the cytoplasm to the extracellular environment, has suggested that vulnibactin is secreted via a type 1 secretory pathway, employing a resistance-nodulation division (RND) efflux system. This study also identified TolC as an essential protein involved with the export of vulnibactin [135].

As documented earlier, fatal *V. vulnificus* infections often occur in individuals with predisposing liver conditions, or high iron serum levels [36, 68]. Accordingly, *in vivo* studies which investigated iron levels and *V. vulnificus* pathogenicity, showed that an increase in iron levels, caused a decrease in the amount of bacteria required to cause an infection from 10^6 to 1 bacterial cells. The study concluded that mice with liver damage were more susceptible to *V. vulnificus* infection [136].

1.8.3 Motility and attachment

In order to establish an infection, many bacteria will often move from the initial site of infection to another location within a host [137]. This motility is often achieved by the presence of flagella and as such flagella is often regarded as an important virulence factor for many pathogenic bacteria [138]. For example, *V. vulnificus* infection is commonly associated with sepsis, therefore depending on the route of infection, the bacterium will have to migrate from the initial site of infection to the bloodstream [14, 139]. Accordingly, genetic mutagenesis studies have demonstrated that the flagellum

is a virulence factor for *V. vulnificus* [140, 141]. Attachment of bacterial cells to a host surface is also important for the establishment of an infection [142]. This is particularly true for *V. vulnificus* cells when invading via the gastrointestinal route, as cells will need to attach and destroy the intestinal cell wall, allowing the bacterium to enter the bloodstream [12].

1.8.3.1 Flagellum

The basic flagellum structure is made up of the basal body, hook and filament [143]. In *V. vulnificus* the following genes encode for hook associated proteins (HAP), *flgK* (HAP1), *flgL* (HAP2) and *flgH* (HAP3), whereas *flgK* and *flgH* form a junction between the hook and filament, with *flgL* forming a capping structure at the end of the flagellum. To understand the role of the flagellum in *V. vulnificus* virulence, mutagenesis studies were performed. The study found that *flgK* and *flgL* mutants, both produced a flagellum which was identifiable by Western blotting, however the flagellum was not attached to the bacteria and was secreted out in to the supernatant [144]. Conversely, the *flgH* mutant produced a very loosely attached flagellum. Investigation into the motility of these mutants showed that both *flgK* and *flgH* were non motile, and all 3 mutants were reduced in their cytotoxicity and adherence to cell culture lines [144]. In a mouse model of infection, *flgL* and *flgH* were attenuated [145]. A mutant containing a deletion in the *flgE* gene is also non-motile, attenuated in an *in vivo* infection model and reduced in adherence and biofilm formation [141]. Similarly disruption to the *flgC* gene leads to a significant decrease in motility, adhesion and cytotoxicity, with the mutant displaying an attenuation in a mouse model of infection [140].

1.8.3.2 Pili

Pili structures on *V. vulnificus* can be imaged using electron microscopy, and have been found to be important for adherence of the bacterium to epithelial cell lines [146]. Furthermore, deletion of the *V. vulnificus* *vvpD* gene, a homologue of the *pilD* gene in *Pseudomonas aeruginosa*, has been shown to effect surface expression of pili [92]. Indicating that *V. vulnificus* surface expressed pili are from the type 4 class, which are involved in attachment and motility [147]. PilD is a peptidase which cleaves the pre-pilin signal on PilA proteins, which are involved with pili generation. Furthermore, mutations to *pilD* in bacteria such as, *P. aeruginosa*, *Aeromonas*

hydrophila and *Legionella pneumophila*, have caused disruption to proteins secreted via the GSP. Similarly for *V. vulnificus*, mutations to the *pilD* gene led to a disruption in the secretion of several extracellular enzymes. For example, one extracellular enzyme was found to localise to the periplasmic space, therefore suggesting the protein is normally secreted via the GSP. The *vvpD* mutant was also attenuated for cytotoxicity to epithelial cell lines, adherence to Hep-2 cells lines and was attenuated in an iron-over loaded mouse model [147].

1.8.4 Bacterial endotoxin

Lipopolysaccharide (LPS), also known as endotoxin, is a molecule made up of a lipid and a polysaccharide region [148]. Molecules of LPS are not secreted but are found situated on the outside of Gram negative bacteria [149]. Due to the LPS molecule making up the outer leaflet of the outer membrane of Gram negative bacteria, LPS is easily accessible to the host immune system, and is a prudent activator of host pro-inflammatory cytokines [148]. In addition to the activation of immune cytokines, LPS can also activate both the innate and adaptive immune response, this can lead to fever, organ failure and ultimately death from septic shock [148, 149].

1.8.4.1 *V. vulnificus* endotoxin

In agreement with what is known about bacterial LPS, exposure of humans to *V. vulnificus* LPS is reported to result in septic shock [150]. Additionally, experimental injection of *V. vulnificus* LPS into rats via the intraperitoneal route has been shown to cause death in as little as 30 minutes [151]. *In vitro* studies of *V. vulnificus* LPS have also shown activation of rat microglia resulting in the release of inflammatory cytokines [150].

A phenomenon associated with *V. vulnificus* infection is why a disproportionate number of males succumb to *V. vulnificus* sepsis compared to females [12, 43, 70]. This un-answered question was investigated by a study carried out in 2001, which looked at the protective mechanisms of oestrogen to sepsis induced by *V. vulnificus* LPS. The study used an *in vivo* mouse model to demonstrate the ability of the female hormone oestrogen to protect against the toxic effects of LPS. The study therefore hypothesised that the female hormone, oestrogen may account for why there are more *V. vulnificus* infections associated with males than with females [70]. Although

the study demonstrated that oestrogen can protect against the endotoxic shock induced by LPS, the exact mechanisms of the protection is yet to be established.

In addition to oestrogen, low density lipoproteins (LDL), are also believed to help protect host organisms from *V. vulnificus* induced sepsis, as it has been shown that the levels of LDL in a patient's serum can affect *V. vulnificus* infection outcome [152]. Although the study demonstrated that serum LDL levels can affect infection outcome, the exact methods by which LDL protect against *V. vulnificus* sepsis is currently undetermined [152]. A more recent study looking at the innate immune response to *V. vulnificus* LPS, demonstrated that the secondary metabolite, Cyclo (Phe-Pro) produced by *V. vulnificus* is able to suppress inflammatory cytokines *in vitro*. The study suggested that Cyclo(Phe-Pro) enables the pathogen to survive in the host by suppressing the inflammatory immune response [153].

1.8.5 Bacterial exotoxins

During bacterial pathogenesis, bacteria employ a range of secreted virulence factors, these virulence factors can be used for both damaging host cells, as well as protecting the invading bacterium from the host's immune response [92, 154]. Likewise, in addition to the virulence factor LPS, described in the above section, *V. vulnificus* also produces an array of secreted virulence factors to aid in the disease process [38, 43].

Toxins secreted by pathogenic bacteria can be divided into three different subclasses, type I toxins, type II toxins and type III toxins [154]. Type I toxins exert their effect at the cell surface and do not require entry into the host cell [92, 154]. The second class of toxins is the type II toxins, these are classified as toxins which cause damage to the integrity of host cell membranes [154], an example of a type II toxin is the Rtx class of toxins [92, 154, 155]. Finally, type III toxins are a group of toxins that are composed of two molecules and are therefore sometimes referred to as A/B toxins [154]. An example of a type III toxin is the well-studied cholera toxin [154]. The B subunit of the toxin generally binds to receptors of the surface of host cells, whereas the A subunit, which contains the enzymatic activity enters the host cell where it causes its deleterious effects [154].

1.8.5.1 V. vulnificus Rtx toxin

Although *V. vulnificus* is known to produce a range of secreted virulence factors, the most extensively studied toxin is the Rtx toxin [154, 156]. The Rtx or “repeats in toxin” is a class of toxin which is found extensively in Gram negative bacteria and can cause a range of biological effects [156]. Bacterial Rtx toxins often contain glycine and aspartate amino acid repeats and are usually secreted via the type 1 secretion system [156].

The RtxA toxin from *V. vulnificus* was first identified as a virulence factor for this pathogen in 2007 [155, 157]; and although the toxin shares significant homology to the Rtx toxin of *V. cholerae*, the RtxA toxin from *V. vulnificus* differs in its mode of action. For example, *V. vulnificus* RtxA has been shown to cause disruption to the cellular membrane of mammalian cells [155], as well as causing cytoskeleton rearrangement and blebbing of cells, ultimately leading to the necrotic cell death of mammalian cells [158]. This is in contrast to the *V. cholerae* Rtx toxin, which has been shown not to disrupt the cellular membrane, but instead causes depolymerisation of actin leading to the rounding up of mammalian cells [155].

The RtxA toxin of *V. vulnificus* is secreted via the T1SS which contains an RtxE ATPase. This was identified following *in vitro* experiments which demonstrated that RtxA could be identified in the supernatant of wild-type *V. vulnificus*, but not in the supernatant of an *rtxE* mutant [159, 160]. The *rtxE* is described as a virulence factor for *V. vulnificus* as the mutant is attenuated in a mouse model of infection. Additionally, the *rtxE* mutant was shown to be more attenuated than a *rtxA* mutant *in vivo*, suggesting that RtxE is involved with the secretion of additional virulence factors other than solely RtxA [159]. Following secretion of the RtxA toxin into host cells, the toxin has been shown to then be processed into two parts. *In vitro* studies have demonstrated that the larger N-terminal region localises to the host cell membrane, whereas the smaller C-terminal region can be detected inside the host cell [161]. The pore produced by the N-terminal fragment has been shown to cause an imbalance of calcium, whereby there is an influx of calcium into host cells leading to an increase in intracellular calcium levels. The study showed that the increase in calcium levels led to mitochondrial dysfunction and ultimately programmed necrotic cell death [161].

A study which monitored the infection process of *V. vulnificus*, by following intragastric inoculation of mice, found that deleting the *rtxA* gene caused a delay in bacterial growth *in vivo*, reduced colonisation of the small intestines and reduced dissemination of the bacteria to other organs such as the liver and spleen. The bacteria were monitored *in vivo* by imaging infected mice and tracking bacteria using luminescence. Overall the study found that the RtxA toxin aids in establishment of an infection and dissemination to other tissues, a loss of the RtxA toxin caused a delay in the establishment of infection and in general, a less severe infection [162].

The majority of the studies which have examined the role of the RtxA toxin from *V. vulnificus*, have used the reference strains, CMCP6, MO6-24/O or YJ016. However, a recent bioinformatic study which assessed the variation in domains associated with the RtxA toxin from 40 *V. vulnificus* isolates found there to be four different variations of the toxin's domain. This bioinformatic study found the most abundant RtxA toxin present in clinical isolates has reduced virulence in comparison to the toxin from environmental isolates. It is believed that the variation in the toxin effector domain arose from recombination events, either with RtxA genes from plasmid DNA or from the *Vibrio* strain, *V. anguillarum*. The authors suggested that strains of *V. vulnificus* are undergoing genetic rearrangement which may ultimately lead to selection of strains that exhibit reduced virulence in humans [163].

1.8.5.2 Extracellular cytolysin/haemolysin

As well as producing a well-studied RtxA toxin, *V. vulnificus* is also known to secrete a 56kDa cytolysin/haemolysin, which is encoded by the *vvhA* gene [43, 164, 165]. Although homologous to the *vvhA* gene of *V. cholerae* [166], the *vvhA* gene from *V. vulnificus* is often used as a *V. vulnificus* species specific housekeeping gene that is commonly used to identify the provenance of isolates [167, 168].

In 1985 the VvhA toxin was purified and characterised in several *in vitro* and *in vivo* experiments [164]. The studies demonstrated that the toxin was heat-labile, hydrophobic and able to cause lysis of red blood cells. Further characterisation of the toxin indicated that the protein was toxic to CHO cells *in vitro*, and lethal in an *in vivo* mouse model of infection [164]. As such VvhA is thought to be a potent *V. vulnificus* toxin due to the disease symptoms generated in mice at very low inoculation levels [164, 169].

To further understand the role of VvhA in *V. vulnificus* virulence, a deletion mutant was made and tested *in vivo*, with mice subsequently challenged via the intraperitoneal and intradermal infection route. Conversely to previous data, the study found that the *vvhA* mutant was not attenuated *in vivo* and virulence of the mutant was comparable to the wild-type strain [170]. This led researchers to believe that the VvhA toxin may not be as important in *V. vulnificus* infection as once believed. To determine whether VvhA was produced *in vivo* during infection, RNA was extracted from the infected mice. The study demonstrated that *vvhA* was indeed expressed during *in vivo* infection, as RT-PCR performed on cDNA generated from the RNA extractions, demonstrated expression of the *vvhA* gene [169]. Several years after the confusion of understanding the role of VvhA in *V. vulnificus* virulence, a study carried out an infection of mice with a *vvhA* mutant via the intra-gastric route, instead of the previously used intra-peritoneal or intra-dermal route [162]. The study found that the *vvhA* mutant was attenuated compared to the wild-type strain, and that VvhA in conjunction with RtxA, is required for gut pathogenesis. Demonstrating that both RtxA and VvhA are required for *in vivo* growth, establishment of an infection and dissemination from the gut to other organs [162]. This study demonstrates the importance of using appropriate models of infection as well as identifying suitable methods of inoculation when studying mutants *in vivo*.

Although there has been much focus on the role of VvhA in *V. vulnificus* pathogenicity, there have been a couple of studies which have attempted to understand the delivery route of VvhA during infection; with one study suggesting outer membrane vesicles (OMV) as a potential secretion route [167]. It is understood that OMV are used by various Gram negative bacteria for the delivery of toxins to host cells and may present as a stress response by bacteria in response to changes in their environment [171]. This may explain why OMV are activated when bacteria enter a human host [171]. An experimental study using immunoblotting demonstrated that *V. vulnificus* produces OMV containing VvhA during *in vitro* infection which mediates apoptosis in epithelial cells [167]. It was shown that the toxin delivered by OMV is VvhA as VvhA null mutants are unable to cause cytotoxicity to cells. The study also observed that OMV interact with cholesterol on host cells to deliver the toxin, as treatment of epithelial cells with a cholesterol sequester inhibits the cytotoxic effects of OMV containing VvhA [167]. This is in

accordance with an additional study that showed cholesterol is required for the binding of VvhA to plasma cell membranes, and as such, removal of cholesterol inhibited VvhA binding to membranes [172].

1.8.5.3 Extracellular proteases produced by *V. vulnificus*

An additional secreted protein by *V. vulnificus* is the extracellular metalloprotease, VvpE [43]. In 1985, this 50.5 kDa protein was shown to function optimally at pH 7-8 and was produced maximally during the late exponential growth phase. As well as being growth phase dependent, VvpE has also been shown to be effected by factors such as temperature, iron levels, oxygen and osmolality [173].

In contrary to original findings described above, recent research has demonstrated that the VvpE protein is 45 kDa, not 50.5kDa and upon secretion is cleaved into two fragments, a 34 kDa protein and a C-terminal pro-peptide that is 11 kDa in length [174]. The original 45 kDa protein is thought to be cleaved into two fragments by extracellular autoprotolysis. During the early growth phase of *V. vulnificus* cells, both the 34 kDa protein and the 45 kDa protein can be found in the supernatant, however it was found that the 34 kDa protein predominates over the 45 kDa protein. Both sized proteins contain proteolytic capabilities. However the 34 kDa protein is more efficient at degrading soluble proteins than insoluble proteins. The 45 kDa protein however is sufficient at maintaining a proteolytic ability that is similar for both insoluble and soluble proteins [174].

After the identification of VvpE, studies aiming to characterise the protease subsequently ensued. Early studies achieved this by carrying out injection of the purified protein into mice [175]. These studies proposed that VvpE was a virulence factor, as mice challenged with the enzyme manifested with disease symptoms such as dermonecrosis and swelling, symptoms commonly seen in wound infected patients [176, 177]. To further validate the claims that VvpE was a virulence factor, research groups synthesised *vvpE* mutants which were assayed in an iron overloaded mouse model of infection, mice were challenged via the subcutaneous route, inter-peritoneal route and by force feeding. However, the *vvpE* mutants did not show any signs of attenuation compared to the wild-type strain [178, 179]. This led authors to concluded that VvpE may not be as an important virulence factor as once

hypothesised [179], or that alternative virulence factor may be able to compensate for the loss of VvpE [178].

Although *vvpE* mutants do not display attenuation in a mouse model of infection, *vvpE* mutants are attenuated in several invertebrate infection models [17]. For example, a *vvpE* mutant fails to cause melanisation in a *Tenebrio molitor* infection model, and additionally a *vvpE* mutant is also attenuated compared to the wild-type strain in *Caenorhabditis elegans* and *Artemia salina* infection models. Demonstrating a possible role for VvpE in invertebrate infection [17].

Even though the involvement of VvpE in mammalian infection is controversial, analysis of *vvpE* mutants *in vitro* demonstrates that the mutants are attenuated compared to the wild-type. For example, a *vvpE* mutant is unable to swarm *in vitro*, this however can be restored by complementing the *vvpE* gene. It has also been further demonstrated that VvpE is able to degrade immunity proteins such as IgA and lactoferrins, suggesting that VvpE may play a role in establishment of infection by aiding *V. vulnificus* in adherence and colonisation, as well as carrying out removal of immunity proteins such as IgA [180]. Furthermore, an insertional knock out mutant of the *vvpE* gene causes a loss in elastase ability [175]. However, although a *vvpE* mutant displays a loss in elastase ability, residual protease activity is still detected, suggesting the presence of additional proteases. This was recently found to be true following the identification of a VvpE-homologue, which has been named VvpM [181]. The role of VvpM in *V. vulnificus* virulence was explored by generation of a recombinant form of the protease. The recombinant VvpM protease was shown to be virulent towards human tissue culture cell lines by inducing apoptosis of the cells, indicating a potential role of VvpM in pathogenesis [181].

1.8.6 Gram negative secretion systems

Given that the previous virulence factors described are predominantly extracellular toxins, there must be a way by which these bacterial toxins are released from the cell. In order to facilitate this interaction with the extracellular milieu many bacterial species employ mechanisms known as secretion systems [182]. Secretion systems can be used not only for the release of toxins, but also for the release of other compounds such as enzymes [183]. Currently there are 6 characterised secretion systems in Gram negative bacteria, named accordingly type 1-6 [182, 184].

The six known secretion systems can be further categorised into either a one-step or two-step mechanism. Type 1, 3, 4, and 6 are all examples of one-step secretion systems, and as the name suggests, proteins are moved from inside the cell to the extracellular space by one continuous movement [185]. Unlike one-step secretion systems, two-step secretion systems secrete proteins that have first been transported from the cytoplasm to the periplasm by either the Sec or twin-arginine (Tat) apparatus [184]. Proteins are then moved from their short stay in the periplasm into the extracellular milieu, by either the type 2 or type 5 secretion system [183, 184]. The Sec pathway is generally involved with the emission of both unfolded or partially folded proteins [186], while folded proteins are generally ejected via the Tat system. The Sec pathway is made up of Sec proteins, known as SecA and SecYEG. SecA is an ATPase and provides the energy for the movement of proteins, whereas SecYEG makes up the translocon apparatus. Sec proteins are trafficked to the periplasm by a N-terminal signal sequence, which is cleaved once proteins arrive in the periplasm [92, 183]. Like Sec-dependent proteins, Tat proteins also contain a signal sequence, however the sequence varies in length from the Sec signal [183], as well as containing a twin-arginine motif [184].

1.8.6.1 *V. vulnificus* secretion systems

Although there are currently six known secretion systems in Gram negative bacteria, the most extensively studied secretion system in *V. vulnificus* is the T2SS. It has previously been shown that the EspC protein is integral for connecting the inner and outer membrane regions of the T2SS [187, 188]. Furthermore deletion of the *espC* gene leads to a disruption in proteins secreted via the T2SS. For example, deletion of the *espC* gene in *V. vulnificus* resulted in diminished secretion of T2SS substrates, such as the VvhA toxin [189]. Accordingly, the *epsC* mutant strain was also defective in haemolytic ability associated with VvhA. The absence of the VvhA protein from the extra cellular milieu of the *espC* mutant strain was also further confirmed by Western blotting using a VvhA antibody which demonstrated that VvhA was not detected in the supernatant of the mutant strain, but was present in the supernatant of the wild-type strain, further validating the role of the T2SS in secretion of VvhA [189]. An *in trans* complementation of the *epsC* gene in the mutant was also able to restore the secretion of the VvhA toxin

In addition to VvhA, the protein VvpE has also been shown to be secreted via the T2SS, as deletion of the gene *epsC* led to a periplasmic accumulation of both VvpE and VvhA [189]. The study concluded that the T2SS is involved with the secretion of both the haemolysin/cytolysin, VvhA and the metalloprotease VvpE [189].

Although *V. vulnificus* is known to encode a T1SS which is believed to be involved with secretion of the well characterised RtxA toxin, the T1SS has not been extensively studied in *V. vulnificus*. However, it has been shown that disruption of the T1SS does not affect the secretion of either VvpE or VvhA, further suggesting that the secretion of VvpE and VvhA by *V. vulnificus* is T2SS dependent [189].

Other than the secretion systems mentioned previously, no other secretion systems have been characterised in *V. vulnificus*. Bioinformatic analysis of *V. vulnificus* genomes has suggested the presence of a T4SS and T3SS due to the identification of *virB* and *sopB*, genes which are associated with the T4SS and T3SS respectively [190, 191]. However, there is a distinct lack of knowledge regarding the secretion systems that are functional in the *V. vulnificus* genome, representing an area which is particularly understudied for this pathogen. This thesis aims to contribute towards this understudied area with the identification of novel T6SSs, which are discussed in more detail in Chapters 4, 5 and 6. A schematic image in Figure 1 represents the secretion systems currently identified in *V. vulnificus*, including the T6SS1 and T6SS2 identified in *V. vulnificus* in the current study, also shown is the currently known effectors for the T1SS, T2SS and T6SS1.

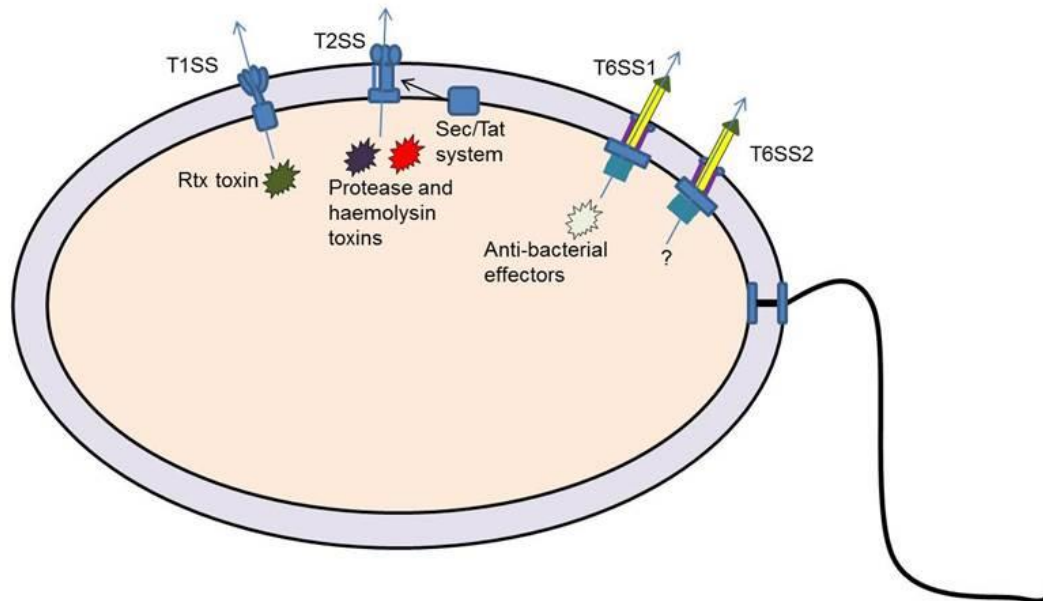


Figure 1.1: Secretion systems in *V. vulnificus*. The image shows a schematic representation of a *V. vulnificus* cell. Included on the diagram is the single polar flagellum, the T1SS, which is believed to secrete the RtxA toxin, the T2SS which secretes the haemolysin, VvhA and protease VvpE. Additionally shown on the diagram is the T6SS1 which contain anti-bacterial properties. The T6SS2 is also shown; however the mode of action of this secretion system is currently undetermined. The T3SS and T4SS have not been included, as currently these two secretion systems have not been characterised beyond bioinformatic identification of one or two genes.

1.9 Study objective

V. vulnificus is a pathogenic bacterium which is known to vary in virulence potential. This has led to the hypothesis that not all strains are equal, with some strains better adapted to causing human infection than others. A possible reason for this may be due to differences in expression of virulence factors, such as those described above. Consequently, this study characterised a panel of strains from different isolation sources that had varying degrees of virulence by analysing their behaviour in several phenotypic assays based around known virulence determinants. The objective of this was to determine whether any of these assays could distinguish strains on the basis of their virulence potential or source of isolation.

Chapter 2 Phenotypic characterisation of *V. vulnificus* isolates

2.1 Introduction and aim

The previous chapter introduced the diverse nature of *V. vulnificus* isolates in terms of virulence potential and genotype [19]. This observation of diversity between strains has led to the hypothesis that not all strains of *V. vulnificus* are equal in pathogenicity, with some strains better adapted to causing human infection than others [114]. This may be due to differences in expression of virulence factors. Therefore the aim of the current study was to determine whether such differences could be characterised through phenotypic assays. The phenotypic assays investigated the following known virulence factors, presence of capsule, protease production, motility and cytotoxicity towards the intestinal barrier model, CaCo-2 cells. In addition, another aim was to identify whether any phenotypic assay findings could demonstrate correlation with, 1), the published *in vivo* mouse data on virulence groupings of these isolates, or 2), source of isolation.

The graph in Figure 2.1 shows the virulence grouping of ten strains selected for study in this thesis as well as the three reference strains, YJ016, MO6-24/O and CMCP6 [13]. The data shown in Figure 2.1 is extracted from a study which investigated the virulence of 69 strains in an iron overloaded mouse model. Virulence was assessed by characterising the infected mice from the following measurements, cfu/g of bacteria in the skin, cfu/g of bacteria in the liver and a decrease in body temperature (<33°C was presumptive of death) [13]. Using these indicators of virulence, strains were grouped from one to five, whereby group one was the least virulent and group five the most virulent. The virulence groups contained the following characteristics; group 1 very low levels of skin infection with almost undetectable liver infection; group 2 low levels of skin infection with undetectable to low levels of liver infection; group 3 high levels of skin infection with undetectable to low levels of liver infection; group 4 high levels of skin infection with moderate to high levels of liver infection; group 5 very high skin infection and very high liver infection.

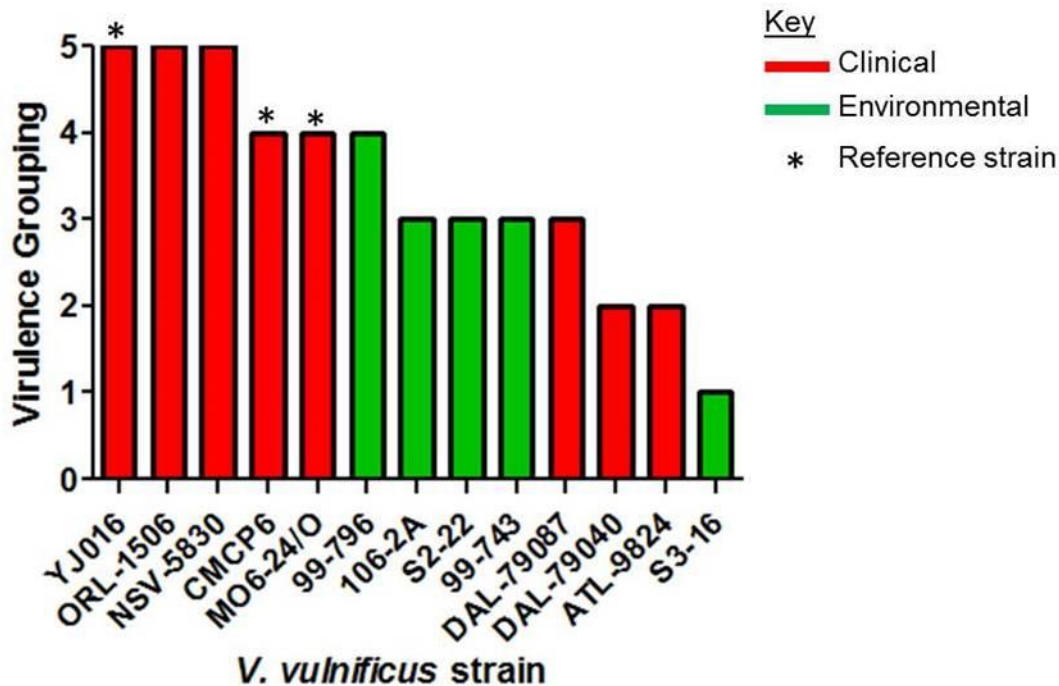


Figure 2.1: Virulence groupings of *V. vulnificus* isolates. Data shown is adapted from Thiaville *et al.*, (2011) for the 10 *V. vulnificus* isolates used in the current study, including the three reference strains, YJ016, CMCP6 and MO6-24/O. Strains were assigned into virulence groupings from one to five depending on the severity of disease symptoms and bacterial load in the skin, liver and spleen.

Therefore, using the data in Figure 2.1, this study aimed to address whether any of the phenotypic assays performed on the ten strains, were able to predict virulence (as determined from the data in Figure 2.1) or source of isolation of a strain.

2.2 Results

2.2.1 Confirmation of *V. vulnificus* strains

Prior to commencing phenotypic characterisation assays the panel of *V. vulnificus* strains were streaked onto *Vibrio* TCBS selective agar to ensure all strains were *V. vulnificus*. The majority of the strains produced characteristic green colonies. One strain however, 99-743, consistently produced yellow colonies. This is not uncommon as it is documented in the literature that a sub-group, ~3-15% of *V. vulnificus* strains are able to ferment sucrose and therefore appear yellow on TCBS agar [74]. To further confirm the provenance of the strains as *V. vulnificus*, a PCR was carried out to identify the presence of *vvhA*, a *V. vulnificus* specific gene which encodes the haemolysin/cytolysin [74]. Figure 2.2 demonstrates that all of the strains are positive for the *vvhA* gene as they produced the expected 520bp PCR product.

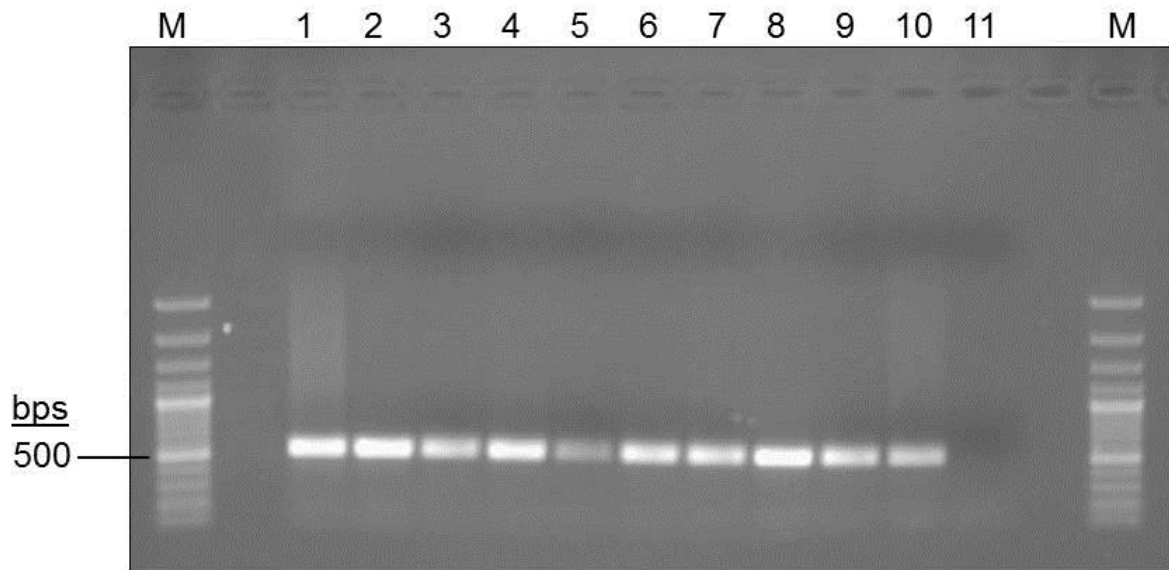
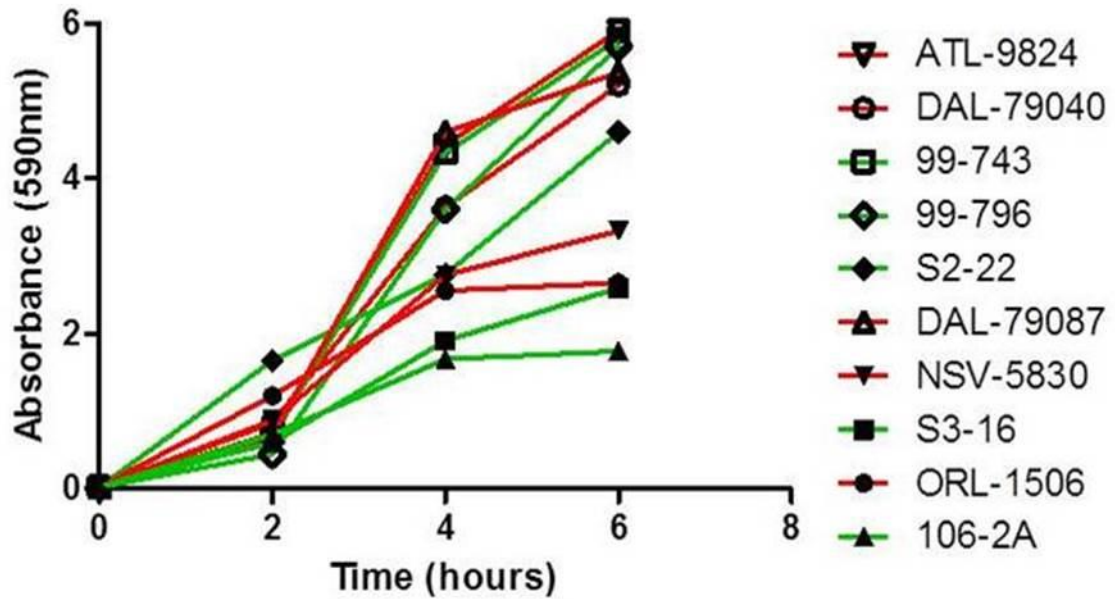


Figure 2.2: PCR confirmation of *vvhA* positive *V. vulnificus* isolates. Gel electrophoresis image of a PCR carried out on genomic DNA from the ten *V. vulnificus* strains using primers *vvhA*_F and *vvhA*_R, to amplify the *vvhA* gene, a marker used to the current study demonstrating that all strains are *V. vulnificus*. The marker indicated with “M” represents a 1kb plus ladder for sizing of DNA fragments. Lanes 1-10 is a 5µl sample of the *vvhA* PCR run for each of the tested strains, lane 11 is a negative control.

2.2.2 Growth characteristics of clinical and environmental *V. vulnificus* isolates

The first phenotypic test analysed the growth of each *V. vulnificus* strain by the construction of growth curves, as it was hypothesised that the ability of some *V. vulnificus* strains to cause a rapid and fulminating disease may be linked to differences in growth. The current study hypothesised that the hyper virulent strains may grow faster than the lesser virulent strains. Additionally growth curves were also determined for each strain to aid in latter characterisation assays, where knowing the average cfu/mL and corresponding OD reading would be required. Figure 2.3(A) shows the growth curves for each strain. Overnight cultures were re-adjusted to an OD_{590nm} of 0.03 and readings were taken every two hours at T0, T2, T4 and T6. Figure 2.3(B) demonstrates the cfu/mL viable counts for the corresponding OD readings at T2, T4 and T6. Viable cell counts were determined by carrying out a Miles and Misra serial dilution.

(A)



(B)

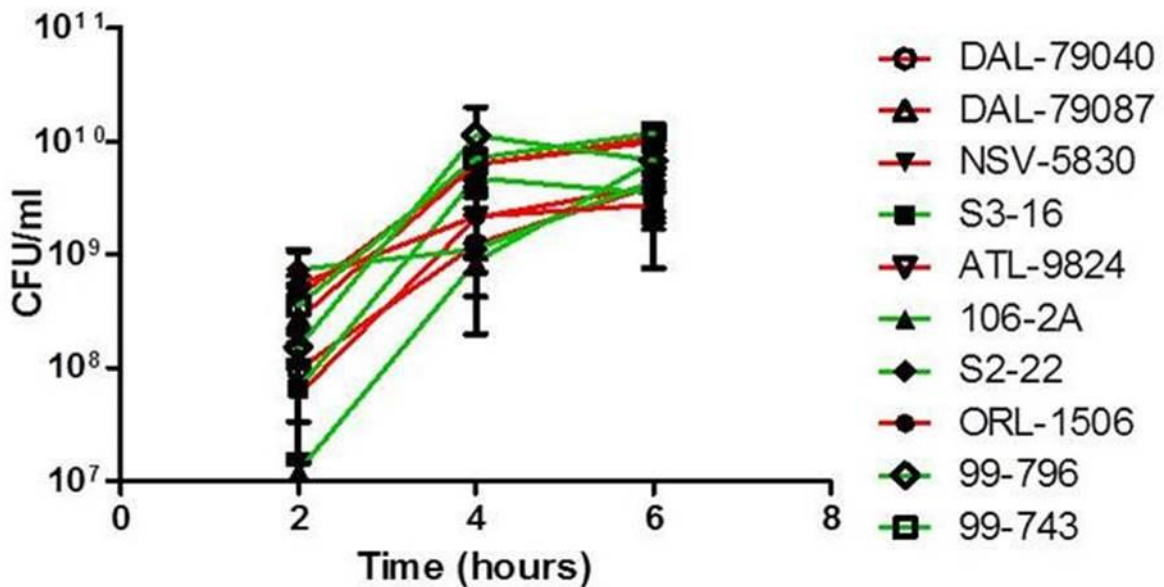


Figure 2.3: Growth characteristic of clinical and environmental *V. vulnificus* isolates. (A) OD_{590nm} readings for *V. vulnificus* growth curves at two hourly intervals, T0, T2, T4, T6 and T8. (B) OD_{590nm} corresponding Miles and Misra serial dilutions, cfu/mL. Clinical isolates are shown in red and environmental isolates are shown in green. The absorbency reading graph shown in (A) was repeated 3 times, the recorded cfu/mL was performed three times in triplicate. Error bars on the graph represent standard error of the mean. Growth curves were performed at 37°C in 2% LB media.

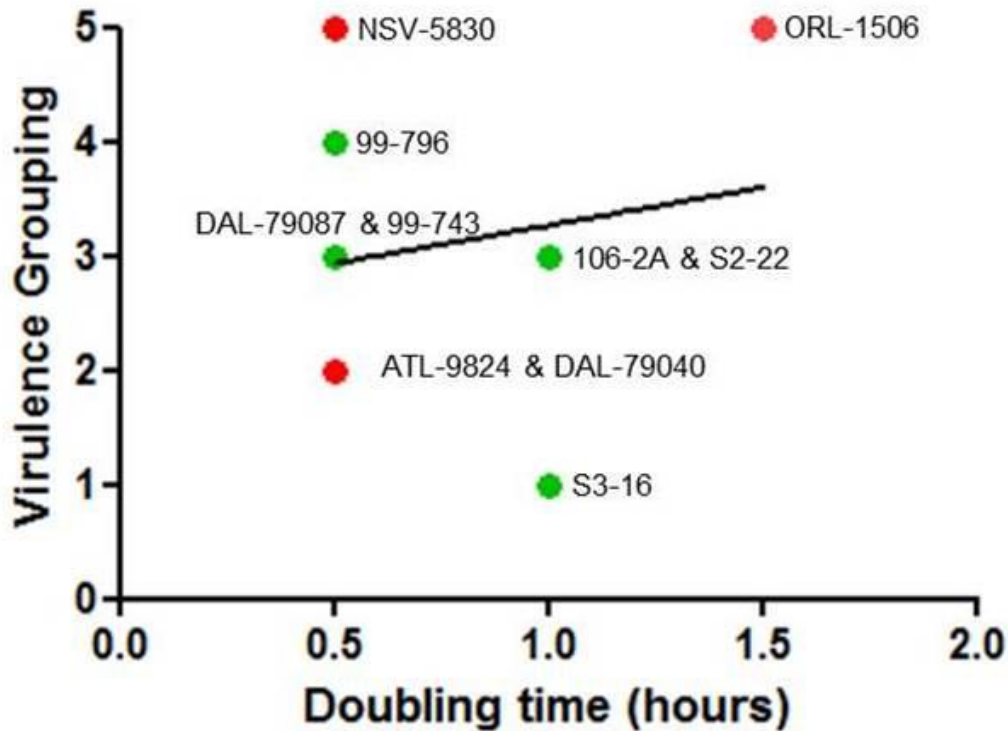


Figure 2.4: Scatter plot of *V. vulnificus* doubling time versus virulence groupings of the strains. The doubling time of the *V. vulnificus* strains were calculated and plotted against each strain's corresponding virulence grouping. Green represents environmental isolates and clinical isolates are shown in red. Each point is labelled with the strains name. The data point for strain DAL-79087 which is a clinical strain is located behind the data point for 99-743. The R-value for the scatter graph is, 0.1832 when analysed using a Pearson correlation.

The results of a two-way ANOVA followed by a post-hoc Tukey test for the growth OD graph shown in Figure 2.3A is shown in Appendix A1. These statistical tests showed that at T0 and T2 there is no statistical significance between the mean values between the strains. This is an expected result as when observing the optical density graph, there is little difference between the strains at time T0 and T2. However, when analysing the later time points, T4 and T6, when the majority of strains are in the exponential phase, there are differences seen between the strains. The significant differences between several of the strains at T4 and T6 are highlighted in yellow, in Appendix A1.

When comparing the strains which have a statistically significant greater mean OD reading at T4, there is no obvious pattern emerging where clinical strains have a higher OD reading than the environmental strains. For example, DAL-79087 and ATL-9824, which are clinical strains, have a higher OD reading than S3-16 which is an environmental strain. Furthermore, the clinical strains, DAL-79040, DAL-79087 and ATL-9824, have a greater OD reading than the environmental strain, 106-2A.

Additionally, DAL-79087 and ATL-9824 have a significantly different OD reading to S3-16. However, other than these differences, there are no other significant differences between the clinical and environmental strains at T4. Demonstrating that not all clinical strains have a higher OD reading than environmental strains. When comparing the OD readings at T6, although there are more significant differences between the strains than at T4, similar results are obtained, in that not all clinical strains produce a significantly greater OD reading compared to environmental strains.

When the growth data is compared to the *in vivo* virulence data for the strains, there is no obvious correlation of hyper virulent strains producing a statistically significant higher OD reading compared to the lesser virulent strains, this is true for both T4 and T6. For example, strain ORL-1506 is a hyper virulent strain, and this strain does not produce a significantly greater OD reading at either T4 or T6 than the least virulent strain, S3-16. Furthermore as shown in Figure 2.4 when the doubling time of each stain is plotted against the virulence data for the strains, the data shows there is a very weak positive correlation, with an R-value equal to 0.1832 when analysed using a Pearson correlation. This data therefore demonstrates that strains producing a higher OD reading are not necessarily more virulent than those producing a lower OD reading and source of isolation does not affect OD readings.

2.2.3 Imaging of capsule on clinical and environmental *V. vulnificus* isolates

The presence of a capsule has been shown to correlate with virulence for *V. vulnificus* strains and through the use of mutagenesis studies the capsule has been identified as a major virulence factor for this pathogen [121, 124]. Although the capsule has been shown to be a virulence factor for this pathogen [120-122, 192], the capsule is not a marker for *V. vulnificus* strains that are hazardous to human health. This has been demonstrated in the published *in vivo* mouse virulence data available for *V. vulnificus* isolates, which shows that both hyper and lesser virulent strains both contain a capsule [13].

Previous capsule studies have shown that there is a difference in capsule production between strains. For instance, there have been reports of some strains possessing a capsule, where as other strains do not [120, 121, 124]. This difference in capsular phenotype has been attributed to deletions in genes involved in capsule production

[123]. Therefore the aim of the capsule phenotypic study was to assess if all the *V. vulnificus* strains used in the current study, possessed a capsule.

Two methods were used to identify the presence or absence of capsule in the current study; they were as follows, colony morphology on 2% NaCl LB-agar streak plates and India ink staining. Colony morphology was used to assess capsule production as it is reported in the literature to be an indicator of encapsulated and non-encapsulated strains, with the former being opaque and the latter translucent [120, 122-125, 193-195]. An additional India ink staining method was also used to assess capsule presence on each strain, as it allows capsule to be imaged using a light microscope.

Streak plates were performed routinely prior to making overnight cultures and the colony morphologies displayed for each strain was opaque, suggesting that all the strains tested were encapsulated. None of the strains displayed the non-encapsulated, translucent phenotype. Figure 2.5 demonstrates representative images of the opaque colony morphology displayed for the ten *V. vulnificus* strains used in the current study.

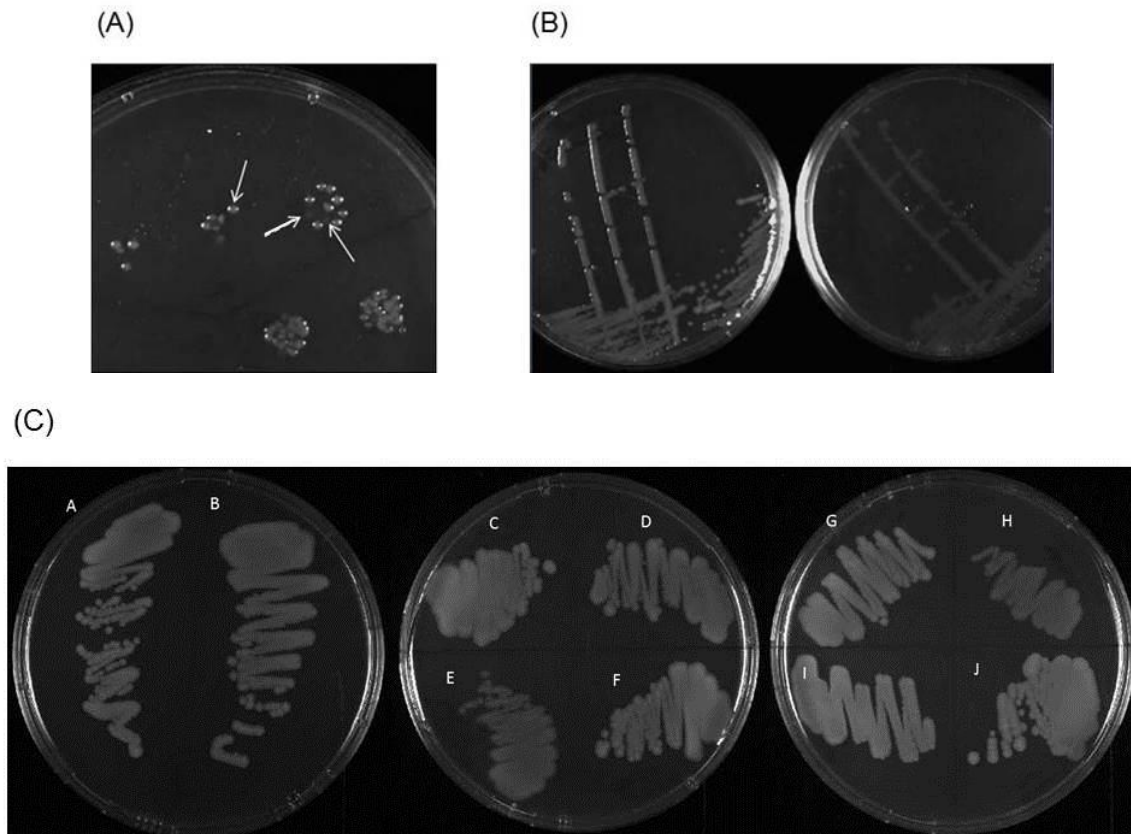


Figure 2.5: Capsule colony morphology of *V. vulnificus* strain on 2% NaCl LB agar plates. (A) Strain S2-22 translucent and opaque colony morphology (colony PCR ensured translucent colonies were *V. vulnificus*). (B) The white arrows indicate translucent colonies. The translucent S2-22 colony variant identified in (A) was re-streaked on to 2% NaCl LB agar alongside the encapsulated version of S2-22, which clearly shows the difference in encapsulated and non-encapsulated colony morphology. (C) Demonstrates streak plates of the ten *V. vulnificus* strains streaked onto 2% NaCl LB agar from freezer stocks. All 10 strains produced the encapsulated phenotype shown (A) ORL-1506, (B) S2-22, (C) DAL-79040, (D) S3-16, (E) 106-2A (F) 99-743, (G) ATL-9824, (H) 99-796, (I) DAL-79087, (J) NSV-5830.

The colonies produced at 37°C on 2% NaCl LB-agar, were highly reminiscent of the encapsulated strain images reported in the literature [124]. Both the clinical and environmental strains produced similar colonies that were circular in shape, raised and with a dense shiny surface that was opaque. There was no difference seen in the colony morphology for either the clinical or environmental strains. The image in Figure 2.5 also contains a *V. vulnificus* strain that is translucent. This strain serves as a translucent control to compare to the opaque strains. The translucent strain is *V. vulnificus* S2-22 and was generated following passage through the infection model, *Galleria mellonella*. The translucent S2-22 colony which was produced following passage through *G. mellonella* was picked and re-streaked as shown in Figure 2.5A. The images in Figure 2.5A demonstrate the difference in colony morphology between translucent and opaque colony variants. Following on from

colony morphology on 2% NaCl LB-agar plates, India ink staining and imaging by microscopy of mid-log culture cells was performed.

India ink is a qualitative, negative staining procedure used for imaging bacterial capsule. The presence of a capsule is indicated by a white halo surrounding cells when they are imaged under a light microscope. The white halo produced around the cells is due to India ink being unable to penetrate the capsule or cell body and therefore provides a dark, negative background when imaging cells using a light microscope. Therefore, to further validate the results seen in Figure 2.5, India ink staining was performed on all of the strains. Figure 2.6 A-J shows the results gained when *V. vulnificus* strains are grown to mid-log phase, in 2% NaCl LB broth at 37°C and stained with India ink. All of the strains analysed, both environmental and clinical contain a capsule, as all strains contain a white halo around the body of the cells. None of the strains appear without a capsule and the images shown are representative of a number of cells analysed.

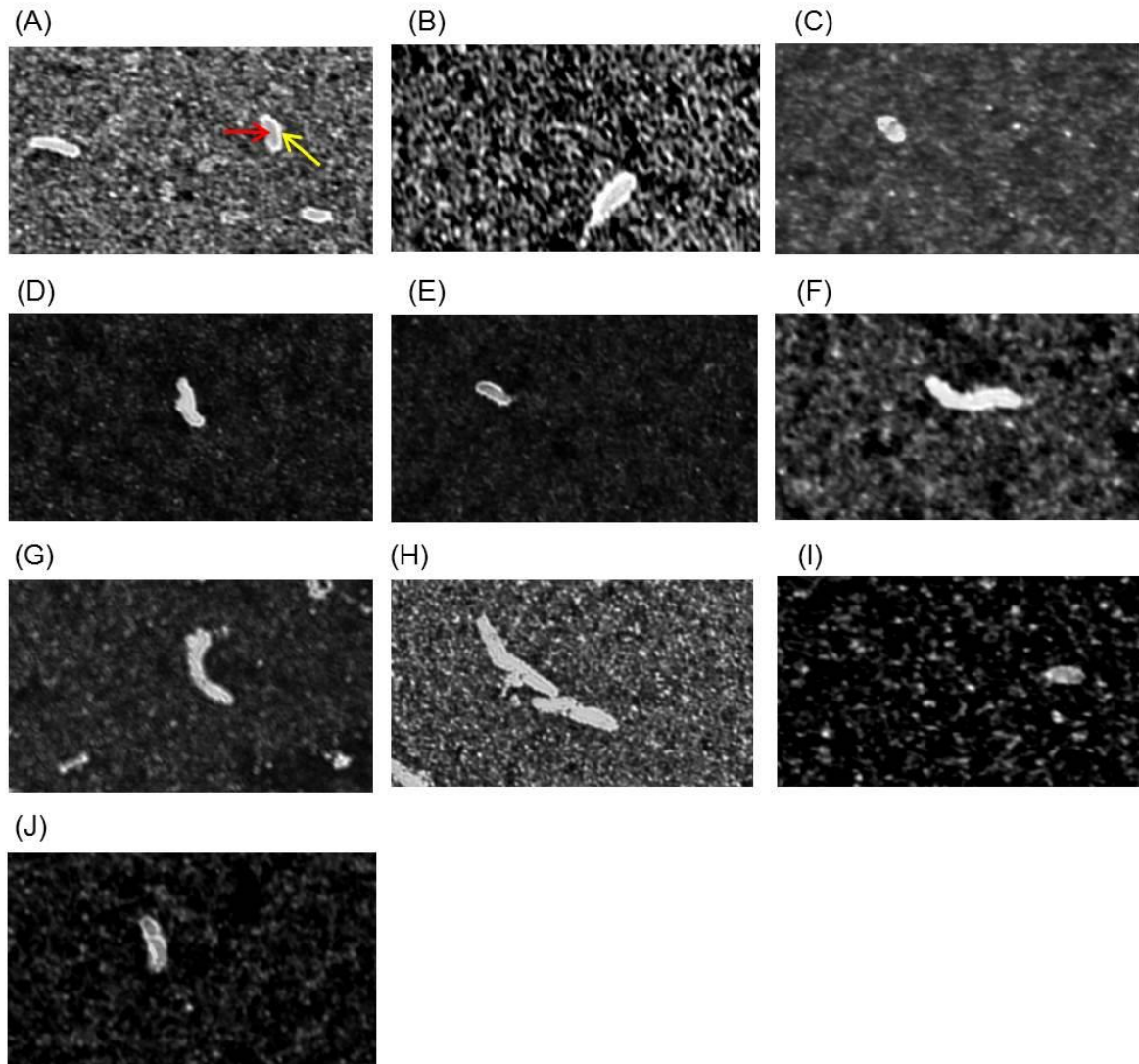


Figure 2.6: Capsule imaging using India ink staining of *V. vulnificus* isolates from clinical and environmental origin. Images A-J are representative images, the yellow arrow on image (A) indicates the capsule and red arrow cell body. (A) *V. vulnificus* 106-2A environmental isolate (B) *V. vulnificus* 99-743 environmental isolate, (C) *V. vulnificus* 99-796 environmental isolate, (D) *V. vulnificus* S3-16 environmental isolate, (E) *V. vulnificus* S2-22 environmental isolate, (F) *V. vulnificus* ATL-9824 clinical isolate, (G) *V. vulnificus* NSV-5830 clinical isolate, (H) *V. vulnificus* ORL-1506 clinical isolate, (I) *V. vulnificus* DAL-79040 clinical isolate, (J) *V. vulnificus* DAL-79087 clinical isolate.

2.2.4 Protease production by clinical and environmental *V. vulnificus* isolates

It has previously been shown that injection of purified VvpE from *V. vulnificus* into mice causes the following manifestations, edema, haemorrhagic damage, dermonecrosis, and an increase in vascular permeability. All of which are disease symptoms often associated with *V. vulnificus* infection. [176, 196-198]. However, the exact role of VvpE in *V. vulnificus* infection is still unclear as although injection of purified VvpE into mice causes disease symptoms commonly associated with *V.*

vulnificus infection, mutagenesis studies have shown that a *vvpE* deletion mutant is not attenuated compared to the wild-type strain [178].

To test the total extracellular protease production of the ten *V. vulnificus* isolates in the current study, a protease assay using azocasein was used. This assay is a quantitative assay which measures a change in absorption using a spectrophotometer. In the assay, azocasein acts as a non-specific substrate for proteases, resulting in hydrolysis and release of the azo dye, causing a colour change that can be quantitatively measured. Figure 2.7 demonstrates the results gained for the azocasein protease assay. To allow for normalisation of growth in the assay, the corresponding growth OD was also calculated for each strain at each time point. For each sample a negative/background control was also performed, this comprised of media being added in place of the bacterial suspension. To normalise for growth and to remove the negative/background the following calculation was performed, (protease OD - negative)/growth OD.

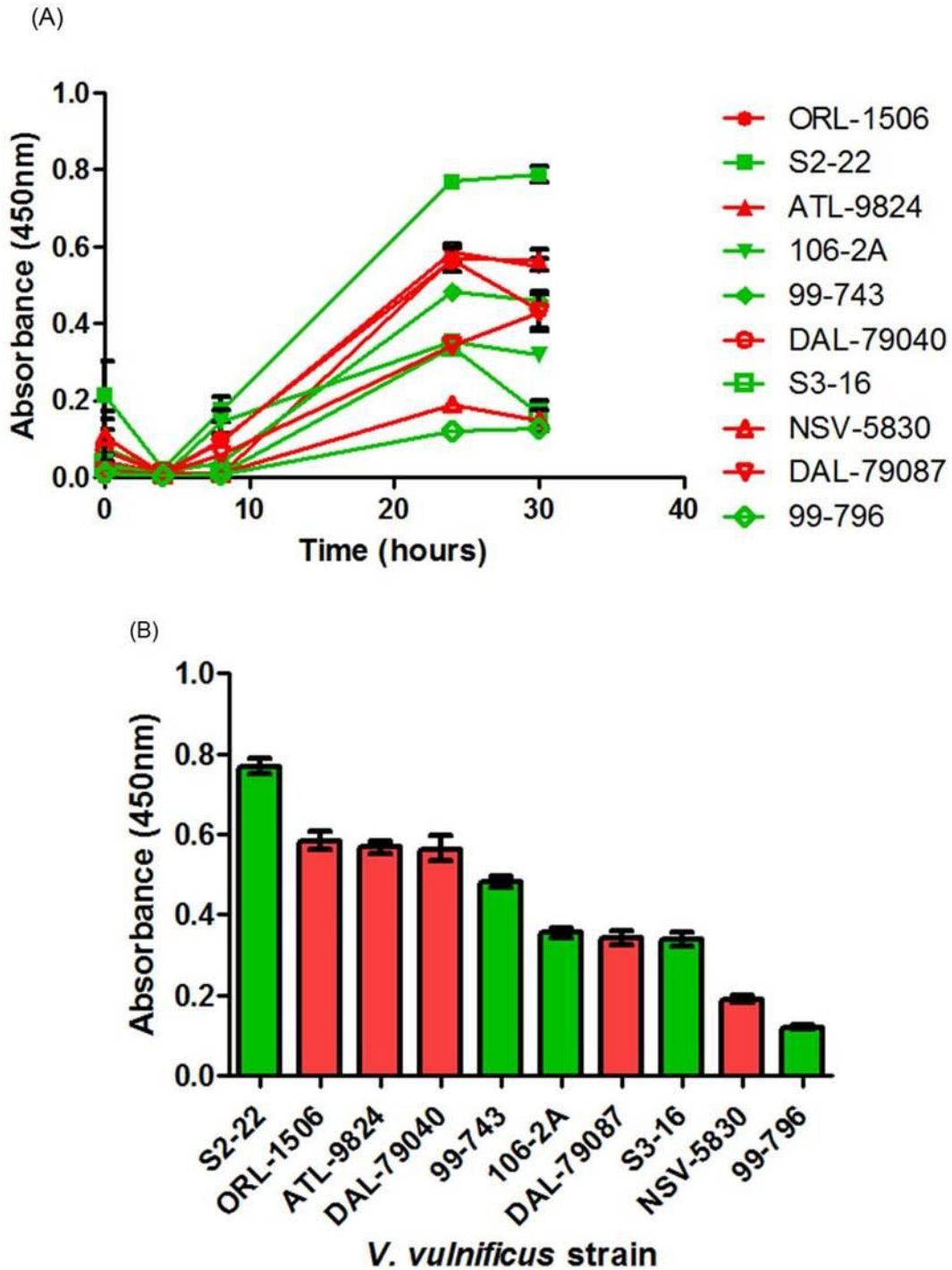


Figure 2.7: Total extracellular protease production from clinical and environmental *V. vulnificus* isolates.

(A) Protease production for ten *V. vulnificus* strains using a qualitative azocasein assay. Results show total protease production assayed at the time points, T0, T4, T8, T24 and T30 which have been normalised for growth and negative background removed. Clinical isolates are shown in red and environmental isolates are shown in green. Experiments were performed three times in triplicate. Error bars represent standard error of the mean. (B) Data extracted from graph (A) at T24, which corresponds to maximal protease production for all the strains. Clinical strains are shown in red and environmental strains shown in green. Error bars represent standard error of the mean.

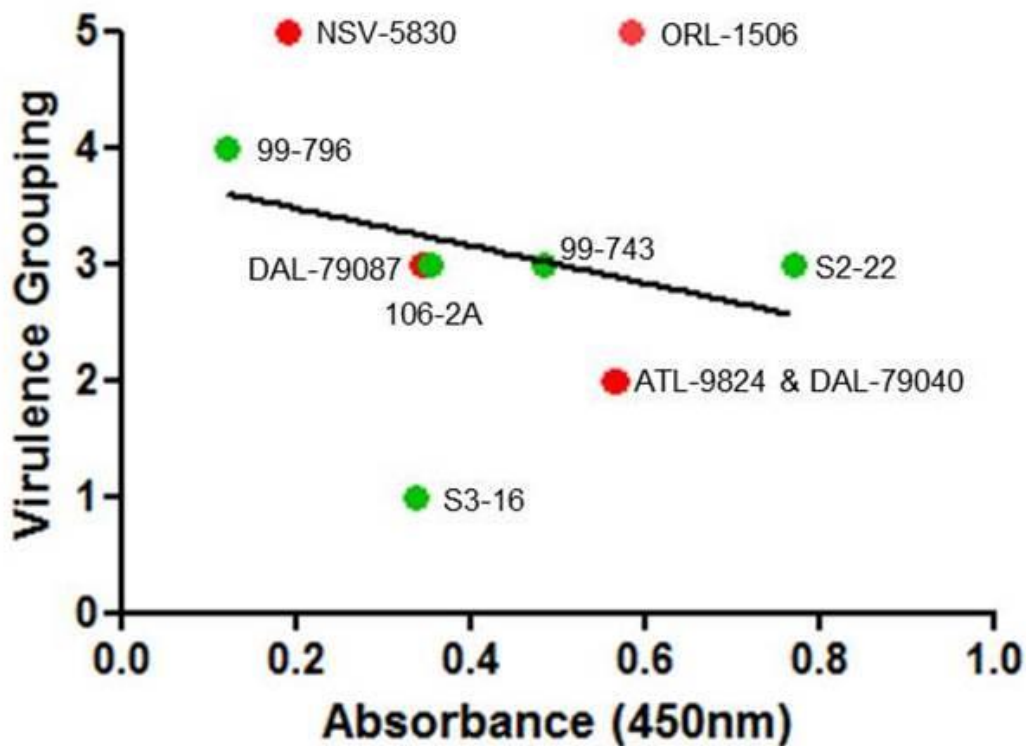


Figure 2.8: Scatter graph of total protease production for *V. vulnificus* strains versus virulence grouping: The graph shows total protease production at T30 for each *V. vulnificus* strain plotted against each strain's corresponding virulence grouping. The R-value calculated following a Pearson correlation is equal to -0.2475. Environmental strains are shown in green and clinical strains shown in red.

Although cells were washed three times at the beginning of the assay, the results show there is some residual protease activity still detected for the strains at T0. However, by the time the cells have reached T4 this has levelled off for all the strains. At T8, the cells begin to show a difference in protease activity, with the greatest difference seen between the strains at T24 and T30. Figure 2.6B represents data extracted from Figure 2.7A for the T24 hour time point. This time point was chosen as it shows maximal protease production for most of the strains.

The data in Figure 2.7B shows that there is no clear grouping of either clinical or environmental strains, which are shown in red and green respectively. Additionally, when this data is compared to the *in vivo* mouse data there is no clear clustering of hyper and lesser virulent strains. Statistical analysis using a one-way ANOVA followed by a post-hoc Tukey test on the results shown in Figure 2.7B showed that the strain ORL-1506, which is a group 5 hyper virulent strain, produces statistically significantly less protease than S2-22, which is a virulence group three strain, but

significantly more protease compared to the strains, 106-2A, 99-743, S3-16, NSV-5830, DAL-79087 and 99-796, where $P < 0.05$. The strains 106-2A, 99-743, S3-16, NSV-5830, DAL-79087 and 99-796 are grouped as virulence groups three, three, one, five, three and four respectively according to the published *in vivo* mouse virulence data, demonstrating that although ORL-1506 is a virulence group five strain, which produces statistically significantly more protease than some virulence group one, three and five strains, it doesn't produce statistically significantly more protease than some other lesser virulent strains, as shown with the example, S2-22 ($P < 0.05$). Additionally it cannot be said that lesser virulent strains produce more protease, as the least virulent group one strain, S3-16, produces significantly less protease than ORL-1506 ($P < 0.05$). Furthermore, the strain 99-796, which is a hyper virulent group four strain, produces significantly less protease compared to all of the strains tested, further indicating that hyper virulent strains do not always produce more protease than lesser virulent strains. In addition to presenting the total protease production, the graph shown in Figure 2.8 demonstrates that there is a very weak correlation of total protease production for the *V. vulnificus* strains when plotted against each strain's corresponding virulence grouping. A Pearson correlation performed on the graph in Figure 2.8 produces an R-value of -0.2475, further demonstrating that there is no significant correlation between a strain's virulence grouping and total protease production.

This data therefore suggests that protease production is not a clear indicator of hyper or lesser virulent *V. vulnificus* strains, and additionally protease production is not a clear indicator of source of isolation. This therefore suggests that there are other factors other than protease which are causing the difference in virulence between *V. vulnificus* strains.

2.2.5 Comparison of motility between clinical and environmental *V. vulnificus* isolates

Motility is an important virulence factor for *V. vulnificus*, as the bacterium must be able to move from the initial site of infection in order to cause the fulminating systemic disease symptoms often associated with this pathogen [13]. The motility of this bacterium is documented as being attributed to a single polar flagellum that allows the organism to be highly motile [141, 199, 200].

To assess the motility of the ten *V. vulnificus* isolates in the current study a motility assay which looked at the swimming ability of each organism was performed. 2 µl of mid-log phase cultures were inoculated into the centre of 0.3% motility agar plates and incubated statically for 24 hours at 37°C. The motility assay was performed three times in triplicate, to reduce error between replicates and ensure the protocol was standardised, For each assay motility agar was melted, cooled to ~50°C and 25 mL poured into each agar plate and allowed to dry in a laminar flow hood for 40 minutes prior to inoculation. Following 24 hour incubation of the inoculated plates, the diameter of the colony for each strain was measured and recorded. Figure 2.9 represents the data gained from the motility assay.

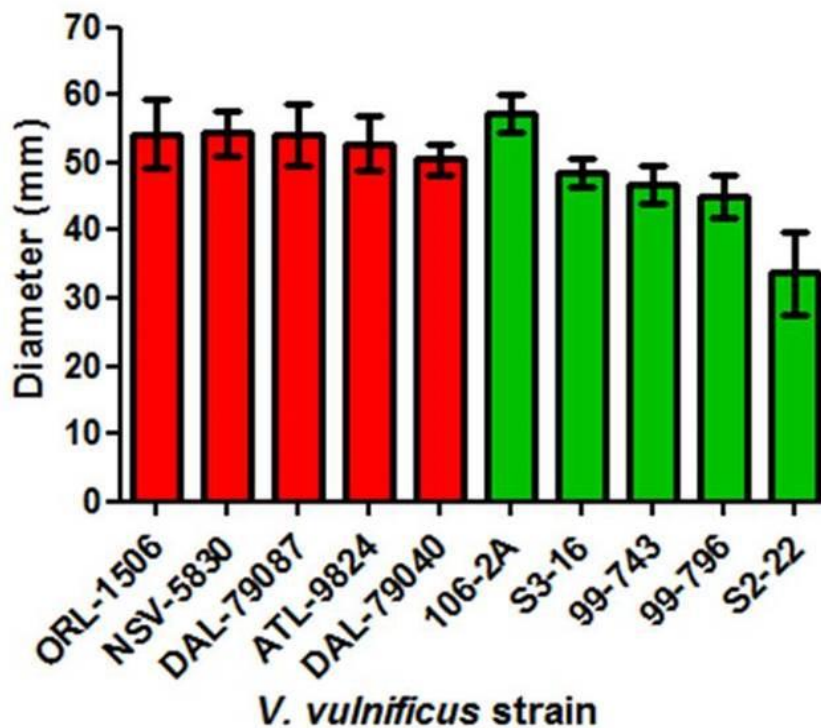


Figure 2.9: Motility of *V. vulnificus* clinical and environmental isolates. Swimming ability of ten *V. vulnificus* cells assayed using motility agar following 24 hour incubation at 37°C. Error bars represent standard error of the mean, experiments were performed at least three times in triplicate for each strain.

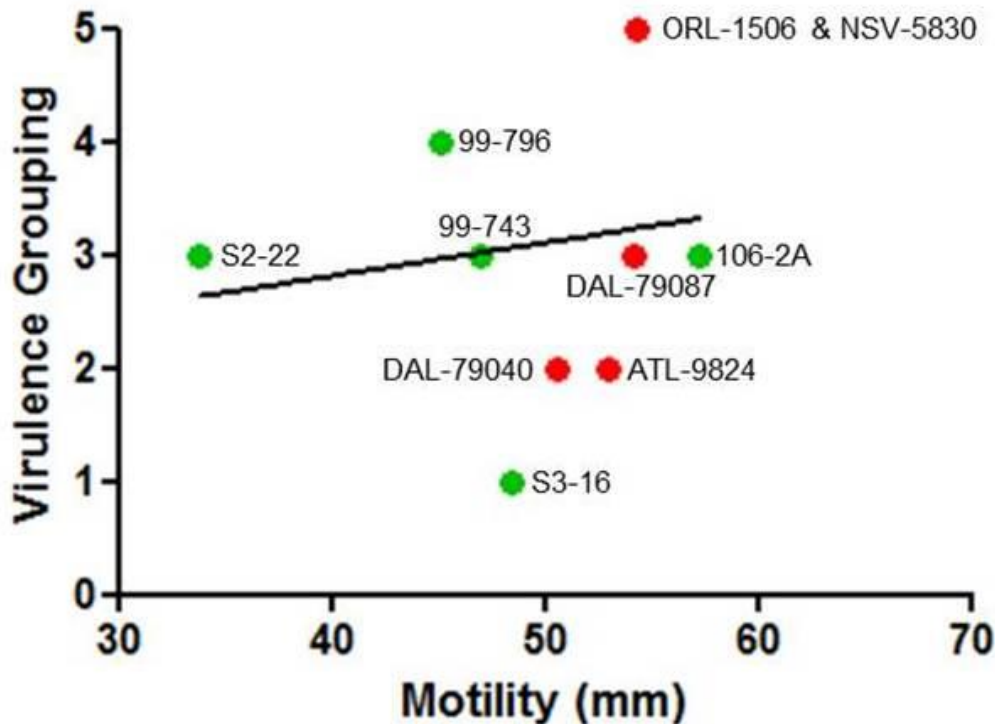


Figure 2.10: Motility of *V. vulnificus* isolates plotted against virulence groupings. The scatter graph shows the motility of clinical and environmental *V. vulnificus* strains plotted against each strain's corresponding virulence grouping. Clinical strains are shown in red and environmental strains shown in green. A Pearson analysis of the correlation between the two groups gives an R-value equal to 0.1547.

On initial inspection of the graph in Figure 2.9 it would appear that the clinical isolates are almost uniform in their motility ability. The environmental strains appear to have more variation between each other, with *V. vulnificus* 106-2A being as motile as the clinical strains, whereas *V. vulnificus* S2-22 is a lot more reduced in its motility. The general trend from the graph is that clinical isolates are more motile than the environmental isolates. However, there is one anomaly which is the environmental strain, 106-2A which is most motile of all the environmental isolates, and appears to be as motile as the clinical isolates. When applying a one-way ANOVA followed a post hoc Tukey test to compare each strain against each other, the results indicate that the clinical strains are not significantly more motile than the environmental strains. The only significant difference between the strains is that ORL-1506, NSV-5830, ATL-9824, DAL-79087 and 106-2A are significantly more motile than S2-22, ($P < 0.05$).

The data does however demonstrate that all of the *V. vulnificus* strains are motile. In comparison to the mouse virulence data the results shows that hyper virulent strains are not necessarily more motile than lesser virulent strains, as hyper virulent strains

are not always significantly more motile than the lesser virulent strains. For example, there is no significant difference between the hyper virulent strain, ORL-1506 and the least virulent strain, S3-16. Furthermore the scatter graph shown in Figure 2.10 demonstrates that there is a very weak positive correlation between motility and strain's virulence grouping, which when analysed using a Pearson correlation gives an R-value equal to 0.1547. This data would therefore suggest that there are other virulence factors, other than motility that play a role in infection.

2.2.6 LDH release from CaCo-2 cells infected with clinical and environmental *V. vulnificus* isolates

The aim of the cytotoxicity assay was to determine if clinical isolates were more cytotoxic than environmental isolates. The results would be used to see if there was a correlation between the LDH cytotoxicity assay and the *in vivo* mouse data on virulence. The hypothesis being that hyper virulent strains, would be more cytotoxic than the lesser virulent strains.

V. vulnificus has been reported in a number of literature articles to be cytotoxic towards *in vitro* cell culture lines [10, 155, 162, 199, 201]. The majority of reports use the following cell lines when investigating *V. vulnificus* cytotoxicity; HeLa cells which is a cell line that was originally established in 1951 from a cervical tumour biopsy [202], Hep-2 cell lines which are often used as a model for a human epithelial cell [203] and are thought to be derived from a larynx cancer [203], and finally the CaCo-2 cell line. The CaCo-2 cell line is often used as a model of the intestinal barrier which was originally isolated from a human colon adenocarcinoma [204]. Therefore the current study chose to assess cytotoxicity using CaCo-2 cells as they present a good model for *V. vulnificus* gastrointestinal infection.

Briefly, CaCo-2 Cells were routinely cultured in DMEM supplemented with 10% foetal calf serum. The CaCo-2 cells were cultured until 70% confluent, at which point cells were passaged into new media or seeded into wells and incubated overnight to allow cells to attach. Following overnight incubation, cells were infected with *V. vulnificus* cells at a MOI of 100 for six hours, as preliminary data indicated that a six hours infection period showed the greatest difference in LDH release between strains.

An initial experiment, shown in Figure 2.11A, comparing the clinical isolate, ORL-1506 and environmental isolate, S2-22, showed that the clinical strain was significantly more cytotoxic towards CaCo-2 cells than the environmental isolate, $P < 0.0001$, when analysed using an unpaired two-tailed student's t-test. The results from this initial experiment demonstrated that a hyper virulent clinical isolate (as denoted from the mouse virulence data), is more cytotoxicity than a lesser virulent environmental isolate.

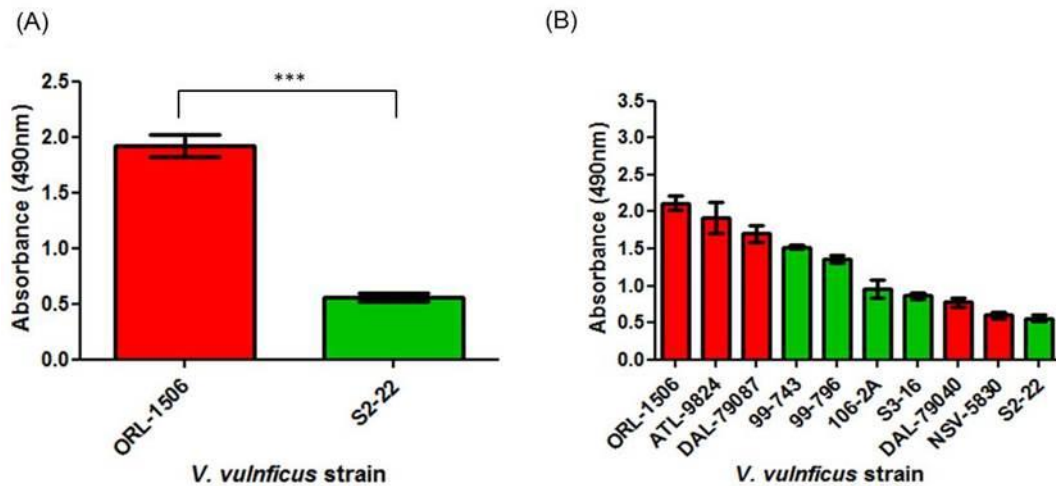


Figure 2.11: LDH cytotoxicity assay on *V. vulnificus* clinical and environmental isolates following incubation with CaCo-2 cells. LDH release from CaCo-2 cells infected with the hyper virulent clinical isolate, ORL-1506 shown in red and the lesser virulent environmental isolate, S2-22 at MOI of 100 for six hours. Experiments were performed three times in triplicate; error bars represent standard error of the mean. Statistical analysis performed using a two-tailed unpaired student's t-test, *** $P < 0.0001$. (B) LDH release from CaCo-2 cells infected with a panel of *V. vulnificus* isolates from clinical and environment isolation, shown in red and green respectively. CaCo-2 cells were infected with a MOI of 100 for six hours at 37°C. Experiments were repeated in at least three times in triplicate and statistical analysis performed using a one-way ANOVA followed by a post hoc Tukey test.

However, when analysing a larger panel of *V. vulnificus* strains, as shown in Figure 2.11B, the results do not follow the initial trend seen in Figure 2.8A. For example, although the 3 clinical strains, ORL-1506, ATL-9824 and DAL-79087 all cluster together as strains that are more cytotoxic towards the CaCo-2 cells, an additional 2 clinical strains, DAL-79040 and NSV-5830 appear less cytotoxic than the environmental strains, 99-743, 99-796 and 106-2A. When compared using a 1-way ANOVA followed by a post-hoc Tukey test, environmental strains, 99-743 and 99-796 are significantly more cytotoxic than the clinical strains, DAL-79040 and NSV-5830. This data demonstrates that clinical strains are not necessarily more cytotoxic than environmental strains, as the assay shows that environmental strains can also be significantly more cytotoxic than clinical strains.

When comparing the LDH assay data to the *in vivo* mouse virulence data, there is no correlation between the two studies. For example, although strain ORL-1506 is highly cytotoxic in the LDH assay, and was grouped as a virulence group five in the mouse study data, when comparing ORL-1506 to NSV-5830, also a virulence group five strain NSV-5830 appears significantly less cytotoxic than ORL-1506 in the LDH assay, $P < 0.0001$, (analysis based on an unpaired two-tailed student's t-test). Additionally NSV-5830, produces low levels of cytotoxicity when compared with the all of the strains tested. Only strain S2-22 produced levels of LDH release lower, but these were not significantly different to strain NSV-5830. In the mouse virulence study, strain S2-22 is grouped as a virulence group three strain and NSV-5830 is grouped as a hyper virulent group five strain. Therefore, as S2-22 is not significantly less cytotoxic than NSV-5830, the results would suggest that the LDH assay is not an assay that can be reliably used to predict virulence. Additionally DAL-79087 also a virulence group three strain, produces significantly more LDH release than NSV-5830, $P < 0.0001$ when compared using an unpaired two-tailed student's t-test. Furthermore as shown in Figure 2.12, when the LDH absorbancy readings for each strain is plotted against each strain's representative virulence group, the data shows there is no strong correlation between LDH release and virulence grouping of a strain. When using a Pearson correlation is applied to the data in Figure 2.12, the data demonstrates a very weak correlation with an R-value equal to 0.2454.

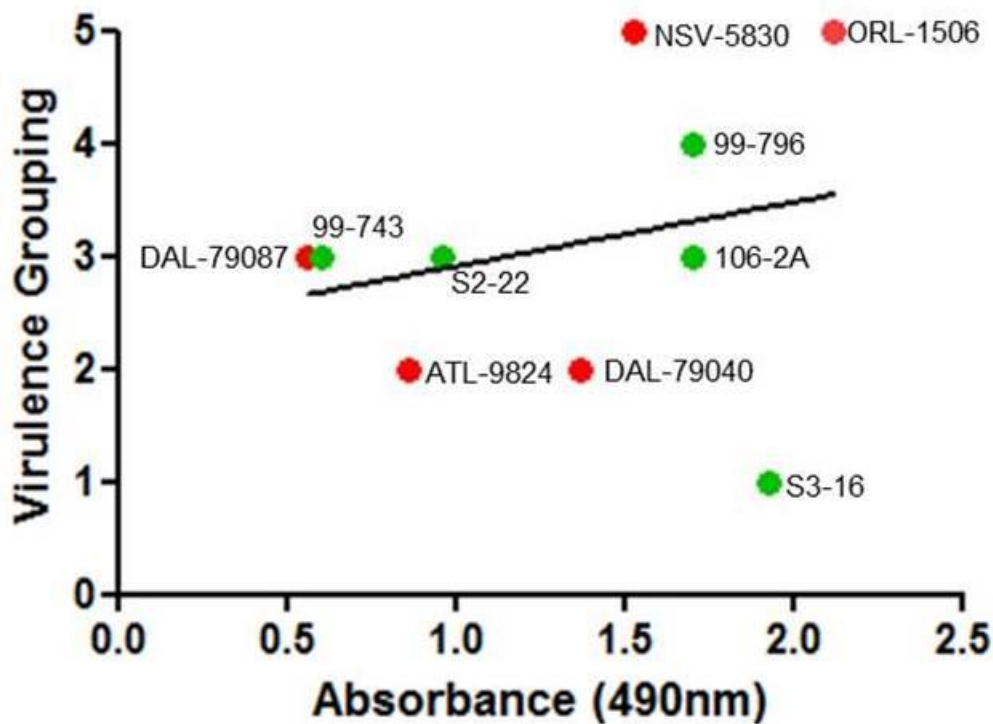


Figure 2.12: LDH release plotted against virulence grouping of each *V. vulnificus* strain. The scatter graph shows LDH absorbance plotted against each strain's corresponding virulence grouping. Environmental strains are shown in green and clinical strains shown in red. A Pearson correlation gives an R-value of 0.2454.

Therefore the data in Figure 2.11B suggests that although preliminary data (Figure 2.11A) identified a clinical strain that was more cytotoxic than an environmental strain, when looking at a larger panel of strains, the trend does not hold true. Furthermore, the cytotoxicity assay is not able to mirror the mouse virulence data in terms of grouping hyper and lesser virulent strains; as the hyper virulent group five strains do not always produce significantly more LDH release from CaCo-2 cells.

2.3 Discussion

The initial aim of these phenotypic assays was to better understand the panel of ten *V. vulnificus* strains in terms of virulence. This was achieved by performing several phenotypic assays focusing on virulence factors that had previously been identified in *V. vulnificus*. The phenotypic assays employed assessed the growth characteristics, capsule, protease production, motility and cytotoxicity of each strain. Initially, the phenotypic data was used to determine whether source of isolation could predict the virulence potential of a strain. As it was hypothesised that clinical isolates maybe more virulent than the environmental isolates, as clinical isolates have

previously been passaged through a human host and therefore may be preselected as being more virulent. Analysis of the phenotypic data however indicated that source of isolation does not equate to virulence potential of a strain. This is in agreement with published data which reported that source of isolation is not an indicator of virulence for *V. vulnificus* strains [13]. Comparison of the phenotypic assay results with the published *in vivo* mouse virulence data demonstrated that none of the phenotypic assays were able to accurately mirror the results seen in the mouse virulence data. For example, hyper virulent strains in the mouse model did not necessarily equate to being more cytotoxic in an *in vitro* tissue culture model.

The current study investigated growth characteristics of *V. vulnificus* strains as it was also hypothesised, that the ability of *V. vulnificus* to cause a rapid and fulminating disease, may be due to difference in growth characteristics between strains. The growth data however disproved this hypothesis. For example, comparison of the strains source of isolation with growth ODs, demonstrated that not all of the clinical strains produced a higher OD reading compared to the environmental strains and vice versa. Furthermore, when the growth curve data is compared with the *in vivo* mouse virulence data, it appears that growth characteristics do not necessarily equate with *V. vulnificus*'s virulence potential. For example, the strain ORL-1506 which is a hyper virulent group five strain does not produce a significantly greater OD reading than S3-16, which is a lesser virulent group one strain. Therefore it can be concluded for this data that growth characteristics are unable to predict the virulence potential of a strain.

Following on from growth characteristics, the study investigated the presence of the capsule on the ten *V. vulnificus* strains. This was carried out as capsule has been shown to be an important virulence factor for pathogenic bacteria, including *V. vulnificus* [120-123, 192]. A classic example of capsule as an essential virulence determinant is in *Burkholderia mallei* [205] and *Streptococcus pneumoniae*, with the latter expressing phase variable capsule production which produces two differing colony morphologies [206]. Similarly it has been reported in the literature that *V. vulnificus* strains are able to produce two types of colony morphology, opaque and translucent which corresponds to encapsulated and non-encapsulated strains respectively [120, 121, 207]. The bacterium is also reported to produce an

intermediate colony morphology which is strains expressing capsule, although at lower levels than opaque strains [123, 193].

To determine if the *V. vulnificus* strains in the current study were encapsulated or non-encapsulated, two methods were employed. The first was by colony morphology and the second method was through the use of India ink staining to image the capsule by using light microscopy. The results from both sets of data indicated that the ten strains of *V. vulnificus* in the current study are all encapsulated.

A possible explanation for the *V. vulnificus* strains in the current study not producing a mixture of opaque and translucent colonies as reported for other *V. vulnificus* strains in the literature [123, 193, 195] could be that the original colonies received by our laboratory were encapsulated and therefore preselected for capsule production. An alternative explanation may be due to the difference in methods used between laboratories, in particular the culture conditions used. In one study that identified three differing *V. vulnificus* colony morphologies, encapsulated, non-encapsulated and intermediate, cells were routinely cultured in HI-broth at 22°C [123]. Additionally, another study often cultured cells at temperatures lower than 37°C [195], or involved temperature shifts to induce the differing colony morphologies [194]. However, the culture conditions used in the current study, were LB broth supplemented with 2% NaCl, or LB-agar supplemented with 2% NaCl, and incubated at 37°C overnight. Therefore the culture conditions used in the current study maybe more supportive of the encapsulated phenotype rather than the non-encapsulated phenotype, which is more apparent at lower temperatures.

The results also showed there was no difference seen between the clinical and environmental strains, in terms of presence or absence of capsule, as all strains from both isolation source produced capsule. This is similar to other observations seen in the literature where capsule production is observed for both clinical and environmental isolates [21, 124]. When the capsule data from this study is compared to the virulence grouping of *V. vulnificus* in the iron-dextran treated mouse model [13], it shows that both hyper virulent strains and lesser virulent strains contain a capsule. This data would therefore suggest that there are other virulence factors causing the difference in virulence potential seen between *V. vulnificus* isolates, and virulence potential is not attributed to capsule alone.

As neither capsule nor growth characteristics were able to identify strains based on virulence potential or source of isolation, the study investigated whether protease production was able to distinguish strains according to virulence potential or source of isolation. As previous research in *P. aeruginosa* has demonstrated that strains unable to produce protease are generally less virulent [208]. Furthermore, it has been shown that both *Bacillus anthracis* [209] and *Clostridium botulinum* produce pathogenic proteases during human infection [210]. The results from this study however, demonstrated that protease production by *V. vulnificus* is not a marker for virulence potential or source of isolation of a strain; as although all of the ten strains were able to produce protease, there was no clear trend between clinical and environmental strains or hyper and lesser virulent strains. This conclusion is unsurprising as the role of protease during *V. vulnificus* infection has not been completely elucidated. For example, it was initially reported that the protease, VvpE produced by *V. vulnificus* was a virulence factor, as when the purified protease was injected into mice, it caused the disease symptoms associated with *V. vulnificus* infection [176, 198]. However, several years later it was shown that a *vvpE* mutant was not attenuated *in vivo* [178]. Whether there are other virulence factors that are able to compensate for the loss of VvpE, allowing the bacterium to cause disease symptoms associated with *V. vulnificus* remains to be identified, as does the exact role of VvpE in *V. vulnificus* pathogenicity. Therefore, the finding that total protease production is unable to predict virulence or source of isolation of a strain is unsurprising.

V. vulnificus motility was also assayed as it was hypothesised that the pathogen's ability to cause a systemic disease may be due to motility, with hyper virulent or clinical strains being more motile than the lesser virulent environmental isolates. Furthermore, early *V. cholerae* studies demonstrated that non-motile *V. cholerae* strains were defective in intestinal colonisation compared to motile strains [211, 212]. To test the motility hypothesis, the strains were assayed using 0.3% motility agar. All of the ten strains tested were motile and able to swim across the agar plate. This was an expected result as *V. vulnificus* is documented as being a highly motile bacterium due to the single polar flagellum [199]. Initial motility results appeared promising with a general trend that clinical isolates were more motile than environmental isolates. However, when statistical analysis was performed, the

results indicated that not all clinical isolates were more motile than environmental isolates. Further comparison of the results with the mouse virulence data demonstrated that there was no correlation between virulence potential and motility. Motility, like capsule, is a virulence factor as demonstrated in mutagenesis studies for *V. vulnificus* [141, 199]. However, it would appear from the results in the current study, that motility on its own is not a marker for strains hazardous to human health, as both hyper and lesser virulent *V. vulnificus* strains are motile, with no statistically significant pattern between hyper and lesser virulent strains and motility. These findings are similar to a study performed on *Bacillus cereus*, which found that motility was not an exclusive marker for distinguishing between virulent and non-virulent strains [213]

The final phenotypic assay to be tested was a cytotoxicity assay using CaCo-2 cells. Cytotoxicity was assessed using an LDH assay which measured the amount of LDH released from the CaCo-2 cells. The amount of LDH released is quantified using a colour change and the LDH released is directly proportional to the number of CaCo-2 cells lysed. Preliminary data from the LDH cytotoxicity assay suggested that there was a correlation between LDH release, and source of isolation, as well as LDH release and virulence potential. For example, the clinical hyper virulent strain, ORL-1506, produced statistically significantly greater LDH release from CaCo-2 cells than S2-22, an environmental lesser virulent strain. However, when a more comprehensive panel of strains was analysed, the results did not follow the same pattern.

In terms of source of isolation, clinical strains did not consistently produce higher absorbancy readings than the environmental strains. This was expected as previous *in vivo* virulence data has shown that source of isolation does not necessarily correlate with the virulence potential [13]. Furthermore, when the LDH assay absorbancy readings were compared with the *in vivo* mouse virulence data, there was no similarity between the virulence study and the current study. For example, hyper virulent strains did not consistently produce more LDH release than the lesser virulent strains. One drawback of comparing the cytotoxicity study with the *in vivo* mouse data, may be that the CaCo-2 cells are a model for intestinal physiology,

whereas the mouse data is based on a wound infection model. This may provide a possible explanation as why there is no similarity between the two studies.

2.4 Conclusion

Analysis of all the phenotypic assays performed in the current study, demonstrated that the testing of just one virulence factor is unable to accurately distinguish between hyper and lesser virulent *V. vulnificus* strains. Furthermore, scatter graphs which plotted the phenotypic data against the virulence groupings of each strain and were analysed using a Pearson correlation demonstrated that the correlations seen between the phenotypic studies and the virulence data available for each strain were very weak. Virulence of a strain was determined based on published results from an *in vivo* virulence model [13]. Furthermore, it was also shown that source of isolation is not an accurate predictor of a strain's virulence potential. For example, clinical isolates are not necessarily more cytotoxic than environmental isolates.

Although previous research has identified numerous virulence factors in *V. vulnificus*, currently not one virulence factor is able to accurately distinguish a hyper virulent strain from a lesser virulent strain. In addition to this, several research groups have compared the genomes of several *V. vulnificus* strains bioinformatically to identify differences in strains and potential virulence markers [214, 215]. Although the comparative genomics research has led to lists of comparative virulence genes being established, the work has not been followed up with laboratory assays to phenotypically characterise the difference between the strains.

Furthermore, the results from the current study's phenotypic assays, which assessed *V. vulnificus* strains for known virulence factors; demonstrated that not one virulence factor could be used to distinguish hyper virulent strains from lesser virulent strains. This demonstrated the need for novel virulence factors to be identified in *V. vulnificus* strains. Therefore the current study postulated that there was a need for a whole genome sequencing (WGS) comparison study to identify novel genetic differences between hyper and lesser virulent strains, which could ultimately be used to distinguish between strains that are hazardous to human health from those that are not. The study aimed in particular to identify differences in genetic regions between the strains, to try and understand the difference in virulence potential between *V. vulnificus* strains. In order to acknowledge this gap in *V. vulnificus* knowledge, it

seemed plausible to perform WGS analysis on the 10 *V. vulnificus* strains with the aim of identifying novel genetic differences.

Chapter 3 Bioinformatic analysis of *V. vulnificus* strains

3.1 Introduction and aim

WGS of a bacterial genome was first carried out in 2005 using Sanger Sequencing [216]. Since then the cost of carrying out WGS has decreased significantly, allowing many research laboratories to carry out WGS of bacterial strains. The use of WGS has led to an eruption in the number of bacterial genomes sequenced, there are currently >6,500 bacterial genomes available on Genbank, with several genomes still in contig formats [217]. Bacterial WGS data has many uses, which can include, mapping of virulence factors, antibiotic resistance surveillance, infection control and drug development [218-220]. Illumina, Ion Torrent, Roche 454 and SOLiD, are several examples of next-generation sequencing (NGS) instruments that can be used to generate WGS data.

The current study used Illumina sequencing to sequence the genomes of the ten *V. vulnificus* isolates described in chapter two. This was done with the aim of identifying genetic differences between the strains, which may account for the difference in virulence between the strains.

3.2 Results

3.2.1 Preparation and sequencing of genomic DNA (gDNA)

Illumina sequencing was carried out on the following *V. vulnificus* strains, ORL-1506, 99-796, 99-743, DAL-79087 and DAL-79040, by Exeter Sequencing Service, University of Exeter, using 250bp paired end reads on the Illumina MiSeq. The sequencing data for the remaining five *V. vulnificus* strains, S2-22, S3-16, 106-2A, ATL-9824 and NSV-5830 was supplied by CEFAS.

Genomic DNA (gDNA) was extracted from *V. vulnificus* isolates using the Promega Wizard® Genomic DNA Purification Kit according to the manufacturer's instructions. In brief two to three colonies of each bacterial strain were picked from an overnight streak plate, sub-cultured into 2% NaCl LB broth and incubated overnight at 37°C at 200rpm. The following morning a 1 mL sample was taken from the overnight culture and gDNA extracted. Once the gDNA had been extracted, a 3 µl sample was electrophoresed through a 1% agarose gel to check the gDNA quality. Quality was checked by ensuring the sample produced a high molecular weight band with no fragmentation. The gDNA sample was then sent to Exeter Sequencing Service

where the necessary library preparation of the sample was carried out, including quantification of DNA using Qubit® Fluorometric Quantitation.

3.2.2 Assembly of *V. vulnificus* raw sequencing reads

The assembly of the raw sequencing data was achieved by using the *de novo* automated assembler, a5 [221]. The a5 pipeline does not require a reference genome to assemble sequencing reads, instead overlapping sequencing reads are built into contiguous reads (contigs), which are then further assembled into scaffolds [221]. The a5 pipeline builds scaffolds using the following five stages, stage one, low quality reads and adapter sequences are removed from the data, stage two, contigs are built using a de Bruijn graph based algorithm, stage three, the contigs are then scaffolded and extended, stage four, the unmapped reads are mapped back to the assembled scaffolds, the miss-assembled reads are detected and broken, finally stage five, broken scaffolds are re-scaffolded. Once the raw sequencing reads had been assembled, the assembly was reviewed using the contigstat programme, which produces statistical data on raw sequencing read assemblies. The data presented in Table 3.1 shows the statistical analysis on the a5 assemblies using the contigstat programme, data presented includes data on the number of scaffolds and the length of the longest scaffold. Once the WGS data had been assembled, scaffolds were then used for downstream analysis such as gene annotation, phylogenetic tree construction and genotyping of strains.

Table 3.1: Statistics on assembly of raw sequencing reads using a5 pipeline. The table shows the basic statistics calculated for the a5 assembly of each bacterial strain. L50 is the length of the smallest scaffold which is equal to or greater than the 50% value. The 50% value is calculated by ordering in the scaffolds, in length from smallest to largest and the length totalled divided by two.

Bacterial Strain	Number of scaffolds	Total length of scaffolds (bps)	Length of longest scaffold (bps)	L50 (bps)
<i>V. vulnificus</i> DAL-79040	46	4,866,902	1,310,740	553,895
<i>V. vulnificus</i> DAL-79087	99	4,891,124	371,595	171,786
<i>V. vulnificus</i> 99-743	81	4,874,281	777,312	204,495
<i>V. vulnificus</i> 99-796	124	4,953,985	541,160	162,757
<i>V. vulnificus</i> S3-16	80	4,982,280	841,250	219,189
<i>V. vulnificus</i> S2-22	81	4,905,980	810,776	202,306
<i>V. vulnificus</i> NSV-5830	105	4,888,328	631,804	274,590
<i>V. vulnificus</i> ATL-9824	77	4,921,179	1,114,370	297,891
<i>V. vulnificus</i> ORL-1506	74	4,866,455	892,373	829,112
<i>V. vulnificus</i> 106-2A	97	4,971,929	1,090,137	223,665
<i>V. vulnificus</i> 106-2A $\Delta icmF$ T6SS1	97	4,956,646	642,096	143,161
<i>V. vulnificus</i> 106-2A $\Delta icmF$ T6SS2	52	4,766,254	606,991	280,075
<i>V. fluvialis</i> NCTC 11327	53	4,947,586	873,156	378,052

3.2.3 Bioinformatic genotyping of *V. vulnificus* strains

As mentioned in chapter one, *V. vulnificus* strains can be sub-categorised based on genotype, one such protocol is the *vcg* typing method [30]. This method is based on the finding that clinical strains contained a region of DNA ~200bp in length, that is generally, but not always, absent from environmental isolates [21]. To further characterise this ~200bp region, surrounding DNA of approximately 700bp was amplified [30]. Following DNA alignment against a reference genome, the authors found that this ~700bp region corresponded to the 3' end of the VV0401 gene, as well as downstream non-coding sequence. From this alignment, typing primers P1, P2 and P3 were designed to distinguish between C and E genotypes [30]. PCRs employing the primers P1 and P3 amplify a region indicative of C-genotypes, commonly associated with clinical isolates. Conversely, primers P2 and P3 amplify a region common to most environmental strains, E-genotypes. This specificity is due to a difference of sequence at the binding region of P1 and P2, which is shown in Figure 3.1.

```
VV JY1306 vcgE      1 ctcaattgacaatgatctcatcactgctatccaaagta
VV YJ016  vcgC      1 agctgccgatagcgatctcgtctccgcgatacaaaaata
```

Figure 3.1. Primer binding sites of *vcg* genotyping primers, P1 and P2. *V. vulnificus* C and E-genotypes can be distinguished using PCR, this method is based on the differences in the primer binding sites of the primers P1 and P2. The primer binding site of P2 is boxed in green and binds to E-genotype strains, which is distinguishable from C-genotype strains that bind primer P1, shown boxed in red. The differences in the DNA base sequence between the C and E-genotypes are also highlighted in red, further demonstrating the difference in DNA sequence between the C and E-genotypes.

Using this information, the current study used a local BLAST search to identify the scaffolds on which the VV0401 gene was located for all of the 10 strains. The scaffolds were then used to generate *in silico* PCRs with the primers P1 and P3, or P2 and P3. Figure 3.2 shows the alignment of the primer binding sites for each of the strains investigated. In addition, each strain's information, in terms of isolation source, virulence potential and *vcg*-type is also tabulated in Table 3.2. Out of the ten strains analysed, the following three strains were omitted, ORL-1506, NSV-5830 and ATL-9824. ORL-1506 and NSV-5830 were omitted as the sequence alignment of these strains was too diverse and did not produce accurate alignments, on the other

hand, the strain ATL-9824 failed to produce a PCR product due to the inability of the P3 primer to bind *in silico*.



Figure 3.2 Sequence alignment of the vcg primer binding sites. Shown in the top half of the image is the sequence alignment for the C-genotype strains, boxed in red is the P1 primer binding site for the reference strain, YJ016. In comparison the E-genotype strain, JY1306 is also shown, highlighted in red are the base pair changes, indicating the difference in DNA sequence between the E-genotype and C-genotype strains. Conversely the E-genotypes are shown in the bottom half of the image. Boxed in green is the P2 site for the reference strain, JY1306. In comparison the YJ016, C-genotype reference strain is also shown. The red bases indicate the difference in base pairs between the C and E-genotype strains. In both images the universal reverse primer P3 is also shown, boxed in blue.

Table 3.2: *V. vulnificus* strain information. The table shows each strain's isolation source, vcg type and virulence grouping according to the published virulence mouse data for each strain. Strains, ORL-1506, NSV-5830 and ATL-9824 were unable to be typed *in silico*.

Strain	Isolation source	vcg type	Virulence group
ORL-1506	Clinical	Unable to type	5
NSV-5830	Clinical	Unable to type	5
99-796	Environmental	C-type	4
106-2A	Environmental	C-type	3
S2-22	Environmental	C-type	3
99-743	Environmental	E-type	3
DAL-79087	Clinical	E-type	3
DAL-79040	Clinical	C-type	2
ATL-9824	Clinical	Unable to type	2
S3-16	Environmental	C-type	1

The binding site of the C-genotype primer, P1 is boxed in red in Figure 3.2. This primer bound to the strains S3-16, S2-22, DAL-79040, 106-2A and 99-796, indicating that these strains are of C-genotype. Conversely, the E-genotype primer, P2 is boxed in green, this primer bound to the strains 99-743 and DAL-79087, identifying

these strains as E-genotype. Although the *vcg* typing method was established to distinguish between strains based on isolation source and provide an indicator of virulence potential [30], the data presented here demonstrates that this method is unable to accurately identify strains based on isolation source or virulence potential. For example, as demonstrated in Table 3.2, strain S3-16 is an environmental strain, yet this is grouped as a C-genotype, furthermore according to the virulence data [13], this strain is a lesser virulent group one strain, demonstrating that the *vcg* genotyping method is unable to accurately predict source of isolation or virulence potential of a strain.

Following on from genotypic characterisation of strains, the bioinformatic data was used to construct phylogenetic trees for the ten *V. vulnificus* strains. This was done to identify if phylogenetic analysis could distinguish strains based on isolation source or virulence potential.

3.2.4 Phylogenetic tree construction for *V. vulnificus* strains from clinical and environmental origin

Phylogenetic trees are often used to study the genetic evolution of organisms. With the advent of WGS producing large amounts of data, generating phylogenetic trees based on single nucleotide polymorphisms (SNPs) has become increasingly popular [222-224]. SNPs are a change in a single nucleotide position in a DNA sequence [92] and are often associated with low mutation rates and evolutionary stability, making them good candidates for studying the evolution of organisms [224]. Studies looking at *Escherichia coli* outbreaks in Europe and antibiotic resistance in *Staphylococcus aureus* are a couple of examples of where SNP analysis has been used for evolutionary analysis [219, 225]. SNP analysis has also recently been used to understand the evolution of the *V. vulnificus* biotype 3 sub-species [226]. Therefore the current study aimed at using SNP analysis to construct phylogenetic trees of *V. vulnificus* biotype 1 strains, with the aim of identifying clusters of strains based on either virulence or source of isolation. Phylogenetic trees were constructed based on SNP profiles, using the pipeline, SNPhylo [223].

In order for the programme SNPhylo to generate phylogenetic trees, the data must be inputted into the pipeline in Variant Call Format (VCF). To achieve this the raw sequencing reads were first trimmed against the reference genome, YJ016 using

“Trim Galore!” listed in the Materials and Methods. Following trimming of adapter sequences using Trim Galore! the reads were converted from SAM to BAM and finally into vcf format, the data was then uploaded to SNPhylo [223], which constructed phylogenetic trees for the ten strains. The assembled trees are shown in Figures 3.3, 3.4 and 3.5. The SNP analysis was carried out on data from chromosome 1 and 2 separately as well as both chromosomes combined. This was done to identify if strains clustered differently depending on the chromosome analysed. Figure 3.3 shows the phylogenetic tree constructed when both chromosomes are combined, whereas Figure 3.4 and 3.5 show the phylogenetic trees constructed when SNPs from either chromosome 1 or chromosome 2 are analysed separately. The length of the branches on the trees corresponds to the amount of change between strains. For example, the longer the branch the larger the amount of difference, the number at the bottom of the figures shows the scale of this change.

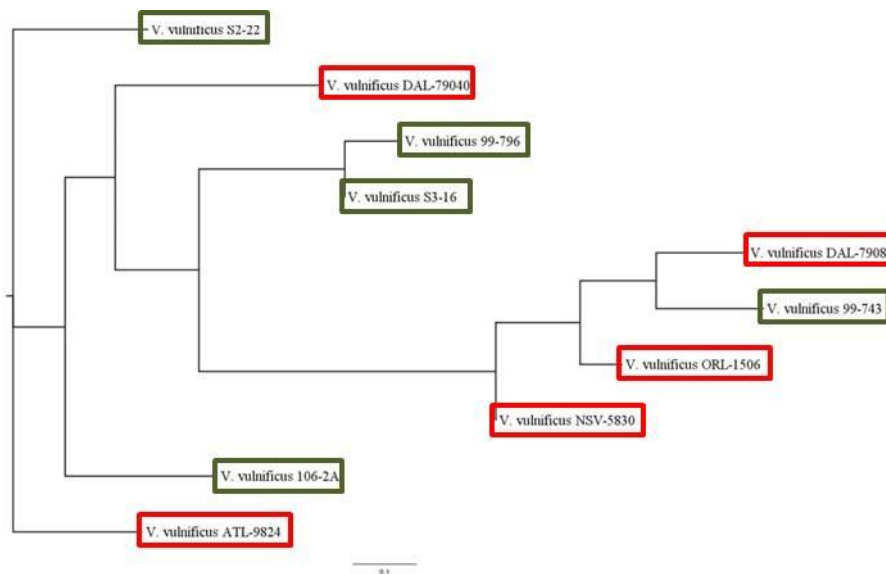


Figure 3.3: Phylogenetic tree constructed from chromosomes one and two for *V. vulnificus*.

The phylogenetic tree constructed when analysing SNPs from chromosomes one and two using SNPhylo. Five clusters are generated for the ten *V. vulnificus* strains analysed, the clusters include strains with varying degrees of virulence potentials, with clinical and environmental isolates, shown in red and green respectively interspersed throughout the clusters. The length of the branches on the trees corresponds to the amount of change, for example the longer the bar the larger the amount of difference between the strains.

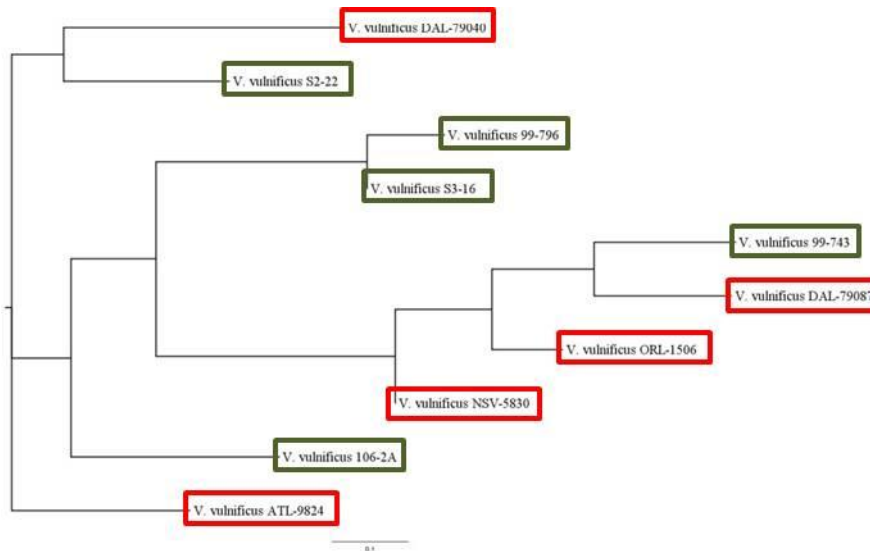


Figure 3.4: Chromosome one constructed phylogenetic tree. SNP analysis of chromosome one for ten *V. vulnificus* strains shows there is no clustering of either clinical or environmental strains, which are shown boxed in red and green respectively. The SNP analysis of chromosome one also shows there is no clustering of hyper and lesser virulent strains. The scale bar shown at the bottom of the images corresponds to the scale of change, which is 0.1.

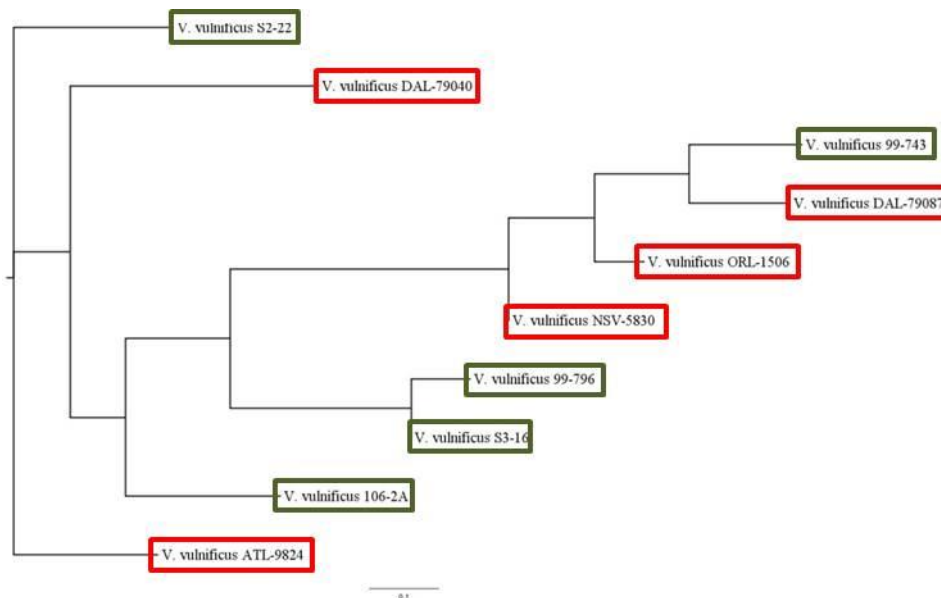


Figure 3.5: Phylogenetic tree constructed based on SNP analysis for chromosome two. Analysis of SNPs in chromosome two for ten *V. vulnificus* strains using SNPhylo demonstrated that there is no clear clustering of either clinical or environmental strains, which are shown in red and green respectively, as both isolates are interspersed through the tree demonstrating that there is no clear clustering of either clinical or environmental strains. Additionally there is also no clear clustering of either hyper or lesser virulent strains, which are also interspersed throughout the tree. Shown at the bottom of the image is the scale bar, which shows the amount of change between each strain.

Comparison of the phylogenetic trees presented in Figures 3.3, 3.4 and 3.5 demonstrates that the SNP analysis produces different results depending on the chromosomes being analysed, in addition to the differences there are also similarities. For example, all of the phylogenetic trees shown produce five groupings

of the strains, however the strains that make up these five groupings differ. Figure 3.3, which illustrates the phylogenetic tree produced when both chromosomes are analysed, shows that the strains split into the following five groups; strains S2-22, ATL-9824 and 106-2A appear as three separate out-groups, whereas DAL-79040, 99-796 and S3-16 make up group four, with DAL-79087, 99-743, NSV-5830 and ORL-1506 making up group five. Analysis of the phylogenetic tree produced for chromosome one in Figure 3.4 suggests that S2-22 is not an out-group as seen in Figure 3.3 and instead clusters with the strain, DAL-79040 in a single clade sharing a common ancestor, making up group one. However, the strain ATL-9824 consistently appears as an out-group, making up group two. Group three is made up of the two strains, S3-16 and 99-796. The largest group, group four is made up of 99-743, DAL-79087, ORL-1506 and NSV-5830. Finally, the strain 106-2A does not appear to cluster with any other strains and appears as an outgroup making the final group, group five. Finally Figure 3.5 which represents the phylogenetic tree constructed for chromosome two, shows the following 5 groups; groups one to four are constructed from the following four outgroup strains, S2-22, DAL-79040, 106-2A and ATL-9824, the remaining strains make up the final fifth group, 99-743, DAL-79087, ORL-1506, NSV-5830, 99-796 and S3-16.

All three phylogenetic analyses produce similar groupings of strains, except for the following strains, S2-22, DAL-79040, S3-16 and 99-796 which are changeable depending on the tree that is analysed. The strain S2-22 appears as an outgroup in Figures 3.3 and 3.5, however in Figure 3.4, the chromosome one analysis, the position of strain S2-22 changes. Instead of appearing as an out-group, it now clusters with DAL-79040. A possible explanation for the changeable position of strain S2-22 maybe due to the chromosome two of DAL-79040 and S2-22 being more divergent, hence why the two strains cluster separately when chromosome two is analysed, but not when chromosome one is analysed. Conversely, S3-16 and 99-796 appear to have a more divergent chromosome one than the strains NSV-5830, ORL-1506, DAL-79087 and 99-743, as when chromosome one, shown in Figure 3.4, is analysed, S3-16 and 99-796 cluster in a group of their own, separate from the strains, NSV-5830, ORL-1506, DAL-79087 and 99-743. However, when chromosome two is analysed S3-16 and 99-796 cluster with the strains NSV-5830,

ORL-1506, DAL-79087 and 99-743, suggesting that the strains are similar in regards to chromosome two, but more divergent with regards to chromosome one.

When comparing the phylogenetic results to the strains' source of isolation, there is no clear clustering of either clinical strains or environmental strains. For example the clinical isolate, ORL-1506 clusters with environmental isolate, 99-743 in each tree analysed. These results are not too dissimilar to the results gained by another research group which demonstrated that *V. vulnificus* strains from both clinical and environmental origin were interspersed throughout a constructed phylogenetic tree, with no cluster being made up of all clinical or all environmental isolates [55]. Comparison of the current study's phylogenetic tree data with the available *in vivo* virulence data [13], indicates that there is no clear clustering of hyper and lesser virulent strains. For example, the virulence group one strain, S3-16 consistently groups with 99-796, a virulence group four strain. Additionally DAL-79087 which is a virulence group three strain is found in a cluster with NSV-5830 and ORL-1506, which are virulence group five strains.

The results presented here demonstrate that *V. vulnificus* phylogenetic tree analysis does not produce clear groupings of strains based on virulence potential, or source of isolation. Therefore the study utilised the WGS data to carry out WGS comparison and gene annotation, to identify genetic differences between the strains. This was performed with the aim of identifying genetic differences that can discriminate between strains of differing virulence potential.

3.2.5 WGS comparison of *V. vulnificus* strains

WGS comparison is the process by which multiple genomes are aligned to a reference genome, allowing for differences and similarities between the genomes to be observed. WGS comparison is becoming increasingly common in the field of microbiology allowing for differences in virulence genes or antibiotic resistance markers to be identified between different strains of bacteria. The current study therefore employed WGS comparison to identify genetic differences between the ten *V. vulnificus* strains used in the current study. WGS comparison was achieved by using the bioinformatic software programmes, MUMmer [227] and Circos [228]. MUMmer was used to align the a5 assembled scaffolds against the reference

genome YJ016, this alignment was visualised using circos [228], and is shown in Figure 3.6.

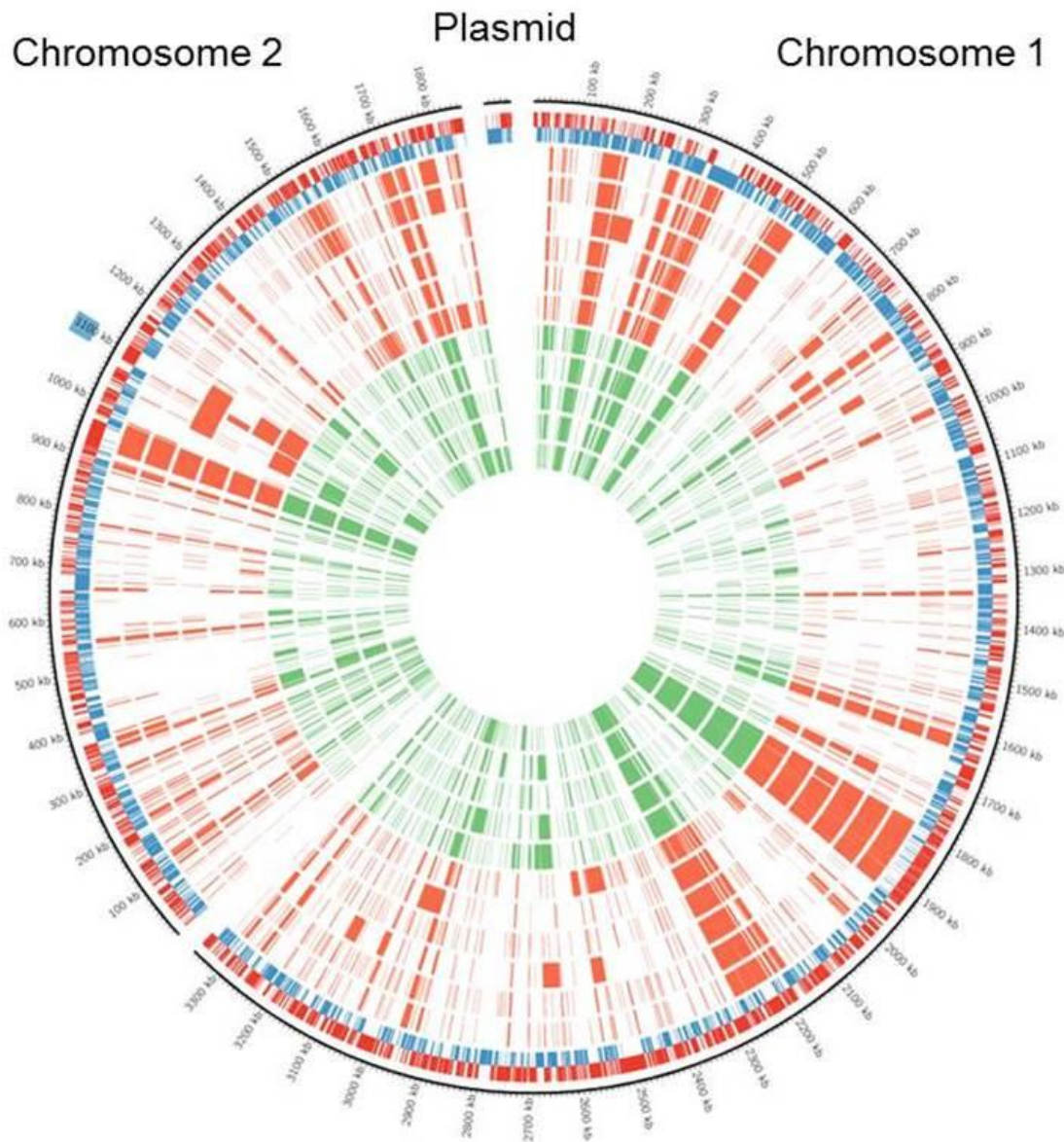


Figure 3.6: Circos visualisation of assembled scaffolds from *V. vulnificus* isolates compared to the reference strain, YJ016. The blocked regions on the diagram indicated regions of DNA in the assembled scaffolds from clinical isolates, shown in red and environmental isolates shown in green that have less than 80% sequence identity compared to the reference strain, YJ016. The reference strain YJ016, is shown on the outside in black, with the red and blue tracks representing the forward and reverse CDS features respectively. Highlighted in blue on the outside is the location of T6SS2 on chromosome two. From the inner circle working out the strains are as follows, 99-743, 99-796, S3-16, S2-22, 106-2A, DAL-79087, DAL-79040, ATL-9824, MO6-24/O, NSV-5830 and ORL-1506

The black outer circle in Figure 3.6 represents the reference strain, YJ016 with the CDSs' on the forward and reverse strands shown in red and blue respectively. The blocked sections of red and green in the inner circles signify the ten clinical and

environmental strains repetitively, as well as an additional reference strain, MO6-24/O also shown. These red and green areas indicate regions of DNA in the assembled scaffolds that have less than 80% sequence identity compared to the reference strain. The data was presented in this way to highlight dissimilarities between the ten query sequences compared to YJ016.

Analysis of Figure 3.6 demonstrates that there are numerous differences in the query sequences compared to the reference strain, as highlighted by the blocked regions of red and green. On the other hand there are also similarities, as there are regions on the diagram that have no blocking of colour, indicating that the regions of DNA are >80% similar when compared to the reference strain. In particular there is a region of no colour which corresponds to the plasmid region of YJ016, this would suggest that the query sequences contain a plasmid. However when this was checked by aligning the trimmed sequencing reads from the ten strains against the plasmid sequence from YJ016, using Bowtie2. The alignment statistics presented in Table 3.3 indicates that there is no alignment between the ten strains and the plasmid from YJ016. This is not to say that the ten strains do not contain a plasmid, as the laboratory preparation used a gDNA extraction kit, listed in the Materials and Methods which is for the extraction of primarily gDNA and not plasmid DNA.

Table 3.3: Alignment rate of *V. vulnificus* strains against the plasmid of YJ016. The table shows the overall alignment rate of trimmed raw sequencing reads from the ten *V. vulnificus* strains against the reference genome, YJ016. Bioinformatic alignment was achieved using the software, Bowtie2.

<i>V. vulnificus</i> strain	Overall alignment against the plasmid of YJ016 (%)
ORL-1506	0
NSV-5830	0
ATL-9824	0
DAL-79087	0
DAL-79040	0
99-796	0
99-743	0
106-2A	0
S3-16	0
S2-22	0

Although the WGS comparison presented in Figure 3.6 demonstrates there are many differences and similarities between the query strains and the reference strain, there is a drawback with this method. The disadvantage of using the WGS comparison method presented in Figure 3.6 is that the data will only show what is not present in the query data compared to the reference data. Therefore if there are additional genes in the query data, these will not be identified, as the unmapped scaffolds will not be mapped. Consequently, if a strain such as ORL-1506 contains genes that YJ016 does not, these genes would not be identified using the presented WGS comparison method and would be grouped into unmapped data. Therefore in order to identify genes that maybe encoded on the unmapped data, an assembly of the un-aligned scaffolds would also need to be performed, making WGS comparison a lengthy task when there are several different query strains being analysed. The current study therefore carried out WGS gene annotation of the assembled scaffolds to identify differences in genes between the strains.

3.2.6 Gene annotation of WGS data

Annotation of WGS data in the current study was achieved by utilising the automated server, RAST [229]. RAST works by blasting predictive ORFs against groups of proteins known as FIGfams, which are families of homologous proteins that share a

common function [230]. Once RAST completes its annotation the data can be downloaded in several different formats [229]. The current study chose to extract the RAST annotation into Excel and manually scrutinise the spreadsheets. This led to the identification of a novel secretion system, known as the type 6 secretion system (T6SS), the genomic location of which is shown in Figure 3.6. A literature search on secretion systems and *V. vulnificus* highlighted that the T6SS had not been previously described in this organism. Further interrogation into the prevalence of this secretion system among the ten strains, identified a difference in the number of T6SSs. All of the sequenced strains contained a T6SS, herein referred to as T6SS2 (annotated in Figure 3.6), whereas three strains, 99-796, S3-16 and 106-2A contained an additional T6SS, herein referred to as T6SS1. Further bioinformatic analysis of the reference genomes, YJ016, MO6-24/O and CMCP6 demonstrated that these strains too contained a T6SS, T6SS2; however they were negative for T6SS1.

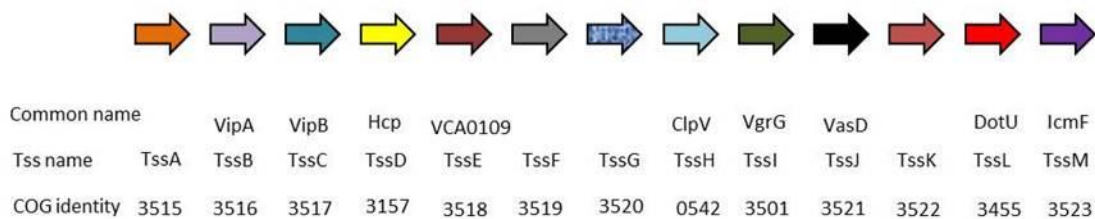
The initial aim of this bioinformatic study was to identify differences in genetic regions that could account for the varying virulence potentials between *V. vulnificus* strains. However, due to the discovery of the T6SS, the study chose to halt further bioinformatic research into investigating genetic differences, and instead focus attention on the T6SS. In particular the study was interested in understanding the role of the additional T6SS, T6SS1 which was only present in a sub-set of strains (99-796, 106-2A and S3-16).

3.2.7 Bioinformatic analysis of the T6SS gene clusters in sequenced *V. vulnificus* strains

Originally identified and characterised in *V. cholerae*, [231] the T6SS has since been described in numerous Gram negative proteobacteria, including *Pseudomonas aeruginosa* [232] *Burkholderia mallei* [233], *Serratia marcescens* [234] and *Campylobacter jejuni* [235]. The minimum set of core proteins required to assemble a functional T6SS [236] are depicted in Figure 3.7A. Supplementary to these core proteins, several bacterial species also contain additional proteins, known as accessory proteins, which are shown in Figure 3.7B. Accessory proteins can include phosphatases and kinases which are involved in the T6SS regulation [232, 237]. The majority of the proteins encoded within the T6SS cluster shown in Figure 3.7 are

named according to historical naming nomenclature. However, to avoid confusion, a new T6SS terminology has arisen, the type six secretion “Tss” nomenclature. Both terminologies are shown in Figure 3.7. However, for the remainder of the study, proteins and genes are generally referred to in accordance with the original nomenclature, except for recently identified T6SS proteins such as the *tssK*, which do not have a common historical name are referred to in accordance with the Tss naming nomenclature.

(A)



(B)



Figure 3.7: The core T6SS proteins and accessory proteins. A) A schematic diagram showing the 13 conserved proteins required for a functional T6SS as determined by Bingle *et al* (2008). B) The image shows a schematic representation of the accessory proteins often associated with the T6SS in some but not all strains harbouring the T6SS(s). Both images have included the COG identity as well as the Tss naming nomenclature for the T6SS proteins, additionally the common name is also indicated for genes which have been either phenotypically investigated or the name commonly referred to in the literature. Image adapted from Coulthurst SJ (2013).

In an attempt to putatively understand the functionality of T6SS1 and T6SS2 in *V. vulnificus*, the secretion systems were examined for the presence of 13 core components. Analysis of the gene organisation demonstrated that both secretion systems contained the 13 genes required for a functional T6SS, as well as several accessory genes. The genetic organisation of T6SS1 is shown in Figure 3.8 and shown in 3.9 is the genetic organisation of T6SS2.

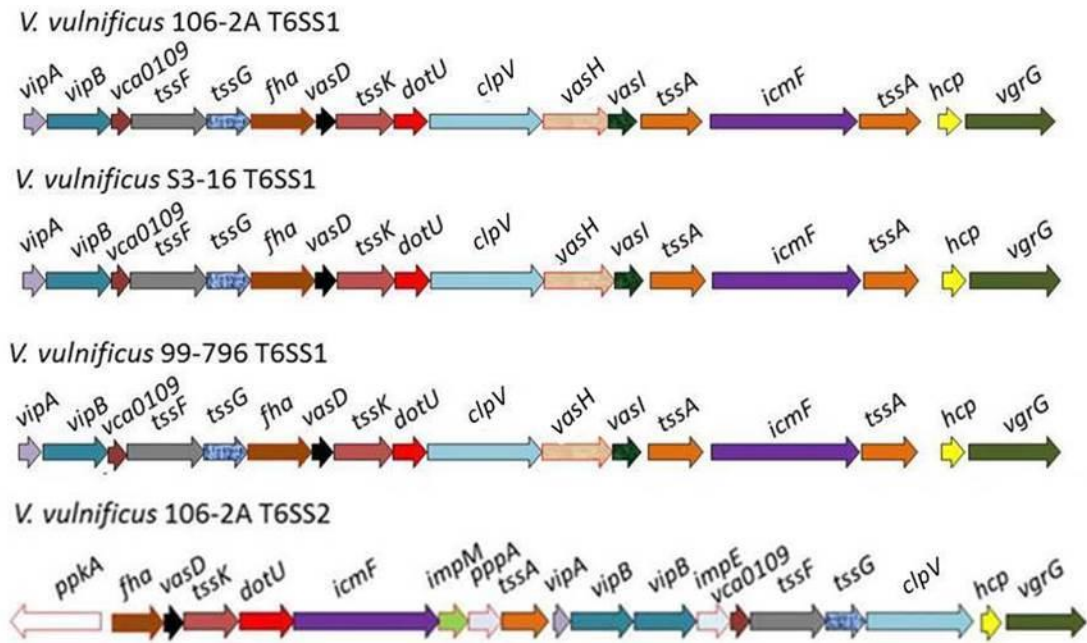


Figure 3.8: Genetic organisation of *V. vulnificus* T6SS1. The schematic gene organisation of T6SS1 from *V. vulnificus* 106-2A, S3-16 and 99-796 is shown. For comparison the genetic organisation of T6SS2 from 106-2A is also shown. T6SS1 contains all of the genes required for a functional T6SS shown outlined in black as well as accessory genes such as *fha* which are outlined in red. The colour coding of the genes corresponds to the colour coding shown in Figure 3.7, the gene organisation shown is taken from the RAST annotation server coupled with BLAST searches to identify COG identities.

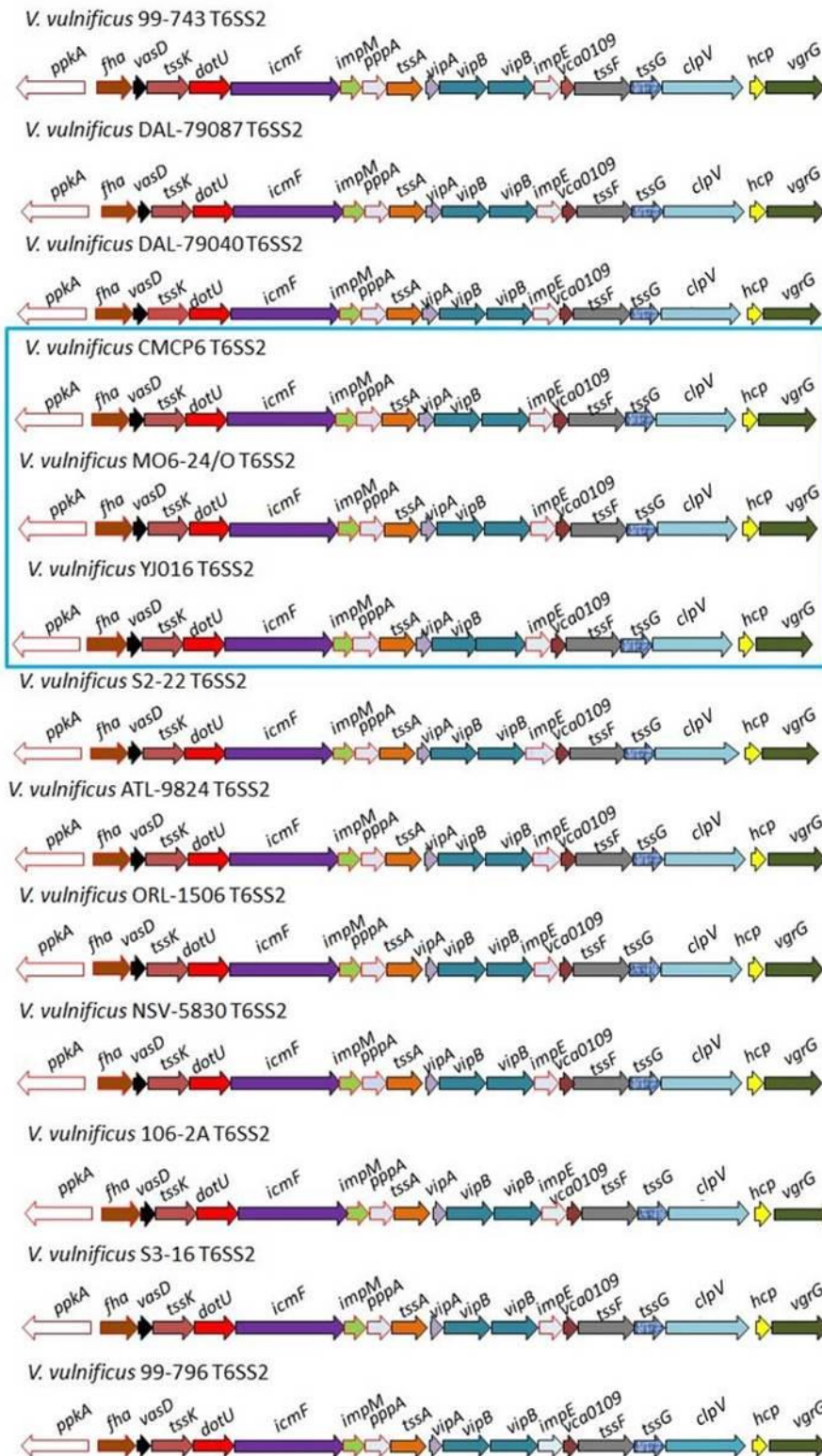


Figure 3.9: The genetic arrangement of *V. vulnificus* T6SS2. The image shows the genetic organisation of the T6SS2 in the ten *V. vulnificus* strains sequenced as well as the reference strains, YJ016, MO6-24/O and CMCP6. T6SS2 contains all of the 13 genes required for a functional T6SS which are outlined in black, as well as several accessory proteins outlined in red. The gene organisation shown is taken from the RAST annotation server coupled with BLAST searches to identify COG identities.

Initial inspection of the *V. vulnificus* reference genome YJ016, found all of the T6SS2 genes to be unannotated. Furthermore, the reference strains MO6-24/O and CMCP6 also contained inaccurate and incomplete annotation, with the majority of the T6SS genes annotated as hypothetical or uncharacterised. In order to identify the T6SS2 in the reference strains, alignment was performed using the sequence of *icmF* from T6SS2. The DNA sequence surrounding this gene was then searched for ORFs using Clone Manager. Each ORF was then subjected to a BLAST search using NCBI to annotate these genes which is shown in boxed region in Figure 3.9. The original mis-annotation of the reference strains may provide a possible explanation as to why this secretion system has not been previously identified in *V. vulnificus*.

Comparison of T6SS1 and T6SS2 in *V. vulnificus*, demonstrates that there are several genetic differences. For example, T6SS2 harbours more accessory components than T6SS1. Additionally the location of genes such as *vipA* and *vipB* differ between the two clusters; T6SS1 encodes *vipA* and *vipB* genes at the distal end of the secretion system locus, whereas T6SS2 harbours *vipA* and *vipB* genes in the middle of the locus. In addition to the differences, there are also similarities, as exemplified by the *hcp* and *vgrG* genes, both of which are located next to each other and at the distal end of the T6SS clusters. The gene organisation of T6SS1 from *V. vulnificus* also shares synteny with the T6SS of *V. cholerae*, as shown in Figure 3.10. In addition to the similarities however, there are also several differences, for example, *V. cholerae*, contains three *vgrG* genes and two *hcp* genes, whereas *V. vulnificus* contains only one of each gene. Additionally, although the majority of the *V. cholerae* T6SS genes are located contiguously on chromosome one, there are copies of the *hcp* gene and *vgrG* gene located on chromosome two, which are distal from the main T6SS locus (as exemplified in Figure 3.10) [238, 239]. An extensive search of the ten *V. vulnificus* genomes highlighted that there were no distal *hcp* or *vgrG* genes.

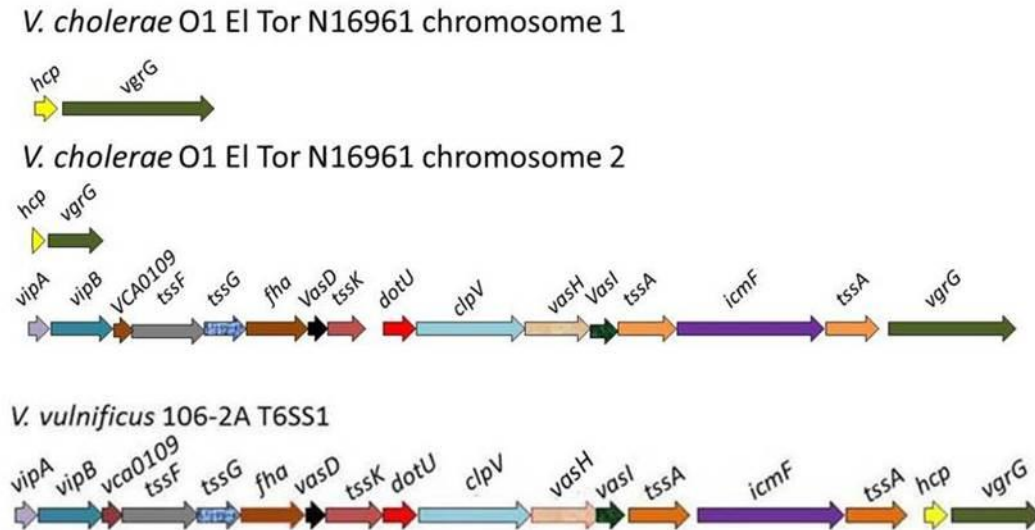


Figure 3.10: Gene organisation of *V. vulnificus* T6SS1 compared to the T6SS gene organisation in *V. cholerae*. The image shows the similarity in gene organisation of the T6SS1 from *V. vulnificus* 106-2A with *V. cholerae* O1 El Tor N16961. There are however several differences such as the number and location of the *hcp* and *vgrG* genes.

Comparison of the strains that harbour T6SS1 with those that are T6SS1 negative, found that all T6SS1 positive strains are environmental isolates, whereas the strains that harbour T6SS2 are from both clinical and environmental origin. In comparison to the *in vivo* virulence data it was found that the majority of the strains that harbour T6SS1, were lesser virulent strains, for example S3-16 and 106-2A are lesser virulent group one and three strains. However, the strain 99-796 which is also T6SS1 positive is a hyper virulent group four strain [13]. Table 3.4 demonstrates the prevalence of both T6SS1 and T6SS2 among the 10 clinical strains, T6SS1 is found only in the environmental strains analysed whereas T6SS2 is present in both clinical and environmental isolates.

Table 3.4: Prevalence of T6SS1 and T6SS2 among the 10 *V. vulnificus* strains analysed. The diagram shows the distribution of T6SSs among the 10 *V. vulnificus* strains. Y indicates the presents of the indicated T6SS, whereas a N indicates the absences of the indicated T6SS. Also shown is the virulence group of a strain and isolation source, E indicates an environmental strain, whereas C indicates a clinical strain.

Strain	Source	Virulence Group	T6SS1	T6SS2
106-2A	E	3	Y	Y
S3-16	E	1	Y	Y
99-796	E	4	Y	Y
99-743	E	3	N	Y
S2-22	E	3	N	Y
DAL-79087	C	3	N	Y
DAL-79040	C	2	N	Y
ATL-9824	C	2	N	Y
NSV-5830	C	5	N	Y
ORL-1506	C	5	N	Y

3.3 Discussion

V. vulnificus biotype 1 strains are opportunistic human pathogens that are known to vary in virulence [13, 36, 43]. The current study hypothesised that this difference in virulence potential maybe due to genetic variations between the strains. Using a WGS approach the study aimed to identify these differences bioinformatically. A total of ten biotype 1 strains were sequenced, which generated WGS data that was then utilised in several downstream analyses, such as phylogenetic tree analysis, WGS comparison and gene annotation. The output data from these downstream analyses was compared to the strains source of isolation and virulence potential.

In order to understand the evolutionary relatedness of the ten *V. vulnificus* strains, phylogenetic trees were constructed based on SNP analysis. The constructed phylogenetic trees were then examined to investigate whether strains produced groups relating to either source of isolation or virulence potential. The phylogenetic trees demonstrated that there was no clear clustering of strains based on either source of isolation or virulence potential. A recent study by Bier *et al.*, [10] generated phylogenetic trees for 53 *V. vulnificus* strains based on multi-locus sequence typing (MLST), with the aim of identifying virulence markers for risk assessment of subsequently identified *V. vulnificus* strains. The study suggested that the *V. vulnificus* strains grouped into two clusters which were based on isolation source.

Cluster I was reported to be made up of predominantly environmental isolates, whereas cluster II was made up of mainly clinical isolates [10]. However, analysis of the phylogenetic tree from this study, which is shown in Figure 3.11, demonstrates that this grouping of strains based on isolation source is not exclusive.

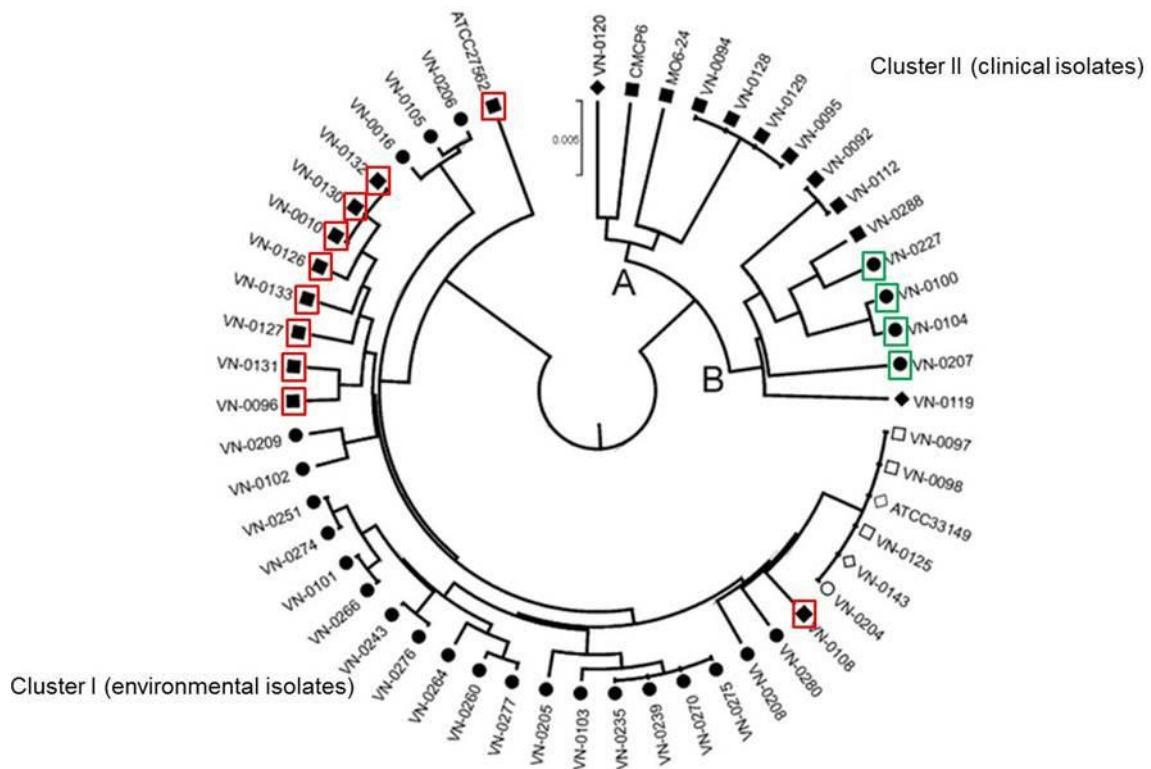


Figure 3.11: Phylogenetic tree generated for *V. vulnificus* strains based on MLST analysis. The image is adapted from Bier *et al.*, (2013), which shows *V. vulnificus* strains group into two clusters, cluster I is associated with environmental isolates, whereas cluster II is made up of clinical isolates. Highlighted in red are clinical isolates that appear in the environmental cluster and highlighted in green are environmental isolates that appear in the clinical cluster. Demonstrating the clusters are not exclusive for grouping either environmental strains or clinical strains.

For example, clinical strains can be observed in the environmental cluster I, as well as environmental isolates appearing in the clinical cluster II. Highlighted in red in Figure 3.11 are the clinical strains that appear in the environmental lineage and highlighted in green are the environmental isolates that cluster in the clinical group, demonstrating that the phylogenetic tree analysis is unable to accurately predict source of isolation of the strains. The phylogenetic trees constructed in the current study were also unable to produce groupings of strains that were exclusively clinical or environmental, as clinical and environmental strains were interspersed throughout the trees. In terms of virulence potential, the phylogenetic trees from the current study were also unable to generate groupings of strains based on virulence potential.

Virulence of the strains was assessed according to the *in vivo* virulence data generated by Thiaville *et al.*, (2011) [13].

As the phylogenetic tree analysis was unable to group *V. vulnificus* strains based on source of isolation or virulence potential, the study utilised the WGS data to perform WGS comparison and gene annotation. This was done with the aim of identifying genetic differences between strains that could account for the varying virulence potentials or isolation source. A similar WGS comparison approach was utilised recently to compare pathogenic and non-pathogenic strains of *Clavibacter*, to better understand the genetic basis of virulence displayed between the strains [240]. WGS comparison of four *V. vulnificus* strains was also been performed by Gulig *et al.*,(2010) [215], with the aim of identifying differences in virulence factors between strains [215]. Prior to bioinformatic analysis the study grouped strains according to clades, based on MLST analysis [31]. The MLST data was also coupled with virulence data for the strains, which was assessed by using an *in vivo* mouse model of virulence [13, 215]. This bioinformatic study identified 80 genes that were specific to the hyper virulent strains and absent from lesser virulent strains. The study suggested that these genes maybe virulence factors that enable the hyper virulent strains to cause systemic infection and death in a mouse model of infection [215]. However, this study was only in two virulent and two non-virulent strains [215].

Similarly, the current study performed WGS comparison of the ten *V. vulnificus* strains with the aim of identifying genetic differences between the strains that may account for the disparity in virulence potentials between the strains. WGS comparison was performed using the bioinformatic software programmes Mummer and Circos, this allowed for the assembled scaffolds for the query strains to be aligned and visualised against the reference genome, YJ016. The alignment demonstrated that there were several differences and similarities between YJ016 and the query sequences. However, the WGS comparison differences were not fully elucidated in the current study as simultaneously to WGS comparison, gene annotation of the WGS data was also performed. This latter method led to the discovery T6SSs, novel secretion systems that had not been previously described in *V. vulnificus*.

The current study chose to carry out gene annotation in parallel with the WGS comparison, as the WGS comparison method utilised in the study has its weaknesses. For example, if the reference strain is negative for genes that are present in the query scaffolds, then these regions will not be mapped to the reference strain, resulting in unmapped regions. One way of identifying these unmapped genomic regions is to carry out a BLAST search of the unaligned regions against the genomes of other organisms in order to identify unmapped genes, a method that Gulig *et al.*, (2010) carried out [215]. However, when several genomes are being analysed this can be a lengthy task, hence the current study carried out whole genome annotation on all strains to examine the differences in genes between the strains. Genetic annotation proved successful for identifying gene differences, as the current study successfully identified two previously unidentified secretion systems, termed T6SS1 and T6SS2. It is possible that if WGS comparison alone was utilised, the T6SS1 may not have been identified, as the reference strain, YJ016 contains only T6SS2 and is negative for T6SS1.

Although the current study aimed to identify genetic differences between the strains, following the identification of the novel T6SSs, the study focused on characterising the secretion systems, in particular T6SS1, as the secretion system shared synteny with genetic organisation of the T6SS in *V. cholerae*. Furthermore, T6SS1 was only present in environmental isolates with a predominance to be associated with lesser virulent *V. vulnificus* strains. Investigation into the genetic organisation of T6SS1 demonstrated that the secretion system contained all of the 13 conserved proteins required for a functional T6SS [236, 237].

Previous phenotypic studies have shown that the T6SS contains anti-prokaryotic capabilities, whereby bacterial strains that harbour a T6SS have a competitive advantage over bacterial strains that do not harbour a cognate T6SS [234, 241-248]. Therefore it was hypothesised that T6SS1 positive *V. vulnificus* strains may have a competitive advantage over the T6SS1 negative strains. To test this hypothesis the study aimed to phenotypically characterise T6SS1 through the use of mutagenesis studies coupled with *in vitro* assays.

3.4 Conclusion

In conclusion to the bioinformatics study, it was found that although the phylogenetic tree analysis of *V. vulnificus* strains did not show any clustering of strains in terms of source of isolation or virulence potential, the gene annotation of WGS data identified novel T6SSs, termed T6SS1 and T6SS2. Although the WGS comparison method showed several genetic differences between the *V. vulnificus* strains analysed, the current study did not investigate these further as attention was focused on understanding the role of the novel T6SSs.

T6SS1 was chosen for further study as it shared synteny with the previously identified and functional T6SS in *V. cholerae* as well as the finding that T6SS1 was only present in a sub-set of strains, with a predominance to be associated with lesser virulent environmental isolates.

Chapter 4 The type 6 Secretion System (T6SS)

4.1 History of the T6SS

4.1.1 The T6SS discovery

Prior to the identification of the T6SS as a bona-fide secretion system [231], there had been much research surrounding the T6SS genes and locus [249-252]. However, despite suggestions of a novel secretion system [253], it wasn't until 2006 that Mekalanos and colleagues carried out a transposon mutagenesis study in *V. cholerae* which ultimately led to the discovery of the novel T6SS [231]. Since then, the T6SS has been identified and characterised in various Gram negative bacteria [234, 235, 248, 254], with *in silico* analysis suggesting that the T6SS is present in 25% of all sequenced Gram negative bacterial genomes [236].

4.1.2 Naming of T6SS components

As briefly mentioned in the Chapter three, 13 core proteins have been identified which are required for the proper assembly of the T6SS [236], these 13 proteins are listed in Table 4.1. Additionally, several species of bacteria have also been shown to encode additional T6SS proteins which are referred to as accessory proteins [237]. Many of the accessory proteins have been shown to be involved with regulation of the T6SS as exemplified by the phosphatase and kinases encoded within the *P. aeruginosa* T6SS cluster [242].

It has also been reported in the literature that the 13 core proteins can be separated into two groups, the membrane associated complex proteins and phage related complex proteins [255, 256]. The membrane associated complex is made up of TssJ/VasD, TssK, TssL/DotU and TssM/IcmF and the phage related complex is made up of proteins which share homology to the bacteriophage tail structure, TssB/VipA, TssC/VipB, TssD/Hcp, TssE/VCA0109, TssF, TssG, TssH/ClpV and TssI/VgrG.

In an attempt to standardise the T6SS naming nomenclature, the terminology "Tss" arose, which is an acronym for "type six secretion" [237, 256]. However, as shown in Table 4.1, several T6SS components are referred to in accordance with historical names. For example, IcmF and Hcp are still used interchangeably with the Tss terminology. However, to avoid confusion this thesis will refer to T6SS components

in accordance with the common/historical nomenclature, with the exception of TssA, TssF, TssG and TssK, which do not have commonly associated names.

Table 4.1: The 13 core proteins required for a functional T6SS

Protein Name (Tss nomenclature/common name)	COG Identity	Function
TssA	3515	Unknown function
TssB / VipA	3516	Similar to the bacteriophage T4 contractile sheath. Interacts with VipB to form sheath around the Hcp [257].
TssC / VipB	3517	Similar to the bacteriophage T4 contractile sheath. Interacts with VipA to form sheath around the Hcp [257].
TssD / Hcp	3157	Forms hexameric rings that stack up on top of each other, hypothesised to form the needle structure of the T6SS [258].
TssE / VCA0109	3518	Believed to be involved with forming the base plate of the T6SS with similarity to the gp25 protein of the T4 bacteriophage [256].
TssF	3519	Unknown function
TssG	3520	Unknown function
TssH / ClpV	0542	Provides the energy for the disassembly of the VipA and VipB sheath [259].
TssI / VgrG	3501	Found at the distal end of the T6SS it forms the puncturing device capped onto the tip of the Hcp protein. Shares homology with the gp27 and gp5 proteins of the T4 bacteriophage [260].
TssJ / VasD	3521	A lipoprotein which is hypothesised to anchor the T6SS to the membrane by interacting with the proteins DotU and IcmF [261].
TssK	3522	A cytoplasmic protein that is hypothesised to form part of the baseplate structure connecting the tail of the T6SS structure to VasD, DotU and IcmF. TssK has also been shown to interact with the sheath protein, VipB [256].
TssL / DotU	3455	DotU shares homology to the type IVb secretion system DotU/IcmH proteins. It is believed that DotU interacts with vasD and IcmF, forming a membrane complex that anchors the T6SS to the cell envelope [262]
TssM / IcmF	3523	Core scaffolding protein of the T6SS [231] and is also believed to be an ATPase and supply energy for the assembly of the T6SS [263].

4.2 The T6SS structure

4.2.1 The phage related complex

The T6SS is a cell puncturing device which as previously mentioned is believed to form an inverted bacteriophage like structure, a schematic diagram of the T6SS structure is depicted in Figure 4.1 [238].

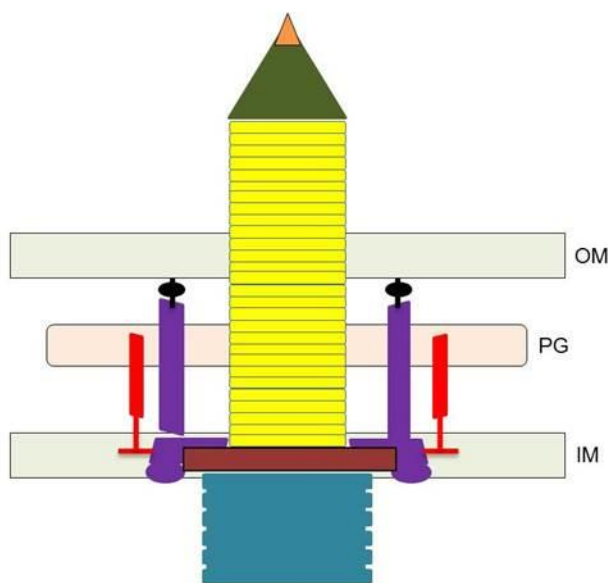


Figure 4.1: Schematic diagram of the T6SS in its contracted form. Shown in blue are the VipA and VipB proteins which form contractile tubes that are structurally similar to the T4 bacteriophage sheath that wrap around the Hcp tube. Upon contraction of the VipA and vipB proteins, the Hcp needle (yellow) is forced up out of the cell. On top of the Hcp needle is the VgrG protein (green), which is the cell puncturing protein. The puncturing action of VgrG is further aided by the PAAR protein (orange), which sharpens the tip of VgrG. The whole T6SS structure is anchored in place by the membrane associated complex consisting of LcmF (purple), DotU (red), VasD (black) and the baseplate structure (brown).

Based on homology studies, the Hcp protein shares similarity to the gp5 tail protein of phage λ [264], and is hypothesised to form the needle structure of the T6SS [258, 265, 266]. More recently experimental evidence has shown that the Hcp protein forms hexameric rings that stack on top of each other in a head to tail manner [258], further suggesting that the Hcp protein forms the needle structure of the T6SS. In addition to being a structural element, Hcp is also believed to be involved with chaperoning T6SS effector proteins [267]. At the distal end of the Hcp needle structure is the VgrG protein. The VgrG protein has been shown to share homology with the gp5 and gp27 proteins of the T4 bacteriophage [260] and is hypothesised to form the puncturing device of the secretion system. It has also recently been shown that several VgrG proteins are partnered to PAAR (Pro-Ala-Ala-Arg) regions. These PAAR regions have been shown to interact with the VgrG protein and are believed to improve the puncturing action of VgrG [268]. In addition to VgrG's structural

capabilities, several VgrG proteins have been shown to contain effector functions. These VgrGs are termed, “evolved VgrGs”, and are distinguishable from structural VgrGs based on the addition of a C-terminal extension [269]. An example of an evolved VgrG is VgrG-1 of *V. cholerae*. This evolved protein has been shown to contain an actin cross-linking domain which is used in virulence towards macrophages [269, 270].

In agreement with the analogy of the T6SS as an inverted bacteriophage structure [238], the T6SS has also been shown to display two differing morphologies. An elongated extended morphology, as well as a shorter contracted morphology (the contracted morphology is shown in Figure 4.1) [271]. Experimental work with *V. cholerae* has demonstrated that the two differing morphologies are due to the VipA and VipB proteins [259]. These proteins are hypothesised to form a sheath like structure that wraps around the Hcp proteins which propel the Hcp needle out of the cell and into neighbouring cells [259]. Time-lapse microscopy on *V. cholerae* cells using green-florescent protein labelled VipA demonstrated that the T6SS sheath goes through cycles of assembly, contraction, disassembly and re-assembly. Although ClpV is not necessarily part of the phage-related complex, the involvement of ClpV is mentioned here briefly as recent research has shown that disassembly of the VipA/VipB sheath is dependent on the ClpV protein, which provides energy for the disassembly [259].

4.2.2 The membrane associated complex, anchoring the T6SS

The tail-sheath like complex of the T6SS secretion system described above, is anchored to the bacterial cell by the VasD, IcmF and DotU complex [256]. DotU and IcmF (Figure 4.1 red and purple) are so named due their homology to the T4SSb, however the VasD protein (Figure 4.1 black) currently has no homology to other identified secretion system proteins [272].

The outer membrane lipoprotein, VasD is anchored in place by association with the outer membrane, it also contains a region that extends into the periplasm which allows for contact with the IcmF protein [273]. Although IcmF can be found residing in the inner membrane, a large proportion of the protein is also found located in the periplasm where it contacts VasD [256]. IcmF is a T6SS scaffolding protein [274] that has also been shown to contain ATPase activity [275]. IcmF is stabilised by

interaction with the DotU protein, [276] a protein that resides mainly in the cytoplasm. However, DotU also contains a C-terminus peptidoglycan binding motif that allows the protein to bind peptidoglycan which further aids in anchoring the T6SS complex to the bacterial membrane [256]. DotU proteins that lack a C-terminal peptidoglycan binding motif, contain the accessory protein, TagL. TagL also contains peptidoglycan binding abilities and therefore in the absence of the DotU motif, TagL anchors the T6SS structure to the cell [277]. A schematic representation of the location of the VasD, IcmF and DotU proteins is shown in Figure 4.1.

Until recently it was unclear how the phage-related portion of the T6SS structure was connected to the trans-membrane spanning complex made up of, VasD, IcmF and DotU. However, recent research has suggested that a baseplate structure made up of TssAEFGK may be involved with connecting the two structures. Recently it has been shown that TssK may play a role in connecting the phage related portion of the T6SS to the membrane associated complex; as TssK has been shown to interact with both IcmF and DotU. [259, 278]. In addition to a connective function, TssK has also been shown to interact with the protein of unknown function, TssA [278]. An additional understudied T6SS protein is VCA0109 (shown in brown in Figure 4.1), the exact role of this protein is still relatively unclear. However, homology studies have indicated that this protein maybe involved with baseplate formation as it is homologous to the protein, gp25 from the T4 bacteriophage [259, 265].

4.3 Anti-eukaryotic properties of the T6SS

Through the use of transposon mutagenesis studies in *V. cholerae*, it was found that a T6SS transposon mutant was attenuated in *Dictyostelium*, a eukaryotic model of infection [231]. This finding was later complemented with *in vitro* studies that demonstrated the T6SS of *V. cholerae* was also involved in virulence towards macrophages. In particular the evolved VgrG, VgrG-1 was shown to prevent phagocytosis by cross-linking actin [270]. The authors also demonstrated that internalisation of *V. cholerae* cells by macrophages activated the T6SS and caused the release of the effector, VgrG-1 [270]. The researchers of this study therefore hypothesised that the T6SS is a mechanism by which internalised *V. cholerae* can prevent macrophages from further phagocytosis and therefore protects the extracellular bacteria. This in turn allows for the dissemination of *V. cholerae*

throughout the human host as internalised *V. cholerae* cells would render the infected macrophages inactive [269]. A schematic representation of this working model proposed by the authors is shown in Figure 4.2. *In vivo* experimentation has also revealed that VgrG-1 causes cross-linking of actin *in vivo*, which is believed to contribute to the inflammatory diarrhoea symptoms commonly associated with *V. cholerae* infection [274]. In addition to VgrG-1, *V. cholerae* also encodes a pore forming T6SS effector, VasX. This effector has been shown to contain anti-prokaryotic properties and is used by *V. cholerae* to target and kill *D. discoideum* [279].

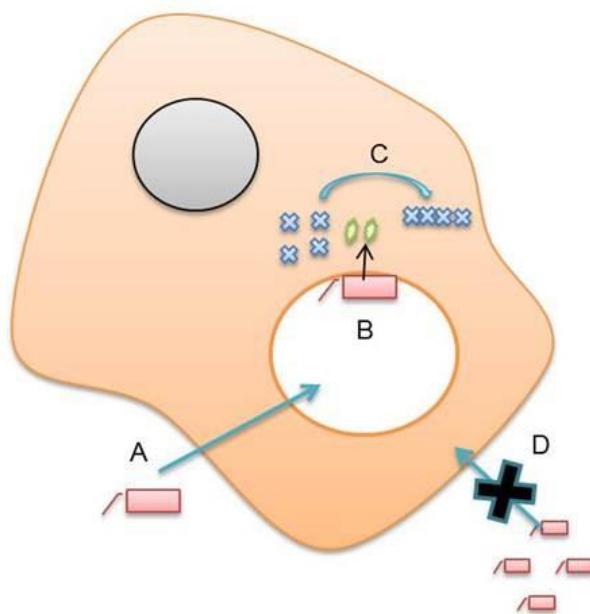


Figure 4.2: Schematic diagram of the anti-eukaryotic properties of the T6SS from *V. cholerae*. The internalisation of *V. cholerae* by macrophages (A) leads to packaging of *V. cholerae* into *V. cholerae* containing vesicles (B), this causes the activation of the T6SS and the release of VgrG-1 (green) into the cytosol of the macrophage. VgrG-1 causes actin cross-linking in the macrophage (C). This renders the macrophage incapable of further phagocytosis, therefore the extracellular *V. cholerae* cells (D) are protected from phagocytosis by the macrophage.

Further examples of the T6SS's anti-eukaryotic properties are exemplified in bacteria from the *Burkholderia* species. For example, many of the T6SS genes in *B. pseudomallei* have been shown to be expressed during *in vivo* infection [280]. In particular, the T6SS-1 of *B. pseudomallei* has been shown to be essential for virulence in a mouse model of infection, as well as playing a role in the formation of mononucleated giant cells (MNGC), a characteristic phenotype associated with *B. pseudomallei* infection [281]. Until recently the T6SS effector responsible for the formation of MNGC was unknown. However, it has been demonstrated in the closely related *B. thailandensis*, that T6SS-5 is essential for mammalian virulence and the protein VgrG-5 is an "evolved VgrG" which is believed to be the key effector involved in the formation of MGNC [282].

Other anti-eukaryotic T6SSs include the T6SS recently identified in *C. jejuni*. This T6SS has been shown to play a role in colonisation *in vivo* as well as the involvement with adherence and invasion *in vitro* [235]. Studies with *P. aeruginosa* also provide evidence that the T6SS is expressed and functional during human infection as the sputum of cystic fibrosis patients infected with *P. aeruginosa* contains Hcp protein. In addition to this finding, Hcp antibodies were also identified in the serum of infected patients [182].

More recently however, the versatility of the T6SS has been demonstrated. As in addition to targeting eukaryotic cells, the T6SS can also target prokaryotic cells. Since this discovery, there has been an explosion in T6SS research and it's anti-prokaryotic properties which are discussed in more detail in the sections below.

4.4 An introduction to anti-prokaryotic T6SS effectors and immunity proteins

The idea that the T6SS was involved with targeting bacterial species was first conceived following the identification of a T6SS protein in *P. aeruginosa* [242, 246]. The Type Six Effector, Tse2, secreted by *P. aeruginosa* was found to specifically target prokaryotic cells in a T6SS contact dependent manner, causing an inhibitory effect on the growth of targeted cells [242]. The inhibitory growth effects of Tse2 were found to be neutralised by the expression of the protein, Tsi2 (Type 6 Secretion System Immunity Protein) [242] and further co-immunoprecipitation experiments demonstrated that both Tse2 and Tsi2 are able to interact with one another [242].

Since the discovery of Tse2 in *P. aeruginosa*, there has been much research aimed at understanding the secretome of anti-prokaryotic T6SSs, and as such knowledge in this field has expanded. It is now widely accepted that in addition to the T6SS encoding anti-bacterial effectors/toxins, the T6SS also encode cognate immunity proteins. These proteins are able to neutralise the deleterious effects of the T6SS toxins, and as such confer protection from the effects of an attacking daughter cell [246, 283, 284].

As a result of the increasing research and knowledge surrounding T6SS anti-prokaryotic toxins, it has become apparent that the toxins can be divided into 3 different classes. An overview of these differing T6SS toxins is discussed in the sections below.

4.5 The differing classes of anti-prokaryotic T6SS toxins

The three different classes of T6SS toxins are divided up as follows, toxins that target the cell wall, toxins that target the cell membrane and toxins that target cytoplasmic nucleic acids [237, 247]. A schematic diagram in Figure 4.3 represents a hypothesised delivery mechanism of T6SS effectors, it should be noted however that although there has been much research into understanding independent effectors of the T6SS, the exact delivery mechanism of these identified T6SS effectors remains unknown [285]. The current hypothesis is that effectors are either fused to structural elements such as the VgrG or PAAR and transported out of an attacker cell and into a prey cell as “specialised effectors”, or translocated as “cargo effectors”, whereby effectors interact directly with structural elements such as the Hcp (as shown in Figure 4.3) [285].

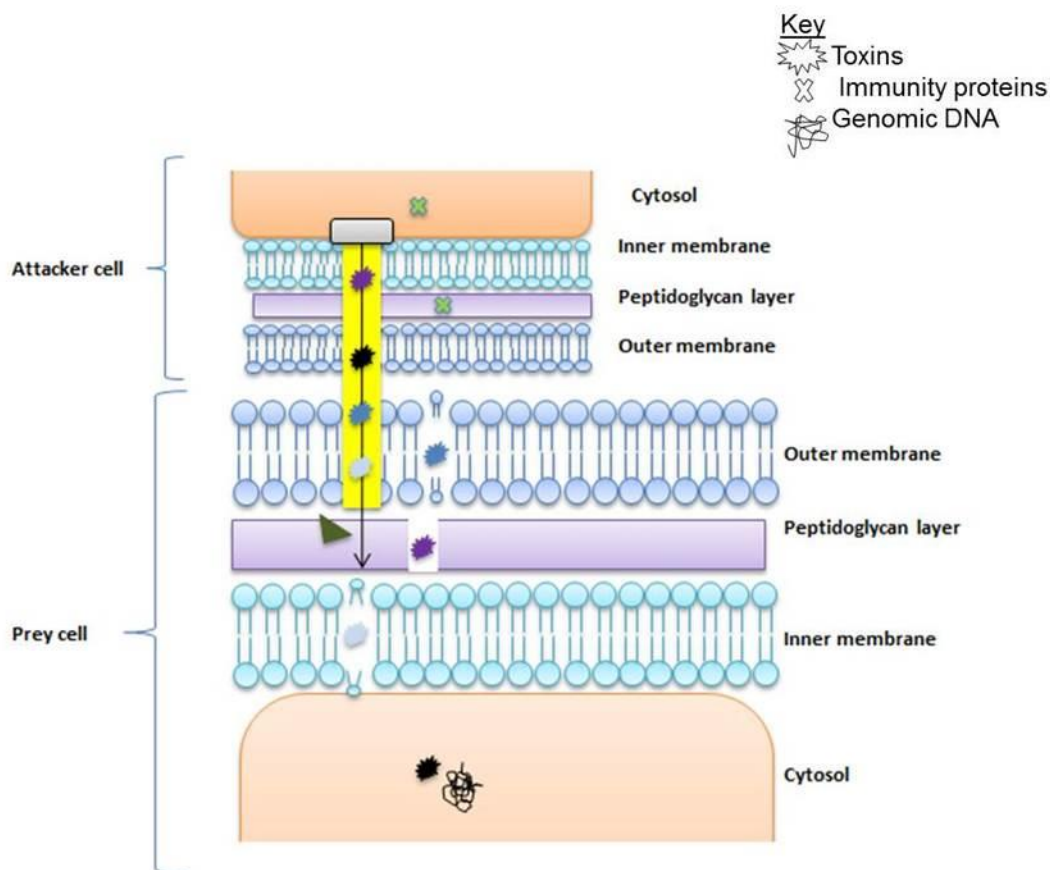


Figure 4.3: Schematic diagram representing T6SS effector transport. The image shows a cross section of the T6SS Hcp needed with effectors being translocated within the Hcp needed from an attacker strain into a prey strain as “cargo effectors”. Upon injection of the T6SS needle into the prey strain, effectors/toxins are released. Toxins can cause damage to integral bacterial components such as the membrane, peptidoglycan layer or DNA of the prey strain. The attacker strain however is protected from the deleterious effects of the toxins by immunity proteins.

4.5.1 Cell wall targeting effectors

Due to the ever expanding field of identified T6SS toxins and immunity proteins, a new nomenclature has been proposed, whereby identified toxins and immunity pairs are named according to the toxin’s target. For example, peptidoglycan amidase T6SS toxins are now named, “Tae”, an acronym for type 6 secretion amidase effector and corresponding cognate immunity proteins are named “Tai”, type 6 secretion amidase immunity [285]. As the name implies, Tae toxins contain amidase activity which allows the toxins to cleave peptidoglycan cross-bridges.

To identify novel Tae/Tai toxin-immunity pairs in T6SS harbouring organisms, a bioinformatic analysis was performed on 193 organisms [286]. This analysis identified 51 putative Tae/Tai pairs which were analysed to compare their evolutionary relatedness. Phylogenetic trees demonstrated that the toxins separated

into four evolutionary distinct clades, designated Tae1-4 [286]. The study characterised each clade *in vitro* by analysing a Tae toxin from each. This demonstrated that the Tae protein contained amidase activity and was toxic when targeted to the periplasm of *E. coli* [286]. An example of a previously identified Tae toxin is Tse1 from *P. aeruginosa*. This toxin was found to cluster in the group one clade of Tae toxins [246], and as such was renamed Tae1^{PA} [286]. Clade two includes BTH_10068 from *B. thailandensis*, also known as Tae2^{BT}, clade three includes PFL_5498 from *P. fluorescens* known as Tae3^{PF} [286], and clade four includes Ssp1 and Ssp2 from *S. marcescens* also known as Tae4.1SM and Tae4.2SM [283].

As well as the Tae proteins, another class of cell wall degrading toxins have been identified. These are known as type 6 secretion glycoside hydrolase effectors, “Tge”, and these effectors can be divided into 3 classes, Tge1-3. Like the Tae toxins, Tge toxins also target bacterial peptidoglycan. However, unlike Tae proteins which cleave peptidoglycan cross-bridges, Tge proteins are able to target the glycan backbone of peptidoglycan, thereby causing damage to the cell [246, 287].

As previously mentioned, T6SS structural elements can also act as effectors, such as the case for the *V. cholerae* evolved VgrG, VgrG-1. Similarly to VgrG-1, *V. cholerae* encodes an additional evolved VgrG protein, VgrG-3. This latter evolved VgrG has been shown to contain a C-terminal domain with peptidoglycan degrading properties and through the use of *in vitro* assays, VgrG-3 has been shown to target bacterial cells in an antagonistic manner [288].

4.5.2 Cell membrane targeting effectors

In addition to targeting the peptidoglycan layer, T6SS toxins are also known to attack the cell membrane. T6SS toxins that attack cell membrane lipids are known as the type 6 secretion lipase effectors “Tle” [289]. Tle effectors are often encoded in genomes adjacent to the VgrG proteins, along with a downstream open-reading frame, which is believed to be the immunity protein [289]. The Tle cognate immunity proteins are known as Tli, type 6 secretion lipase immunity, which are able to neutralise the toxic effects of the Tle proteins [289, 290]. It has been suggested that the Tle proteins exert their effect on the cell membrane from within the periplasmic

space, this is because the cognate immunity proteins, Tli localise to the periplasmic space [289].

A bioinformatic approach demonstrated that there are 5 families of Tle proteins, named Tle1-5. Tle1, Tle2 and Tle5 have been experimentally examined in *B. thailandensis* [289], *V. cholerae* [289, 290] and *P. aeruginosa* [289] respectively and it has been demonstrated that all are able to act as antibacterial effectors [289]. The Tle effector present in *V. cholerae* was identified as a T6SS secreted protein following comparative secretome analysis of a wild-type strain with a T6SS transposon mutant. This identified the Tle effector was named TseL and was bioinformatically shown to contain a lipase domain. *In vitro* assays demonstrated that TseL in conjunction with the other T6SS effectors, VasX and VgrG-3 was required for bacterial targeting [290].

4.5.3 DNA targeting effectors

Recent studies have also shown that the T6SS can produce toxins that are able to target cellular DNA. Recombinant hot spot (Rhs) proteins in *Dickya dadanti* have been shown to damage DNA as the Rhs proteins carry nuclease domains that have been shown to degrade cellular DNA. In particular, the Rhs proteins, RhsA and RhsB were shown to be involved with intracellular bacterial competition in *D. dadanti* [291]. It was found that the Rhs elements were found either linked to *vgrG* or *hcp* genes or next to other T6SS genes. In accordance with T6SS toxins, RhsA and RhsB were also found to have corresponding immunity proteins [291].

4.6 The role of the T6SS in bacterial communities

Due to the T6SS toxins capabilities to disrupt major bacterial cell components, it is hypothesised that a role of the T6SS is bacterial competition. The identification of immunity proteins co-occurring with toxins to protect kin cells, further adds to this evidence. Additionally, T6SSs harbouring anti-prokaryotic capabilities are not generally found in bacteria that are often found in isolation [248]. Furthermore it has also been demonstrated that several bacterial species activate their T6SS in response to differing environmental cues. For example, at low cell densities *P. aeruginosa* [292], *V. cholerae* [293] and *V. parahaemolyticus* [254] activate certain T6SSs. This has led researchers to suggest that the T6SS may be used to set up a

niche, whereby at low cell densities the T6SS is activated in order to displace other competing bacteria. Alternatively, environmental cues such as temperature, salinity and pH can cause activation of the T6SS, which bacteria may use as signals to detect that they have entered a host or certain environment that may contain competing bacteria [243, 254, 294].

In addition to the hypothesis that bacteria harbouring a T6SS engage in inter-species targeting, it has also been shown for *V. cholerae* [295] and *S. marcescens* [234], that the T6SS is used in intra-species targeting. This can be achieved when there is a difference in toxin and immunity pairs between competing strains. It is unsurprising that the T6SS may be used in this way as strains occupying the same niche will be in competition with each other for nutrients and space. Therefore having a mechanism by which strains of a certain genotype can predominate will give a fitness advantage to the competing genotype. It is often seen in both the laboratory setting and in the natural environment that one genotype of a species will often dominate [247] which, among other factors, may be due to the T6SS.

4.7 Monitoring T6SS functionality

One of the most commonly cited ways of identifying a functional T6SS *in vitro* is to monitor the secretion of the well-known T6SS associated protein, Hcp. Hcp is reported as being the most abundant protein of the T6SS [258] and can often be detected in culture filtrates. It is believed that the Hcp is detected in the supernatant due to shearing off from the cells [234] which is often detected by methods such as Western blotting and mass spectrometry [231, 234, 263, 296]. Indeed, the initial key experiment used to identify the T6SS as a bona fide secretion system was a Western blot, which demonstrated detection of Hcp in both the cell lysate and culture filtrate of the wild-type *V. cholerae* strain, V52. However, following disruption to the T6SS scaffolding protein, IcmF, the Hcp was unable to be secreted. As such Hcp was only detected in the cell lysate and not in the culture filtrate.

4.8 Monitoring T6SS killing *in vitro*

In addition to monitoring the functionality of the T6SS, the associated bacterial killing phenotype can also be monitored *in vitro*. A set of experiments designed by Mekalanos and colleagues using time-lapse fluorescent microscopy demonstrated

the killing abilities of the *P. aeruginosa* T6SS when cultured in the presence *V. cholerae*, a T6SS positive organism [297]. Intriguingly these experiments showed that the T6SS in *P. aeruginosa* is not always constitutively expressed [298], and moreover, the T6SS of *P. aeruginosa* is able to locate where an attack is being presented, and assemble the T6SS in a specific location within the cell to mount a counter attack [297]. Often, *P. aeruginosa* sister cells can be seen attacking each other when monitored using time lapse fluorescent microscopy, a phenomenon which was termed “T6SS duelling” by the authors [297]. The same study demonstrated that the detection of an attack and the mounting of a counter attack is not distinguishable in *V. cholerae* cells, as it is believed that *V. cholerae* cells exhibit much higher T6SS activity, whereby cells are continually firing the T6SS, and firing of the T6SS is not specific as seen in *P. aeruginosa* [297]. *P. aeruginosa* only exhibits T6SS activity in certain regions of the cell, suggesting that the activity is due to cells detecting a stimulus, and reacting.

Time-lapse fluorescence microscopy has also been used to demonstrate that *P. aeruginosa* will preferentially target cells that first mount an attack on *P. aeruginosa* [299]. For example, when bacterial cultures of *V. cholerae* harbouring an intact T6SS are mixed with *P. aeruginosa* cultures, *V. cholerae* will spontaneously fire the T6SS, when the T6SS contacts *P. aeruginosa*, *P. aeruginosa* will mount a counter attack by detecting where it has been targeted and assemble the T6SS in the location to target the *V. cholerae* cells [298]. *V. cholerae* cells that have been targeted by *P. aeruginosa* then display a morphological rounding shape and die. However, it was shown when *V. cholerae* cells that were deficient in T6SS assembly were mixed with *P. aeruginosa*, *P. aeruginosa* did not target these cells. This phenomenon of a T6SS attack only being mounted once an attack had already been made was termed “tit-for-tat” [298].

In order to assess the anti-prokaryotic properties of the T6SS in a more simplified manner than using time lapse fluorescent microscopy, a co-culturing method has been established [234, 245, 254]. This is a method by which a T6SS attacker strain is cultured statically on an agar plate in the presence of a susceptible or T6SS negative strain, designated prey [245]. Co-culturing of the prey strain with either the wild-type attacker strain, or a T6SS mutant attacker strain with a dysfunctional T6SS, allows analysis of the prey strains survival. A prey strain that is targeted by the T6SS

will survive significantly better when co-cultured with a T6SS mutant strain than when co-cultured with a wild-type attacker strain [234, 245, 248, 254, 295]. Prey and attacker strains are cultured in unison on agar plates as T6SS killing has been shown to be contact dependent, whereby the addition of filter paper between prey and attacker cells on agar plates is known to abrogate T6SS killing [245]. So far the T6SS has only been shown to be toxic to Gram negative bacterial species [241, 244, 254, 285]. This is due to the finding that the T6SS is ineffective at targeting Gram positive organisms and yeasts such as, *Candida albicans* or *Saccharomyces cerevisiae* [245].

4.9 Study objectives

WGS data demonstrated that *V. vulnificus* contains two T6SS, termed T6SS1 and T6SS2. The study chose to investigate T6SS1 further as it shared synteny with the previously described and functional T6SS of *V. cholerae*. Furthermore, this secretion system was found exclusively in environmental strains, with a predominance to be associate with the lesser virulent strains. The study aimed to assess T6SS1 functionality by Western blotting, to monitor secretion of the T6SS1 associated protein, Hcp.

Chapter 5 Phenotypic characteristics of T6SS1
from *V. vulnificus* 106-2A

5.1 Introduction and aim

WGS analysis carried out in the current study identified novel T6SSs in *V. vulnificus* strains. The data showed that all of the ten strains sequenced contained a T6SS termed T6SS2. However, three strains, 106-2A, S3-16 and 99-796 contained an additional T6SS, termed T6SS1. A literature search on *V. vulnificus* and secretion systems confirmed that the T6SS had not been previously described in this species.

This recently discovered bacterial secretion system has been shown to have numerous functions, including the secretion of both anti-eukaryotic and anti-prokaryotic effectors. Analysis of the T6SS1 genetic organisation described in Chapter three, demonstrated that T6SS1 had synteny with the well characterised T6SS of *V. cholerae*. In addition, T6SS1 appeared to be more prevalent in strains of environmental origin and as such may be more ubiquitous in *V. vulnificus* strains. Therefore the T6SS1 was chosen for further investigation.

5.2 Results

5.2.1 The T6SS1 is functional in *V. vulnificus* 106-2A.

Secretion of the T6SS hallmark protein Hcp is generally accepted as the gold-standard method for assessing T6SS functionality. Hcp secretion can be assessed by using methods such as Western blotting and mass spectrometry [234, 236, 254, 270, 300]. Detection of Hcp in culture filtrate is believed to be due to shearing off of the protein from cells [234, 269, 301]. The current study performed Western blotting, using an antibody against the Hcp protein to determine the functionality of T6SS1 in *V. vulnificus*. The Hcp antibody was supplied by Dr. Stefan Pukatzki, from the University of Alberta, Canada. The antibody was originally raised against the peptide region, AGTSGSDDWRKPIEA, from Hcp in *V. cholerae* [269]. This same sequence was present in Hcp from *V. vulnificus* T6SS1 and therefore allows for cross reactivity with *V. vulnificus*.

In order to study this novel secretion system, the biotype 1 strain 106-2A was selected. This strain is an environmental isolate, originally cultured from the Gulf of Mexico, and has been shown to exhibit medium virulence in a mouse model of infection [13]. To assess functionality of T6SS1, *V. vulnificus* 106-2A cells were grown at 23°C, 30°C and 37°C in LB or LB supplemented with 3% NaCl. These

conditions were investigated as previous *V. parahaemolyticus* T6SS research demonstrated that temperature and salinity effects T6SS functionality. Proteins were extracted as detailed in the Materials and Methods from cells grown under the differing conditions. In brief, 25 mL cultures were grown to an OD₅₉₀ of 1.5. A 20 mL sample of the cells was then centrifuged and the supernatant filtered and precipitated using TCA to obtain the culture filtrate proteins. Precipitated proteins were quantified using a BCA assay and along with whole cell lysate, subjected to SDS-PAGE. Proteins were then transferred to a nitrocellulose membrane which was Ponceau S stained to ensure proteins had been transferred and that protein loadings were equal. The stain was then removed and the membrane subjected to Western blotting using the Hcp antibody.

Figure 5.1 shows the temperature dependent secretion of the T6SS1 associated Hcp protein at approximately 23kDa on the Western blots. Hcp can be detected in the culture filtrate at 23°C and 30°C (lane 2, Figure 5.1A and B), but not at 37°C (lane 6 Figure 5.1B). Furthermore, supplementation of LB broth with 3% NaCl causes a decrease in the Hcp band intensities at 23°C and 30°C (lane 3 and 4, Figure 5.1A and B), suggesting that salinity may have an inhibitory effect on Hcp secretion from T6SS1. At 37°C in LB-only (lane 5, Figure 5.1A) there is a substantial amount of Hcp detected in the cell lysate, suggesting that the *hcp* gene is being expressed, however, Hcp cannot be detected in the supernatant (lane 6, Figure 5.1A), suggesting that at 37°C the T6SS1 is not fully functional. Furthermore, cells grown at 37°C, in LB supplemented with 3% NaCl (lanes 7, Figure 5.1A), exhibit a significant decrease in the amount of Hcp in the cell lysate, further suggesting that increasing NaCl levels may have an inhibitory effect on *hcp* expression. Control samples run on the Western blot shown in Figure 5.1 include the wild-type *V. cholerae* V52 strain (provided by Dr. Stefan Pukatzki), against which the Hcp antibody was raised. A negative control is provided by the *V. cholerae* V52 mutant strain, with *hcp1* and *hcp2* deleted (provided by Dr. Stefan Pukatzki). A further negative control was also included, *C. difficile*, as the antibody does not bind to any of the *C. difficile* proteins, this negative control demonstrates the specificity of the Hcp antibody.

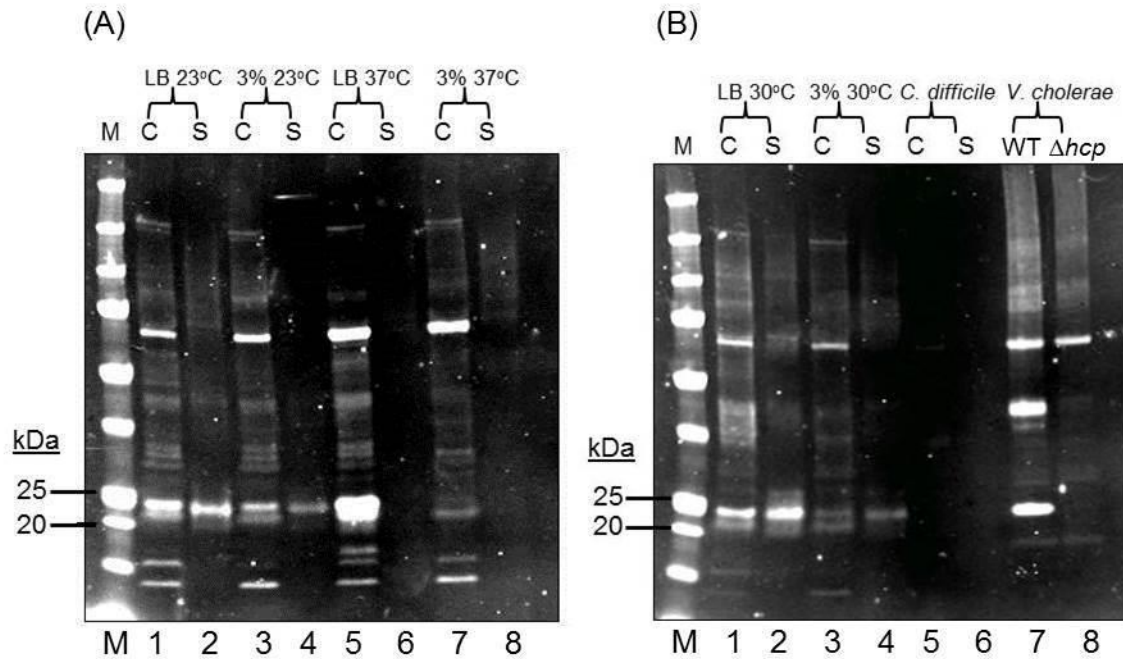


Figure 5.1: Western blot images demonstrating expression and secretion of Hcp. (A) *V. vulnificus* cells lysate (C) and culture filtrates (S) from cells grown at 23°C and 37°C in LB with and without 3% NaCl. Hcp detection at ~23 kDa, corresponding Ponceau S stains shown in Appendix A2. (B) Cell lysate (C) and supernatant (S) from *V. vulnificus* cells grown as 30°C in LB and LB supplemented with 3% NaCl, Hcp detected at ~23 kDa. *V. cholerae* V52 cell lysate run as a positive control (*V. cholerae* WT), showing detection of Hcp at ~23 kDa (lane 7). Negative controls provided by *V. cholerae* $\Delta hcp1\Delta hcp2$ (*V. cholerae* Δhcp , lane 8), and *C. difficile* (lanes 6 and 6). Protein samples loaded equalled 14 μ g of protein/lane. Protein marker is represented with (M). Indicated above each lane are the temperature and media conditions. Both images are representative images of Western blots carried out on protein extractions from three independent experiments.

In conclusion, these results suggest that the T6SS1 is active at 23°C and 30°C but inactive at 37°C; with increasing NaCl concentrations causing an inhibitory effect on both the expression and secretion of Hcp. Following on from these functionality experiments, a T6SS1 mutant was generated in 106-2A in order to confirm the molecular basis of this phenotype.

5.2.2 Production and confirmation of $\Delta icmF1$ and $\Delta icmF2$ mutants in *V. vulnificus* 106-2A

Direct and random mutagenesis are two examples of reverse genetic analysis commonly used to characterise novel microbial genes [302]. A directed mutagenesis study usually involves an initial hypothesis being made about a certain gene, this gene is then mutated either by insertion, or deletion, allowing for the gene of interest to be characterised. It was hypothesised that the expression and secretion of Hcp by *V. vulnificus* is due to a functional T6SS1. To test this hypothesis an in-frame deletion mutant of *icmF* in strain 106-2A was constructed (In addition to generating a

T6SS1 $\Delta icmF$ mutant a similar mutant in T6SS2 was also synthesised simultaneously to act a control in downstream phenotypic assays).

The *icmF* gene was chosen for deletion as it encodes a core scaffolding protein which is required for the correct assembly of the T6SS [231, 236]. Studies have shown targeted disruption of *icmF* renders the T6SS non-functional, as assessed by the inability of the secretion system to translocate Hcp [231]. Therefore, the current study used Western blotting to assess T6SS functionality by monitoring the relative amounts of Hcp in culture filtrate of the wild-type strain and of the $\Delta icmF$ mutant. Construction of unmarked in-frame mutants of *icmF* in T6SS1 and T6SS2 was achieved by utilising the counter-selectable suicide vector, pDM4 [115, 131, 162, 179, 199, 303-306]. The strategy used to construct pDM4 deletion vectors is outlined in Figure 5.2.

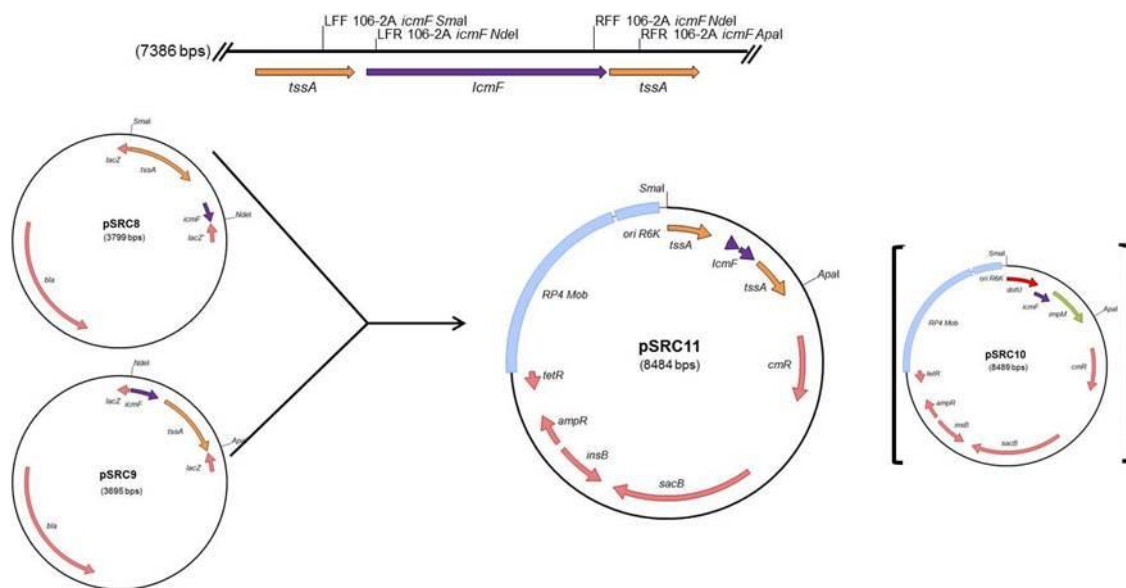


Figure 5.2: Construction of suicide vector pSRC11. Flanking regions either side of *icmF* were PCR amplified using the primers indicated. These regions were then ligated into holding vectors to generate pSRC8 and pSRC9. The cloned regions were excised and ligated into pDM4, creating pSRC11. The resultant mutant essentially had ~ 3000bp of the central portion of the *icmF* gene deleted. A similar construct, pSRC10 was generated in a comparable way.

The intermediate constructs pSRC8 and pSRC9 shown in Figure 5.2 were generated by PCR amplification of left and right flanks from *icmF* (primers used are listed in the materials and methods, in addition the gene sequence of *icmF* is available in Appendix A3 and A4 for T6SS1 and T6SS2 respectively). These plasmids were then sent for sequencing to ensure the fidelity of the PCR. Correctly sequenced upstream

and downstream fragments were then digested with *Sma*I and *Nde*I and *Nde*I and *Apa*I respectively and ligated into *Sma*I and *Apa*I digested pDM4. This produced pSRC11, which contained the *icmF* flanking regions from T6SS1. A similar plasmid, pSRC10 was made with in-frame deletion of *icmF* from T6SS2.

Both pSRC10 and pSRC11 were then introduced separately into *V. vulnificus* 106-2A by tri-parental mating. Confirmation of the integration of each plasmid into the genome to generate first cross-over integrants was confirmed by selecting chloramphenicol resistant clones. The mechanism of production of a first cross-over integrant is depicted in Figure 5.3.

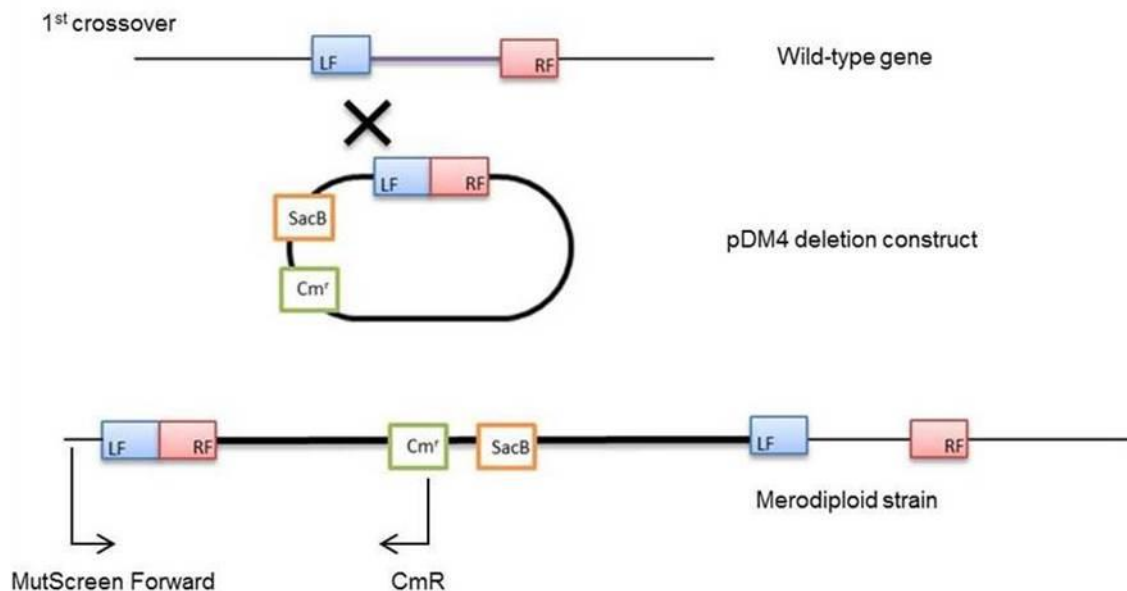


Figure 5.3: Schematic representation of the integration of a suicide vector into the *V. vulnificus* genome. Integration of the deletion construct into the *V. vulnificus* genome by homologous recombination of the left flanking region is shown. Black arrows indicate binding regions of MutScreen Forward and CmR. LF= left flanking region of target gene, RF = right flanking region of target gene, purple line = middle of target gene, cm = chloramphenicol resistance cassette, SacB = *sacB* gene encoded on pDM4 for counter selection. Thick black line = pDM4 backbone, thin black line = bacterial genome, arrows indicate binding of exemplified primers. Image adapted from Reytrat *et al.*, (1998).

First cross-over integrants were checked by PCR using the primers MutScreen Forward and CmR or MutScreen Reverse and CmF, Figure 5.3. CmF and CmR were designed to bind within the suicide plasmid whereas MutScreen Forward and Reverse were designed to bind distal to the flanking regions. Generation of a PCR product could thus only be achieved following successful integration of the suicide

plasmid into the genome. The provenance of the first cross over integrants was further checked using the *V. vulnificus* specific primers, *vvhA* forward and reverse.

Confirmed first cross over integrants were then plated onto LB agar plates containing 5% sucrose. This was performed in order to select for second cross-over integrants which had successfully excised the suicide vector from the genome. This process is schematically represented in Figure 5.4.

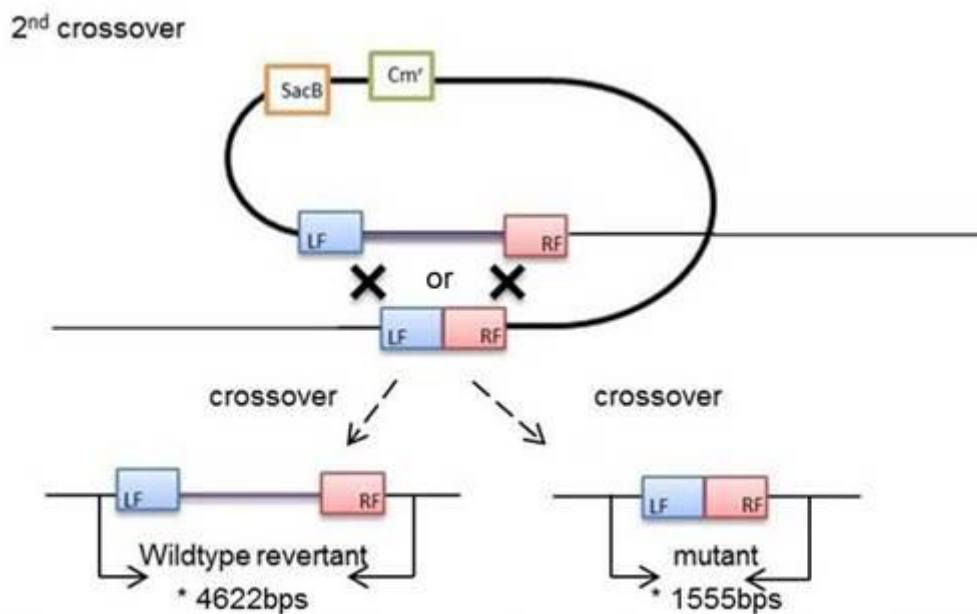


Figure 5.4: Schematic representation of the 2nd homologous cross-over event. 2nd crossover homologous recombination occurring at the right flank produces a mutant, recombination at the left flank produces a wild-type revertant. LF= left flanking region of target gene, RF = right flanking region of target gene, purple line = middle of target gene, cm = chloramphenicol resistance cassette, SacB = *sacB* gene encoded on pDM4 for counter selection. Thick black line = pDM4 backbone, thin black line = bacterial genome, thick arrows = MutScreen primers, * = Length of PCR product generated using MutScreen primers against *icmF*. Image adapted from Reyrat *et al.*, (1998).

During the second cross-over event the plasmid is excised from the genome and the integrant recombines to form either a mutant or a wild-type revertant. To ensure clones produced during the second cross over were negative for the plasmid, colonies were streaked onto both sucrose and chloramphenicol plates. Chloramphenicol sensitivity and an ability to grow in the presence of sucrose indicated that the suicide plasmid had been lost. In addition, clones were genetically checked using PCR to ensure the *icmF* gene had been replaced with a truncated version. PCRs were performed using the primers MutScreen Forward and Reverse

for the *icmF* gene in either T6SS1 or T6SS2. This allowed for the distinction between wild-type revertants and mutant clones based on PCR product sizes, revertants produce a product 4622bps in length, while mutants generated a smaller 1555bps fragment. The primers additionally ensured the excision of the plasmid from that 2nd crossover clones as the primers bound within the genome. Confirmed $\Delta icmF$ clones were referred to as either “ $\Delta T6SS1$ mutant” or “ $\Delta T6SS2$ mutant”, which refers to $\Delta icmF$ in T6SS1 and T6SS2 accordingly. As such, from here on this thesis will refer to $\Delta icmF$ mutants as “ $\Delta T6SS1$ mutant” or “ $\Delta T6SS2$ mutant”.

The gel electrophoresis image presented in Figure 5.5 confirms an *icmF* mutant in T6SS1, using the MutScreen primers. Lane one shows the PCR product generated when wild-type gDNA is used as template for the MutScreen primers, amplifying a band 4622bps in length. The same PCR using gDNA from 106-2A $\Delta T6SS1$ produces a band 1555bp shown in lane two. A negative control using nuclease free water in place of gDNA is shown in lane three.

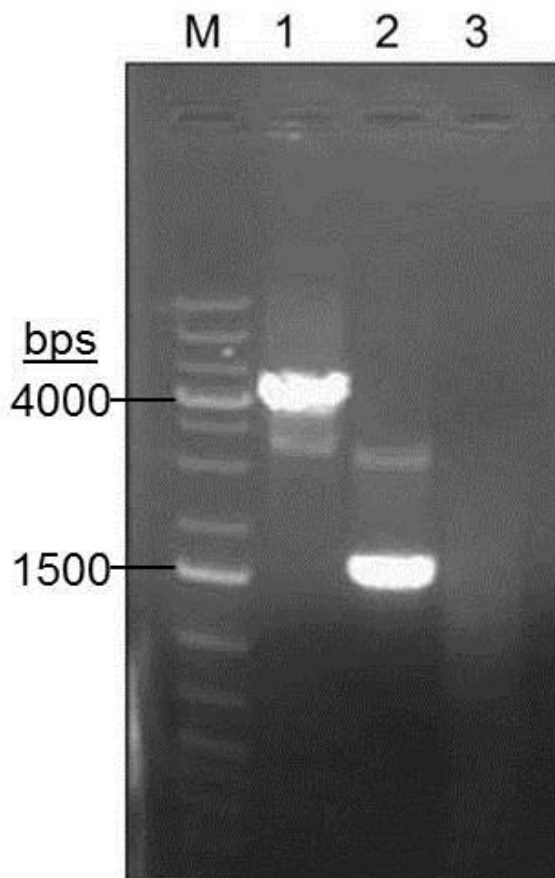


Figure 5.5: Gel electrophoresis image of PCR to confirm an *icmF* mutant in *V. vulnificus* 106-2A T6SS1. PCR bands generated when using the MutScreen forward and reverse primers. Lane one, wild-type *icmF* gene, 4622bps; lane two, mutated *icmF* gene, 1555bps; lane three, negative control; M, Fermentas 1kb plus ladder. Appendix A5 shows a similar gel electrophoresis image for the *icmF* deletion in T6SS2.

To further confirm the mutation of the *icmF* gene in T6SS1 and to ensure no other mutation had occurred in the genome, the mutant was sent for WGS. Figure 5.6A shows a WGS comparison of assembled scaffolds from the wild-type strain, *V. vulnificus* 106-2A, and the mutant strain, *V. vulnificus* 106-2A Δ T6SS1.

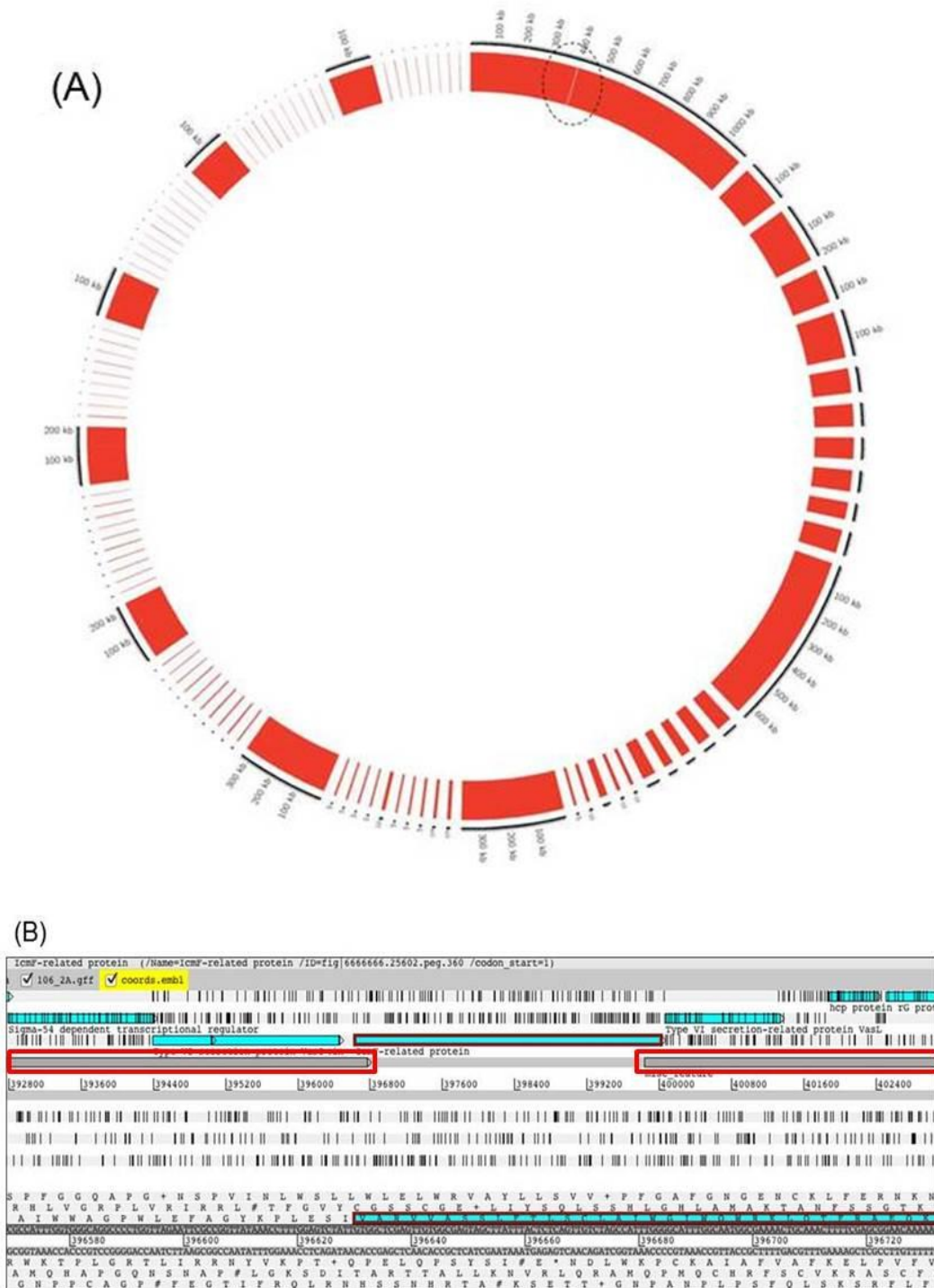


Figure 5.6: WGS comparison of *V. vulnificus* 106-2A and *V. vulnificus* 106-2A Δ T6SS1. Black outer fragments represent scaffolds from the wild-type strain, *V. vulnificus* 106-2A. Blocked inner red regions represent *V. vulnificus* 106-2A Δ T6SS1 scaffolds. Red blocks represent regions of DNA in the mutant sequence with >80% homology compared to regions of DNA in the wild-type sequence. Regions of DNA with <80% homology are represented with no colour. The hashed circle highlights a difference in the alignment between the wild-type and mutant scaffolds. This region corresponds to the deleted *icmF* gene. (B) Wild-type sequencing reads are represented with the grey shaded track lines, associated ARTEMIS annotation for sequencing reads are represented with blue arrows above the grey. Over-laid onto the wild-type sequencing reads is the mutants strain annotation highlighted in red boxes. This demonstrated that the missing region in the mutant strain, shown in the middle of the boxed red regions corresponds to the *icmF* gene in the wild-type strain.

MUMmer [227] and Circos [228] created the WGS comparison in Figure 5.6A. The image was generated using the wild-type and mutant scaffolds, denoted by black and red respectively. The blocked red regions represent DNA sequence in the mutant that is >80% homologous to the wild-type strain. Genetic sequences with <80% homology are shown with no colour and represent a “gapped” region. The hashed circle in Figure 5.6A shows a region that is absent in the mutant strain yet is present in the wild-type strain. Characterisation of this deleted region was achieved by uploading the genetic co-ordinates from the wild-type strain and mutant strain to ARTEMIS, a gene annotation programme [307]. The co-ordinates corresponded to the *icmF* gene which was present in 106-2A wild-type, but absent in 106-2A Δ T6SS1, as shown in Figure 5.6B.

5.2.3 A Δ T6SS1 mutant of *V. vulnificus* is deficient for Hcp secretion

Functionality of T6SS1 was phenotypically assessed by monitoring secretion of the Hcp protein in LB at 30°C, as Hcp was shown to be maximally expressed at this temperature, as seen in Figure 5.1. The Western blot in Figure 5.7 shows detection of the Hcp in the cell lysate and the supernatant (lanes one and two) for the wild-type strain. However, Δ T6SS1 cells grown under the same conditions are deficient for Hcp secretion as Hcp is only detected in the cell lysate (lane three) and not in the supernatant (lane four). This demonstrated that deletion of the *icmF* gene in T6SS1 renders the secretion system non-functional. Furthermore, Figure 5.7 acts as an internal control for Hcp secretion in the wild-type strain, as Hcp is not detected in the supernatant of Δ T6SS1, demonstrating that the Hcp identified in the culture filtrate of the wild-type strain is due to secretion and not cell lysis.

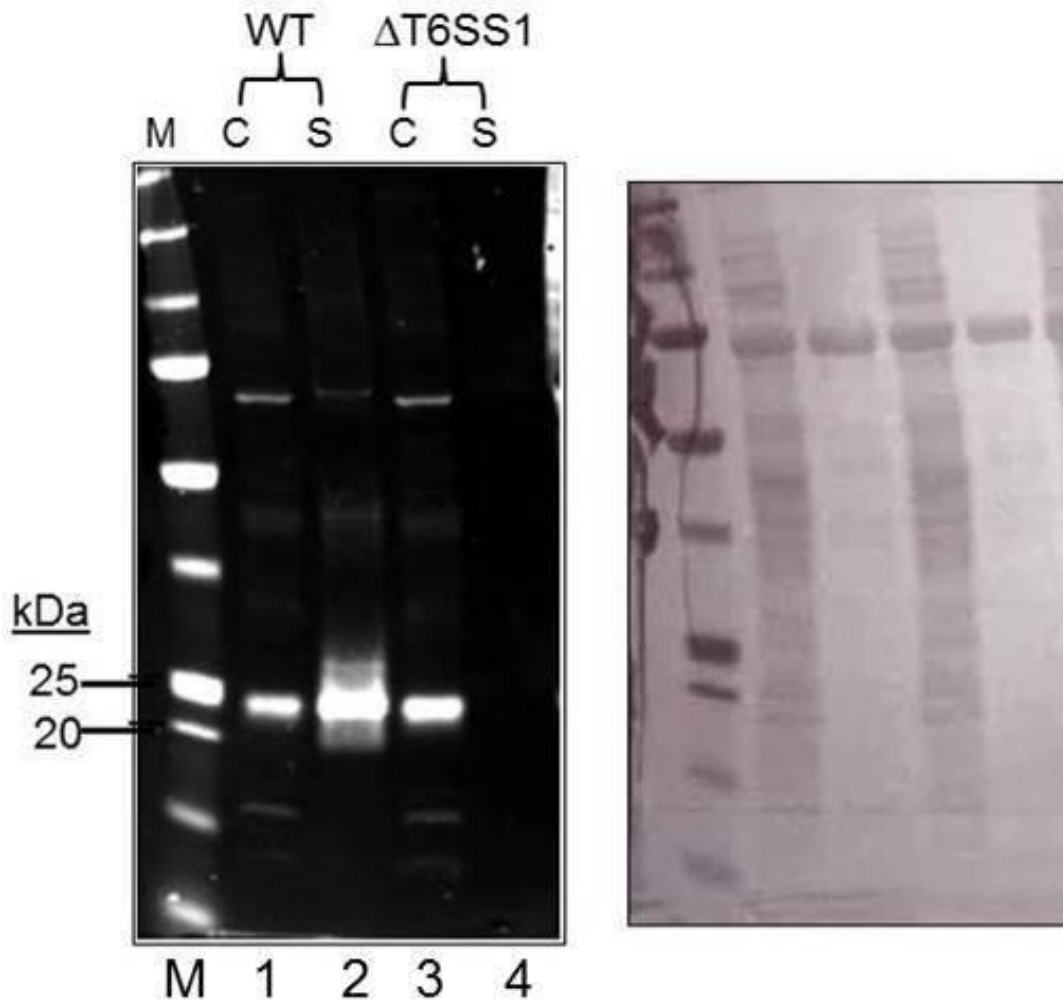


Figure 5.7: Assessment of Hcp secretion from *V. vulnificus* 106-2A wild-type and *V. vulnificus* 106-2A Δ T6SS1. Cell lysate (C) and supernatant (S) for wild-type (WT) and Δ T6SS1 mutant (Δ T6SS1) grown in LB at 30°C. Hcp protein detected at ~23kDa in lanes 1 and 2, lane 4 is absent for Hcp secretion for the Δ T6SS1 mutant. Protein marker (M), 16.00 μ g protein/lane. The image is a representative image of Western blots carried out on protein extractions from three independent experiments.

In conclusion, the Western blot demonstrates that secretion of Hcp in 106-2A is due to T6SS1. Disruption of this secretion by introduction of an in-frame deletion to *icmF* renders the system non-functional, as assessed by monitoring Hcp localisation using Western blotting.

5.2.4. The hypothesised role of T6SS1 in *V. vulnificus* 106-2A

As discussed in Chapter four, the T6SS was initially discovered as a virulence factor against eukaryotic cells [231, 270]. However, following the discovery of a T6SS anti-bacterial effector in *P. aeruginosa* [242], many of the recent T6SS studies have focused on the system's novel anti-prokaryotic properties [234, 236-238, 241, 242, 244-248, 254, 269, 297, 298, 301, 308, 309]. Experimental study of the system's

ability to target bacterial cells is generally evaluated using co-culture killing assays, as described in section 4.8.

The current study hypothesised that the T6SS1 of *V. vulnificus* would contain anti-prokaryotic properties, as functionality experiments shown in Figure 5.1 demonstrated that the secretion system was active at environmental temperatures. Conversely the system is inactive at 37°C and as such the current study speculated that T6SS1 was unlikely to target eukaryotic cells. To test the hypothesised ability of T6SS1 to target bacterial cells, co-culture killing assays were performed. The prey strains chosen for investigation included a T6SS1 negative *V. vulnificus* strain, 99-743, as it was hypothesised that T6SS1 positive *V. vulnificus* cells would have a competitive advantage over T6SS1 negative *V. vulnificus* strains. In addition to 99-743, the prey strain, *V. fluvialis* NCTC 11327 was also chosen as it is likely that *V. vulnificus* would encounter *V. fluvialis* in the natural environment as they share similar environmental niches. Prior to commencing the co-culturing assays, growth curves were performed. This allowed for the assessment of growth for the prey and attacker strains before commencing downstream phenotypic assays.

5.2.5 Growth characteristics of *V. vulnificus* 106-2A wild-type, 106-2A Δ T6SS1, 106-2A Δ T6SS2, *V. vulnificus* 99-743 and *V. fluvialis*

Growth curves for the followings strains, *V. vulnificus* 106-2A wild-type, 106-2A Δ T6SS1, 106-2A Δ T6SS2, *V. vulnificus* 99-743 and *V. fluvialis* NCTC 11327 were performed in LB at 30°C. These conditions were selected as downstream co-culturing assays would be performed at this temperature. 30°C was preferred over 23°C as *V. vulnificus* cultures grew slower at the latter temperature. Supplementary to assessing the strains growth characteristics, the data also allowed for the Δ T6SS1 and Δ T6SS2 mutants to be monitored to ensure the introduced genetic mutations did not cause any pleiotropic effects on growth.

The graph in Figure 5.8 displays the growth data for each of the tested strains. Statistical analysis by means of a two-way ANOVA, followed by a post-hoc Tukey test was performed on the growth curves, the results of which are shown in Appendix A6.

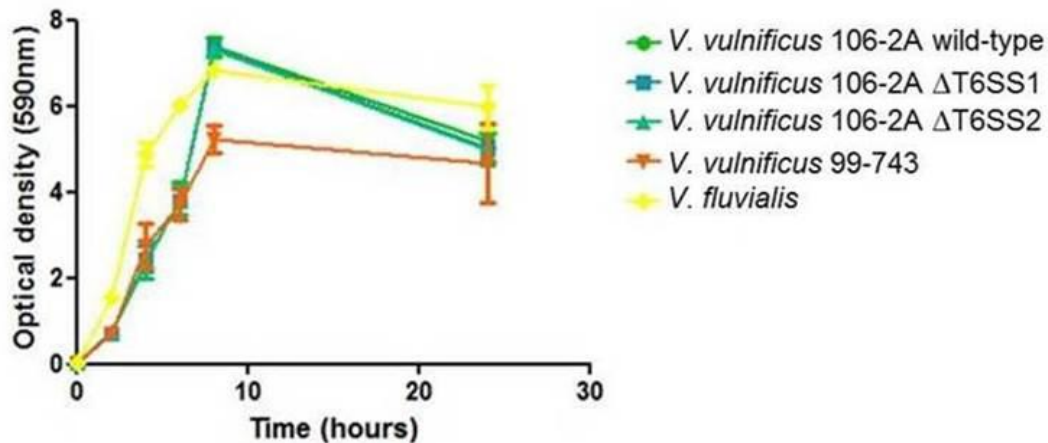


Figure 5.8: Growth curves *Vibrio* strains. Growth curves were performed in LB at 30°C, shaking. The OD_{590nm} reading for the time points, 0, 2, 4, 6, 8 and 24 hours is presented. Each growth curve was repeated three times in triplicate, error bars represent standard error of the mean. Statistical analysis of the growth curves was performed using a two-way ANOVA shown in Appendix A2.

Statistical analysis on the growth curves demonstrated that there is no significant difference in the mean OD_{590nm} values of 106-2A and the corresponding ΔT6SS1 and ΔT6SS2 mutants, indicating that the introduced genetic mutations do not cause pleiotropic effects on growth. There is also no significant difference at T0 and T2 for any of the strains tested. However, at time points, T4, T6 and T8 *V. fluvialis* produces statistically significantly higher OD_{590nm} readings compared to the other strains.

In conclusion, the growth curves demonstrate that the genetic mutations to *icmF* of T6SS1 or T6SS2 does not cause any pleiotropic effects on growth. Furthermore, the growth curves show that the tested strains produce similar OD readings, information that was required for downstream phenotypic assays.

5.2.6 T6SS1 positive *V. vulnificus* 106-2A can target T6SS1 negative *V. vulnificus* 99-743

To test the hypothesis that T6SS1 positive *V. vulnificus* strains have a competitive advantage over T6SS1 negative strains, co-culture killing assays were performed, as previously described in section 4.8. The initial prey strain tested was the T6SS1 negative *V. vulnificus* strain, 99-743. Killing assays were performed as documented in the Materials and Methods. In brief, the prey and attacker strains were grown to an OD_{590nm} 1.0, and then adjusted to an OD_{590nm} 0.8, and mixed at a 3:1 ratio of attacker to prey. The co-culture plates were incubated at 30°C for 5 hours. Following

incubation, the growth was scraped off and re-suspended in sterile PBS. Serial dilutions were then spotted onto TCBS plates. TCBS agar plates containing serial dilutions for T0 and T5 were then incubated at 37°C. The *Vibrio* selective agar, TCBS was used for enumeration as *V. vulnificus* 106-2A, Δ T6SS1 and Δ T6SS2 colonies appear green, whereas *V. vulnificus* 99-743 colonies are yellow, therefore allowing for the quantification of both strains based on colony colour. Incubation of the enumeration plates was performed at 37°C as the T6SS1 is inactive at this temperature and therefore T6SS targeting between the strains should not occur. An illustrative image is shown in Figure 5.9, demonstrating the ability of yellow and green serial dilution colonies to be distinguished.

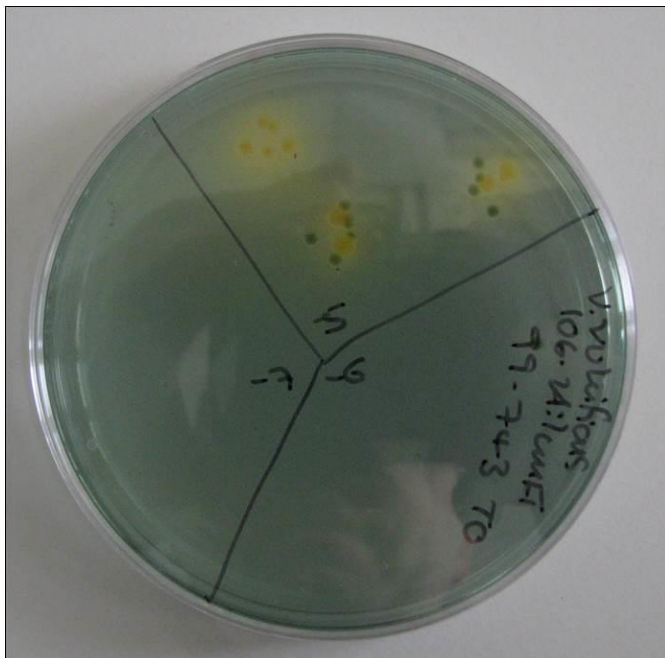


Figure 5.9: Miles and Misra TCBS agar serial dilution plate. Green and yellow colonies produced from co-culture serial dilutions of *V. vulnificus* 106-2A and *V. vulnificus* 99-743 on TCBS agar.

Data for the co-culture killing assays used to assess the anti-prokaryotic targeting properties of *V. vulnificus* 106-2A T6SS1 are shown in Figure 5.10. Assays were performed using the prey strain, 99-743 in co-culture with either 106-2A wild-type or Δ T6SS1. In addition to assessing the targeting abilities of Δ T6SS1, Δ T6SS2 was also included as a control. This was done to establish whether T6SS2 played a role in targeting bacterial species. The raw data gained from the co-culturing killing assays is shown in in Figure 5.11, the raw data was used to calculate the fold change in survival of the prey and attacker strains using the equation, output (cfu/mL)/input (cfu/mL), which is shown in Figure 5.10.

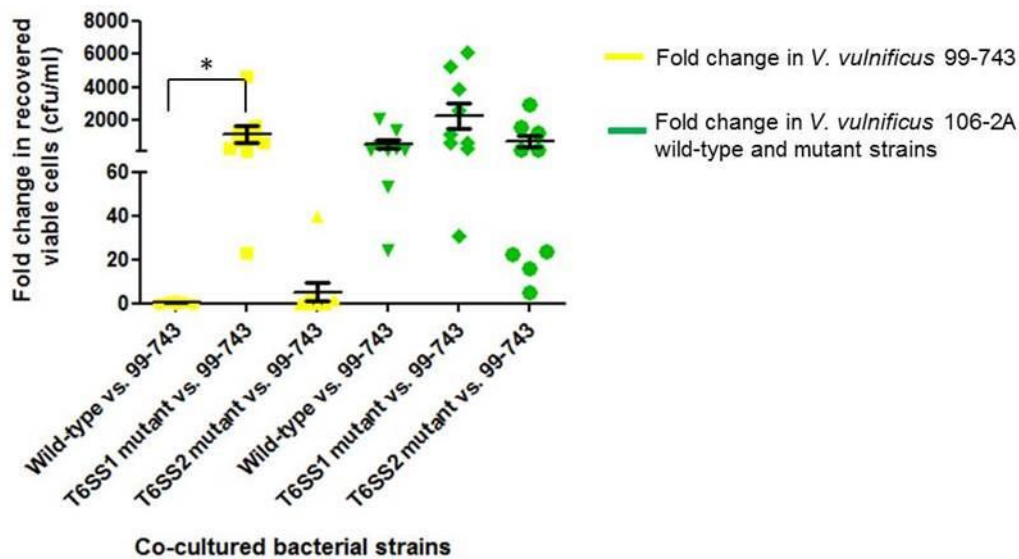


Figure 5.10: The T6SS1 of *V. vulnificus* 106-2A can be utilised to target the T6SS1 negative *V. vulnificus* strain, 99-743. The fold change in cfu/ml of the T6SS1 negative prey strain, *V. vulnificus* 99-743 shown in yellow when co-cultured with the attacker strains, *V. vulnificus* 106-2A wild-type, Δ T6SS1 mutant or Δ T6SS2 mutant. Survival of the attacker strains are depicted in green on the graph. The x-axis represents the strains used in individual co-culture killing assay. Assays were performed three times in triplicate, each spot on the graph represents a co-culture killing assay and error bars show standard error of the mean. Statistics were performed using the unpaired two-way Student's t-test, * $P < 0.05$.

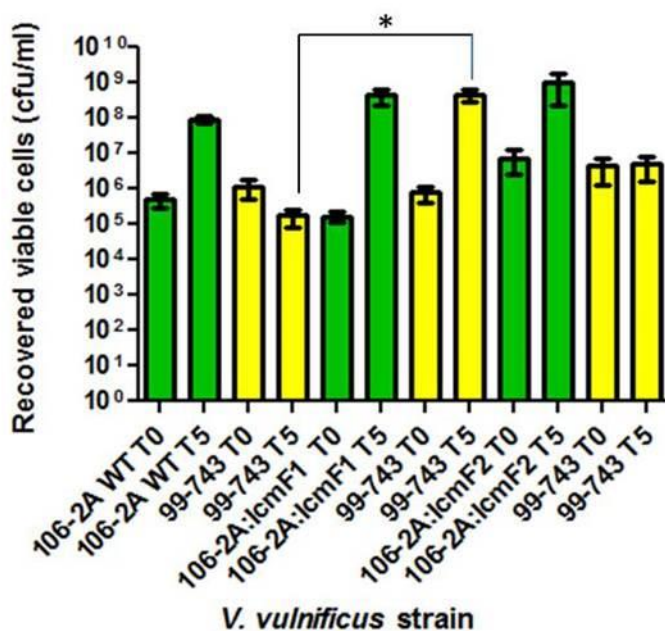


Figure 5.11: The T6SS1 of *V. vulnificus* 106-2A can target a T6SS1 negative *V. vulnificus* strain. The graph represents raw data gained from viable cfu/mL produced at T0 and at T5 for the attacker strains *V. vulnificus* 106-2A wild-type (106-2A WT), Δ T6SS1 mutant (106-2A:lcmF1), Δ T6SS2 mutant (106-2A:lcmF2) shown in green and the prey strain, *V. vulnificus* 99-743 (99-743) shown in yellow following co-culture assays. To the right of each attacker strain is the corresponding prey strain which were co-cultured together. Experiments were performed three times in triplicate, error bars show standard error of the mean. Statistics were performed using the unpaired 2-way Student's t-test, * $P < 0.05$.

Assessment of the graph in Figure 5.10 shows the fold change in recovery of viable cells for the prey strain, 99-743 (depicted in yellow) is greatly increased when co-cultured with the T6SS1 mutant. Recovery of 99-743 is almost three logs higher

when grown with the T6SS1 mutant compared to the wild-type strain. A statistical comparison using the student's t-test demonstrates that this difference is significant where $P < 0.05$. To ensure that the observed killing of 99-743 was due to T6SS1 and not T6SS2, the T6SS2 mutant strain was also used in co-culture killing assays. As seen in Figure 5.10, there is no difference in the recovery of 99-743 when co-cultured with Δ T6SS2 or with the wild-type strain. Analysis using the student's-t-test further demonstrates that there is no significant difference in the survival of 99-743 when co-cultured with either the wild-type strain or Δ T6SS2. Therefore the killing of 99-743 is due to the functionality of T6SS1 and not T6SS2.

Included on the graph is the survival of the attacker strains, 106-2A wild-type, Δ T6SS1 and Δ T6SS2, shown in green. The recovery of the attacker strains is comparable to recovered 99-743 cells when co-cultured with Δ T6SS1. Statistical analysis demonstrates there is no significant difference in the recovery of either the wild-type, Δ T6SS1 or Δ T6SS2 mutants when co-cultured with 99-743, demonstrating that 99-743 does not target 106-2A strains. In conclusion, this data shows that a T6SS1 positive strain exhibits anti-prokaryotic properties against a T6SS1 negative *V. vulnificus* strain. This suggests that T6SS1 positive strains have a competitive advantage over strains that are T6SS1 negative. Furthermore, the killing of 99-743 seen by *V. vulnificus* 106-2A wild-type is attributed to the T6SS1 as a deletion in T6SS2 has no effect.

5.3 Discussion

WGS annotation of ten *V. vulnificus* strains identified novel secretion systems termed T6SS1 and T6SS2. As these novel secretion systems had not been previously described in *V. vulnificus*, the T6SS was chosen for investigation. In particular T6SS1 was evaluated as the gene organisation of T6SS1 has synteny to the previously described and functional T6SS in *V. cholerae* V52 [231]. Furthermore, the T6SS1 was only present in a sub-set of environmental strains, with a predominance to be associated with lesser virulent strains.

T6SS functionality can be assessed by monitoring the secretion of Hcp [231]. Therefore the functionality of T6SS1 was assessed by Western blotting to monitor Hcp secretion. This demonstrated that the T6SS1 was fully functional at 23°C and 30°C, but not at 37°C. This is different to results gained in *V. cholerae* V52, which

contains a T6SS that is functional at 37°C as assessed by the secretion of Hcp [231]. This difference in temperature regulation of the T6SS between *V. cholerae* and *V. vulnificus* is unsurprising as other bacterial species also show differences in T6SS thermoregulation [254, 310]. For example, *V. parahaemolyticus* has been shown to contain two T6SSs which are differentially regulated by temperature [254] and *Yersinia pseudotuberculosis* has four T6SS, which are differentially regulated by temperature [310]

In addition to temperature, the current study investigated the effect on changing salinity levels on T6SS1 associated Hcp secretion, as previous studies in *V. parahaemolyticus* and *V. cholerae* [243] have demonstrated that differing salinity concentrations effect the secretion of T6SS proteins [254]. The results from the current study found that increasing salinity levels caused an inhibitory effect on the secretion of Hcp from T6SS1.

Comparison of T6SS1 in *V. vulnificus* studied here, with the T6SSs in *V. parahaemolyticus* demonstrates that the expression and secretion of Hcp from T6SS1 of *V. vulnificus* is similar to the expression and secretion of Hcp from T6SS2 in *V. parahaemolyticus* [254]. For example, *V. parahaemolyticus* T6SS2 associated Hcp was found to be expressed at 23°C, 30°C and 37°C. However, secretion was only detected in LB at 23°C and 30°C, but not at 37°C [254], akin to the results seen here for *V. vulnificus* for T6SS1. However, with the addition of NaCl to the media, *V. parahaemolyticus* does not secrete Hcp from T6SS2, which is different to *V. vulnificus*, which secretes Hcp from T6SS1 with the addition of NaCl, although at lower levels than when cells are grown in LB alone. Conversely the Hcp from T6SS1 of *V. parahaemolyticus* is expressed only at 23°C and 30°C but not 37°C. The secretion of Hcp from T6SS1 in *V. parahaemolyticus* however, is only detected at 30°C in high salt concentrations and to a lesser extent at 23°C in low salt conditions [254]. These results would suggest that T6SS1 from *V. vulnificus* 106-2A shares a similar secretion and expression pattern to T6SS2 from *V. parahaemolyticus* in terms of temperature regulation. However, the effect of salinity on the regulation on the T6SS differs between the two bacteria.

An alternative example of T6SS salinity regulation is also exemplified in *V. cholerae*. For example, although the T6SS of non-O1 and non-O139 *V. cholerae* strains, such

as V52 is constitutively active in standard laboratory LB media [311], the T6SS of the *V. cholerae* O1 strain, A1552 is active in high salinity solutions. The finding that *V. cholerae* A1552 is active when in the presence of high salinity is unsurprising given that *V. cholerae* is often found in coastal and estuarine environments. These findings in *V. cholerae* A1552 disagree with the findings presented here for *V. vulnificus*, where increasing salinity levels has an inhibitory effects on T6SS1. However, in terms of thermoregulation regulation the T6SS1 of *V. vulnificus* and the T6SS of *V. cholerae* A1552 are similar as they are both functional at 23°C, but inactive at 37°C.

In addition to temperature and osmolality regulation several T6SSs also show post translational regulation, as exemplified by the common nosocomial pathogen, *P. aeruginosa*. This pathogen encodes three T6SSs, named accordingly HSI-I to HSI-III. It has been shown that HSI-I is regulated post-translationally by a serine-threonine phosphatase and a serine-threonine kinase, encoded by PppA and PpkA respectively [232]. In wild-type *P. aeruginosa* it has been shown that HSI-I does not secrete Hcp under normal laboratory conditions. However, deletion of *pppA* results in a constitutively active T6SS, whereby Hcp is secreted. Conversely, deletion of *ppkA* eliminates T6SS activation [232]. Deletion of *pppA* causes T6SS activation as in the wild-type strain, PppA antagonises PpkA. PpkA is activated by an unknown environmental signal which causes dimerization and autophosphorylation of PpkA. The autophosphorylation of PpkA leads to binding and phosphorylation of FHA (fork head association domain) which ultimately leads to the secretion of Hcp [232]. Recent research has also shown that TagR and TagF can promote and repress HSI-I secretion of Hcp respectively [312, 313].

Although the T6SS1 of *V. vulnificus* does not contain a serine-threonine phosphatase or a serine-threonine kinase, findings from this study show that T6SS2 encodes genes for *pppA*, *ppkA* and *fha*. This may suggest that *V. vulnificus* T6SS2 may display regulation similar to the HSI-I of *P. aeruginosa*. This may propose an area for further *V. vulnificus* research as the current study did not investigate the functionality of T6SS2.

The secretion of Hcp was attributed to T6SS1 as an *icmF* deletion mutant in T6SS1 was deficient for Hcp secretion. Other research groups have previously deleted the *icmF* gene in several other bacterial species which has successfully disrupted the

secretion system [182, 231, 296, 314]. Deletion of the *icmF* gene from T6SS1 in *V. vulnificus* rendered the secretion system non-functional, as assessed by Western blotting to monitor the secretion of the Hcp protein. The T6SS1 mutant also provided an internal control demonstrating that the Hcp detected in the supernatant of the wild-type strain was due to secretion and not cell lysis.

The T6SS has previously been shown to target bacterial cells [234, 237, 238, 241, 242, 245, 247, 297, 298, 301, 315]. It was therefore hypothesised that the T6SS1 of *V. vulnificus* 106-2A may contain anti-prokaryotic properties as it was active at lower temperatures such as 23°C and 30°C which are akin to those in the environment, but inactive at 37°C. Due to the inactivation of T6SS1 at 37°C, it was speculated that the T6SS was unlikely to be anti-eukaryotic. In order to test the ability of the T6SS1 to target bacterial cells, the T6SS1 mutant was compared to the wild-type strain in co-culture assays. In addition to the T6SS1 mutant, a T6SS2 mutant was also assessed to understand whether the T6SS2 mutant had any effect on targeting bacterial cells. The co-culture assays were performed on agar surfaces as previous research had demonstrated that the T6SS is unable to target prey cells when cultured in broth [315, 316]. Additionally, preliminary data in the current study demonstrated that the T6SS1 is unable to target prey cells when co-cultured in broth but can when co-cultured on a solid surface.

The study hypothesised that T6SS1 positive *V. vulnificus* cells may have a competitive advantage over *V. vulnificus* cells that are T6SS1 negative. Therefore co-culture assays were performed using the *V. vulnificus* T6SS1 negative strain, 99-743. The results from the co-culture killing assay demonstrated that 99-743 was able to survive significantly better when co-cultured with the T6SS1 mutant strain compared to the wild-type strain. However, when the co-culture killing assay was performed with the T6SS2 mutant there was no significant difference in the recovery of 99-743 compared to the wild-type strain, demonstrating that T6SS1 gives *V. vulnificus* 106-2A a competitive advantage over the T6SS1 negative strain, 99-743.

The ability for the T6SS1 positive strains to target the T6SS1 negative strains, maybe due to the difference in toxin and immunity proteins encoded by the strains. A similar study carried out in *V. cholerae* demonstrated that *V. cholerae* displays intra-species specific competition where it was postulated that certain strains contain

compatibility sets of toxins and immunity proteins. Therefore strains which express cognate toxins and immunity proteins are able to co-exist, whereas *V. cholerae* strains containing different toxin and immunity proteins are unable to co-exist. This is due to the ability of T6SS immunity proteins to neutralise cognate toxins [284]. The toxin and cognate immunity protein pairs allow *V. cholerae* cells to distinguish between self and non-self-cells as well as allowing the bacteria to engage in competitive intra-species competition [295]. This work in *V. cholerae* was further followed up with bioinformatic analysis of toxin and immunity protein pairs which further supports the hypothesis that different strains of *V. cholerae* contain different compatibility pairs of toxins and immunity proteins, allowing for the competitive behaviour seen between strains *in vitro* [288]. In light of the findings regarding bacterial species containing differing classes of T6SS toxins and cognate immunity proteins allowing for bacterial cells to engage in intra and inter-species targeting, the current study hypothesised that *V. vulnificus* may too contain specific toxins and cognate immunity proteins that are specific to strains encoding T6SS1, which may allow T6SS1 positive strains to target T6SS1 negative strains. For example T6SS1 positive *V. vulnificus* strains may contain compatible toxins and immunity proteins, enabling the strains to discriminate between self and non-self. However, the T6SS1 negative strains may not encode cognate immunity proteins to the toxins encoded by T6SS1 positive strains, therefore T6SS1 positive strains can their cognate toxins to target the T6SS1 negative *V. vulnificus* strains in an antagonistic manner. However further research would need to be carried out in order to identify toxins and immunity pairs specific to T6SS1 to verify this hypothesis. Figure 5.12 demonstrates the working hypothesis that T6SS1 of *V. vulnificus* is involved with intra-species targeting.

Although this study did not investigate the secreted toxins of T6SS1 experimentally, it is likely that the effectors are Rhs elements. As the genes encoded adjacent to the *vgrG* of T6SS1 are *rhs* genes. Similarly, the T6SS *rhs* genes encoded by *D. dadanti* are found adjacent to *vgrG* genes. Furthermore, studies in *D. dadanti* demonstrated that the *rhs* genes were involved in bacterial completion and degradation of cellular DNA. Therefore, the current study speculates that the *rhs* genes found adjacent to the T6SS1 locus of *V. vulnificus* may have similar properties [291].

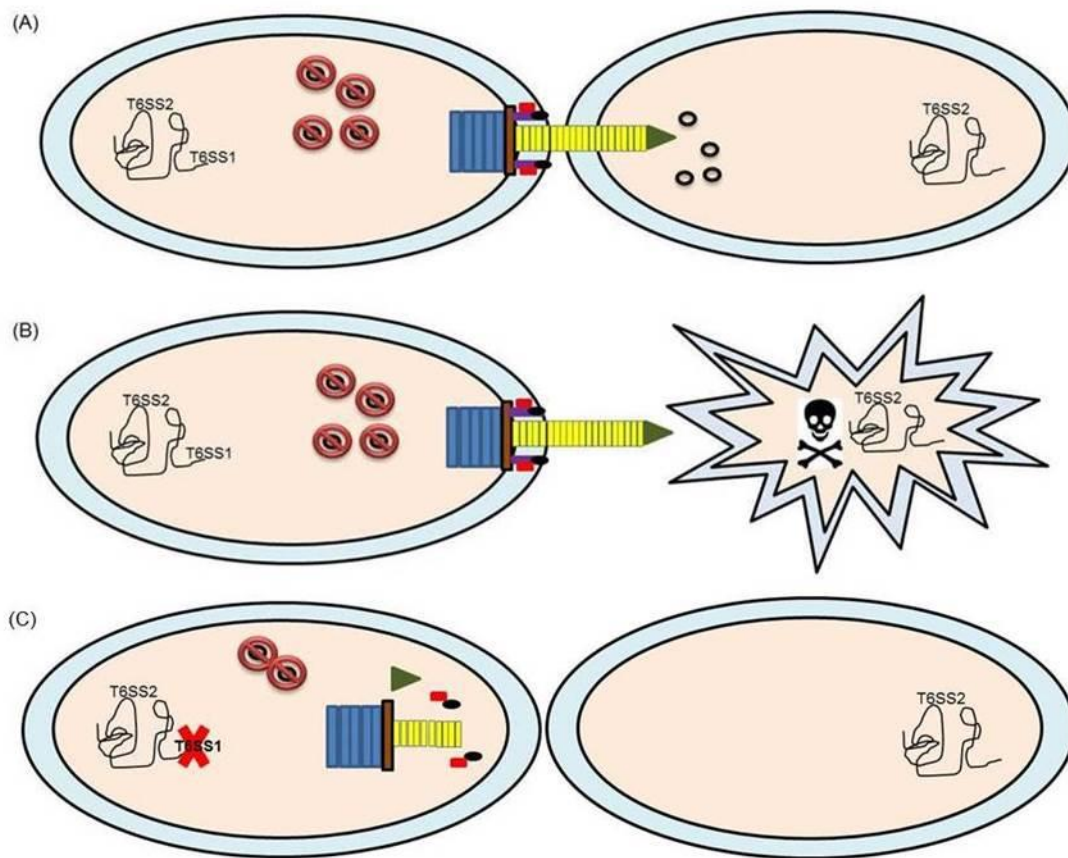


Figure 5.12: T6SS1 of *V. vulnificus* is involved with intra-species targeting. Image (A) represents a *V. vulnificus* cell encoding T6SS1 and T6SS2 targeting a T6SS1 negative cell with an assembled T6SS1. Translocation of the toxins represented in black renders the T6SS1 negative cells unable to survive (B). However, as seen in (B) the T6SS1 positive cell is not susceptible to the deleterious effects of the toxins as T6SS1 also encodes cognate immunity proteins, denoted by red circles which neutralises the toxins. (C) A non-functional T6SS1 due to a deletion in the *icmF* gene shown in purple is no longer able to build a functional T6SS1, therefore the T6SS1 negative strain is not targeted and it able to survive.

The current study also hypothesised that T6SS1 may play a role in understanding the bigger *V. vulnificus* research question which has plagued many scientists working on this organism for several years, the question of, “why are there relatively few serious cases of *V. vulnificus* human infection given the natural prevalence and virulence potential of this bacterium?” With this question in mind, the current study hypothesised that the lesser virulent T6SS1 positive *V. vulnificus* strains are able to target hyper virulent strains naturally in the marine environment, therefore there are less hyper virulent strains occurring naturally which may result in a decreased incidence of serious human infection. The current study poses this as a hypothesis as out of the ten strains analysed bioinformatically, all of the T6SS1 positive strains were of environmental origin. Furthermore analysis of the virulence potential of these

strains, as assessed by the virulence data from the *in vivo* mouse studies [13], demonstrated that T6SS1 is predominantly identified in lesser virulent strains. For example, the T6SS1 positive strain S3-16 is virulence group one and produces very low levels of skin infection with almost undetectable liver infection [13]. Furthermore, strain 106-2A is a low virulence group three strain, which although is associated with high levels of skin infection it produces undetectable to low levels of liver infection, demonstrating that these two strains are unable to produce a fatal systemic disease which is often associated with death in *V. vulnificus* infected patients. There was one strain however, 99-796 which was a hyper virulent group four strain producing high levels of skin infection with moderate to high levels of liver infection. Therefore further research understanding the prevalence of the T6SS1 in *V. vulnificus* strains from both clinical and environmental origin with varying virulence potentials would need to be undertaken to validate the hypothesis detailed above.

5.4 Conclusion

In conclusion, the current study identified that the T6SS1 of *V. vulnificus* 106-2A is functional at 23°C and 30°C in LB and LB supplemented with 3% NaCl. Functionality was assessed by monitoring the secretion of Hcp by Western blotting. It was also noted that although *hcp* is expressed at 37°C, the Hcp protein is not secreted, indicating that T6SS1 is not fully functional at 37°C. Hcp secretion was attributed to T6SS1 as a T6SS1 mutant containing an in-frame deletion of *icmF* was unable to secrete Hcp. The T6SS1 mutant was also used in a co-culture killing assays with the *V. vulnificus* T6SS1 negative prey strain, 99-743. These results demonstrated that T6SS1 positive *V. vulnificus* 106-2A has a competitive advantage over T6SS1 negative, *V. vulnificus* 99-743, as 99-743 survives significantly better when co-cultured with the T6SS1 mutant compared to the wild-type strain. Furthermore, assessment of the Δ T6SS2 mutant demonstrates that the competitive advantage of *V. vulnificus* 106-2A is due to T6SS1 and not T6SS2.

The current study additionally found that T6SS1 may provide a possible explanation to one of the major question surrounding this bacterium, “Why are there so few serious *V. vulnificus* associated infections given the natural prevalence and abundance of this pathogen occurring naturally in the environment?” The current study found that the majority of the hyper virulent *V. vulnificus* strains are T6SS1

negative, whereas several of the lesser virulent strains are T6SS1 positive. Therefore, the current study has hypothesised that the limited number of serious human infection associated attributed to *V. vulnificus* may be due to the lesser virulent T6SS1 positive strains targeting the hyper virulent T6SS1 negative strains in the environment.

**Chapter 6 The inter-species targeting abilities
of *V. vulnificus* T6SS1**

6.1 Introduction and aim

The T6SS is documented in the literature to be involved with intra-species targeting [295]. Accordingly, it was shown in the previous chapter that *V. vulnificus* engages in intra-species targeting as evidenced by a T6SS1 positive strain killing a T6SS1 negative strain, demonstrating that T6SS1 positive *V. vulnificus* cells have a competitive advantage over T6SS1 negative cells. In addition to intra-species targeting, the literature reports that the T6SS is also involved in inter-species competition [234, 241, 245, 254, 297, 298, 317]. Therefore, the current study hypothesised that T6SS1 of *V. vulnificus* may be involved in targeting bacterial species other than *V. vulnificus*. To test this hypothesis, the *Vibrio* species, *V. fluvialis* was used as a prey strain in co-culture assays. As well as testing an alternative *Vibrio* species, the study also tested a non-*Vibrio* species, *B. thailandensis* in co-culture assays. Furthermore, the study also investigated the virulence of T6SS2 towards the eukaryotic infection model, *G. mellonella*. As previously published research has demonstrated that the T6SS is involved in targeting eukaryotic cells [231, 233, 248, 269, 270, 274, 282].

The study also used a Δ T6SS2 *V. vulnificus* strain in all of the assays, as it was hypothesised that T6SS1 may be specific to intra-species targeting and T6SS2 may be involved with inter-species competition or virulence towards eukaryotic cells.

6.2 Results

6.2.1 *V. vulnificus* can utilise T6SS1 to target an alternative *Vibrio* species

To further investigate the specificity of T6SS1 to target other *Vibrio* species, the co-culture killing assay was repeated with the prey strain, *V. fluvialis* NCTC 11327. Similarly to 99-743, *V. fluvialis* appears yellow on TCBS, allowing for *V. fluvialis* colonies to be distinguished from *V. vulnificus* colonies on enumeration plates. In addition to Δ T6SS1, Δ T6SS2 was also assayed to test whether T6SS2 was able to target *V. fluvialis* cells, as although T6SS2 was not involved with targeting T6SS1 negative *V. vulnificus* strains, it was hypothesised that T6SS1 may be specific to targeting *V. vulnificus* species and T6SS2 may be involved in targeting other *Vibrio* species.

The co-culture results are shown in Figure 6.1 which demonstrates that the fold change in the recovery of *V. fluvialis* NCTC 11327 (shown in yellow) is significantly greater when co-cultured with Δ T6SS1 compared to when co-cultured with the wild-type strain. Statistical analysis of this difference using a student's t-test indicates that the difference is significant, where $P < 0.005$. Evaluation of *V. fluvialis* recovery when co-cultured with Δ T6SS2, demonstrates that there is no difference in the survival of *V. fluvialis* when co-cultured with either the Δ T6SS2 strain or the wild-type strain. These results therefore demonstrate that the killing seen by the wild-type strain is due to T6SS1 and not T6SS2, as a mutation to T6SS2 does not affect the survival of *V. fluvialis* in a co-culture assay. The raw data for the graph shown in Figure 6.1 is shown in Figure 6.2.

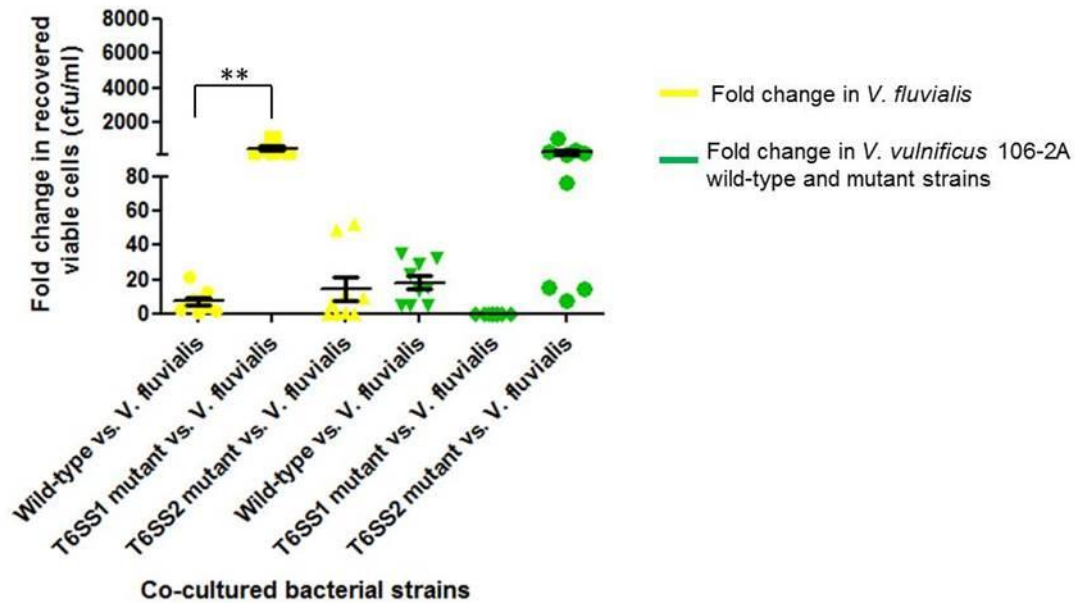


Figure 6.1: *V. vulnificus* 106-2A is able to utilise T6SS1 to target *V. fluvialis* during co-culture. Shown in yellow is the fold change in growth (cfu/mL) for the prey strain, *V. fluvialis* when co-cultured with the attacker strains *V. vulnificus* 106-2A wild-type, Δ T6SS1 mutant or Δ T6SS2 mutant, shown in green. Strains used in individual co-culture assays are shown on the x-axis. Assays were performed three times in triplicate, each spot on the graph represents a co-culture killing assay and error bars show standard error of the mean. Statistics were performed using the unpaired two-way Student's t-test, ** $P < 0.005$.

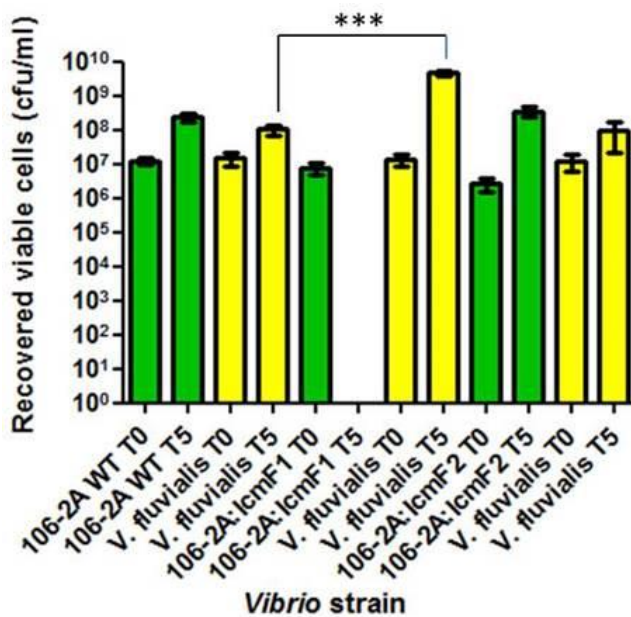


Figure 6.2: *V. vulnificus* 106-2A can target *V. fluvialis* in a T6SS1 dependent manner.

Raw data gained following co-culture with the attacker strains, *V. vulnificus* 106-2A wild-type (106-2A WT), Δ T6SS1 mutant (106-2A:lcmF1), Δ T6SS2 mutant (106-2A:lcmF2) shown in green and the prey strain, *V. fluvialis* (*V. fluvialis*) shown in yellow at 30°C for 5 hours. Shown in green are the results gained for the attacker strains at T0 and T5 and shown in yellow are the results for the prey strain at T0 and T5. To the right of each attacker strain shown in green is the corresponding prey strain shown in yellow. *V. fluvialis* survives significantly better when co-cultured with Δ T6SS1 mutant compared to co-culture with 106-2A wild-type strain. There is no recovery of any Δ T6SS1 mutant colonies following co-culture with *V. fluvialis*. Experiments were performed three times in triplicate, error bars

show standard error of the mean. Statistics were performed using the unpaired 2-way Student's t-test, *** $P < 0.0005$.

Conversely to the results gained in Figure 5.10, the Δ T6SS1 shown in green in Figure 6.1 is unable to survive in the presence of the prey strain, *V. fluvialis*. Furthermore, analysis of the recovery of the attacker strains, Δ T6SS2 and wild-type also show a decrease in growth when compared to Figure 5.10. For example,

Δ T6SS2 and wild-type show a \sim 2-log and \sim 1-log increase respectively in growth when co-cultured with *V. fluvialis*, however when the same strains are co-cultured with 99-734, there is \sim 3-log increase in growth. Additionally the raw data shown in Figure 6.2 shows there is no recovery of any T6SS1 mutant cells following co-culture with *V. fluvialis*. This led to the hypothesis that *V. fluvialis* may contain a functional T6SS that was active at 37°C and was able to target *V. vulnificus* on the TCBS enumeration plates. This hypothesised targeting of *V. fluvialis* against *V. vulnificus*, would account for the inability to recover Δ T6SS1 cells, as these cells would be unable to mount an attack on *V. fluvialis* due to Δ T6SS1 being unable to assemble a functional T6SS.

To test the hypothesis that *V. fluvialis* was killing *V. vulnificus* at 37°C on the TCBS enumeration plates, antibiotic resistant attacker and prey strains were generated. *V. vulnificus* 106-2A wild-type, Δ T6SS1 and Δ T6SS2 were engineered to harbour trimethoprim resistance encoded on the plasmid pSCrhaB3 (Figure 6.3) whereas *V. fluvialis* was made chloramphenicol resistant by introducing the plasmid, pBHR-RFP (Figure 6.3). The antibiotic resistance allowed for the prey and attackers strains to be enumerated separately on selective plates following the co-culture killing assay rather than in concurrence on TCBS plates, thereby removing the ability for the strains to target one another on the enumeration plates.

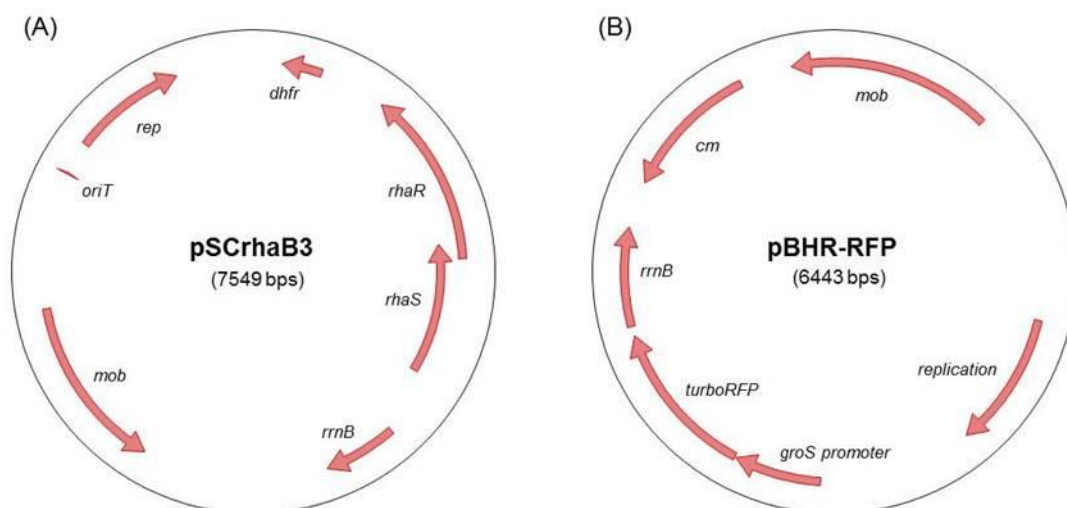


Figure 6.3: Plasmid maps for pSCrhaB3 and pBHR-RFP. The plasmid maps represent the genes encoded on each plasmid. In particular, trimethoprim resistance is encoded by *dhfr* on pSCrhaB3 and chloramphenicol resistance by *cm* on pBHR-RFP.

6.2.2 *V. fluvialis* NCTC 11327 can target *V. vulnificus* 106-2A Δ T6SS1 at 37°C

The results of the co-culture killing assays using the antibiotic resistant strains are shown in Figure 6.4. Assessment of the graph demonstrates that the prey strain, *V. fluvialis* is able to survive significantly better when co-cultured with Δ T6SS1 than when co-cultured with the wild-type strain. The data from this co-culture assay, which uses antibiotic resistant strains, also shows that there is no significant difference in the survival of *V. fluvialis* when co-cultured with either Δ T6SS2 or the wild-type strain, demonstrating that the killing seen by the wild-type strain is due to T6SS1 and not T6SS2.

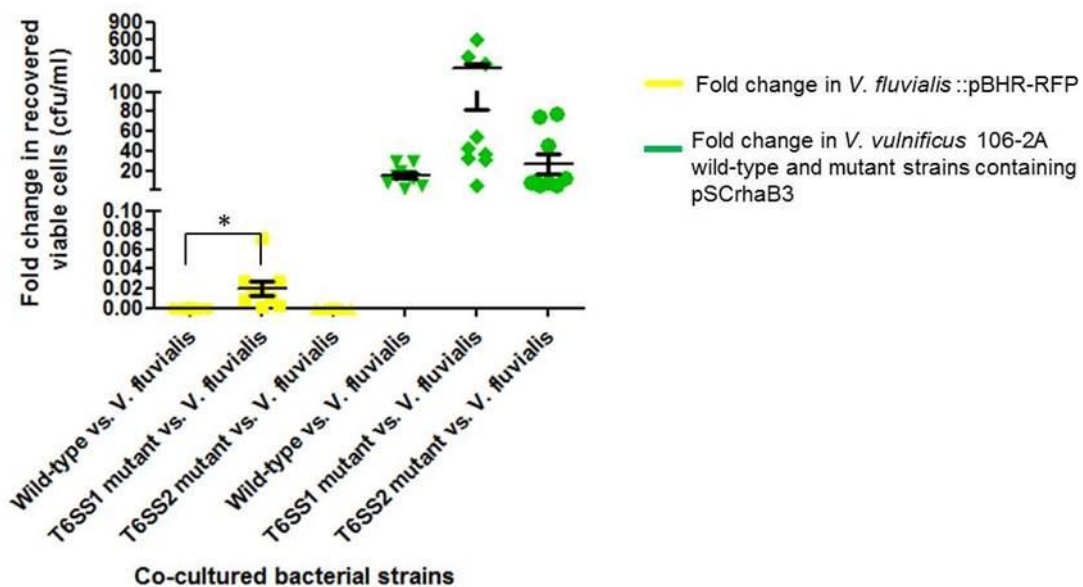


Figure 6.4: Genetically engineered antibiotic resistant strains demonstrate that the T6SS1 of *V. vulnificus* 106-2A can target *V. fluvialis* NCTC 11327 at 30°C. Fold change in growth (cfu/ml) of the prey and attacker strains when enumerated using antibiotic selective plates. Shown in yellow is the prey strain *V. fluvialis* and shown in green is the attacker strains, *V. vulnificus* 106-2A wild-type, Δ T6SS1 mutant or Δ T6SS2 mutant. Assays were performed three times in triplicate, each spot on the graph represents a co-culture killing assay and error bars show standard error of the mean. Statistics were performed using the unpaired two-way Student's t-test, * $P < 0.05$.

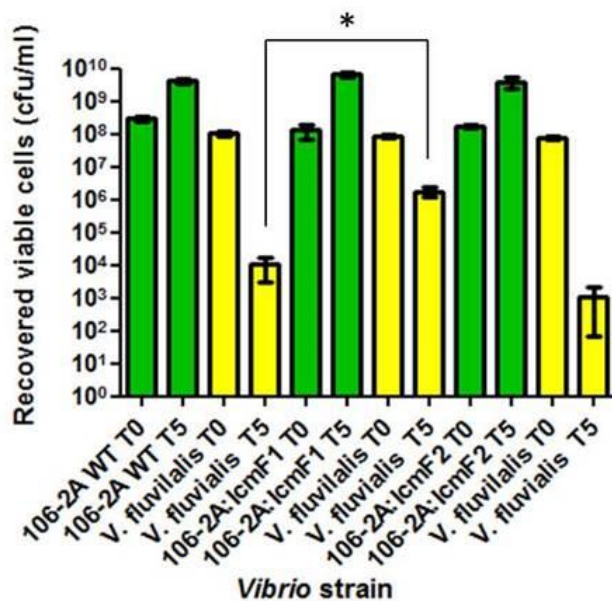


Figure 6.5: Co-culture killing assay using genetically engineered antibiotic resistant prey and attacker strains.

Co-culture assay using the attacker strains, *V. vulnificus* 106-2A wild-type (106-2A WT), Δ T6SS1 mutant (106-2A:lcmF1), Δ T6SS2 mutant (106-2A:lcmF2) shown in green and the prey strain, *V. fluvialis* (*V. fluvialis*) shown in yellow, followed by enumeration of strains using antibiotic selection plates. Shown in green are the results gained for the attacker strains at T0 and T5 and shown in yellow are the results for the prey strain at T0 and T5. To the right of each attacker strain shown in green is the corresponding prey strain shown in yellow. Results show *V. fluvialis* survives significantly better when cultured with Δ T6SS1 mutant compared to 106-2A wild-type strain. Assays were performed 3 times in triplicate, each spot on the graph represents a co-culture killing assay and error bars show standard error of the mean. Statistics were

performed using the unpaired 2-way Student's t-test, * $P < 0.05$.

Analysis of the survival of the attacker strains when enumerated separately using antibiotic selection plates, demonstrates that *V. fluvialis* can no longer target Δ T6SS1, as survival of Δ T6SS1 is comparable to wild-type levels. This is due to the strains not being in contact on the enumeration plates. Furthermore, the raw data in Figure 6.5 demonstrates that following co-culture with *V. fluvialis*, Δ T6SS1 cells can be recovered when using the antibiotic enumeration plates, unlike the previous experiment in which Δ T6SS1 cells could not be recovered when enumerated on TCBS agar plates when *V. fluvialis* is present.

The data presented in Figure 6.6 further highlights the difference in survival of *V. vulnificus* Δ T6SS1 when enumerated on TCBS agar compared to the antibiotic plates following co-culture with *V. fluvialis* the graph in Figure 6.4 was generated. Figure 6.6 shows the fold-change levels for the *V. vulnificus* attacker strains shown in green when enumerated on TCBS agar. Shown in red, is the *V. vulnificus* attacker strains survival when enumerated on antibiotic plates. The graph shows the fold change in Δ T6SS1 survival is significantly greater when enumerated on antibiotic selection plates compared to TCBS agar plates, where $P < 0.05$, when compared using the student's t-test.

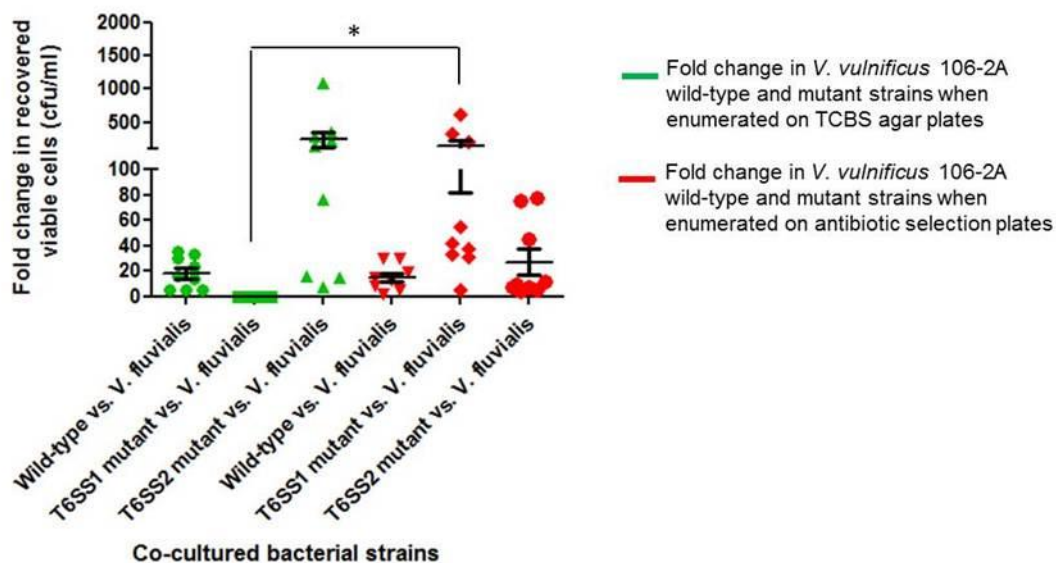


Figure 6.6: Survival of *V. vulnificus* strains when enumerated on either TCBS agar plates or antibiotic selection plates, following co-culture with *V. fluvialis*. Fold change in recovery of the attacker strains, *V. vulnificus* 106-2A wild-type, Δ T6SS1 mutant or Δ T6SS2 mutant when co-cultured with *V. fluvialis*. Shown in green is the fold change in recovery for *V. vulnificus* 106-2A wild-type, Δ T6SS1 mutant or Δ T6SS2 when enumerated on TCBS agar plates and shown in red is fold change in recovery for *V. vulnificus* 106-2A wild-type, Δ T6SS1 mutant or Δ T6SS2 when enumerated on antibiotic selection plates. Assays were performed three times in triplicate, each spot on the graph represents a co-culture killing assay and error bars show standard error of the mean. Statistics were performed using the unpaired two-way Student's t-test, * $P < 0.05$.

It was also noted that the fold change in *V. fluvialis* recovery was different between Figure 6.1 and Figure 6.4. It was therefore speculated that the difference could be due to the instability of the antibiotic resistance plasmid in *V. fluvialis*, which could lead to the antibiotic killing of *V. fluvialis* on antibiotic enumeration plates. To test this hypothesis a plasmid stability test was carried out. The graph in A7 of the Appendix illustrates the results gained for plasmid stability test in *V. fluvialis*, which was performed as detailed in the Materials and Methods. The results demonstrate that the plasmid is not stable during the five hour co-culture conditions when there is no selection pressure present, as there is a statistically significant difference in the cfu/mL counts between the TCBS agar plates and the antibiotic plates, where $P < 0.05$, when analysed using the student's t-test. In addition to the instability of the plasmid, the difference in *V. fluvialis* survival between Figure 6.1 and Figure 6.4 may also be due the antibiotic on the enumeration plates and the temperature shift from 30°C to 37°C causing a stress on the cells, which may cause the cells to enter a viable but non-culturable state.

6.2.3 WGS sequencing of *V. fluvialis* NCTC 11327

As the current study hypothesised that *V. fluvialis* NCTC 11327 contained a T6SS that was targeting *V. vulnificus* at 37°C, WGS was carried out on the *V. fluvialis* NCTC 11327 strain to identify a T6SS locus. The data generated from WGS was assembled using a5 and annotated using the RAST server. Using a combination of the RAST and NCBI BLAST searches of ORFs, two T6SSs were found in *V. fluvialis*, these T6SSs termed VF T6SS1 and VF T6SS2 are shown in Figure 6.7.

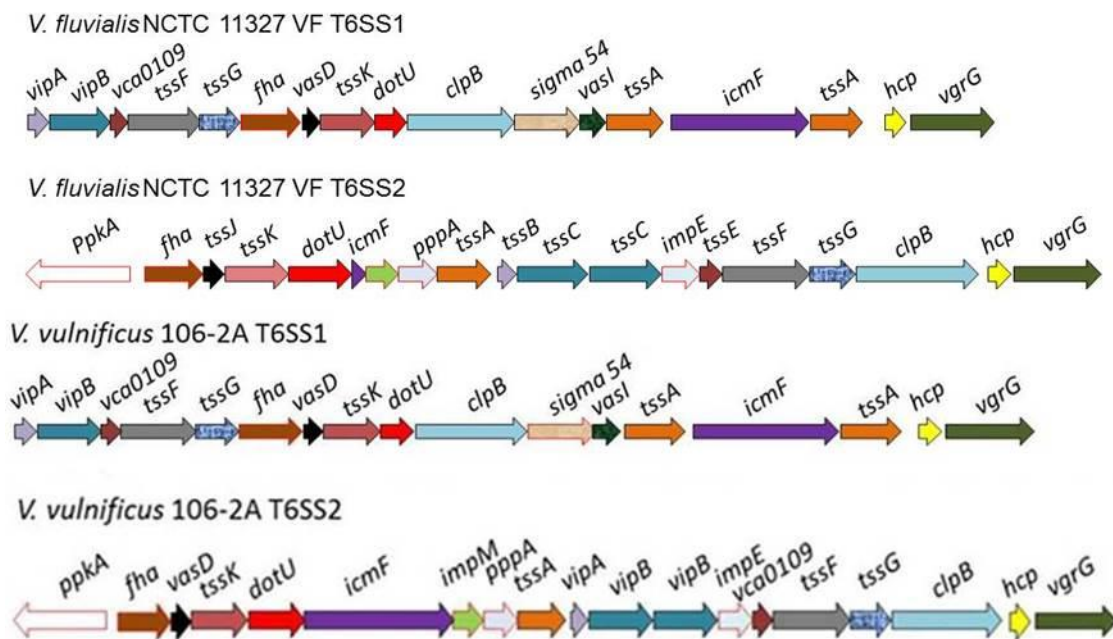


Figure 6.7: The gene organisation of the 2 T6SSs from *V. fluvialis* NCTC 11327. Schematic gene organisation for the 2 T6SSs, denoted VF T6SS1 and VF T6SS2 identified in *V. fluvialis* NCTC 11327 by RAST annotation of assembled WGS scaffolds. For comparison the T6SS1 and T6SS2 from *V. vulnificus* 106-2A is also shown.

The gene organisations of the T6SSs in *V. fluvialis* were compared to the genetic organisation of the T6SSs in *V. vulnificus*. This demonstrated a high degree of synteny between the two secretion systems. For example, *V. fluvialis* contains a T6SS, denoted VF T6SS1 (Figure 6.7) that was identical in gene organisation to T6SS1 of *V. vulnificus*. The second T6SS identified in *V. fluvialis*, denoted VF T6SS2 (Figure 6.7) had synteny with the T6SS2 of *V. vulnificus*. However the *icmF* gene in the second secretion system identified in *V. fluvialis* contained an uncharacteristically short *icmF* gene.

In conclusion, the current study has shown that *V. vulnificus* is able to target *V. fluvialis* at 30°C in a T6SS1 dependent manner. However, inactivation of the T6SS1

by way of an in frame deletion to the *icmF* gene renders the secretion system non-functional, allowing for *V. fluvialis* to target *V. vulnificus* at 37°C. This was demonstrated as following co-incubation of TCBS enumeration plates at 37°C, the study was unable to recover *V. vulnificus* Δ T6SS1 cells. However, when the strains were engineered to harbour antibiotic resistance and enumerated separately on antibiotic selection plates, *V. fluvialis* was no longer able to target *V. vulnificus* Δ T6SS1. In light of these findings the study performed WGS on *V. fluvialis* NCTC 11327, as it was hypothesised that the targeting ability of *V. fluvialis* may be due to a T6SS. Analysis of WGS data demonstrated that *V. fluvialis* contained two T6SSs, termed VF T6SS1 and VF T6SS2. Although this study has demonstrated that *V. fluvialis* contains two T6SSs, further investigation is needed to determine whether they are functional. In addition, mutagenesis studies would need to be performed to determine whether the targeting of *V. vulnificus* by *V. fluvialis* is due to VF T6SS1, VF T6SS2, a combination of both, or an alternative factor.

6.2.4 The T6SS1 of *V. vulnificus* 106-2A is involved in killing non-*Vibrio* species

The demonstrated ability of T6SS1 from *V. vulnificus* to target a T6SS1 negative *V. vulnificus* strain and other *Vibrio* species, led to the hypothesis that the T6SS1 may also be able to target other non-*Vibrio* species. To test this hypothesis, co-culture killing assays were performed with *B. thailandensis* as prey. Enumeration of *V. vulnificus* was performed on TCBS agar plates. *B. thailandensis* was engineered to harbour chloramphenicol resistance by the introduction of the plasmid pBHR-RFP and was enumerated on chloramphenicol plates. This was done as TCBS does not support the growth of *B. thailandensis* and *V. vulnificus* cannot grow in the presence of chloramphenicol. Fold change in recovered viable cfu/mL for *B. thailandensis* following co-culture with either *V. vulnificus* 106-2A wild-type, Δ T6SS1 or Δ T6SS2 is presented in Figure 6.8.

The results show that T6SS1 is able to successfully target *B. thailandensis* in T6SS1 dependent manner. The results indicate that the killing is due to T6SS1 and not T6SS2 as there is no significant difference between the survival of *B. thailandensis* when it is co-cultured with either 106-2A wild-type or Δ T6SS2. Additionally shown in Figure 6.8 is the fold change in growth of *V. vulnificus* strains when co-cultured with *B. thailandensis*. The results show that *V. vulnificus* is able to survive in the presence

of *B. thailandensis* as there is an increase in the fold change of recovered viable cells for all the *V. vulnificus* strains tested. The raw data for Figure 6.8 is presented in Figure 6.9.

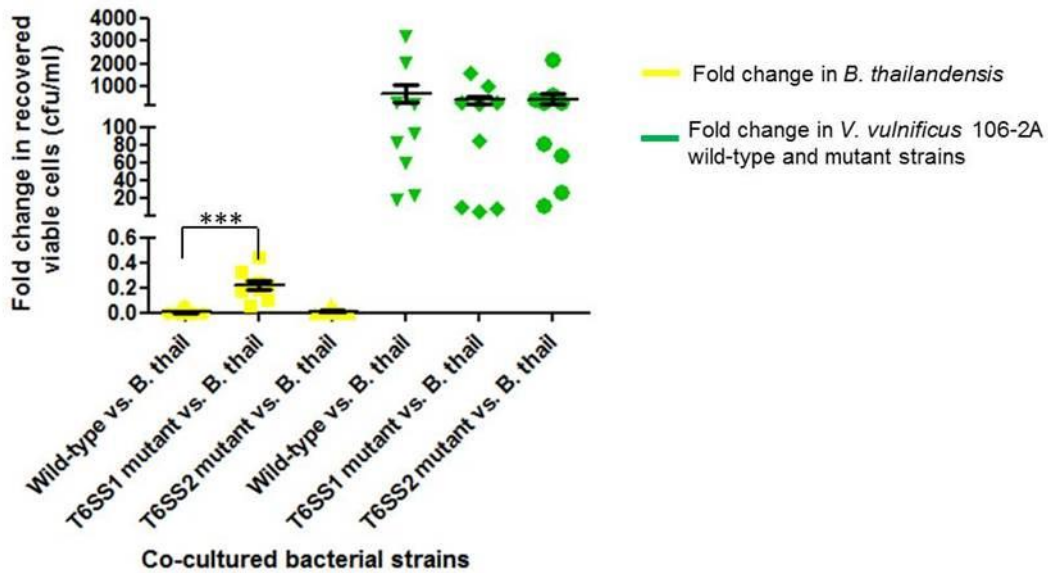


Figure 6.8: The T6SS1 from *V. vulnificus* 106-2A is able to target *B. thailandensis* E264 during a co-culture assay. The fold change in the recovery (cfu/ml) of the prey strain, *B. thailandensis* is shown in yellow when co-cultured with either *V. vulnificus* 106-2A wild-type, Δ T6SS1 mutant or Δ T6SS2 mutant, the x-axis displays strain used in a single co-culture assay. Shown in green is the fold change in recovery for the attacker strains, *V. vulnificus* 106-2A wild-type, Δ T6SS1 mutant or Δ T6SS2 mutant. Assays were performed three times in triplicate, each spot on the graph represents a co-culture killing assay and error bars show standard error of the mean. Statistics were performed using the unpaired two-way Student's t-test, *** $P < 0.0005$.

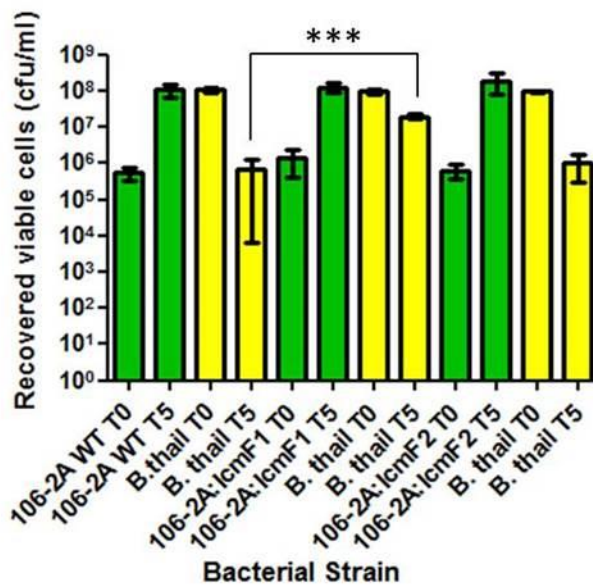


Figure 6.9: T6SS1 from *V. vulnificus* 106-2A is able to target *B. thailandensis*. Co-culture assay using the attacker strains, *V. vulnificus* 106-2A wild-type (106-2A WT), Δ T6SS1 mutant (106-2A:lcmF1), Δ T6SS2 mutant (106-2A:lcmF2) shown in green and the prey strain, *B. thailandensis* (B. thail) shown in yellow. Shown in green are the results gained for the attacker strains at T0 and T5 and shown in yellow are the results for the prey strain at T0 and T5. To the right of each attacker strain shown in green is the corresponding prey strain shown in yellow. Results show *B. thailandensis* survives significantly better when cultured with Δ T6SS1 mutant compared to 106-2A wild-type strain. Experiments were performed three times in triplicate, error bars show standard error of the mean. Statistics were performed using the unpaired 1-way Student's t-test, * $P < 0.0005$.

6.2.5 *V. vulnificus* contains alternative mechanisms for attacking *B. thailandensis* other than T6SS1

Although the results shown in section 6.2.4 demonstrate that *V. vulnificus* can target *B. thailandensis* in a T6SS1 dependent manner, it was noted that the fold-change in growth for *B. thailandensis* was much lower than for the fold change in growth of *V. fluvialis* as shown in Figure 6.1. Therefore the study hypothesised that *V. vulnificus* may produce effectors other than those secreted by T6SS1 that may target *B. thailandensis*. To test this hypothesis a negative control was also assayed, this was where *B. thailandensis* was mixed with LB in place of the attacker strain. The study did not include the Δ T6SS2 mutant in the assay as according to the data shown in Figure 6.6, targeting of *B. thailandensis* by *V. vulnificus* 106-2A is due to T6SS1 and not T6SS2. The graph in Figure 6.10 shows the fold change in recovered viable cells when *B. thailandensis* is co-cultured with either *V. vulnificus* 106-2A wild-type, Δ T6SS1 and LB media (negative control). The raw data for the graph shown in Figure 6.10 is presented in Figure 6.11.

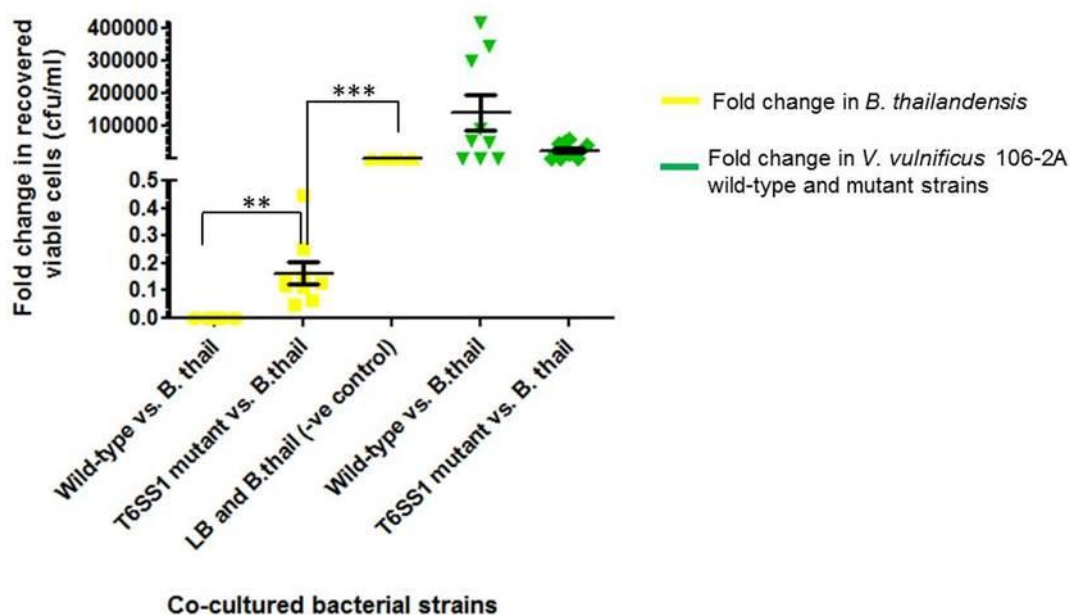


Figure 6.10: Co-culture killing assay with *V. vulnificus* and *B. thailandensis* with a 24 hour incubation period. The fold change in recovery (cfu/ml) of the prey strain, *B. thailandensis* is shown in yellow when co-cultured with either *V. vulnificus* 106-2A wild-type, Δ T6SS1 mutant or LB as a negative control. Shown in green is the fold change in recovery of the attacker strains, *V. vulnificus* 106-2A wild-type and Δ T6SS1 mutant. Assays were performed three times in triplicate, each spot on the graph represents a co-culture killing assay and error bars show standard error of the mean. Statistics were performed using the unpaired two-way Student's t-test, ** $P < 0.005$, *** $P < 0.0005$.

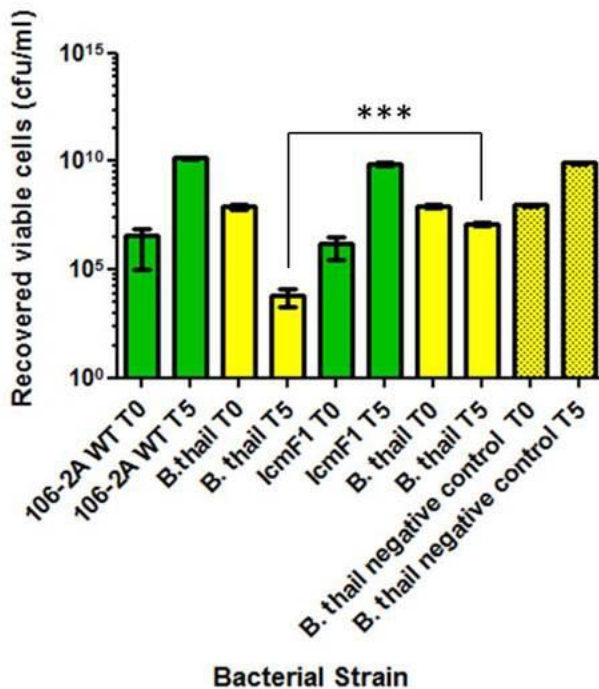


Figure 6.11: Co-culture killing assay with *V. vulnificus* and *B. thailandensis* with a 24 hour incubation period. Co-culture assay using the attacker strains, *V. vulnificus* 106-2A wild-type (106-2A WT) and Δ T6SS1 mutant (106-2A:lcmF1) shown in green and the prey strain, *B. thailandensis* (B. thail) shown in yellow were performed for 24 hours. Shown in green are the results gained for the attacker strains at T0 and T24 and shown in yellow are the results for the prey strain at T0 and T24. To the right of each attacker strain shown in green is the corresponding prey strain shown in yellow. Results show *B. thailandensis* survives significantly better when cultured with Δ T6SS1 mutant compared to 106-2A wild-type strain, however residual prey *B. thailandensis* is still able to survive following a longer incubation period. Experiments were performed three times in triplicate, error bars show standard error of the mean. Statistics were performed using the unpaired 1-way

Student's t-test, * $P < 0.0005$.

The results in Figure 6.10 show the survival of *B. thailandensis* is significantly greater when co-cultured with the T6SS1 mutant compared to the wild-type strain. Furthermore, comparison of the *B. thailandensis* negative control compared with *B. thailandensis* recovery when cultured with Δ T6SS1, shows that *B. thailandensis* is able to survive significantly better in the negative control. This suggests that *V. vulnificus* may produce other factors other than T6SS1 effectors that can target *B. thailandensis*; furthermore the negative control demonstrates that the reduction of *B. thailandensis* when co-cultured with the wild-type strain is due to *V. vulnificus* and not due to the assay conditions.

Secondary to the negative control, the study increased the co-culture incubation period from five hours to 24 hours. This was done as it was noted that following co-culture with *V. vulnificus* 106-2A wild-type there was residual *B. thailandensis* cells that were able to survive the co-culture period. A result which was seen in the majority of co-culture assays performed in this study. Therefore the current study hypothesised that a longer co-incubation may remove the ability of residual prey cells to survive. This hypothesis was tested by incubating the co-culture cells for 24 hours instead of five hours. However, the image in Figure 6.10 shows that a longer incubation period does not improve the killing ability of *V. vulnificus* 106-2A wild-type

as residual *B. thailandensis* cells are still recovered, as seen in Figure 6.10 and Figure 6.11.

In conclusion this study has shown that the T6SS1 of *V. vulnificus* can target both *Vibrio* and non-*Vibrio* species, allowing T6SS1 positive *V. vulnificus* cells to partake in both intra and inter-species targeting. The study has additionally demonstrated that *V. vulnificus* can produce effectors other than T6SS1 effectors which are able to target alternative Gram negative bacterial species.

6.2.9 The effects of *V. vulnificus* T6SS2 on *Galleria mellonella*

As the T6SS1 from *V. vulnificus* 106-2A had been shown to efficiently target prokaryotic cells, it was questioned whether T6SS2 from *V. vulnificus* 106-2A was able to target eukaryotic cells. To test this hypothesis the infection model *G. mellonella* was used. Preliminary experiments, demonstrated that *V. vulnificus* was virulent towards *G. mellonella* when challenged using a bacterial load $\sim 10^7$ cfu/10 μ l at 37°C in 24 hours, therefore a bacterial load of 10^5 cfu/10 μ l was used to challenge *G. mellonella* in further studies. The lower dose was used to ensure not all strains were killed rapidly to allow an assessment of killing over a longer period of time. The infection was carried out at 37°C and not 30°C as a preliminary study shown in Appendix A8 with one time point assayed at 24 hours, demonstrated that the T6SS2 mutant was attenuated at 37°C but not at 30°C. To further validate the results seen in the preliminary infection model a full infection study was carried out. The infection study was repeated three times and with groups of ten larvae used for each strain, larvae were monitored for death at time points, 24, 30 and 48 hours post challenge. Death was assessed by an unresponsiveness to touch.

The survival graph shown in Figure 6.12 illustrates the data gained for the infection study using *V. vulnificus* 106-2A wild-type and the Δ T6SS1 and Δ T6SS2 mutants, Δ T6SS1 was included as a control.

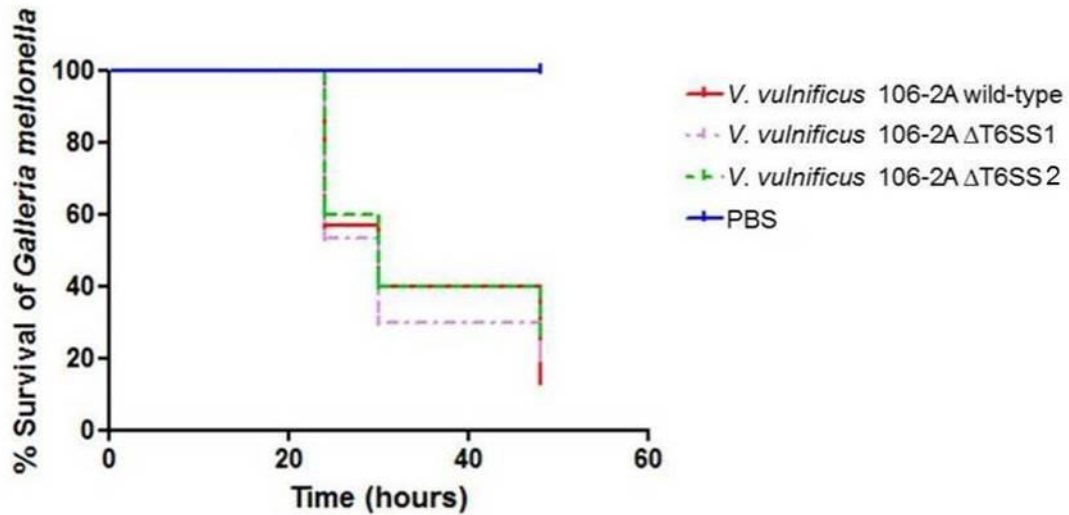


Figure 6.12: *Galleria mellonella* infection study using *V. vulnificus* 106-2A wild-type and T6SS1 and T6SS2 mutants incubated at 37°C. The survival graph demonstrates the survival (%) of *G. mellonella* following challenge with either *V. vulnificus* 106-2A wild-type or the ΔT6SS1 mutant or ΔT6SS2 mutant. *G. mellonella* were challenged with 10⁵ cfu/ml of each strain which had been grown to mid-log phase at 37°C. Shown in blue is *G. mellonella* survival following PBS injection. Larvae were assessed for death at T24, T30 and T48 hours. Experiments were performed three times where n=10.

The results indicate that although preliminary studies suggested that ΔT6SS2 may be attenuated compared to the wild-type strain when incubated at 37°C, repeats of this study show that neither ΔT6SS1 nor ΔT6SS2 are attenuated at 37°C compared to the wild-type strain, as there is no statistically significant difference between the strains. All of the *G. mellonella* injected with PBS as a negative control survived, which demonstrate that the effects seen in the infected galleria are due to the bacteria and are not due to any of the other effects from the study such as the injecting process.

6.3 Discussion

Using a co-culture assay Chapter five demonstrated that T6SS1 of *V. vulnificus* 106-2A can target the T6SS1 negative *V. vulnificus* strain, 99-743. It was therefore hypothesised that T6SS1 may also be able to target alternative Gram negative bacteria. To test this, the study explored the ability of T6SS1 to target the alternative *Vibrio* species, *V. fluvialis* NCTC 11327 and the alternative Gram negative species, *B. thailandensis*. The study included the ΔT6SS2 mutant as a control in all co-culture assays as it was further speculated that T6SS1 may be specific to targeting *V. vulnificus* and T6SS2 may be involved with targeting alternative Gram negative species.

The results from the co-culture assays demonstrated that T6SS1 was responsible for targeting *V. fluvialis* at 30°C, however T6SS2 was not. The presented data further revealed that at 37°C *V. fluvialis* can target Δ T6SS1 *V. vulnificus* cells. As co-enumeration of *V. fluvialis* and *V. vulnificus* Δ T6SS1 on TCBS enumeration plates demonstrated that *V. vulnificus* Δ T6SS1 was unable to survive, as no cells were recovered on the enumeration plates. However, when the cells were engineered to contain antibiotic resistance plasmids and the cells were enumerated separately, the study was able to recover *V. vulnificus* Δ T6SS1 cells. Therefore, the study hypothesised that *V. fluvialis* may contain a T6SS that could target *V. vulnificus* at 37°C when *V. vulnificus* T6SS1 is inactive. To identify whether *V. fluvialis* contained a T6SS, WGS and gene annotation was performed. This revealed that *V. fluvialis* contains two T6SSs, termed VF T6SS1 and VF T6SS2, both of which share synteny to the genetic organisation of T6SS1 and T6SS2 from *V. vulnificus*. A literature search on *V. fluvialis* and secretion systems found that a bioinformatic study has previously described the presence of the T6SS in *V. fluvialis* [318]. However, whether the T6SS is functional remains to be elucidated as the study did not follow up the findings with functionality tests. Therefore, although it is possible that the T6SSs encoded by *V. fluvialis* may be targeting *V. vulnificus* at 37°C, further mutagenesis studies in *V. fluvialis* would need to be performed to test whether the secretion systems are functional at 37°C and whether they are able to target *V. vulnificus* cells.

Ingestion of *V. vulnificus* can lead to life threatening septicaemia that can progress to death [20, 36]. *V. fluvialis* on the other hand, is more commonly associated with occasional diarrhoeal diseases, and is very rarely associated with septicaemia [318, 319]. *V. vulnificus* infection is often correlated with the consumption of raw or uncooked oysters [36], in addition to oysters containing *V. vulnificus*, oysters are also known to harbour the pathogen, *V. fluvialis* [319-321]. It is also documented in the literature that oysters are often colonised by a mixture of *Vibrio* species and not one particular strain [13, 319, 320]. As *V. fluvialis* can target *V. vulnificus* at 37°C, this also may provide a possible explanation of why there are relatively few serious *V. vulnificus* infections compared to the natural prevalence of this bacterium in the environment.

For example, if the majority of the *V. vulnificus* strains in the environment are T6SS1 negative, then upon human ingestion of an oyster contaminated with both *V. vulnificus* and *V. fluvialis*, the temperature would be elevated to 37°C, a temperature at which *V. fluvialis* can target *V. vulnificus*. Once inside a human *V. fluvialis* may target *V. vulnificus*, which may lead to control of *V. vulnificus* within the host, which may contribute to the low levels of *V. vulnificus* disease observed. These claims however would need to be further assessed by carrying out experimental work to understand the role of the T6SS *in vivo* in both an oyster and human model of infection.

In addition to demonstrating the ability of T6SS1 to target alternative *Vibrio* species, the current study also demonstrated that the T6SS1 of *V. vulnificus* 106-2A was able to target non-*Vibrio* species, by performing co-culture assays with the prey strain, *B. thailandensis*. These studies showed that *V. vulnificus* 106-2A was able to target *B. thailandensis* in a T6SS1 dependent manner. Furthermore the current study also showed that *V. vulnificus* produces effectors other than T6SS1 effectors that are able to target *B. thailandensis* in an antagonistic manner.

The literature describes *B. thailandensis* as containing 5 T6SSs [248]. The T6SS1 and T6SS5 of *B. thailandensis* have distinct roles in pathogenicity, with T6SS1 involved in targeting prokaryotic cells and T6SS5 involved in targeting eukaryotic cells [248]. Although the T6SS1 of *B. thailandensis* can efficiently target bacteria species such as *Pseudomonas putida*, *Pseudomonas fluorescens* and *Serratia proteamaculans*, it was unable to successfully target *Vibrio* species such as *V. cholerae* and *V. parahaemolyticus* [248]. Therefore it is unsurprising that *V. vulnificus* was also not targeted by *B. thailandensis*. However, *V. vulnificus* could target *B. thailandensis*. The results in the current assay are comparable to the *B. thailandensis* data presented by Schwarz *et al.*, [248] as the competition assays were both performed at 30°C and therefore it cannot be said that it is unlikely that the T6SS of *B. thailandensis* is inactive due to difference temperatures [248]. In addition to demonstrating that the T6SS1 of *V. vulnificus* could target *B. thailandensis* the assay conditions demonstrated that there was a significant difference in the survival of *B. thailandensis* when it was grown with either LB alone or the T6SS1 mutant. This would suggest that there are other factors produced by *V. vulnificus* other than

T6SS1 effectors that can target *B. thailandensis*. This is unsurprising as it has been shown that different bacterial species produce an array of antimicrobial compounds other than effectors from the T6SS that are involved with targeting other bacterial cells [322, 323].

To further characterise the T6SSs in *V. vulnificus*, the wild-type strain, 106-2A and Δ T6SS1 and Δ T6SS2 mutants were assayed in a eukaryotic model of infection. As previous literature reports have demonstrated that the T6SS is able to target eukaryotic cells [231, 237, 245, 274]. Therefore, the current study investigated the anti-eukaryotic properties of T6SS2 using a *G. mellonella* model of infection, as it was hypothesised that like *B. thailandensis*, the two T6SSs in *V. vulnificus* 106-2A may have distinct roles in virulence. Whereby T6SS1 is involved with targeting prokaryotic cells and T6SS2 is involved with targeting eukaryotic cells. However, the results from the current study demonstrated that *V. vulnificus* T6SS2 was not virulent towards *G. mellonella*, the Δ T6SS1 mutant was also assayed as a control which had no effect on the *G. mellonella*. This is unsurprising as T6SS1 is inactive at 37°C, furthermore the results for T6SS1 are in agreement with previously published data for *S. marcescens*, which demonstrated that the anti-prokaryotic T6SS of *S. marcescens* is ineffective at targeting *G. mellonella* [234].

6.4 Conclusion

In conclusion, the current study has shown that *V. vulnificus* 106-2A can utilise its T6SS1 to target a range of Gram negative bacterial species, such as *B. thailandensis* and *V. fluvialis*. However the study further demonstrated that at 37°C a Δ T6SS1 mutant of *V. vulnificus* 106-2A can be targeted by *V. fluvialis*. WGS sequencing of this *V. fluvialis* strain demonstrated that *V. fluvialis* encodes two T6SSs, which share synteny with T6SS1 and T6SS2 of *V. vulnificus*. However, further mutagenesis research would be required to elucidate if these secretion systems are targeting *V. vulnificus* at 37°C.

In addition to testing the anti-prokaryotic abilities of T6SS1, the anti-eukaryotic effects of T6SS1 and T6SS2 were also tested in the eukaryotic infection model, *G. mellonella*. However the results demonstrated that neither a Δ T6SS1 or Δ T6SS2 mutant was attenuated for virulence.

Following on from the characterisation of T6SS1, complementation of the *icmF* gene was attempted, this was done to understand if *in trans* complementation of the *icmF* gene restored the Δ T6SS1 mutant phenotypes to wild-type levels.

Chapter 7 Complementation of T6SS1 in *V. vulnificus* 106-2A

7.1 Introduction and aim

The current study generated in-frame *icmF* deletion mutants in T6SS1 and T6SS2 in *V. vulnificus* 106-2A. The Δ T6SS1 mutant was used in Western blot experiments to attribute the secretion of the hall mark Hcp protein in 106-2A wild-type to T6SS1. Furthermore, the Δ T6SS1 mutant was used in several co-culture assays to demonstrate that the T6SS1 of *V. vulnificus* 106-2A is responsible for targeting several different Gram negative species.

To confirm that the phenotypic effects seen in the Δ T6SS1 mutant were due to the in-frame deletion of *icmF*, the Δ T6SS1 mutant strain was complemented with a wild-type copy of the *icmF* gene. Previous T6SS complementation studies in *V. cholerae* have demonstrated that an *icmF* deletion mutant was successfully complemented using the arabinose inducible expression vector, pBAD24 [231]. Therefore the current study aimed to complement 106-2A Δ T6SS1 using a similar approach.

7.2 Results

7.2.1 Construction of a complementing plasmid, pSRC14

The current study utilised the expression vector, pBAD24 for complementation. This method was chosen as an *icmF* deletion mutant in *V. cholerae* V52 was successfully complemented using a pBAD24 derivative plasmid [245, 295]. The pBAD24 vector contains the P_{BAD} promoter allowing for the controlled expression of proteins. In addition, the vector contains a Shine-Dalgarno ribosome binding site and a start codon. To construct the pBAD24 complement vector the wild-type *icmF* gene was amplified from *V. vulnificus* 106-2A using the primers, *icmF1* Final F pBAD *Sma*I and *icmF1* Final R pBAD *Sph*I, as shown in Figure 7.1.

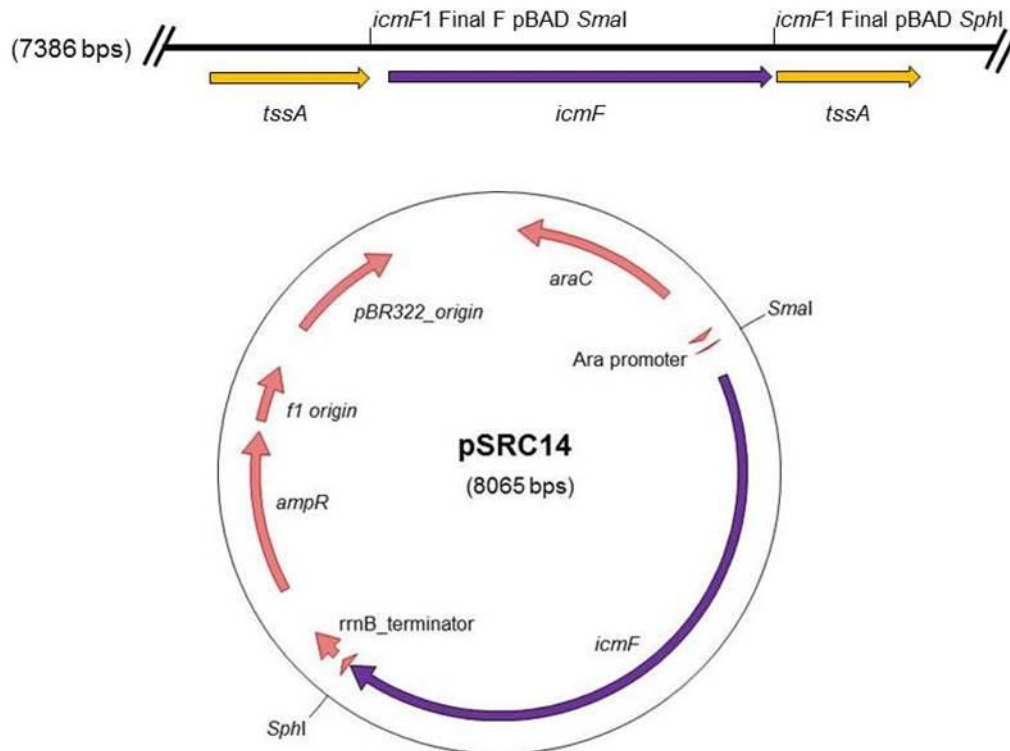


Figure 7.1: Construction of the complement plasmid, pSRC14. The complementation plasmid, pSRC14 was generated by amplifying the *V. vulnificus* 106-2A wild-type *icmF* gene using the primers indicated. The correctly sequenced *icmF* gene was ligated into pBAD24, following digestion of the pBAD24 vector with *SmaI* and *SphI* restriction enzymes. The resulting complement vector, pSRC14 is shown.

The ~3500bp *icmF* gene from T6SS1 was amplified using the KOD Xtreme™ Hot Start DNA Polymerase, which enables amplification of long DNA templates. Following PCR amplification, the gel purified *icmF* gene was A-tailed as detailed in the Materials and Methods and ligated into the pGEM-T-easy holding vector, to produce pSRC13. pSRC13 was then sequenced. To ensure the entire length of the *icmF* was fully sequenced, a primer walking method was utilised using the primers, Seq_1 - Seq_5, including M13F, M13R, *icmF1* Final F pBAD *SmaI* and *icmF1* Final R pBAD *SphI*. Correctly sequenced *icmF* regions were then digested with *SmaI* and *SphI* and ligated into *SmaI* and *SphI* digested pBAD24. These ligations were then transformed into *E. coli* S17 cells.

Potential *E. coli* clones containing pSRC14 (Figure 7.1) were checked by a restriction digest on the mini-prepped plasmids using *SmaI* and *SphI*. The digestion profile shown in Figure 7.2, demonstrates that 6 clones tested gave the correct

digestion profile. The 3554bp band corresponds to the *icmF* gene, with the pBAD24 backbone producing a 4511bp band.



Figure 7.2: Gel electrophoresis image of the digestion profile for pSRC14 using *SmaI* and *SphI*. An uncut control of each pSRC14 clone is shown in lanes 1, 5, 9, 13, 17 and 21. A corresponding double digest, using *SmaI* and *SphI* is shown to the right of each uncut plasmid, lanes, 2, 6, 10, 14, 17 and 22. Control single digests are also shown to the right of each double digest using *SmaI* or *SphI*, demonstrating that both enzymes cut. The DNA ladder marker used is indicated with (M). Double digests produce the 3554bp and 4511bp bands, which correspond to the *icmF* gene and pBAD24 backbone respectively. Singularly cut pSRC14 produces a band 8065bp.

pSRC14 was then conjugated into *V. vulnificus* 106-2A Δ T6SS1 using the helper strain *E. coli* pRK2013. Following conjugation, potential *V. vulnificus* clones containing pSRC14 were checked by PCR. Figure 7.3 is a gel electrophoresis image of a PCR carried out using the primers *icmF1* Final F pBAD *SmaI* and *icmF1* Final R pBAD *SphI* on mini-preps from two complemented clones. This PCR amplified the wild-type *icmF* gene from the plasmid DNA (Figure 6.3, lanes 1 and 2). In addition, the truncated mutated *icmF* gene from the mutant's gDNA was also amplified (Figure 7.3, lanes 1 and 2), indicating that some gDNA also came through in the plasmid preparation. This produced two bands as seen in the gel electrophoresis image in Figure 7.3. This result confirms the successful construction of a complementing strains containing, pSRC14.

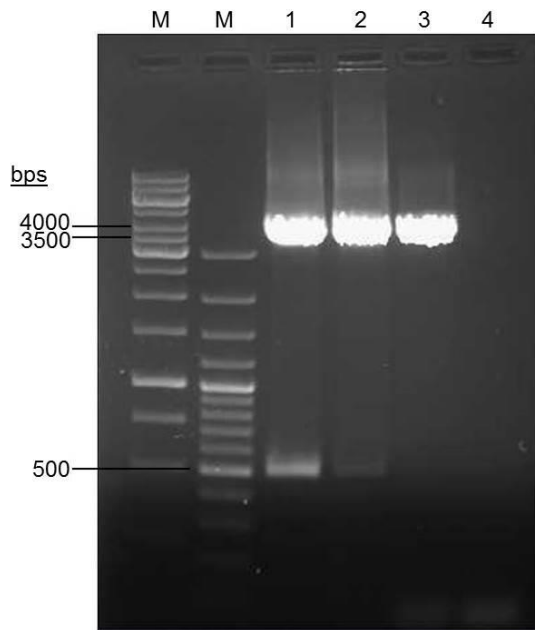


Figure 7.3 Gel electrophoresis image of a PCR carried out on *V. vulnificus* 106-2A Δ T6SS1 clones containing pSRC14. Lanes 1 and 2 show the amplification of the wild-type *icmF* gene, 3554bp in length from plasmid DNA. In addition, the truncated *icmF* gene, 497bp in length was amplified from the gDNA which was pulled through during the plasmid preparation. A positive control run in lane 3 is wild-type gDNA showing the amplification of the wild-type *icmF* gene. Lane 3 is a negative control. Lanes M contain the DNA ladders.

7.2.2 Complementation of Δ T6SS1 with pSRC14.

To assess whether pSRC14 complemented *V. vulnificus* 106-2A Δ T6SS1, Western blotting using the Hcp antibody was performed to identify restored Hcp secretion. *V. vulnificus* Δ T6SS1 cells containing pSRC14 were grown as described previously in Chapter five, with the addition of 0.1% w/v arabinose. Cells were grown to mid-log phase and then prepared for protein extraction and Western blotting as detailed in the Materials and Methods.

The Western blot in Figure 7.4 shows that Hcp can be detected in both the cell lysate and the supernatant of *V. vulnificus* 106-2A wild-type (lanes 1 and 2). As seen previously (Figure 5.7) Hcp is only detected in the cell lysate of the 106-2A Δ T6SS1 mutant strain (lanes 3). In lane 8 it can be seen that there appears to be some Hcp in the culture filtrate of Δ T6SS1::pSRC14. This suggests that pSRC14 has successfully complemented the mutation in Δ T6SS1. There is no detection of Hcp in the supernatant for the empty vector control, Δ T6SS1::pBAD24 (lane 6). Therefore Hcp detected in the supernatant of the complement strain can be assumed to be due to complementation by pSRC14.

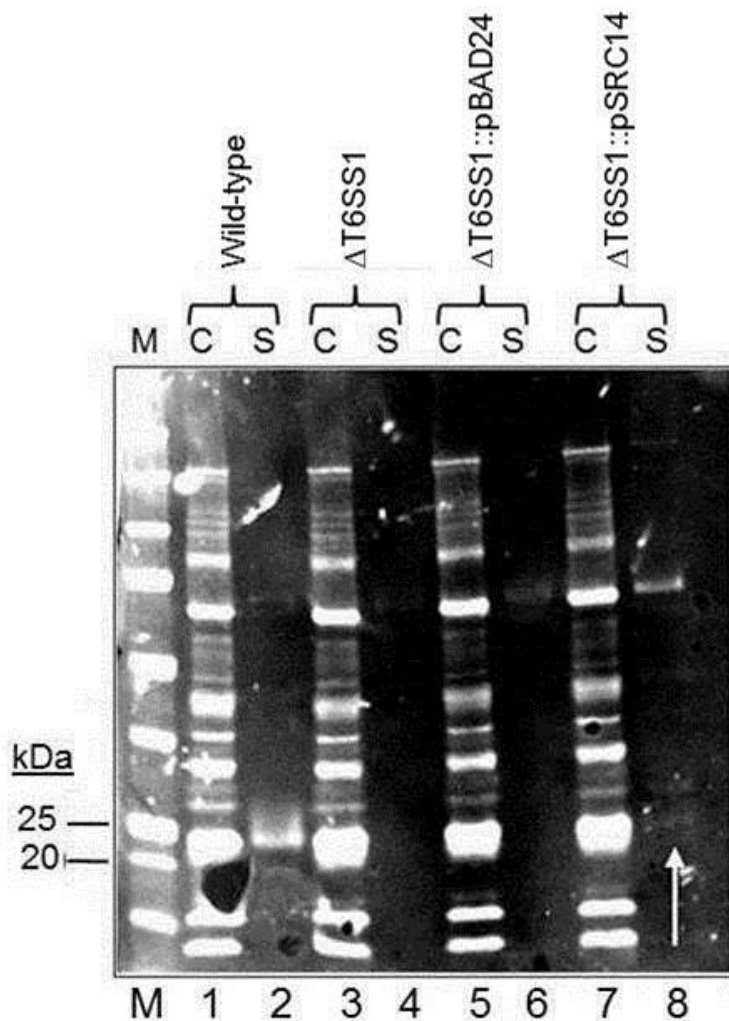


Figure 7.4: Western blot using anti-Hcp antibody to detect Hcp secretion in a $\Delta icmF$ complement strain. *V. vulnificus* cells lysate (C) and culture filtrates (S) from cells grown at 30°C in LB supplemented with 0.1% arabinose. Hcp detection ~23 kDa, Hcp detection in $\Delta T6SS1::pSRC14$ is indicated with a white arrow ~23 ug protein/lane. Corresponding Ponceau S stains shown in Appendix A9. Protein marker is represented with (M).

Figure 7.4 also shows that there is a marked difference in secretion of Hcp between *V. vulnificus* 106-2A wild-type and $\Delta T6SS1::pSRC14$, with the latter having a significantly reduced amount of observed Hcp in the culture filtrate. Therefore the study performed an optimisation experiment to monitor levels of Hcp secretion in $\Delta T6SS1::pSRC14$.

7.2.3 Optimisation of Hcp secretion by 106-2A $\Delta T6SS1::pSRC14$

Optimisation experiments to maximise expression levels of Hcp secretion from $\Delta T6SS1::pSRC14$ were conducted using the following conditions; an overnight culture of the complement strain was back diluted to an OD_{590nm} of 0.03 and then grown to an OD_{590nm} of 0.18. The cells were then induced with 0.1% v/v arabinose and at four and six hours post induction samples were taken for protein preparation as outlined in the Materials and Methods. During the optimisation experiment an additional clone was also included to see if the impaired Hcp secretion seen in the complement strain in Figure 7.4 was due to an irregular clone. The Western blot

image in Figure 7.5 demonstrates the results gained from the optimisation experiment using two different complemented strains.

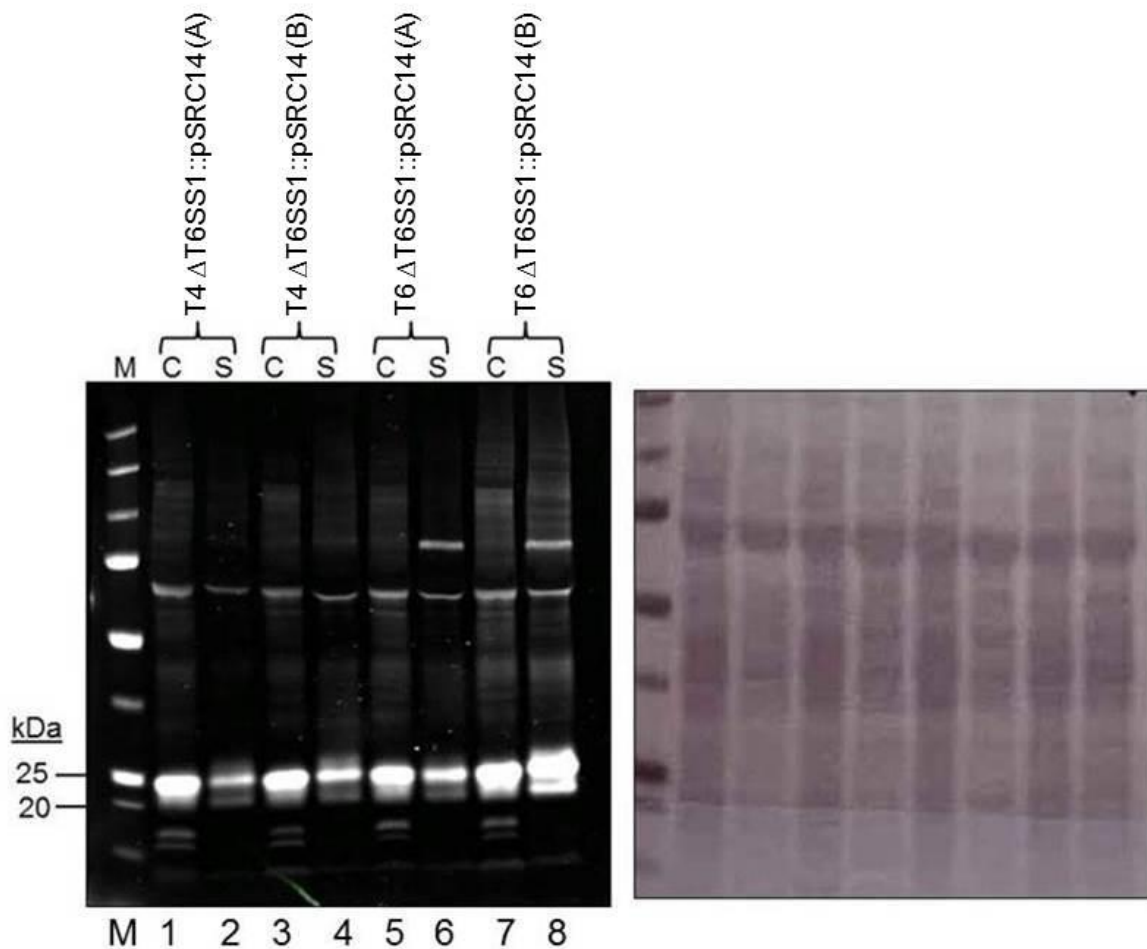


Figure 7.5: Optimisation Western blot using anti-Hcp antibody to detect Hcp secretion in an *icmF* complemented mutant. Cells lysate (C) and culture filtrates (S) from two $\Delta T6SS1::pSRC14$ clones, A and B grown at 30°C in LB supplemented with 0.1% arabinose. T4 and T6, indicated above each lane correspond to samples taken for protein preparation following 0.1% arabinose induction. Hcp detection ~23 kDa, corresponding Ponceau S stains shown. ~30 ug protein/lane. Protein marker is represented with (M).

Analysis of Figure 7.5 shows that Hcp can be detected in both the cell lysate and the supernatant at both T4 and T6 for clones A and B (lanes 1-8). However, at T6 the culture filtrate shows signs of cell lysis, as judged by detection of additional bands in the supernatant that are also present in the cell lysate, which cannot be identified at T4. As there was no clear differences between the clones A and B in terms of levels of Hcp expression, clone A was chosen for further optimisation.

Following on from the initial optimisation experiment, the Western blot was repeated including the strains, 106-2A wild-type, 106-2A $\Delta T6SS1$, $\Delta T6SS1::pBAD24$ as

controls. The 106-2A wild-type, 106-2A Δ T6SS1, 106-2A Δ T6SS1::pBAD24 and 106-2A Δ T6SS1::pSRC14 were grown in LB alone to an OD_{590nm} of 1.5 and proteins extracted, no arabinose was added to the media. The complement and empty vector strains however were induced with 0.1% arabinose at an OD_{590nm} of 0.18 and grown to an OD_{590nm} 3.0, which is the OD at four hour post induction.

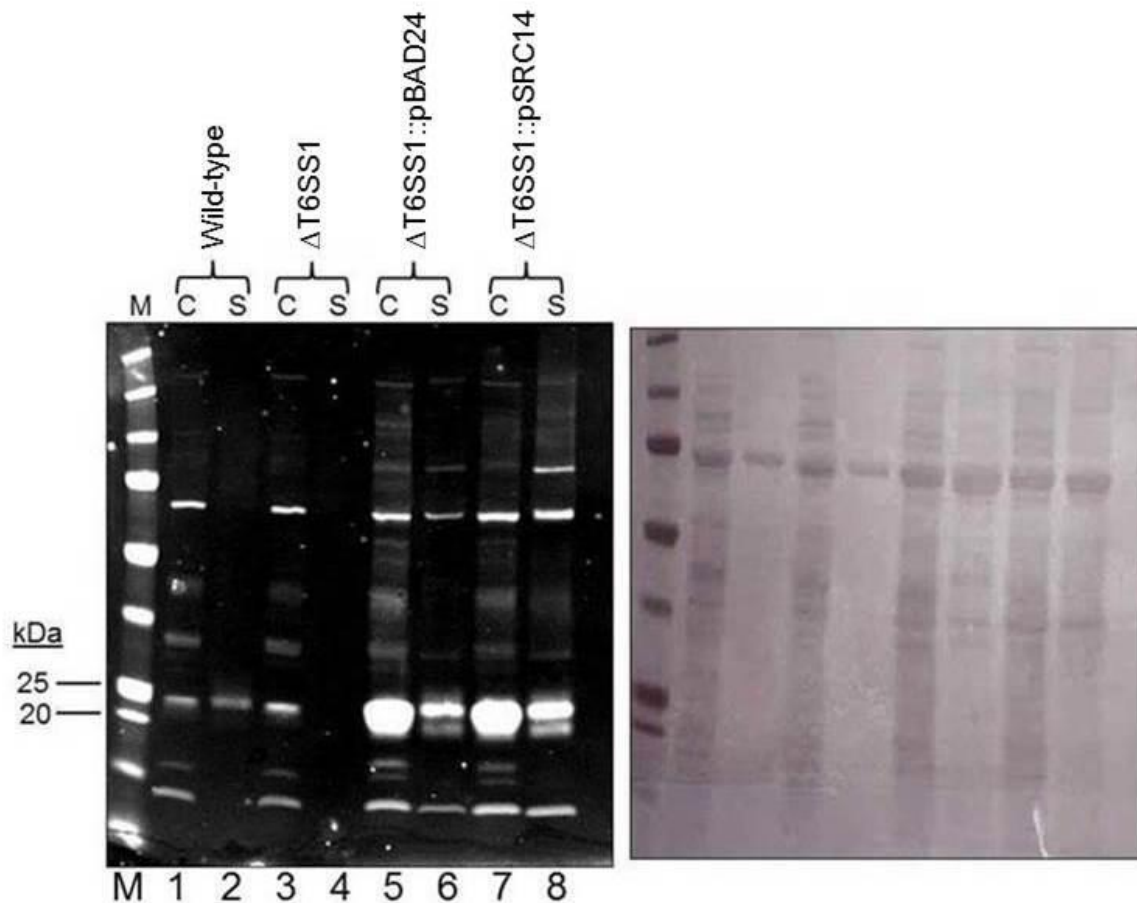


Figure 7.6: Western blot using anti-Hcp antibody to detect Hcp secretion. *V. vulnificus* cells lysate (C) and culture filtrates (S) from cells grown at 30°C in LB, Δ T6SS1::pBAD24 and Δ T6SS1::pSRC14 were induced with 0.1% arabinose. Hcp can be detected at ~23 kDa, corresponding Ponceau S is shown, ~30 ug protein/lane. Protein marker is represented with (M). Indicated above each lane are the samples run in each lane. Image is a representative Western blot carried out on protein extractions from two independent experiments.

The results in Figure 7.6 show Hcp is detected in the cell lysate and the supernatant of the 106-2A wild-type strain (lanes 1 and 2), whereas Hcp is only detected in the cell lysate for the Δ T6SS1 mutant (lane 3). On analysis of the T6SS1 complement strain, Δ T6SS1::pSRC14 there was detection of Hcp in both the cell lysate and supernatant (lanes 7 and 8), indicating potential complementation. However, analysis of the empty vector strain, Δ T6SS1::pBAD24, also showed detection of Hcp both in the cell lysate and the supernatant (lanes 5 and 6). This was an unexpected

result as the empty vector strain should give results akin to the $\Delta T6SS1$ mutant. Further evaluation of the Western blot in Figure 7.6 also shows a higher detection of Hcp in the supernatant of $\Delta T6SS1::pSRC14$ and $\Delta T6SS1::pBAD24$ compared to the wild-type strain. A possible explanation for this increase in Hcp detection maybe due to growth at a higher OD for $\Delta T6SS1::pSRC14$ and $\Delta T6SS1::pBAD24$ compared to the wild-type and mutant strain. Although there is equal loading of total protein for each sample on the Western blot, as demonstrated by the Ponceau S stain, there is a higher abundance of certain proteins. For example, the prominent higher molecular weight band which is detected in the Ponceau S stain is more prominent for samples grown to a higher OD. Due to the detection of Hcp in the supernatant of $\Delta T6SS1::pBAD24$, the Hcp identified in $\Delta T6SS1::pSRC14$ could not be assumed to be due to the *in trans* complementation of the *icmF* mutation.

Investigative work to ensure that pBAD24 had been transformed into the $\Delta T6SS1$ mutant strain was conducted by PCR. Primers *icmF1* Final F pBAD *SmaI* and *icmF1* Final R pBAD *SphI* were used on gDNA extracted from two different stocks of $\Delta T6SS1::pBAD24$ to ensure the strains were of T6SS1 background. Figure 7.7 shows the amplification of the truncated version of *icmF*, demonstrating that $\Delta T6SS1::pBAD24$ is indeed a T6SS1 mutant. Proteins were again extracted from both these two stocks as described previously and Hcp secretion monitored by Western blotting. The Western blot image shown in Figure 7.8 clearly identified Hcp detection in the supernatant of both stocks.



Figure 7.7: Gel electrophoresis image of a PCR carried out on *V. vulnificus* 106-2A Δ T6SS1 pBAD24. The gel electrophoresis image shows a PCR carried out using the primers *icmF1* Final F pBAD SmaI and *icmF1* Final R pBAD SphI on gDNA extracted from *V. vulnificus* 106-2A Δ T6SS1 pBAD24. The image shows the truncated *icmF* gene is amplified at 497bp in *V. vulnificus* 106-2A Δ T6SS1 pBAD24, in lanes 1 and 2. This demonstrates that the empty vector strain, *V. vulnificus* 106-2A pBAD24, is indeed a mutant and does not contain a copy of the wild-type gene. As a control gDNA was also extracted from *V. vulnificus* 106-2A wild-type demonstrating the amplification of the wild-type gene at 3554bp in lane 3, a negative control was also run in lane 4 demonstrating no amplification of any bands. The 100bp plus ladder is indicated in lane M, with the sizes at 4000bps, 3500bps and 500bps indicated, bps= base pairs.

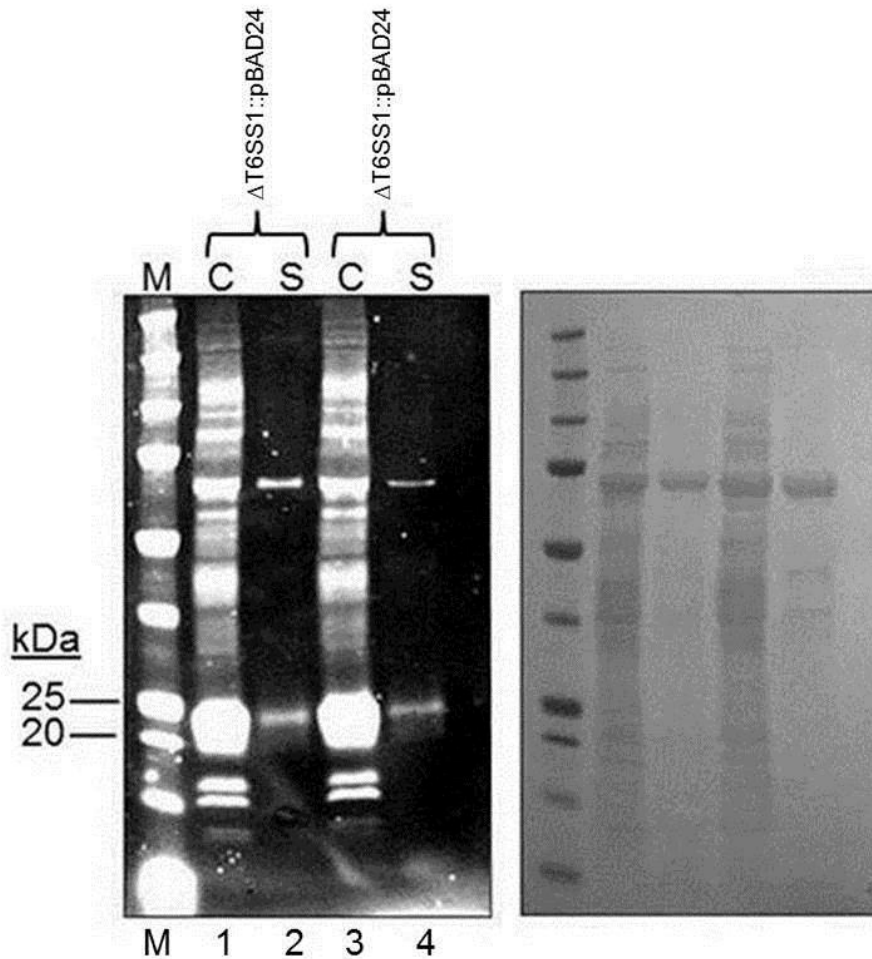


Figure 7.8: Western blot using anti-Hcp antibody to detect Hcp secretion in *V. vulnificus* 106-2A Δ T6SS1::pBAD24. Cells lysate (C) and culture filtrates (S) from *V. vulnificus* 106-2A Δ T6SS1::pBAD24 cells from two separate stocks grown at 30°C in LB supplemented with 0.1% arabinose. Hcp can be detected at ~23 kDa, corresponding Ponceau S is shown. Protein marker is represented with (M).

7.2.4 Analysis of *icmF* transcription from T6SS1

Investigative PCRs had demonstrated that $\Delta T6SS1::pBAD24$ was indeed of $\Delta T6SS1$ mutant background. Therefore the study sought to monitor the transcription of *icmF* in $\Delta T6SS1::pBAD24$. *icmF* transcription was also evaluated in the control strains, 106-2A wild-type, 106-2A $\Delta T6SS1$ and $\Delta T6SS1::pSRC14$. Transcription of *icmF* was monitored by growing cells as described previously, followed by RNA extraction using the Qiagen RNeasy Mini Kit according to the manufacturer's instructions. Extracted RNA was treated with DNase to remove residual DNA using the Life Technologies TURBO™ DNase kit according the manufacturer's instructions and subjected to a PCR using *V. vulnificus* specific housekeeping primers, *vvhA* forward and reverse to ensure complete removal of DNA from the RNA samples. RNA was then reverse transcribed to generate cDNA as described in the Materials and Methods. cDNA samples were then ethanol precipitated to concentrate the samples and a PCR performed using the housekeeping primers *vvhA* forward and reverse to ensure cDNA had been generated. Following a positive result using the housekeeping primers, a PCR was performed using the primers MutScreen Forward and Reverse. These primers were chosen as they bind to the *tssA* genes flanking the *icmF* gene. The gel electrophoresis image in Figure 7.9 shows the PCR bands generated with the primers MutScreen Forward and Reverse.

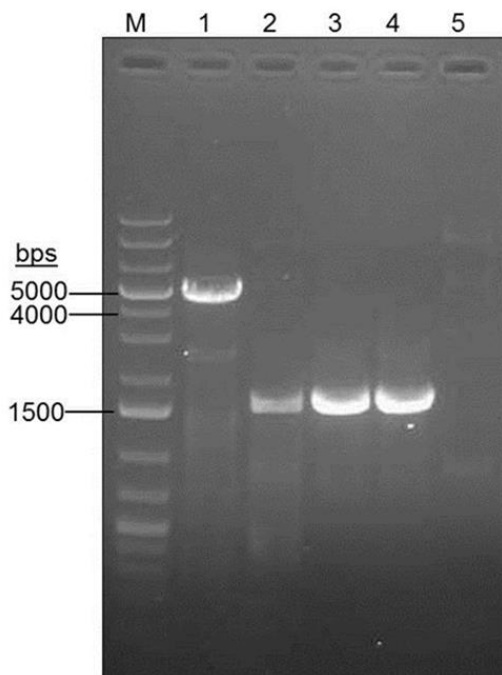


Figure 7.9: Gel electrophoresis image on cDNA using the MutScreen primers. Lane 1 contains, *V. vulnificus* 106-2A wild-type, amplifying a band ~4622bp lane 2, 106-2A $\Delta T6SS1$ (1573bp), lane 3, 106-2A $\Delta T6SS1::pBAD24$ (1573bp), lane 4 106-2A $\Delta T6SS1::pSRC14$ (1573bp) and lane 5 contains a negative control. Fermentas 1kb plus DNA ladder is shown in lane M.

Analysis of Figure 7.9 shows cDNA *icmF* bands for the strains, 106-2A wild-type, 106-2A Δ T6SS1, Δ T6SS1::pBAD24 and Δ T6SS1::pSRC14. Truncated *icmF* is expressed in the strains, 106-2A Δ T6SS1, Δ T6SS1::pBAD24 and Δ T6SS1::pSRC14 further demonstrating that Δ T6SS1::pBAD24 is a mutant and is not expressing a wild-type version of the *icmF* gene. Furthermore the gel image in Figure 7.9 also shows that the generated *icmF* mutation has no effected the expression of the genes flanking *icmF*. Figure 7.9 however does not show whether wild-type *icmF* is being expressed in from pSRC14 in Δ T6SS1::pSRC14, therefore a PCR was performed on the cDNA samples again using the primers, *icmF1_screen* F and *icmF1_screen* R.

The primers, *icmF1_screen* F and *icmF1_screen* R were designed as they amplify a 234bp region internal to the wild-type *icmF* gene, therefore a PCR product will only be generated when wild-type *icmF* is being expressed. Δ T6SS1 will not generate a PCR product as the internal region of the *icmF* has been deleted. Figure 7.10 shows the gel electrophoresis image of a PCR carried out on cDNA using the primers, *icmF1_screen* F and *icmF1_screen* R for Δ T6SS1::pBAD24 and Δ T6SS1::pSRC14

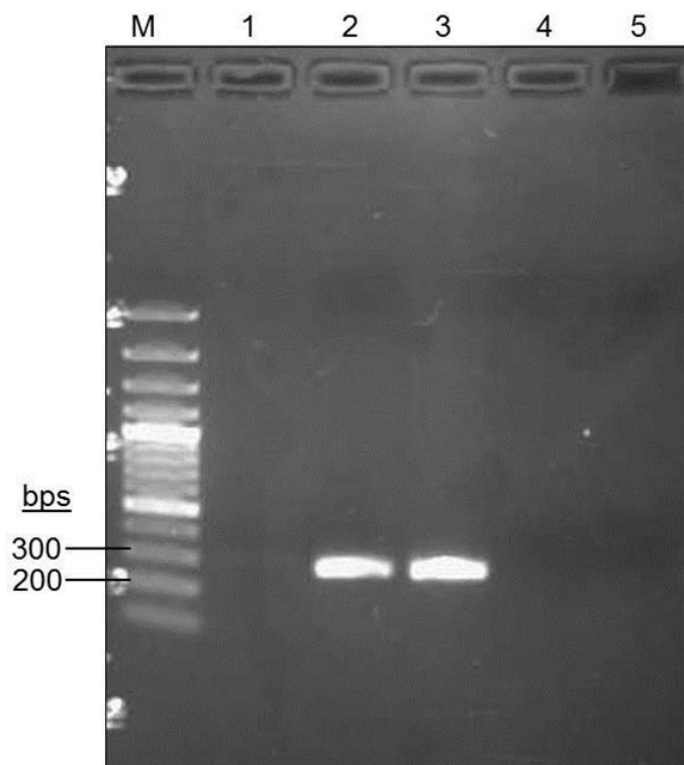


Figure 7.10: Monitoring wild-type *icmF* expression. Lane 1 contains, 106-2A Δ T6SS1::pBAD24, lane 2, 106-2A Δ T6SS1::pSRC14. gDNA controls are run in lanes 3-4. Lane 3, 106-2A wild-type, lane 4, 106-2A Δ T6SS1 and lane 5, negative control. Fermentas 100bp plus DNA ladder is shown in lane M.

Figure 7.10 shows cDNA from $\Delta T6SS1::pBAD24$ (lane 1) is negative for the internal region of *icmF*, demonstrating that this strain does not contain wild-type *icmF*. However, in $\Delta T6SS1::pSRC14$ (lane 2) the internal region of the *icmF* gene is being amplified. The results in Figure 7.10 coupled with the results in Figure 7.9 indicate that the wild-type *icmF* gene is expressed from pSRC14.

In conclusion, the results of these sections demonstrate that the *icmF* gene is being transcribed in $\Delta T6SS1::pSRC14$ from pSRC14. However, Western blot analysis demonstrated that in addition to the observation that Hcp is secreted into the supernatant of this strain, Hcp is also observed in the supernatant of $\Delta T6SS1::pBAD24$. Due to time constraints an initial qualitative killing assay was performed to determine whether, $\Delta T6SS1::pSRC14$ displayed a killing phenotype similar to 106-2A wild-type.

7.2.5 *V. vulnificus* 106-2A $\Delta T6SS1$ pBAD24:*icmF* is unable to restore the killing phenotype associated with T6SS1.

Earlier experiments detailed in this Chapter show that Hcp can be detected in the culture filtrate of $\Delta T6SS1::pSRC14$. Therefore due to time constraints a qualitative killing assay was designed to assess the killing of $\Delta T6SS1::pSRC14$ using the prey strain, *V. vulnificus* 99-743. The qualitative assay was performed using TCBS agar as detailed in the Materials and Methods. TCBS agar was chosen as the prey strain 99-743 can be distinguished from the attacker strains, 106-2A wild-type, 106-2A $\Delta T6SS1$, $\Delta T6SS1::pBAD24$ and $\Delta T6SS1::pSRC14$ based on colour differences. The prey strain, 99-743 appears yellow on TCBS agar whereas the attacker strains listed above appear green. This colour difference allowed for the growth of each strain to be assessed when in co-culture on TCBS agar plates. The results of the qualitative co-culture assays are shown in Figure 7.11.

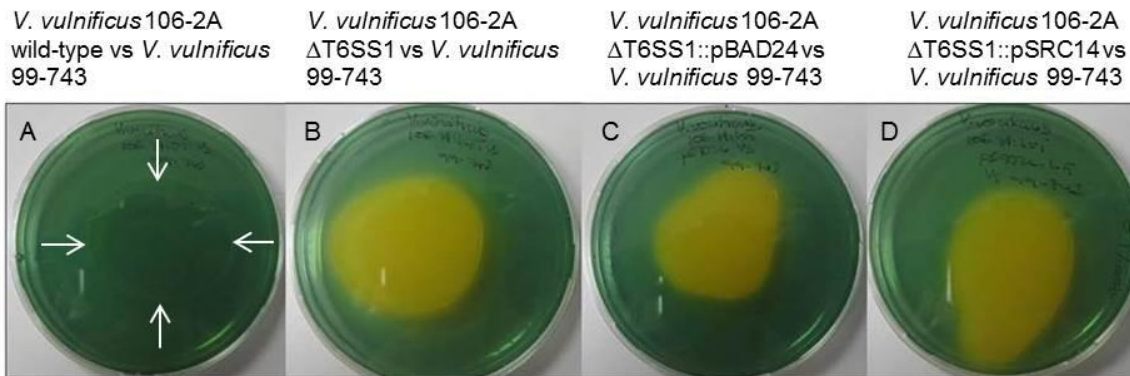


Figure 7.11: Qualitative killing assay to monitor T6SS1 associated killing. Image (A) shows *V. vulnificus* 106-2A wild-type is able to target *V. vulnificus* 99-743 as there is only green growth on the plate with minimal yellow growth around the perimeter of growth as indicated with white arrows. (B) The T6SS1 mutant strain, *V. vulnificus* Δ T6SS1 is unable to target *V. vulnificus* 99-743 as there is only yellow growth observed on the plate. (C) Δ T6SS1::pBAD24 co-cultured with 99-743 produces a phenotype comparable to Δ T6SS1. (D) Δ T6SS1::pSRC14 is unable to restore the killing phenotype associated with T6SS1 as there is only yellow growth on the TCBS plate which is comparable to the yellow growth observed for Δ T6SS1.

Co-culture of 106-2A wild-type with 99-743 shown in Figure 7.11 (A) shows mainly green growth on the TCBS agar plate with minimal yellow growth surrounding the growth perimeter. This result shows that 99-743 is unable to grow well when co-cultured with 106-2A wild-type. However, following co-culturing of 99-743 with 106-2A Δ T6SS1 (Figure 7.11 B) only yellow growth is observed on the plate, indicating that 99-743 is able to grow. The reason for no green growth observed on plates B-D in Figure 7.11 is due to the 24 hour incubation period used. Previous experiments conducted in this study have shown that leaving TCBS plates longer than overnight incubation causes diffusion of yellow across the plate, therefore masking the presences of any green growth. Comparison of the co-culture plate containing 99-743 and Δ T6SS1 (Figure 7.11B) with the co-culture plate containing 99-743 and Δ T6SS1::pSRC14 (Figure 7.11 D), shows no differences in the observed yellow growth, indicating that pSCR14 is unable to restore the killing phenotype associated with 106-2A wild-type (Figure 7.11 A). This result demonstrate that successful complementation was not achieved.

7.3 Discussion

The current study aimed to complement 106-2A Δ T6SS1 using the arabinose inducible vector, pSRC14. pSRC14 was generated by cloning a copy of the wild-type *icmF* gene into the pBAD24 vector to produce, pSRC14. pSRC14 was conjugated

into 106-2A Δ T6SS1, generating 106-2A Δ T6SS1::pSRC14. To assess whether pSRC14 complemented 106-2A Δ T6SS1, Western blotting using the Hcp antibody was used to monitor Hcp secretion. Although initial experiments indicated complementation of 106-2A Δ T6SS1 using pSRC14, as assessed by the presence of Hcp in the culture filtrate, further Western blots using the control strain, Δ T6SS1::pBAD24 were also positive for Hcp in the culture filtrate. Therefore, the Hcp detected in the culture filtrate of Δ T6SS1::pSRC14 could not be assumed to be due to complementation. Further studies monitoring *icmF* transcription identified expression of the *icmF* gene from pSRC14, however a quantitative co-culture killing assay demonstrated that Δ T6SS1::pSRC14 is unable to restore T6SS1 killing to levels that are comparable to the wild-type strain.

The current study hypothesised that Hcp detection in the culture filtrate of Δ T6SS1::pSRC14 and Δ T6SS1::pBAD24 may be due to cell lysis, therefore future work for the current study would be to repeat the Western blots using a control antibody to monitor cell lysis. An example of a lysis control protein is cytosolic RNA polymerase. For example, if RNA polymerase, an internal cytosolic protein is identified in the culture filtrate in addition to the Hcp protein, then this may suggest cell lysis.

A similar approach to complementing a T6SS *icmF* mutant in *V. cholerae* has been demonstrated [295]. This study amplified the wild-type *icmF* gene which was ligated into pBAD24. The resulting complement vector was able to successfully restore Hcp secretion in a T6SS *icmF* mutant as monitored by Western blotting. In addition to monitoring Hcp secretion, the study used an antibody against the internal cytosolic protein RNA polymerase to monitor for cell lysis. The same study also reported partial complementation of the killing phenotype [245, 295]. Conversely the current study was unable to restore the killing phenotype using the complement strain Δ T6SS1::pSRC14.

The current study speculated the ampicillin added to the media as a selection pressure for the vectors, pSRC14 and pBAD24 may have caused cells lysis, leading to detection of Hcp in the culture filtrate. This was hypothesised as ampicillin is a bacteriocidal antibiotic which causes lysis of bacterial cells by interfering with the proper arrangement of bacterial cell walls [92, 324].

Although it is possible that ampicillin may cause cell lysis of $\Delta T6SS1::pBAD24$ and $\Delta T6SS1::pSRC14$, leading to detection of Hcp in the culture filtrate, this is unlikely as pBAD24 and pSRC14 contain the *bla* gene. This gene encodes for β -lactamase, an enzyme that provides resistance to the antibiotic ampicillin [325]. Therefore it is unlikely that the ampicillin which is added to the media is causing the cells to lyse. In addition the cells containing pSRC14 and pBAD24 are growing exponentially in media containing ampicillin which is evident by the increasing OD readings, therefore it is unlikely that the cells are lysing. Furthermore, the detection of Hcp in the culture filtrate is comparable to the levels of Hcp in the culture filtrate of the wild-type strain, indicating that the Hcp is likely being secreted and is not due to residual Hcp from lysed cells.

An alternative hypothesis for the detection of Hcp in the culture filtrate of $\Delta T6SS1::pBAD24$, is ampicillin causing activation of an alternative secretion system such as T6SS2, which may cause secretion of the internally accumulated Hcp from a mechanism other than T6SS1. This study hypothesises that ampicillin may cause activation of T6SS2 as previous research has demonstrated that sub-inhibitory levels of kanamycin can activate HSI-I T6SS genes in *P. aeruginosa* [326]. Therefore, the current study hypothesises that ampicillin may cause activation of an alternative secretion system in *V. vulnificus*, possibly T6SS2, as antibiotics have been shown to effect T6SS activation in *P. aeruginosa* [326]. Therefore if ampicillin activates T6SS2, it is possible that Hcp from T6SS1 is trafficked out of the cell via T6SS2. An example of a protein in the literature being secreted by a mechanism other than its cognate system is the EspC protein of enteropathogenic *E. coli*, where it has been shown that EspC is secreted to the by the T5SS, but is then translocated by the T3SS. Therefore it is possible that the Hcp from T6SS1 may be incorporated and secreted out of cells by T6SS2 [327].

As with the data presented for *P. aeruginosa*, the current study also did not observe any killing of the prey strain, *V. vulnificus* 99-743 when co-cultured with either the complement strain, $\Delta T6SS1::pSRC14$ or the $\Delta T6SS1::pBAD24$. Therefore this may suggest that pSRC14 is unable to fully complement $\Delta T6SS1$. However, as suggested above, ampicillin may activate T6SS2 which may lead to the secretion of the T6SS1 protein, Hcp. However, the hypothesis of T6SS2 activation would need to

be followed up with further work to assess whether T6SS2 are activated in the presences of ampicillin and furthermore, a key experiment would be to monitor Hcp secretion in a double T6SS1 and T6SS2 mutant containing pBAD24, to observe whether Hcp is able to be secreted.

7.4 Conclusion

The results from the current study demonstrated that the *icmF* gene encoded on pSRC14 is expressed. However, the ability for pSRC14 to complement the secretion of Hcp is inconclusive, as Hcp is also observed in the culture filtrate of the control, strain Δ T6SS1::pBAD24. Furthermore a qualitative killing assay showed that the strain, Δ T6SS1::pSRC14 is unable to restore phenotypic co-culture killing to wild-type levels.

Future work for the complementation study would be to repeat Western blots with an internal control antibody to monitor for cell lysis. In addition, the co-culture assays should be repeated to give quantitative data as this would identify if Δ T6SS1::pSRC14 is able to partially restore killing, a phenotype which the qualitative assay cannot determine. In addition to this, complementation with an alternative expression vector should also be attempted as a different vector may be able to better complement *icmF*.

7.5 Concluding summary and future work

V. vulnificus biotype 1 strains are known to vary significantly in virulence potential. Therefore the initial aim of this PhD was to characterise 5 clinical and 5 environmental isolates in several *in vitro* phenotypic assays, to identify whether any *in vitro* assay correlated with either, the published *in vivo* mouse data on virulence groupings of the *V. vulnificus* isolates, or with source of isolation. However, the data from these analyses demonstrated that not one phenotypic assay could accurately predict source of isolation or virulence potential of a strain. The study therefore performed WGS to identify genetic differences between the strains, with the aim of identifying genetic makers which correlated with either source of isolation or virulence potential of the strains.

WGS comparison data demonstrated that the *V. vulnificus* isolates tested contained many genetic differences. In addition to WGS comparison the study also carried out

WGS gene annotation. The gene annotation method quickly led to the discovery of previously undescribed novel T6SSs in *V. vulnificus*. Therefore the study halted further bioinformatic investigation into evaluating the genetic differences between the strains, and instead focused attention on the T6SSs. Although the study identified 2 T6SSs, termed T6SS1 and T6SS2, the study chose to investigate T6SS1, as T6SS1 shared synteny to the previously described T6SS in *V. cholerae*. In addition to this finding, it was noted that T6SS1 was only present in environmental isolates, with a predominance to be associated with lesser virulent strains.

The functionality of T6SS1 was assessed by Western blotting to monitor the expression and secretion of the T6SS associated protein, Hcp. This demonstrated that T6SS1 displayed thermoregulation, whereby T6SS1 was active at 23°C and 30°C, but was inactive at 37°C. Further phenotypic characterisation using co-culturing assays showed that T6SS1 displayed anti-prokaryotic properties which allowed a T6SS1 positive *V. vulnificus* strain to target *B. thailandensis*, *V. fluvialis* and a T6SS1 negative *V. vulnificus* strain.

The findings presented in this thesis contributes to the *V. vulnificus* field of research as WGS comparison data has demonstrated that *V. vulnificus* strains harbour genetic differences. Future bioinformatic studies analysing these genetic differences may identify genetic markers which could potentially distinguish hyper virulent strains that are hazardous to human health from lesser virulent strains that do not pose a risk to human health. The current study has also identified novel previously undescribed T6SSs in *V. vulnificus*, termed T6SS1 and T6SS2. Although T6SS2 was not characterised extensively in the current study, this is an area of research that could be explored in the future.

Based on the phenotypic T6SS1 data presented in this thesis, the current study hypothesises that this newly characterised secretion system may play a role in understanding one of the major questions surrounding *V. vulnificus*, “why are there relatively few serious human infections attributed to *V. vulnificus*, given the natural occurrence and virulence potential of this pathogen?” The following paragraphs will outline the new hypothesis that the current study has generated as well as the future work that would need to be employed to elucidate these hypotheses.

Analysis of the current study's cohort of strains found that T6SS1 is only found in environmental isolates with a predominance to be associated with strains exhibiting lower virulence. As the T6SS1 was rarely identified among hyper virulent strains, the current study hypothesises that in the natural marine environment, lesser virulent T6SS1 positive strains can target the hyper virulent T6SS1 negative strains. This would allow for the lesser virulent strains to predominate in the environment. If this statement is true then the likelihood of humans being exposed to a hyper virulent strain would be low. As a result there would be a much lower incidence of humans presenting with septicaemia, a disease symptom more commonly associated with hyper virulent strains. Instead the majority of humans would present with gastroenteritis and disease symptoms which are more commonly associated with lesser virulent strains. Therefore, it is proposed that although there is a high abundance of *V. vulnificus* bacteria occurring in the environment, the prevalence of hyper virulent strains is low, maybe potentially as a result of the T6SS1 dependent intra-species killing, resulting in only a few serious human infections occurring.

In order to test the hypothesis outlined above, a study identifying the prevalence of the T6SS1 among *V. vulnificus* strains of known isolation and virulence would need to be performed. This would identify whether the T6SS1 is found solely in environmental isolates as well as elucidate the prevalence of the T6SS1 among hyper and lesser virulent strains. In addition an *in vivo* co-culturing infection model would need to be designed to test whether the killing that occurs *in vitro* can also occur *in vivo*.

In addition to the finding that T6SS1 is involved with intra-species targeting, the study also found that that a lesser virulent pathogen, *V. fluvialis* could target a Δ T6SS1 mutant strain. This observation may also provide an explanation as to why there is relatively few serious human infection attributed to *V. vulnificus* given the natural prevalence and virulence potential of *V. fluvialis*. For example, the current study identified that at 30°C *V. vulnificus* could target *V. fluvialis* in a T6SS1 dependent manner. However, at 37°C *V. fluvialis* was able to target the Δ T6SS1 mutant strain. Due to this finding, the current study speculates that if a human ingests a contaminated oyster containing both *V. vulnificus* and *V. fluvialis*, upon

entry into the human host the temperature would be elevated to 37°C, allowing *V. fluvialis* to target *V. vulnificus*.

Therefore the current study hypothesises that *in vivo* *V. vulnificus* may be displaced by *V. fluvialis*, allowing *V. fluvialis* to predominate. *V. fluvialis* is often associated with milder disease symptoms such as gastroenteritis and is rarely associated with septicaemia. With this in mind, the disease symptoms displayed in the human host would be that of *V. fluvialis*. In order to test this hypothesis, experiments would need to be performed to understand the natural microflora in oysters. In addition to this an *in vivo* co-culturing study would also need to be performed to test whether the targeting ability of *V. fluvialis* displayed *in vitro* also occurs *in vivo*.

Further T6SS1 characterisation work could lead to the identification of T6SS1 effectors. Preliminary mass spectrometry data analysing the secretome of 106-2A wild-type and 106-2A Δ T6SS1, demonstrated that T6SS1 proteins such as Hcp could be identified in the culture filtrate of the wild-type strain but not in the mutant strain. However, a more thorough and in depth analysis of the two secretomes would need to be performed to fully elucidate novel effectors of T6SS1.

Chapter 8 Materials and Methods

8.1 Bacterial strains and mammalian cell lines

8.1.1 Bacterial strains

All bacterial strains used in the current study are listed in Table 8.1.

Table 8.1: Bacterial strains used in this study

Bacterial strains	Description	Source
<i>V. vulnificus</i>		
ORL-1506	Wild-type, clinical isolate	CEFAS
ATL-9832	Wild-type, clinical isolate	CEFAS
NSV-5830	Wild-type, clinical isolate	CEFAS
DAL-79087	Wild-type, clinical isolate	CEFAS
DAL-79040	Wild-type, clinical isolate	CEFAS
S3-16	Wild-type, environmental isolate	CEFAS
S2-22	Wild-type, environmental isolate	CEFAS
99-796	Wild-type, environmental isolate	CEFAS
99-743	Wild-type, environmental isolate	CEFAS
106-2A	Wild-type, environmental isolate	CEFAS
106-2A Δ T6SS1	106-2A with in-frame deletion of <i>icmF</i> from T6SS1	This study
106-2A Δ T6SS2	106-2A with in-frame deletion of <i>icmF</i> from T6SS2	This study
106-2A pSCrhaB3	Wild-type strain containing pSCrhaB3 (Tp ^r)	This study
106-2A Δ T6SS1 pSCrhaB3	106-2A Δ <i>icmF1</i> containing pSCrhaB3 (Tp ^r)	This study
106-2A Δ T6SS2 pSCrhaB3	106-2A Δ <i>icmF2</i> containing pSCrhaB3 (Tp ^r)	This study
<i>V. vulnificus</i> 99-743 pBHR4-RFP	<i>V. vulnificus</i> 99-743 containing pBHR4-RFP (Cm ^r)	This study

<i>E. coli</i>		
DH5 α	Cloning host	Lab stock
TOP10	Cloning host	Invitrogen
S17 λ pir	Cloning host and donor strain	Lab Stock
<i>V. cholerae</i>		
V52	Wild-type strain (Sm ^r)	Dr. S. Pukatizki
V52 $\Delta hcp1 \Delta hcp2$	V52 with in-frame deletion of <i>hcp1</i> and <i>hcp2</i> (Sm ^r)	Dr. S. Pukatizki
<i>C. difficile</i>		
630 Δerm	630 containing a deletion of a gene encoding an erythromycin cassette	Dr. S. Michell
<i>V. fluvialis</i>		
NCTC 11327	Wild-type strain	CEFAS
NCTC 11327 pBHR-RFP	<i>V. fluvialis</i> NCTC 11327 containing pBHR4-RFP (Cm ^r)	This study
<i>B. thailandensis</i>		
E264 pBHR-RFP	<i>B. thailandensis</i> containing pBHR-RFP (Cm ^r)	Dr. Claudia Hemsley

8.1.2 Mammalian cell lines

All mammalian cell lines used in the current study are listed in Table 8.2

Table 8.2. Mammalian cell line used in this study

Cell line	Description	Source
CaCo-2	Human cells originally derived from a colorectal adenocarcinoma from a 72year old Caucasian male	Lab stock

8.2 Media

All media used in the current study is listed in Table 8.3

Table 8.3. Growth media for bacterial and mammalian cells used in this study

Media	Composition	Supplier
LB broth	10g peptone, 5g yeast extract, 5g sodium chloride, made up to 1 L with Milliq water and autoclaved	Fisher Scientific
LB agar	10g peptone, 5g yeast extract, 5g sodium chloride, 20g agar made up to 1 L with Milliq water and autoclaved	Fisher Scientific
2% NaCl LB broth	10g peptone, 5g yeast extract, 25g sodium chloride, made up to 1 L with Milliq water and autoclaved, supplemented with 2% (w/v) NaCl	Fisher Scientific supplemented 2% Sodium chloride, from Sigma-Aldrich
2% NaCl LB agar	10g peptone, 5g yeast extract, 25g sodium chloride, 20g agar made up to 1 L with Milliq water and autoclaved, supplemented with 2% (w/v) NaCl	Fisher Scientific supplemented 2% Sodium chloride, from Sigma-Aldrich
TCBS agar	Peptone from casein 5g, peptone from meat 5g, yeast extract 5g, sodium citrate 10g, sodium thiosulfate 10g, ox bile 5g, sodium cholate 3g, sucrose 20g, sodium chloride 10g, iron(III) citrate 1g, thymol blue 0.04g, bromothymol blue 0.04g, agar-agar 14g, 1L Milliq water	Thermo Scientific
10% Sucrose Agar	10g Tryptone, peptone, 5g yeast extract, 266 mL Water and autoclaved, supplemented with 133 mL of filter sterilised 30% sucrose solution	All reagents are from Oxoid, except sucrose from Sigma

0.3% Motility agar	5g Tryptone, 10g sodium chloride, 1.675g bacto agar, 500 mLs Milliq water and autoclaved	Oxoid
EMEM	1 mM sodium pyruvate, 2 mM L-glutamine, 1500 mg/L sodium bicarbonate	ATCC
Leibovitz's Medium (L-15)	Supplemented with 10% non-heat treated fetal bovine serum	Life Technologies

8.3 Routine culturing of bacterial strains

8.3.1 Culturing of *V. vulnificus* cells

The 10 *V. vulnificus* strains were received into the laboratory from CEFAS on LB-agar slopes. Strains were inoculated into 2% LB broth and incubated overnight at 37°C with agitation. 2 mL aliquots of overnight broth cultures were then stored at -80°C, in 12% glycerol. Re-culturing of strains from -80°C was performed by re-streaking strains onto either TCBS agar or 2% NaCl LB agar and incubating overnight at 37°C or 30°C where indicated. Where appropriate media was supplemented with trimethoprim at 100 µg/mL or chloramphenicol at 10 µg/mL.

8.3.2 Culturing of other *Vibrio* species and *Burkholderia thailandensis*

V. cholerae was routinely cultured on LB agar or in LB broth supplemented with streptomycin at 50 mg/mL and incubated at 37°C. *V. fluvialis* was routinely cultured in LB broth or on LB agar supplemented with chloramphenicol at 10 µg/mL where appropriate and incubated at 30°C. *B. thailandensis* was routinely cultured in LB broth or on LB agar supplemented with chloramphenicol at 50 µg/mL and incubated at 30°C.

8.3.3 Culturing of *E. coli* cells

E. coli strains were generally cultured in LB broth or on LB agar and where appropriate supplemented with antibiotics at the following concentration, ampicillin, 100 µg/mL, chloramphenicol 35 µg/mL, kanamycin 50 µg/mL and trimethoprim 100 µg/mL and incubated at 37°C.

8.4 Routine culturing of mammalian cells

8.4.1 Routine culturing of CaCo-2 cells

For long term storage CaCo-2 cells were stored either in liquid nitrogen or in glycerol at -80°C in 90% non-heat treated foetal bovine serum (FBS) and 10% DMSO. Re-culturing of CaCo-2 cells was performed by culturing cells in a T25 culture flask with 5 mL of 37°C pre-warmed EMEM supplemented with 10% non-heat treated FBS and incubated at 37°C in a humidified incubator aerated with 5% CO₂. At 80% confluence, cells were passaged into T75 flasks. CaCo-2 cells were not passaged past passage 20 (P20).

8.4.2 Passaging of CaCo-2 cells

CaCo-2 cells were washed with 5 mL PBS and detached using 1.5 mL trypsin with incubation at 37°C for 5 minutes. Following detachment cells were re-suspended in 10.5 mL 37°C pre-warmed EMEM supplemented with 10% non-heat treated FBS. CaCo-2 cells were then split 1:3 into T75 flasks and suspended in 12 mL pre-warmed EMEM supplemented with 10% non-heat treated FBS. Passages were non performed passed P20.

8.5 In vitro phenotypic assays

8.5.1 *V. vulnificus* growth curves

Growth curves were routinely performed by sub-culturing 2-3 colonies into 2% NaCl LB broth or LB only broth. Broths were incubated overnight at either 37°C or 30°C where indicated with agitation and OD_{590nm} read. At T0 25 mL of 2% NaCl broth or 25 mL of LB broth was inoculated to OD_{590nm} 0.03 with overnight *V. vulnificus* cultures and incubated at either 37°C or 30°C. Samples were taken at designated hourly time points, OD_{590nm} read and Miles and Misra serial dilutions (1:10) performed. Triplicate 10 µl dilutions were spotted onto LB agar plates and incubated. Average cfu/ mL for each triplicate time point was recorded.

8.5.2 Capsule colony morphology

Streaks of *V. vulnificus* strains were performed on 2% NaCl LB agar plates. Following incubation at 37°C colony morphology was assessed and images recorded using BioRad ChemiDoc™ using the Quantity One version 4.6.9.

8.5.3 India ink staining of capsule

V. vulnificus cells grown on 2% NaCl LB agar were sub-cultured into 2% NaCl LB broth and incubated at 37°C. Overnight broths were inoculated to OD_{590nm} 0.03 and grown to mid-log (OD_{590nm} 1.0). 1 µl cultures were then mixed with 10 µl of India ink spotted onto a glass microscopy slide. India ink cultures were smeared across the slide and allowed to air dry. Air dried slides were then saturated with 1 mL of crystal violet for 1 minute. Slides were then washed with distilled water and air dried. Capsule was imaged using the brightfield settings of the Zeiss Axioplan Epifluorescence Microscope.

8.5.4 Azocasein protease assay

Total protease activity in *V. vulnificus* supernatant was determined according to the protease protocol described by Shao and Hor (2000) [328]. In brief, 2 mL overnight *V. vulnificus* broths grown in 2% NaCl LB at 37°C were centrifuged and washed 3 times in 2% NaCl LB broth and inoculated into 2% NaCl broth at dilution of 1 in 100 and incubated at 37°C 200 rpm. At T0, T4, T8, T24 and T30 the growth OD_{590nm} was read and triplicate 500 µl samples of bacterial supernatant were mixed with equal volumes of azocasein solution (5 mg/mL), incubated at 37°C for 15 minutes and protein precipitated with 1 mL trichloroacetic acid (TCA). Samples were then centrifuged and the supernatant mixed with equal volumes of 0.5 M NaOH. OD_{450nm} was then read. A negative control reading at OD_{450nm} was also conducted at each time point by mixing 500 µl 2% NaCl broth with 500 µl azocasein, incubated at 37°C, protein precipitated with 1 mL TCA and equal volumes of 0.5 M NaOH added.

8.5.5 Motility assay

Motility agar described in Table 8.3 was melted, cooled to ~50°C and 25 mL poured into agar plates. Plates were air-dried in a laminar flow hood for 40 minutes and inoculated with 2 µl of mid-log *V. vulnificus* (OD_{590nm} 1.0) cultures (1 inoculation per agar plate x3 plates for each strain). Inoculated plates were then incubated at 37°C for 24 hours before motility recorded in mm.

8.5.6 LDH cytotoxicity assay

CaCo-2 cells were harvested from a T75 routine culturing flask as detailed in section 8.4.1, with minor alterations. Following detachment, CaCo-2 cells were re-

suspended in 4.5 mL of EMEM supplemented with 10% non-heat treated FBS and enumerated using a haemocytometers. Cells were then seeded into 24 well plates at a density of 1.4×10^5 / mL, and incubated at 37°C overnight with 5% CO₂ to allow for attachment.

Following attachment, CaCo-2 cells were overlaid with 1 mL mid-log phase *V. vulnificus* cultures re-suspended in L-15 media at a density of 1.4×10^7 cfu/mL equating to a MOI of 100 (*V. vulnificus* cells were also enumerated in parallel by plating out using serial dilutions of to ensure the MOI equated to 100). Bacterial infected CaCo-2 cells were then incubated at 37°C for 6 hours without aeration. Infections were performed in triplicate for each strain and negative control consisting of CaCo-2 cells overlaid with 1mL L-15 media performed on each 24 well plate. At T6 the supernatant was removed and centrifuged at 5000 rpm for 5 minutes. LDH release from the CaCo-2 cells was then determined using the Promega CytoTox 96® Non-Radioactive Cytotoxicity Assay kit in accordance with the manufacturer's instructions. In brief, 50 µl of supernatant was removed and mixed with 50 µl of LDH substrate in a 96 well plate and incubated in the dark at room temperature for 30 minutes. Following incubation 50 µl of stop solution was added and the absorbance read at OD_{490nm} using the Bio-Rad model 680 microplate reader recorded.

8.5.7 G. mellonella infection assay

Prior to infection waxmoth larvae, *G. mellonella* were weighed and only larvae between 2.0 - 3.0 g with no signs of melanisation were used for infection studies. Overnight cultures of *V. vulnificus* grown in LB at 37°C were re-adjusted to a cell density of $\sim 1 \times 10^7$ cfu/ mL and *G. mellonella* larvae were challenged with 10 µl (equating to $\sim 1 \times 10^5$ cfu/10 µl) doses of *V. vulnificus* cells into the upper right abdominal proleg using a 25 µl Hamilton Microlitre™ syringe 800 series with removable needle (Sigma). *V. vulnificus* cells were also enumerated in parallel by plating out using serial dilutions of the infective dose to ensure $\sim 1 \times 10^5$ cfu/10 µl was the input. Infected larvae were then incubated at 37°C and monitored for signs of infection, death was recorded when larvae failed to respond to touch.

8.5.8 Co-culture killing assays

Overnight cultures of prey (either *V. vulnificus* 99-743, *V. fluvialis* NCTC 11327 or *B. thailandensis* E264) and attacker strains (*V. vulnificus* 106-2A wild-type, Δ T6SS1 or Δ T6SS2) grown in LB with antibiotics where appropriate at 30°C were re-adjusted to an OD_{590nm} 0.03 and grown to OD_{590nm} 1.0. Cells were then re-adjusted to OD_{590nm} 0.8 and mixed at a ratio of 3:1, attacker to prey. 200 µl of mixed cultures were then spotted onto LB agar plates, 3 plates per co-culture and incubated at 30°C for 5 hours. Following incubation the co-culture growth was scraped off and re-suspended in 1 mL PBS. Subsequent 10-fold serial dilutions were performed and triplicate 10 µl spots spotted onto enumeration plates for prey and attacker strains. Enumeration plates were then incubated at 37°C overnight. The average cfu/ mL was recorded for each triplicate dilution.

8.5.9 Qualitative co-culture killing assay

Prey and attacker strains were prepared as described in section 8.5.8, with the minor alteration that 200 µl of mixed cultures were spotted onto TCBS agar plates and incubated at 30°C for 24 hours. Following incubation the colour of each co-culture growth was assessed and recorded.

8.5.10 Plasmid stability testing

Overnight broth culture of *V. fluvialis* NCTC11327::pBHR-RFP grown in LB supplemented with 10 µg/mL chloramphenicol at 30°C, was re-adjusted to OD_{590nm} 0.03 and grown to OD_{590nm} 1.0. Cells were then adjusted to OD_{590nm} 0.8 and 1 mL samples mixed with 3 mL LB. 200 µl was spotted onto LB agar and incubated at 30°C for 5 hours. Following incubation the growth was re-suspended in 1 mL PBS and Miles and Misra serial dilutions (1:10) in PBS performed. Triplicate 10 µl spots of the dilutions were then inoculated onto both LB only agar plates and LB agar plates containing 10 µg/mL chloramphenicol. The inoculation plates were then incubated at 37°C and the growth for each recorded. The average cfu/mL was recorded for each triplicate dilution.

8.6 Molecular genetics

8.6.1 gDNA extraction

All gDNA in this study was extracted using the Promega Wizard® Genomic DNA Purification Kit according to the manufacturer's instructions for Gram negative bacteria. Eluted gDNA was quantified using the Nanodrop reader and stored at 4°C. gDNA preparations for WGS analysis were further quantified using Qubit® Fluorometric Quantitation and analysed using gel electrophoresis to ensure the gDNA was of high quality and not fragmented.

8.6.2 Plasmid extraction

All plasmid preparation for this study were performed using the Qiagen QIAprep Spin Miniprep Kit, according to the manufacturer's instructions, with the minor adjustments of 10 mL starting cultures used instead of 1-5 mL and DNA elution performed using 35 µl of nuclease free water. Preparations were stored at 4°C.

8.6.3 PCR for fragments less than 1000bps

PCR amplification of DNA regions less than 1000bps were routinely performed using 1 µl of 5 U/µl HotStartTaq polymerase (Qiagen), 10 µl of 10X HotStartTaq polymerase buffer, 5X Q Solution, 1µl forward and 1µl reverse oligonucleotides (50 pmol/µl), 1 µl dNTPs (20 Mm each), 5 µl DNA and nuclease free water to a final volume of 50 µl. A typical reaction consisted of an initial denaturation at 96° C for 15 minutes, followed by 30 cycles of denaturation at 94°C for 1 minute, annealing at 65°C for 1 minute, extension at 72°C for 1.5 minutes and a final extension at 72°C for 7 minutes.

8.6.4 PCR for fragments greater than 1000bps

PCR amplification of DNA regions greater than 1000bps were routinely performed using 0.5 µl of 1 U/µl KOD Xtreme™ Hot Start DNA Polymerase (Novagen), 12.5 µl 2X Xtreme buffer, 0.25 µl forward and 0.25 µl reverse oligonucleotides (50 pmol/µl), 0.5 µl dNTPs (20 mM each), 2 µl DNA and nuclease free water to a final volume of 25 µl. A typical reaction consisted on an initial denaturation step at 94° C for 2 minutes followed by 35 cycles of denaturation at 98°C for 10 seconds, annealing at 57°C for 30 seconds and an extension at 68°C for 6.5 minutes.

8.6.5 Agarose gel electrophoresis

Separation of DNA fragments based on size was performed using agarose gel electrophoresis. 0.8%-1% w/v agarose (Sigma) was dissolved in 100 mL 1X TAE (Tris-acetate 40 mM, EDTA 1mM made up in Milliq water to 1X solution) with 10 µl 10X SYBR®Safe DNA gel stain (Invitrogen). Following separation DNA was visualised using the UV transilluminator, BioRad ChemiDoc™ and imaged using Quantity One version 4.6.9.

8.6.6 DNA gel purification

DNA bands excised from 0.8% w/v agarose gels were processed using QIAquick Gel Extraction kit (Qiagen) as per manufacturer's instructions.

8.6.7 Restriction digestion

A typical digest of 1 µg of DNA was mixed with 10X restriction enzyme digest buffer, 10X BSA, 1 µl restriction enzyme and nuclease free water to a final volume of 50 µl. Reactions were incubated as per manufacturer's instructions, followed by gel electrophoresis to either visualise or purify fragments.

8.6.8 Ligation

Ligations typically consisted of 150 ng of digested vector, 1 µl T4 ligase (New England BioLabs) 10X T4 DNA ligase buffer, enzyme and insert to a final volume of 20 µl. Reactions were incubated at 15°C overnight. Amount of insert was calculated using the equation detailed below, to give 150 ng of insert at a vector to insert ratio of 3:1.

$$\text{Amount of insert} = (150 \text{ (size of insert kb / size of vector kb)}) \times 3$$

8.6.9 A-tailing of PCR fragments

1–4 µl of gel purified PCR product was mixed with 2 µl 5X GoTaq® buffer, 2 µl 1 mM dATP, 1 µl of 5 u/µl GoTaq Flexi® DNA Polymerase, 0.6 µl of 25 mM MgCl₂ (All reagents Promega ®) and made up to a final volume of 10µl with nuclease free water. Samples were then incubated at 70°C for 15-30 minutes. A 1-2 µl sample was then used in downstream ligation reactions.

8.6.10 Reverse transcription PCR (RT-PCR)

Total RNA was extracted from overnight *V. vulnificus* 106-2A wild-type and 106-2A Δ T6SS cells that had been adjusted to OD_{590nm} 0.03 and grown to OD_{590nm} 1.5, for 106-2A Δ T6SS1::pBAD24 and 106-2A Δ T6SS1::pSRC14 cells were grown to OD_{590nm} 3.0. Total RNA was extracted using RNeasy Mini Kit (Qiagen) according to the manufacturer's instructions. RNA was subjected to DNase treatment using the Turbo™ DNase (Life Technologies) according to the manufacturer's instructions. A PCR was carried out using the species specific *V. vulnificus* housekeeping primers *vvhA* forward and reverse to ensure RNA samples were DNA free. DNA-free RNA was then reverse transcribed into cDNA using SuperScript™ III Transcriptase (Invitrogen), according to the manufacturer's instructions. In brief, 5 μ l RNA was mixed with 2 μ l random primers (Invitrogen), 1 μ l dNTPs (10 mM each) and 12 μ l nuclease free water and heated to 65°C for 5 minutes, incubated on ice for 1 minute and centrifuged briefly. The sample was then mixed with 4 μ l 5X First Strand Buffer, 1 μ l 0.1 M DTT, 1 μ l RNase OUT, 1 μ l SuperScript III Reverse Transcriptase. The sample was then incubated at 25°C for 5 minutes, followed by 50°C for 30 minutes and 70°C for 15 minutes. 1.5 μ l of RNase H was added to a 30 μ l sample and cDNA was ethanol precipitated at -20°C overnight.

8.6.11 Production of chemically competent *E. coli*

Overnight cultures of *E. coli* were inoculated into LB broth (1:100) and incubated at 37°C to OD₅₉₀ 0.5 – 0.7, followed by incubation on ice for 30 minutes and centrifugation at 3000 rpm for 10 minutes at 4°C. Centrifuged samples were re-suspended in 30 mL ice cold 0.1 M CaCl₂ and incubated on ice for 30 minutes. Cells were then centrifuged at 3000 rpm for 10 minutes at 4°C, and samples re-suspended in 700 μ l 0.1 M CaCl₂ and 300 μ l of 50% glycerol. 50 μ l aliquotes cells were stored at -80°C.

8.6.12 Heat shock transformations

Chemically competent *E. coli* cells were thawed on ice and mixed with 2 μ l of ligation reaction and incubated on ice for 30 minutes, heat shocked at 42°C for 30 seconds and returned to ice. 250 μ l of 37°C pre-warmed LB was immediately added to recover cells, followed by incubation at 37°C for 1 hour at 200 rpm. 500-700 μ l of

37°C pre warmed LB was then added and 200 µl spread onto LB agar plates containing appropriate antibiotic selection and incubated for at 37°C.

8.6.13 Tri-parental conjugation of plasmids into *Vibrio* strains

The helper strain *E. coli* pRK2013 harbouring a kanamycin resistance cassette was used for all tri-parental conjugations. 1 mL samples from overnight cultures of the helper strain, donor strain and *Vibrio* strain were grown at 37°C in LB, and supplemented with antibiotics where appropriate. Overnight broth cultures were centrifuged at 13,000 rpm for 2 minutes and samples were re-suspended in 200 µl LB media. 100 µl from the donor and helper strain were then added to a 1 mL centrifuged sample of the *Vibrio* strain. 100 µl of each suspension was then spotted onto LB plates and incubated at 37°C overnight. Following incubation the growth from each plate was re-suspended in 1 mL PBS and 100 µl spread onto TCBS agar plates containing appropriate antibiotics. Following 2-3 days incubation at 37°C, potential transformant colonies were re-streaked onto TCBS agar supplemented with appropriate antibiotics. Transformants positive for antibiotic resistance were mini-prepped to ensure the presence of the resistance plasmid. *V. vulnificus* colonies were also species checked by PCR using the housekeeping primers, *vvhA* forward and reverse.

8.6.14 Generation of deletion constructs in *V. vulnificus*

Unmarked in-frame deletion mutants of *icmF* in T6SS1 and T6SS2 were constructed using pSRC10 and pSRC11, listed in Table 8.5. In brief, flanking primers with incorporated restriction enzymes listed in Table 8.4 were used to amplify *icmF* flanking regions. These regions were ligated into the intermediate constructs, pSRC6-9 listed in Table 8.5. Correctly sequenced flanking regions were digested and ligated into pDM4 generating, pSRC10 and pSRC11. pSRC10 and pSRC11 were mobilised into *V. vulnificus* by tri-parental mating (section 8.6.12). First cross over integrants were checked by PCR using the MutScreen primers listed in Table 8.4 and plating integrants onto chloramphenicol plates to check for resistance. The excision of the deletion plasmid from the first cross over integrants was induced by plating onto 5% sucrose agar listed in Table 8.3. PCR using the MutScreen primers listed in Table 8.4 were used to distinguish wild-type revertants from mutants.

8.7 Primers and plasmids

8.7.1 Primers

All primers used in the current study are listed in Table 8.4

Table 8.4. Primers used in this study

Primer Name	Description	Primer Sequence 5'–3'
<i>vvhA</i> Forward	<i>V. vulnificus</i> housekeeping gene	ACTGCGGTACAGGTTGG
<i>vvhA</i> Reverse	<i>V. vulnificus</i> housekeeping gene	CGCCACCCACTTTCGGGCC
LFF 106-2A <i>icmF1 Smal</i>	106-2A T6SS1 left flanking region <i>IcmF</i> forward	TGCCCCGGGAGTGATTGGTCTGAGGCCATTG
LFR 106-2A <i>icmF1 NdeI</i>	106-2A T6SS1 left flanking region <i>IcmF</i> reverse	TGCATATGTATCGGGTCTTGACGTAAGTGG
RFF 106-2A <i>icmF1 NdeI</i>	106-2A T6SS1 right flanking region <i>IcmF</i> forward	TGCATATGTGGGCATTCTTTTCGATTGTTAG
RFR 106-2A <i>icmF1 ApaI</i>	106-2A T6SS1 right flanking region <i>IcmF</i> reverse	TTGGGCCCCCTCGGCACGATAAAGCTCTCTC
LFF 106-2A <i>icmF2 Smal</i>	106-2A T6SS2 right flanking region <i>IcmF2</i> forward	TGCCCCGGGACCAGAGTGCGGATTATATTTTC
LFR 106-2A <i>icmF2 NdeI</i>	106-2A T6SS2 left flanking region <i>IcmF2</i> reverse	TGCATATGAATAACCAACAAACGGTTAAAG
RFF 106-2A <i>icmF2 NdeI</i>	106-2A T6SS2 right flanking region <i>IcmF2</i> forward	TACATATGGCAAGGCCGCAATCTCGCAAAG
RFR 106-2A <i>icmF2 ApaI</i>	106-2A T6SS2 right flanking region <i>IcmF2</i> reverse	TCGGGCCCTGCCAATTTGAGGTAAACCATC
M13 Forward	Sequencing primer	TGTAAAACGACGGCCAGT

M13 Reverse	Sequencing primer	CAGGAAACAGCTATGAC
LFF_ <i>icmF</i> _MutScreen	T6SS1 cross over confirmation primer	GGCGGAAAGTGGAACAAAGC
RFR_ <i>icmF</i> _MutScreen	T6SS1 cross over confirmation primer	TACTCGGTTTGCTGGTACTC
LFF_ <i>icmF2</i> _MutScreen	T6SS2 cross over confirmation primer	CGGCTGTGTTAGTCAGTGTG
RFR_ <i>icmF2</i> _MutScreen	T6SS2 cross over confirmation primer	CTCATTTCGATCACCGTTACC
CmF	First crossover integrant primer forward	ATGGAGAAAAAATCACTGGATATACCACC
CmR	First crossover integrant primer reverse	TTACGCCCCGCCCTGCCACTCATCGCAGTA
<i>icmF1</i> Final F pBAD _{SmaI}	Complement <i>icmF</i> gene	ACGTCCCGGGATGTGGAAATTCATTGTCGG
<i>icmF1</i> Final pBAD _{SphI}	Complement <i>icmF</i> gene	CTGAGCATGCTTAATAAAGAGTTTTAGACA
<i>icmF</i> _screen F	RNA screening primer	CCATTGGCCCTAAAGTTG
<i>icmF</i> _screen R	RNA screening primer	GATCTGCGGTAAATCGG
Seq_1	Primer walking sequencing primer for <i>icmF</i> in pBAD24	GTGCTCGTTTACGAG
Seq_2	Primer walking sequencing primer for <i>icmF</i> in pBAD24	TTTGCGGGAACTTG
Seq_3	Primer walking sequencing	TCAGCGTGTCTACAG

	primer for <i>icmF</i> in pBAD24	
Seq_4	Primer walking sequencing primer for <i>icmF</i> in pBAD24	GATCCAAGATGCGCC
Seq_5	Primer walking sequencing primer for <i>icmF</i> in pBAD24	TGGCTTATAGCCATG

8.7.2 Plasmids

All plasmids used in the current study are listed in Table 8.5

Table 8.5. Plasmids used in this study

Plasmid	Description	Source
pGEM-T Easy	High copy number cloning vector (Amp ^r)	Promega
pDM4	Suicide vector (Cm ^r , <i>sacB</i>)	[303]
pRK2013	Conjugation, helper strain (Km ^r)	Lab stock
pSRC6	pGEM®-T Easy containing 106-2A <i>lcmF2</i> left flanking region from T6SS2	This Study
pSRC7	pGEM®-T Easy containing 106-2A <i>lcmF2</i> right flanking region from T6SS2	This Study
pSRC8	pGEM®-T Easy containing 106-2A <i>lcmF1</i> left flanking region from T6SS1	This Study
pSRC9	pGEM®-T Easy containing 106-2A <i>lcmF1</i> right flanking region from T6SS1	This Study
pSRC10	pDM4 containing containing NdeI ligated 106-2A <i>lcmF2</i> left flank and right flank from T6SS2	This Study
pSRC11	pDM4 containing containing NdeI ligated 106-2A <i>lcmF1</i> left flank and right flank from T6SS1	This Study

pSCrhaB3	Vector containing Tp ^r cassette	Dr. C. Hemsley
pBHR4-RFP	Vector containing Cm ^r cassette	Dr. C. Hemsley
pSRC13	pGEM-T-easy vector containing <i>icmF</i> gene from T6SS1	This study
pBAD24	Arabinose inducible expression vector (Amp ^r)	LGC Standards
pSRC14	pBAD24 vector containing <i>icmF1</i> complement gene	This study

8.8 Preparation of protein samples

8.8.1 Culture filtrate and cell lysate preparations

Overnight LB broth cultures of *V. vulnificus* grown at 30°C were re-adjusted to OD_{590nm} 0.03 in 25 mL and grown to OD_{590nm} 1.5. A 21 mL sample was centrifuged at 4000 rpm for 5 minutes at 4°C. The supernatant was filter sterilised using a Millipore 0.22 µm filter and protein precipitated by adding 5 mL of 100% TCA (w/v) dissolved in distilled water. The proteins were precipitated overnight at 4°C.

A 1 mL sample from the overnight bacterial culture was adjusted to OD_{590nm} 1.0, centrifuged at 5000 rpm for 3 minutes and re-suspended in 50 µl BugBuster® Protein Extraction Reagent (Novagen) and incubated at room temperature for 20 minutes with rocking. Following incubation, 25 µl of PBS and 25 µl 4X NuPAGE® LDS Sample Buffer (Invitrogen) was added to the cell lysate and stored at 4°C overnight. BugBuster was prepared by adding 1 µl Benzonase® (Novagen) and 1 µl rLysozyme™ (Novagen) to 1 mL 1X BugBuster® Protein Extraction Reagent.

Following overnight protein precipitation, a 2 mL sample was centrifuged at 20,000 g for 5 minutes at 4°C, the supernatant removed and an additional 2 mL sampled added and centrifuged. This was repeated for the entire ~26 mL precipitated protein solution. The final centrifugation step used 1 mL of ice-cold acetone to wash the cells and performed at 20,000 g for 5 minutes. The acetone was removed and the protein dried at 95°C for ~ 50 seconds and re-suspended in 100 – 200 µl of PBS. Proteins were then quantified using the BCA assay.

8.8.2 Quantification of proteins

Culture filtrate proteins were quantified using the Thermo Scientific™ Pierce™ BCA™ Protein Assay Kit prepared according to the manufacturer's instructions. Quantification of proteins was achieved in a 96-well plate containing 180 µl of working BCA reagent mixed with 10 µl of protein (highly concentrated protein was diluted to 1 in 10 or 1 in 100) and incubated at 37°C. Absorbance of the samples was read at OD_{570nm}.

8.8.3 SDS-PAGE

Quantified protein samples were mixed with 4X NuPAGE® LDS Sample Buffer to a final 1X concentration and heated at 95°C for 10 minutes with the cell lysate preparations. Prior to loading pre-cast NuPAGE® 4-12 % Bis-Tris Gels 1.0 mm x 12 wells (Novex) were rinsed with distilled water and secured into a XCell SureLock® mini cell. The gel was submerged in 1X NuPAGE® MES SDS Running Buffer (Life Technologies) and a 3 µl sample of the Odyssey® One-Color Protein Molecular Weight Marker (Licor) was loaded onto the gel with 10 µl of each sample loaded per lane, the gel was then run at 180 V for 50 minutes.

8.8.4 Western blotting

SDS-separated proteins were transferred to a nitrocellulose membrane included in the iBlot® Transfer Stacks (Novex) using the iBlot® Dry Blotting System (Invitrogen). The protein membrane was then rinsed with water and stained with Ponceau S to ensure equal loadings of protein samples. The Ponceau S stain was removed using 0.1% (w/w) sodium hydroxide and rinsed with water. Membranes were blocked with blocking buffer PBS-T (0.1% (v/v) Tween-20 in PBS) supplemented with 1.5% (w/v) of skimmed milk powder and incubated for 30 minutes at room temperature with rocking. Membranes were then incubated overnight at 4°C. Following incubation membranes were incubated at room temperature for 30 minutes rocking and then rinsed with PBS-T washing buffer. Membranes were then incubated with primary Hcp antibody made up in blocking solution at a 1:500 dilution for 90 minutes at room temperature with rocking. Following incubation the membrane was washed with PBS-T for 5 minutes rocking and removed, the wash step was repeated a further 2 more times before the secondary IRDye 680LT Goat anti-Rabbit IgG (H + L) (Licor) fluorescent antibody made up in blocking buffer at a 1:20,000 dilution was applied for

90 minutes at room temperature with rocking. The secondary antibody was then removed following the wash steps as described previously. The membrane was scanned using the Odyssey CLx infra-red scanner (Licor) and imaged using Image Studio, version 4.0.

8.9 Bioinformatic methods

8.9.1 Whole genome sequencing

Whole genome sequencing was performed by Exeter Sequencing Services at the University of Exeter using 250bp paired end reads on the Illumina MiSeq Desktop Sequencer.

8.9.2 Assembling and annotating scaffolds

Raw sequencing reads were assembled into scaffolds using the automated pipeline a5 [221]. Assembled a5 scaffolds were automatically annotated using RAST version 2.0 [229]. Both a5 and RAST were used according to the default setting.

8.9.3 Generating phylogenetic trees

Phylogenetic trees were constructed using the automated pipeline, SNPPhylo [223]. Raw sequencing reads were first trimmed using Trim Galore and aligned to the reference genome, YJ016 using Bowtie version 2.0. Following alignment, SNPs were called using SAMtools. SAMtools view was used to convert files from .SAM to .BAM format. .BAM files were sorted using SAMtools sort and indexed using SAMtools index. Finally SAMtools mpileup was utilised to compute and store all possible genotype variants into Variant Call Format (VCF), which is the required format for SNPPhylo. Following SNPPhylo process according to the default setting the phylogenetic trees were visualised using FigTree version 1.4.2.

8.9.4 WGS comparison to identify gaps in the alignment between the query sequences and the reference genome

WGS comparison was performed using the programme MUMmer. Prior to comparison, assembled scaffolds were aligned to the reference genome, YJ016, using NUCmer according to the fairly similar sequences default setting. Alignments were then parsed using show-coords and filtered using deltafilter. A MUMmerplot was used to visualise the query sequences alignment against the reference strain in

a scatter plot format. Data was then imported into Excel and sorted according to the start of the alignment in YJ016. Gaps were calculated by extracting the “gap” co-ordinates from Excel and uploading to Circos. Circos was utilised to visualise the comparison of gaps between the query sequences and the reference genome. The forward and reverse tracks on the WGS comparison for the reference strain represent CDS features extracted from Genbank.

8.9.5 WGS comparison between Δ T6SS1 mutant and wild-type strain.

Comparison was performed as detailed in section 8.9.4, however gaps were not calculated in Excel and the instead co-ordinates were uploaded to Circos for visualisation.

References

1. Hollis, D.G., et al., *Halophilic Vibrio species isolated from blood cultures*. J Clin Microbiol, 1976. **3**(4): p. 425-31.
2. Blake, P.A., et al., *Disease caused by a marine Vibrio. Clinical characteristics and epidemiology*. N Engl J Med, 1979. **300**(1): p. 1-5.
3. Reichelt, J.L., P. Baumann, and L. Baumann, *Study of genetic relationships among marine species of the genera Beneckeia and Photobacterium by means of in vitro DNA/DNA hybridization*. Arch Microbiol, 1976. **110**(1): p. 101-20.
4. Farmer, J.J., 3rd, *Vibrio ("Beneckeia") vulnificus, the bacterium associated with sepsis, septicaemia, and the sea*. Lancet, 1979. **2**(8148): p. 903.
5. Changchai, N. and S. Saunjit, *Occurrence of Vibrio parahaemolyticus and Vibrio vulnificus in retail raw oysters from the eastern coast of Thailand*. Southeast Asian J Trop Med Public Health, 2014. **45**(3): p. 662-9.
6. Takemura, A.F., D.M. Chien, and M.F. Polz, *Associations and dynamics of Vibrionaceae in the environment, from the genus to the population level*. Front Microbiol, 2014. **5**: p. 38.
7. Baker-Austin, C., et al., *pilF polymorphism-based real-time PCR to distinguish Vibrio vulnificus strains of human health relevance*. Food Microbiol, 2012. **30**(1): p. 17-23.
8. Froelich, B. and J.D. Oliver, *The interactions of Vibrio vulnificus and the oyster Crassostrea virginica*. Microb Ecol, 2013. **65**(4): p. 807-16.
9. Kustus, R.J., C.J. Kuehl, and J.H. Crosa, *Power plays: iron transport and energy transduction in pathogenic vibrios*. Biometals, 2011. **24**(3): p. 559-66.
10. Bier, N., et al., *Genotypic diversity and virulence characteristics of clinical and environmental Vibrio vulnificus isolates from the Baltic Sea region*. Appl Environ Microbiol, 2013. **79**(12): p. 3570-81.
11. Froelich, B.A., et al., *Apparent loss of Vibrio vulnificus from North Carolina oysters coincides with a drought-induced increase in salinity*. Appl Environ Microbiol, 2012. **78**(11): p. 3885-9.
12. Gulig, P.A., K.L. Bourdage, and A.M. Starks, *Molecular Pathogenesis of Vibrio vulnificus*. J Microbiol, 2005. **43 Spec No**: p. 118-31.
13. Thiaville, P.C., et al., *Genotype is correlated with but does not predict virulence of Vibrio vulnificus biotype 1 in subcutaneously inoculated, iron dextran-treated mice*. Infect Immun, 2011. **79**(3): p. 1194-207.
14. Horseman, M.A. and S. Surani, *A comprehensive review of Vibrio vulnificus: an important cause of severe sepsis and skin and soft-tissue infection*. Int J Infect Dis, 2011. **15**(3): p. e157-66.
15. Mahmud, Z.H., et al., *Occurrence, seasonality and genetic diversity of Vibrio vulnificus in coastal seaweeds and water along the Kii Channel, Japan*. FEMS Microbiol Ecol, 2008. **64**(2): p. 209-18.
16. Li, Z., et al., *Genome sequence of the human-pathogenic bacterium Vibrio vulnificus type strain ATCC 27562*. J Bacteriol, 2012. **194**(24): p. 6954-5.
17. Ha, C., et al., *Quorum sensing-dependent metalloprotease VvpE is important in the virulence of Vibrio vulnificus to invertebrates*. Microb Pathog, 2014. **71-72**: p. 8-14.
18. Oliver, J.D., *The viable but non-culturable state in the human pathogen Vibrio vulnificus*. FEMS Microbiol Lett, 1995. **133**(3): p. 203-8.

19. Williams, T.C., M. Ayrapetyan, and J.D. Oliver, *Implications of chitin attachment for the environmental persistence and clinical nature of the human pathogen Vibrio vulnificus*. Appl Environ Microbiol, 2014. **80**(5): p. 1580-7.
20. Bross, M.H., et al., *Vibrio vulnificus infection: diagnosis and treatment*. Am Fam Physician, 2007. **76**(4): p. 539-44.
21. Warner, J.M. and J.D. Oliver, *Randomly amplified polymorphic DNA analysis of clinical and environmental isolates of Vibrio vulnificus and other vibrio species*. Appl Environ Microbiol, 1999. **65**(3): p. 1141-4.
22. Arias, C.R., et al., *Intraspecific Differentiation of Vibrio vulnificus Biotypes by Amplified Fragment Length Polymorphism and Ribotyping*. Appl Environ Microbiol, 1997. **63**(7): p. 2600-6.
23. Amaro, C., et al., *Evidence that water transmits Vibrio vulnificus biotype 2 infections to eels*. Appl Environ Microbiol, 1995. **61**(3): p. 1133-7.
24. Broza, Y.Y., et al., *Genetic diversity of the human pathogen Vibrio vulnificus: A new phylogroup*. Int J Food Microbiol, 2012. **153**(3): p. 436-43.
25. Vickery, M.C., et al., *A real-time PCR assay for the rapid determination of 16S rRNA genotype in Vibrio vulnificus*. J Microbiol Methods, 2007. **68**(2): p. 376-84.
26. Biosca, E.G., et al., *First record of Vibrio vulnificus biotype 2 from diseased European eel, Anguilla anguilla L*. Journal of Fish Diseases, 1991. **14**(1): p. 103-109.
27. Bisharat, N., et al., *Clinical, epidemiological, and microbiological features of Vibrio vulnificus biogroup 3 causing outbreaks of wound infection and bacteraemia in Israel*. Israel Vibrio Study Group. Lancet, 1999. **354**(9188): p. 1421-4.
28. Yokochi, N., et al., *Distribution of virulence markers among Vibrio vulnificus isolates of clinical and environmental origin and regional characteristics in Japan*. PLoS One, 2013. **8**(1): p. e55219.
29. Nilsson, W.B., et al., *Sequence polymorphism of the 16S rRNA gene of Vibrio vulnificus is a possible indicator of strain virulence*. J Clin Microbiol, 2003. **41**(1): p. 442-6.
30. Rosche, T.M., Y. Yano, and J.D. Oliver, *A rapid and simple PCR analysis indicates there are two subgroups of Vibrio vulnificus which correlate with clinical or environmental isolation*. Microbiol Immunol, 2005. **49**(4): p. 381-9.
31. Bisharat, N., et al., *The evolution of genetic structure in the marine pathogen, Vibrio vulnificus*. Infect Genet Evol, 2007. **7**(6): p. 685-93.
32. Cohen, A.L., et al., *Emergence of a virulent clade of Vibrio vulnificus and correlation with the presence of a 33-kilobase genomic island*. Appl Environ Microbiol, 2007. **73**(17): p. 5553-65.
33. Roig, F.J., et al., *pilF Polymorphism-based PCR to distinguish vibrio vulnificus strains potentially dangerous to public health*. Appl Environ Microbiol, 2010. **76**(5): p. 1328-33.
34. Canigrall, I., et al., *Detection of Vibrio vulnificus in seafood, seawater and wastewater samples from a Mediterranean coastal area*. Microbiol Res, 2010. **165**(8): p. 657-64.
35. Tsao, C.H., et al., *Seasonality, clinical types and prognostic factors of Vibrio vulnificus infection*. J Infect Dev Ctries, 2013. **7**(7): p. 533-40.
36. Daniels, N.A., *Vibrio vulnificus oysters: pearls and perils*. Clin Infect Dis, 2011. **52**(6): p. 788-92.

37. Shapiro, R.L., et al., *The role of Gulf Coast oysters harvested in warmer months in Vibrio vulnificus infections in the United States, 1988-1996*. *Vibrio Working Group*. J Infect Dis, 1998. **178**(3): p. 752-9.
38. Strom, M.S. and R.N. Paranjpye, *Epidemiology and pathogenesis of Vibrio vulnificus*. *Microbes Infect*, 2000. **2**(2): p. 177-88.
39. Blackwell, K.D. and J.D. Oliver, *The ecology of Vibrio vulnificus, Vibrio cholerae, and Vibrio parahaemolyticus in North Carolina estuaries*. J Microbiol, 2008. **46**(2): p. 146-53.
40. Motes, M.L., et al., *Influence of water temperature and salinity on Vibrio vulnificus in Northern Gulf and Atlantic Coast oysters (Crassostrea virginica)*. *Appl Environ Microbiol*, 1998. **64**(4): p. 1459-65.
41. Randa, M.A., M.F. Polz, and E. Lim, *Effects of temperature and salinity on Vibrio vulnificus population dynamics as assessed by quantitative PCR*. *Appl Environ Microbiol*, 2004. **70**(9): p. 5469-76.
42. Paz, S., et al., *Climate change and the emergence of Vibrio vulnificus disease in Israel*. *Environ Res*, 2007. **103**(3): p. 390-6.
43. Jones, M.K. and J.D. Oliver, *Vibrio vulnificus: disease and pathogenesis*. *Infect Immun*, 2009. **77**(5): p. 1723-33.
44. Frank, C., et al., *Vibrio vulnificus wound infections after contact with the Baltic Sea, Germany*. *Euro Surveill*, 2006. **11**(8): p. E060817 1.
45. Torres, L., et al., *Wound Infection due to Vibrio vulnificus in Spain*. *Eur J Clin Microbiol Infect Dis*, 2002. **21**(7): p. 537-8.
46. Partridge, D.G., et al., *Vibrio vulnificus: an unusual mode of acquisition and novel use of rapid susceptibility testing*. *J Clin Pathol*, 2009. **62**(4): p. 370-2.
47. Mertens, A., et al., *Halophilic, lactose-positive Vibrio in a case of fatal septicemia*. *J Clin Microbiol*, 1979. **9**(2): p. 233-5.
48. Mouzopoulos, G., et al., *Lower extremity infections by vibrio vulnificus*. *Chirurgia (Bucur)*, 2008. **103**(2): p. 201-3.
49. Hoi, L., et al., *Occurrence of Vibrio vulnificus biotypes in Danish marine environments*. *Appl Environ Microbiol*, 1998. **64**(1): p. 7-13.
50. Melhus, A., T. Holmdahl, and I. Tjernberg, *First documented case of bacteremia with Vibrio vulnificus in Sweden*. *Scand J Infect Dis*, 1995. **27**(1): p. 81-2.
51. Haenen, O.L., et al., *Vibrio vulnificus outbreaks in Dutch eel farms since 1996: strain diversity and impact*. *Dis Aquat Organ*, 2014. **108**(3): p. 201-9.
52. Paydar, M. and K.L. Thong, *Prevalence and genetic characterization of Vibrio vulnificus in raw seafood and seawater in Malaysia*. *J Food Prot*, 2013. **76**(10): p. 1797-800.
53. Rai, K.R., et al., *Study of medically important Vibrios in the sewage of Katmandu Valley, Nepal*. *Nepal Med Coll J*, 2012. **14**(3): p. 212-5.
54. Lee, S.H., B.H. Chung, and W.C. Lee, *Retrospective analysis of epidemiological aspects of Vibrio vulnificus infections in Korea in 2001-2010*. *Jpn J Infect Dis*, 2013. **66**(4): p. 331-3.
55. Reynaud, Y., et al., *Molecular typing of environmental and clinical strains of Vibrio vulnificus isolated in the northeastern USA*. *PLoS One*, 2013. **8**(12): p. e83357.
56. Vugia, D.J., et al., *Impact of 2003 state regulation on raw oyster-associated Vibrio vulnificus illnesses and deaths, California, USA*. *Emerg Infect Dis*, 2013. **19**(8): p. 1276-80.

57. Weis, K.E., et al., *Vibrio illness in Florida, 1998-2007*. Epidemiol Infect, 2011. **139**(4): p. 591-8.
58. Kumamoto, K.S. and D.J. Vukich, *Clinical infections of Vibrio vulnificus: a case report and review of the literature*. J Emerg Med, 1998. **16**(1): p. 61-6.
59. Matsuoka, Y., et al., *Accurate diagnosis and treatment of Vibrio vulnificus infection: a retrospective study of 12 cases*. Braz J Infect Dis, 2013. **17**(1): p. 7-12.
60. Oliver, J.D., *Wound infections caused by Vibrio vulnificus and other marine bacteria*. Epidemiol Infect, 2005. **133**(3): p. 383-91.
61. Vinh, D.C., et al., *Vibrio vulnificus Septicemia After Handling Tilapia Species Fish: A Canadian Case Report and Review*. Can J Infect Dis Med Microbiol, 2006. **17**(2): p. 129-32.
62. Morris, J.G., Jr., *Cholera and other types of vibriosis: a story of human pandemics and oysters on the half shell*. Clin Infect Dis, 2003. **37**(2): p. 272-80.
63. Lewis, P.R., et al., *Septicaemia secondary to Vibrio vulnificus cellulitis*. Commun Dis Intell Q Rep, 2005. **29**(3): p. 305-7.
64. Borenstein, M. and F. Kerdel, *Infections with Vibrio vulnificus*. Dermatol Clin, 2003. **21**(2): p. 245-8.
65. Yamamoto, T., et al., *[Noncholera vibrio infections (V. parahaemolyticus, V. vulnificus and others)]*. Nihon Rinsho, 2003. **61 Suppl 3**: p. 811-22.
66. Zaidenstein, R., et al., *Clinical characteristics and molecular subtyping of Vibrio vulnificus illnesses, Israel*. Emerg Infect Dis, 2008. **14**(12): p. 1875-82.
67. Haq, S.M. and H.H. Dayal, *Chronic liver disease and consumption of raw oysters: a potentially lethal combination--a review of Vibrio vulnificus septicemia*. Am J Gastroenterol, 2005. **100**(5): p. 1195-9.
68. Chen, Y., T. Satoh, and O. Tokunaga, *Vibrio vulnificus infection in patients with liver disease: report of five autopsy cases*. Virchows Arch, 2002. **441**(1): p. 88-92.
69. Ward, R.J., et al., *Iron and the immune system*. J Neural Transm, 2011. **118**(3): p. 315-28.
70. Merkel, S.M., et al., *Essential role for estrogen in protection against Vibrio vulnificus-induced endotoxic shock*. Infect Immun, 2001. **69**(10): p. 6119-22.
71. Jackson, J.K., R.L. Murphree, and M.L. Tamplin, *Evidence that mortality from Vibrio vulnificus infection results from single strains among heterogeneous populations in shellfish*. J Clin Microbiol, 1997. **35**(8): p. 2098-101.
72. Kobayashi, T., et al., *[a New Selective Isolation Medium for the Vibrio Group; on a Modified Nakanishi's Medium (Tcbs Agar Medium)]*. Nihon Saikingaku Zasshi, 1963. **18**: p. 387-92.
73. Koenig, K.L., J. Mueller, and T. Rose, *Vibrio vulnificus. Hazard on the half shell*. West J Med, 1991. **155**(4): p. 400-3.
74. Kim, S.J., C.M. Kim, and S.H. Shin, *Virulence characteristics of sucrose-fermenting Vibrio vulnificus strains*. Korean J Lab Med, 2010. **30**(5): p. 507-10.
75. Klontz, K.C., et al., *Syndromes of Vibrio vulnificus infections. Clinical and epidemiologic features in Florida cases, 1981-1987*. Ann Intern Med, 1988. **109**(4): p. 318-23.
76. Li, L., et al., *The importance of the viable but non-culturable state in human bacterial pathogens*. Front Microbiol, 2014. **5**: p. 258.

77. Xu, H.S., et al., *Survival and viability of nonculturable Escherichia coli and Vibrio cholerae in the estuarine and marine environment*. Microb Ecol, 1982. **8**(4): p. 313-23.
78. Besnard, V., et al., *Environmental and physico-chemical factors induce VBNC state in Listeria monocytogenes*. Vet Res, 2002. **33**(4): p. 359-70.
79. Asakura, H., et al., *Differential expression of the outer membrane protein W (OmpW) stress response in enterohemorrhagic Escherichia coli O157:H7 corresponds to the viable but non-culturable state*. Res Microbiol, 2008. **159**(9-10): p. 709-17.
80. Cook, K.L. and C.H. Bolster, *Survival of Campylobacter jejuni and Escherichia coli in groundwater during prolonged starvation at low temperatures*. J Appl Microbiol, 2007. **103**(3): p. 573-83.
81. Oliver, J.D., *The viable but nonculturable state in bacteria*. Journal of Microbiology, 2005. **43**: p. 93-100.
82. Lleo, M.M., et al., *mRNA detection by reverse transcription-PCR for monitoring viability over time in an Enterococcus faecalis viable but nonculturable population maintained in a laboratory microcosm*. Appl Environ Microbiol, 2000. **66**(10): p. 4564-7.
83. Lleo, M.M., M.C. Tafi, and P. Canepari, *Nonculturable Enterococcus faecalis cells are metabolically active and capable of resuming active growth*. Syst Appl Microbiol, 1998. **21**(3): p. 333-9.
84. Nowakowska, J. and J.D. Oliver, *Resistance to environmental stresses by Vibrio vulnificus in the viable but nonculturable state*. FEMS Microbiol Ecol, 2013. **84**(1): p. 213-22.
85. Oliver, J.D., L. Nilsson, and S. Kjelleberg, *Formation of nonculturable Vibrio vulnificus cells and its relationship to the starvation state*. Appl Environ Microbiol, 1991. **57**(9): p. 2640-4.
86. Linder, K. and J.D. Oliver, *Membrane fatty acid and virulence changes in the viable but nonculturable state of Vibrio vulnificus*. Appl Environ Microbiol, 1989. **55**(11): p. 2837-42.
87. Smith, B. and J.D. Oliver, *In situ and in vitro gene expression by Vibrio vulnificus during entry into, persistence within, and resuscitation from the viable but nonculturable state*. Appl Environ Microbiol, 2006. **72**(2): p. 1445-51.
88. Kong, I.S., et al., *Role of catalase and oxyR in the viable but nonculturable state of Vibrio vulnificus*. FEMS Microbiol Ecol, 2004. **50**(3): p. 133-42.
89. Oliver, J.D., et al., *Entry into, and resuscitation from, the viable but nonculturable state by Vibrio vulnificus in an estuarine environment*. Appl Environ Microbiol, 1995. **61**(7): p. 2624-30.
90. Ayrapetyan, M., T.C. Williams, and J.D. Oliver, *Interspecific quorum sensing mediates the resuscitation of viable but nonculturable vibrios*. Appl Environ Microbiol, 2014. **80**(8): p. 2478-83.
91. Oliver, J.D. and R. Bockian, *In vivo resuscitation, and virulence towards mice, of viable but nonculturable cells of Vibrio vulnificus*. Appl Environ Microbiol, 1995. **61**(7): p. 2620-3.
92. Willey, J.M., Sherwood, L., Woolverton, C. J., & Prescott, L. M. , *Prescott, Harley, and Klein's microbiology*. 2008, New York: McGraw-Hill Higher Education.
93. Wakeman, C.A. and E.P. Skaar, *Metalloregulation of Gram-positive pathogen physiology*. Curr Opin Microbiol, 2012. **15**(2): p. 169-74.

94. Wilson, J.W., et al., *Mechanisms of bacterial pathogenicity*. Postgrad Med J, 2002. **78**(918): p. 216-24.
95. Litwin, C.M., S.A. Boyko, and S.B. Calderwood, *Cloning, sequencing, and transcriptional regulation of the Vibrio cholerae fur gene*. J Bacteriol, 1992. **174**(6): p. 1897-903.
96. Litwin, C.M. and S.B. Calderwood, *Role of iron in regulation of virulence genes*. Clin Microbiol Rev, 1993. **6**(2): p. 137-49.
97. Muhldorfer, I., et al., *Regulation of the Shiga-like toxin II operon in Escherichia coli*. Infect Immun, 1996. **64**(2): p. 495-502.
98. Calderwood, S.B. and J.J. Mekalanos, *Iron regulation of Shiga-like toxin expression in Escherichia coli is mediated by the fur locus*. J Bacteriol, 1987. **169**(10): p. 4759-64.
99. Litwin, C.M. and S.B. Calderwood, *Cloning and genetic analysis of the Vibrio vulnificus fur gene and construction of a fur mutant by in vivo marker exchange*. J Bacteriol, 1993. **175**(3): p. 706-15.
100. Litwin, C.M. and B.L. Byrne, *Cloning and characterization of an outer membrane protein of Vibrio vulnificus required for heme utilization: regulation of expression and determination of the gene sequence*. Infect Immun, 1998. **66**(7): p. 3134-41.
101. Webster, A.C. and C.M. Litwin, *Cloning and characterization of vuuA, a gene encoding the Vibrio vulnificus ferric vulnibactin receptor*. Infect Immun, 2000. **68**(2): p. 526-34.
102. Lee, H.J., et al., *Regulation of fur expression by RpoS and fur in Vibrio vulnificus*. J Bacteriol, 2003. **185**(19): p. 5891-6.
103. Lee, H.J., et al., *Positive regulation of fur gene expression via direct interaction of fur in a pathogenic bacterium, Vibrio vulnificus*. J Bacteriol, 2007. **189**(7): p. 2629-36.
104. Lee, H.J., et al., *Regulation of haemolysin (VvhA) production by ferric uptake regulator (Fur) in Vibrio vulnificus: repression of vvhA transcription by Fur and proteolysis of VvhA by Fur-repressive exoproteases*. Mol Microbiol, 2013. **88**(4): p. 813-26.
105. Kim, I.H., et al., *The fur-iron complex modulates expression of the quorum-sensing master regulator, SmcR, to control expression of virulence factors in Vibrio vulnificus*. Infect Immun, 2013. **81**(8): p. 2888-98.
106. Kim, S.M., et al., *LuxR homologue SmcR is essential for Vibrio vulnificus pathogenesis and biofilm detachment, and its expression is induced by host cells*. Infect Immun, 2013. **81**(10): p. 3721-30.
107. Popat, R., et al., *Collective sensing and collective responses in quorum-sensing bacteria*. J R Soc Interface, 2015. **12**(103).
108. Diggle, S.P., S.A. Cruz, and M. Camara, *Quorum sensing*. Curr Biol, 2007. **17**(21): p. R907-10.
109. Bruhn, J.B., et al., *Quorum sensing signal molecules (acylated homoserine lactones) in gram-negative fish pathogenic bacteria*. Dis Aquat Organ, 2005. **65**(1): p. 43-52.
110. Valiente, E., et al., *Vibrio vulnificus produces quorum sensing signals of the AHL-class*. FEMS Microbiol Ecol, 2009. **69**(1): p. 16-26.
111. Kim, S.Y., et al., *Regulation of Vibrio vulnificus virulence by the LuxS quorum-sensing system*. Mol Microbiol, 2003. **48**(6): p. 1647-64.

112. Shin, N.R., et al., *Regulation of proinflammatory mediator production in RAW264.7 macrophage by Vibrio vulnificus luxS and smcR*. FEMS Immunol Med Microbiol, 2004. **41**(2): p. 169-76.
113. Shin, N.R., D.Y. Lee, and H.S. Yoo, *Analysis of gene expression in mouse alveolar macrophages stimulated with quorum-sensing mutants of Vibrio vulnificus*. Jpn J Infect Dis, 2008. **61**(5): p. 402-6.
114. Starks, A.M., et al., *Pathogenesis of infection by clinical and environmental strains of Vibrio vulnificus in iron-dextran-treated mice*. Infect Immun, 2000. **68**(10): p. 5785-93.
115. Kim, J.S., et al., *Induction of manganese-containing superoxide dismutase is required for acid tolerance in Vibrio vulnificus*. J Bacteriol, 2005. **187**(17): p. 5984-95.
116. Rhee, J.E., et al., *Identification of the cadBA operon from Vibrio vulnificus and its influence on survival to acid stress*. FEMS Microbiol Lett, 2002. **208**(2): p. 245-51.
117. Rhee, J.E., K.S. Kim, and S.H. Choi, *CadC activates pH-dependent expression of the Vibrio vulnificus cadBA operon at a distance through direct binding to an upstream region*. J Bacteriol, 2005. **187**(22): p. 7870-5.
118. Rhee, J.E., et al., *AphB influences acid tolerance of Vibrio vulnificus by activating expression of the positive regulator CadC*. J Bacteriol, 2006. **188**(18): p. 6490-7.
119. Jeannin, P., et al., *Outer membrane protein A (OmpA): a new pathogen-associated molecular pattern that interacts with antigen presenting cells-impact on vaccine strategies*. Vaccine, 2002. **20 Suppl 4**: p. A23-7.
120. Joseph, L.A. and A.C. Wright, *Expression of Vibrio vulnificus capsular polysaccharide inhibits biofilm formation*. J Bacteriol, 2004. **186**(3): p. 889-93.
121. Yoshida, S., M. Ogawa, and Y. Mizuguchi, *Relation of capsular materials and colony opacity to virulence of Vibrio vulnificus*. Infect Immun, 1985. **47**(2): p. 446-51.
122. Zuppardo, A.B. and R.J. Siebeling, *An epimerase gene essential for capsule synthesis in Vibrio vulnificus*. Infect Immun, 1998. **66**(6): p. 2601-6.
123. Rosche, T.M., B. Smith, and J.D. Oliver, *Evidence for an intermediate colony morphology of Vibrio vulnificus*. Appl Environ Microbiol, 2006. **72**(6): p. 4356-9.
124. Simpson, L.M., et al., *Correlation between virulence and colony morphology in Vibrio vulnificus*. Infect Immun, 1987. **55**(1): p. 269-72.
125. Wright, A.C., et al., *Phenotypic evaluation of acapsular transposon mutants of Vibrio vulnificus*. Infect Immun, 1990. **58**(6): p. 1769-73.
126. Chatzidaki-Livanis, M., M.K. Jones, and A.C. Wright, *Genetic variation in the Vibrio vulnificus group 1 capsular polysaccharide operon*. J Bacteriol, 2006. **188**(5): p. 1987-98.
127. Tan, L.K., G.M. Carlone, and R. Borrow, *Advances in the development of vaccines against Neisseria meningitidis*. N Engl J Med, 2010. **362**(16): p. 1511-20.
128. Simpson, L.M. and J.D. Oliver, *Siderophore production by Vibrio vulnificus*. Infect Immun, 1983. **41**(2): p. 644-9.
129. Kuehl, C.J. and J.H. Crosa, *The TonB energy transduction systems in Vibrio species*. Future Microbiol, 2010. **5**(9): p. 1403-12.

130. Kustusch, R.J., C.J. Kuehl, and J.H. Crosa, *The ttpC gene is contained in two of three TonB systems in the human pathogen Vibrio vulnificus, but only one is active in iron transport and virulence.* J Bacteriol, 2012. **194**(12): p. 3250-9.
131. Alice, A.F. and J.H. Crosa, *The TonB3 system in the human pathogen Vibrio vulnificus is under the control of the global regulators Lrp and cyclic AMP receptor protein.* J Bacteriol, 2012. **194**(8): p. 1897-911.
132. Kim, C.M., et al., *Vibrio vulnificus vulnibactin, but not metalloprotease VvpE, is essentially required for iron-uptake from human holotransferrin.* Biol Pharm Bull, 2006. **29**(5): p. 911-8.
133. Nishina, Y., et al., *Significant role of an exocellular protease in utilization of heme by Vibrio vulnificus.* Infect Immun, 1992. **60**(5): p. 2128-32.
134. Sun, H.Y., et al., *Vibrio vulnificus metalloprotease VvpE has no direct effect on iron-uptake from human hemoglobin.* J Microbiol, 2006. **44**(5): p. 537-47.
135. Kawano, H., et al., *The RND protein is involved in the vulnibactin export system in Vibrio vulnificus M2799.* Microb Pathog, 2014. **75**: p. 59-67.
136. Wright, A.C., L.M. Simpson, and J.D. Oliver, *Role of iron in the pathogenesis of Vibrio vulnificus infections.* Infect Immun, 1981. **34**(2): p. 503-7.
137. Josenhans, C. and S. Suerbaum, *The role of motility as a virulence factor in bacteria.* Int J Med Microbiol, 2002. **291**(8): p. 605-14.
138. Duan, Q., et al., *Flagella and bacterial pathogenicity.* J Basic Microbiol, 2013. **53**(1): p. 1-8.
139. Ruppert, J., et al., *Two cases of severe sepsis due to Vibrio vulnificus wound infection acquired in the Baltic Sea.* Eur J Clin Microbiol Infect Dis, 2004. **23**(12): p. 912-5.
140. Ran Kim, Y. and J. Haeng Rhee, *Flagellar basal body flg operon as a virulence determinant of Vibrio vulnificus.* Biochem Biophys Res Commun, 2003. **304**(2): p. 405-10.
141. Lee, J.H., et al., *Role of flagellum and motility in pathogenesis of Vibrio vulnificus.* Infect Immun, 2004. **72**(8): p. 4905-10.
142. Archambaud, M., *[Bacterial adherence: virulence factor in upper urinary tract infections].* Rev Prat, 1993. **43**(9): p. 1069-71.
143. Homma, M., et al., *Hook-associated proteins essential for flagellar filament formation in Salmonella typhimurium.* J Bacteriol, 1984. **157**(1): p. 100-8.
144. Young Kim, S., et al., *Roles of Flagellar Hook Associated Proteins in Vibrio vulnificus Motility and Virulence* Journal of Bacteriology and Virology 2008. **38**(1): p. 1 - 10.
145. Soo Young Kim, H.Y.H., Joon Haeng Rhee, and Sun Sik Chung, *Roles of Flagellar Hook-Associated Proteins in Vibrio vulnificus Motility and Virulence* Journal of Bacteriology and Virology, 2008. **38**(1): p. 1-10.
146. Gander, R.M. and M.T. LaRocco, *Detection of piluslike structures on clinical and environmental isolates of Vibrio vulnificus.* J Clin Microbiol, 1989. **27**(5): p. 1015-21.
147. Paranjpye, R.N., et al., *The type IV leader peptidase/N-methyltransferase of Vibrio vulnificus controls factors required for adherence to HEp-2 cells and virulence in iron-overloaded mice.* Infect Immun, 1998. **66**(12): p. 5659-68.
148. Bosshart, H. and M. Heinzelmann, *Targeting bacterial endotoxin: two sides of a coin.* Ann N Y Acad Sci, 2007. **1096**: p. 1-17.
149. Rhee, S.H., *Lipopolysaccharide: basic biochemistry, intracellular signaling, and physiological impacts in the gut.* Intest Res, 2014. **12**(2): p. 90-5.

150. Mayer, A.M., et al., *Vibrio vulnificus* MO6-24/O lipopolysaccharide stimulates superoxide anion, thromboxane B(2), matrix metalloproteinase-9, cytokine and chemokine release by rat brain microglia in vitro. *Mar Drugs*, 2014. **12**(4): p. 1732-56.
151. McPherson, V.L., et al., *Physiological effects of the lipopolysaccharide of Vibrio vulnificus on mice and rats*. *Microbios*, 1991. **67**(272-273): p. 141-9.
152. Park, K.H., et al., *Low density lipoprotein inactivates Vibrio vulnificus cytolysin through the oligomerization of toxin monomer*. *Med Microbiol Immunol*, 2005. **194**(3): p. 137-41.
153. Kim, K., et al., *Cyclo(Phe-Pro) produced by the human pathogen Vibrio vulnificus inhibits host innate immune responses through the NF-kappaB pathway*. *Infect Immun*, 2015.
154. Ramachandran, G., *Gram-positive and gram-negative bacterial toxins in sepsis: a brief review*. *Virulence*, 2014. **5**(1): p. 213-8.
155. Lee, J.H., et al., *Identification and characterization of the Vibrio vulnificus rtxA essential for cytotoxicity in vitro and virulence in mice*. *J Microbiol*, 2007. **45**(2): p. 146-52.
156. Linhartova, I., et al., *RTX proteins: a highly diverse family secreted by a common mechanism*. *FEMS Microbiol Rev*, 2010. **34**(6): p. 1076-112.
157. Liu, M., et al., *The HlyU protein is a positive regulator of rtxA1, a gene responsible for cytotoxicity and virulence in the human pathogen Vibrio vulnificus*. *Infect Immun*, 2007. **75**(7): p. 3282-9.
158. Kim, Y.R., et al., *Vibrio vulnificus RTX toxin kills host cells only after contact of the bacteria with host cells*. *Cell Microbiol*, 2008. **10**(4): p. 848-62.
159. Lee, B.C., et al., *Vibrio vulnificus rtxE is important for virulence, and its expression is induced by exposure to host cells*. *Infect Immun*, 2008. **76**(4): p. 1509-17.
160. Lee, B.C., et al., *Comparative analysis of proteins in the culture supernatants of human intestinal epithelial cells infected with the wild-type and rtxE mutant of Vibrio vulnificus*. *Int J Mol Med*, 2011. **28**(5): p. 855-65.
161. Kim, Y.R., et al., *A bacterial RTX toxin causes programmed necrotic cell death through calcium-mediated mitochondrial dysfunction*. *J Infect Dis*, 2013. **207**(9): p. 1406-15.
162. Jeong, H.G. and K.J. Satchell, *Additive Function of Vibrio vulnificus MARTX(Vv) and VvhA Cytolysins Promotes Rapid Growth and Epithelial Tissue Necrosis During Intestinal Infection*. *PLoS Pathog*, 2012. **8**(3): p. e1002581.
163. Kwak, J.S., H.G. Jeong, and K.J. Satchell, *Vibrio vulnificus rtxA1 gene recombination generates toxin variants with altered potency during intestinal infection*. *Proc Natl Acad Sci U S A*, 2011. **108**(4): p. 1645-50.
164. Gray, L.D. and A.S. Kreger, *Purification and characterization of an extracellular cytolysin produced by Vibrio vulnificus*. *Infect Immun*, 1985. **48**(1): p. 62-72.
165. Kreger, A. and D. Lockwood, *Detection of extracellular toxin(s) produced by Vibrio vulnificus*. *Infect Immun*, 1981. **33**(2): p. 583-90.
166. Yamamoto, K., et al., *The cytolysin gene of Vibrio vulnificus: sequence and relationship to the Vibrio cholerae E1 Tor hemolysin gene*. *Infect Immun*, 1990. **58**(8): p. 2706-9.

167. Kim, Y.R., et al., *Outer membrane vesicles of Vibrio vulnificus deliver cytolysin-hemolysin VvhA into epithelial cells to induce cytotoxicity*. Biochem Biophys Res Commun, 2010. **399**(4): p. 607-12.
168. Neogi, S.B., et al., *A highly sensitive and specific multiplex PCR assay for simultaneous detection of Vibrio cholerae, Vibrio parahaemolyticus and Vibrio vulnificus*. Lett Appl Microbiol, 2010. **51**(3): p. 293-300.
169. Lee, S.E., et al., *Production of Vibrio vulnificus hemolysin in vivo and its pathogenic significance*. Biochem Biophys Res Commun, 2004. **324**(1): p. 86-91.
170. Wright, A.C. and J.G. Morris, Jr., *The extracellular cytolysin of Vibrio vulnificus: inactivation and relationship to virulence in mice*. Infect Immun, 1991. **59**(1): p. 192-7.
171. Ellis, T.N. and M.J. Kuehn, *Virulence and immunomodulatory roles of bacterial outer membrane vesicles*. Microbiol Mol Biol Rev, 2010. **74**(1): p. 81-94.
172. Yu, H.N., et al., *Membrane cholesterol is required for activity of Vibrio vulnificus cytolysin*. Arch Microbiol, 2007. **187**(6): p. 467-73.
173. Shao, C.P. and L.I. Hor, *Regulation of metalloprotease gene expression in Vibrio vulnificus by a Vibrio harveyi LuxR homologue*. J Bacteriol, 2001. **183**(4): p. 1369-75.
174. Park, J., et al., *Two forms of Vibrio vulnificus metalloprotease VvpE are secreted via the type II general secretion system*. J Microbiol, 2008. **46**(3): p. 338-43.
175. Kothary, M.H. and A.S. Kreger, *Production and partial characterization of an elastolytic protease of Vibrio vulnificus*. Infect Immun, 1985. **50**(2): p. 534-40.
176. Kothary, M.H. and A.S. Kreger, *Purification and characterization of an elastolytic protease of Vibrio vulnificus*. J Gen Microbiol, 1987. **133**(7): p. 1783-91.
177. Miyoshi, S. and S. Shinoda, *Role of the protease in the permeability enhancement by Vibrio vulnificus*. Microbiol Immunol, 1988. **32**(10): p. 1025-32.
178. Jeong, K.C., et al., *Construction and phenotypic evaluation of a Vibrio vulnificus vvpE mutant for elastolytic protease*. Infect Immun, 2000. **68**(9): p. 5096-106.
179. Fan, J.J., et al., *Isolation and characterization of a Vibrio vulnificus mutant deficient in both extracellular metalloprotease and cytolysin*. Infect Immun, 2001. **69**(9): p. 5943-8.
180. Kim, C.M., et al., *Vibrio vulnificus metalloprotease VvpE is essentially required for swarming*. FEMS Microbiol Lett, 2007. **269**(1): p. 170-9.
181. Lee, M.A., et al., *VvpM, an extracellular metalloprotease of Vibrio vulnificus, induces apoptotic death of human cells*. J Microbiol, 2014. **52**(12): p. 1036-43.
182. Filloux, A., A. Hachani, and S. Bleves, *The bacterial type VI secretion machine: yet another player for protein transport across membranes*. Microbiology, 2008. **154**(Pt 6): p. 1570-83.
183. Filloux, A., *Protein Secretion Systems in Pseudomonas aeruginosa: An Essay on Diversity, Evolution, and Function*. Front Microbiol, 2011. **2**: p. 155.
184. Coulthurst, S.J. and T. Palmer, *A new way out: protein localization on the bacterial cell surface via Tat and a novel Type II secretion system*. Mol Microbiol, 2008. **69**(6): p. 1331-5.

185. Fronzes, R., P.J. Christie, and G. Waksman, *The structural biology of type IV secretion systems*. Nat Rev Microbiol, 2009. **7**(10): p. 703-14.
186. Saier, M.H., Jr., *Protein secretion and membrane insertion systems in gram-negative bacteria*. J Membr Biol, 2006. **214**(2): p. 75-90.
187. Sikora, A.E., et al., *Proteomic analysis of the Vibrio cholerae type II secretome reveals new proteins, including three related serine proteases*. J Biol Chem, 2011. **286**(19): p. 16555-66.
188. Korotkov, K.V., et al., *Structural and functional studies of EpsC, a crucial component of the type 2 secretion system from Vibrio cholerae*. J Mol Biol, 2006. **363**(2): p. 311-21.
189. Hwang, W., et al., *Functional characterization of EpsC, a component of the type II secretion system, in the pathogenicity of Vibrio vulnificus*. Infect Immun, 2011. **79**(10): p. 4068-80.
190. Rama Adiga, I.K., Indrani Karunasagar, *Molecular Docking Studies of Type III Secretion System Effector SopB Homolog in Vibrio vulnificus* Computer Science Systems Biology, 2011. **4**(1): p. 16-20.
191. Rama Adiga, I.K., Indrani Karunasagar, *Outer membrane protein secretin of type III secretion system of Vibrio vulnificus: structure prediction and orientation*. Open Access Bioinformatics, 2011. **3**: p. 61-66.
192. Wright, A.C., et al., *Identification of a group 1-like capsular polysaccharide operon for Vibrio vulnificus*. Infect Immun, 2001. **69**(11): p. 6893-901.
193. Wright, A.C., et al., *Differential expression of Vibrio vulnificus capsular polysaccharide*. Infect Immun, 1999. **67**(5): p. 2250-7.
194. Grau, B.L., M.C. Henk, and G.S. Pettis, *High-frequency phase variation of Vibrio vulnificus 1003: isolation and characterization of a rugose phenotypic variant*. J Bacteriol, 2005. **187**(7): p. 2519-25.
195. Grau, B.L., et al., *Further characterization of Vibrio vulnificus rugose variants and identification of a capsular and rugose exopolysaccharide gene cluster*. Infect Immun, 2008. **76**(4): p. 1485-97.
196. Miyoshi, S., et al., *The C-terminal domain promotes the hemorrhagic damage caused by Vibrio vulnificus metalloprotease*. Toxicon, 2001. **39**(12): p. 1883-6.
197. Miyoshi, S., et al., *Histamine-releasing reaction induced by the N-terminal domain of Vibrio vulnificus metalloprotease*. Life Sci, 2003. **72**(20): p. 2235-42.
198. Miyoshi, N., et al., *Purification and characterization of Vibrio vulnificus protease*. Microbiol Immunol, 1987. **31**(1): p. 13-25.
199. Kim, S.Y., et al., *Contribution of six flagellin genes to the flagellum biogenesis of Vibrio vulnificus and in vivo invasion*. Infect Immun, 2014. **82**(1): p. 29-42.
200. Kim, S.M., D.H. Lee, and S.H. Choi, *Evidence that the Vibrio vulnificus flagellar regulator FlhF is regulated by a quorum sensing master regulator SmcR*. Microbiology, 2012. **158**(Pt 8): p. 2017-25.
201. Goo, S.Y., et al., *Identification of OmpU of Vibrio vulnificus as a fibronectin-binding protein and its role in bacterial pathogenesis*. Infect Immun, 2006. **74**(10): p. 5586-94.
202. Callaway, E., *Deal done over HeLa cell line*. Nature, 2013. **500**(7461): p. 132-3.
203. Masters, J.R., *HeLa cells 50 years on: the good, the bad and the ugly*. Nat Rev Cancer, 2002. **2**(4): p. 315-9.

204. Fogh, J., J.M. Fogh, and T. Orfeo, *One hundred and twenty-seven cultured human tumor cell lines producing tumors in nude mice*. J Natl Cancer Inst, 1977. **59**(1): p. 221-6.
205. DeShazer, D., et al., *Identification of a Burkholderia mallei polysaccharide gene cluster by subtractive hybridization and demonstration that the encoded capsule is an essential virulence determinant*. Microb Pathog, 2001. **30**(5): p. 253-69.
206. Kadioglu, A., et al., *The role of Streptococcus pneumoniae virulence factors in host respiratory colonization and disease*. Nat Rev Microbiol, 2008. **6**(4): p. 288-301.
207. Lee, K.J., et al., *Role of capsular polysaccharide (CPS) in biofilm formation and regulation of CPS production by quorum-sensing in Vibrio vulnificus*. Mol Microbiol, 2013. **90**(4): p. 841-57.
208. Holder, I.A. and C.G. Haidaris, *Experimental studies of the pathogenesis of infections due to Pseudomonas aeruginosa: extracellular protease and elastase as in vivo virulence factors*. Can J Microbiol, 1979. **25**(5): p. 593-9.
209. Young, J.A. and R.J. Collier, *Anthrax toxin: receptor binding, internalization, pore formation, and translocation*. Annu Rev Biochem, 2007. **76**: p. 243-65.
210. Dolly, J.O. and K.R. Aoki, *The structure and mode of action of different botulinum toxins*. Eur J Neurol, 2006. **13 Suppl 4**: p. 1-9.
211. Guentzel, M.N., and L.J. Berry, *Motility as a virulence factor for Vibrio cholerae*. Infection and Immunity, 1975. **11**: p. 890-897.
212. Jones, G.W. and R. Freter, *Adhesive properties of Vibrio cholerae: nature of the interaction with isolated rabbit brush border membranes and human erythrocytes*. Infect Immun, 1976. **14**(1): p. 240-5.
213. Kamar, R., et al., *Pathogenic potential of Bacillus cereus strains as revealed by phenotypic analysis*. J Clin Microbiol, 2013. **51**(1): p. 320-3.
214. Morrison, S.S., et al., *Pyrosequencing-based comparative genome analysis of Vibrio vulnificus environmental isolates*. PLoS One, 2012. **7**(5): p. e37553.
215. Gulig, P.A., et al., *SOLiD sequencing of four Vibrio vulnificus genomes enables comparative genomic analysis and identification of candidate clade-specific virulence genes*. BMC Genomics, 2010. **11**: p. 512.
216. Fleischmann, R.D., et al., *Whole-genome random sequencing and assembly of Haemophilus influenzae Rd*. Science, 1995. **269**(5223): p. 496-512.
217. Edwards, D.J. and K.E. Holt, *Beginner's guide to comparative bacterial genome analysis using next-generation sequence data*. Microb Inform Exp, 2013. **3**(1): p. 2.
218. Koser, C.U., M.J. Ellington, and S.J. Peacock, *Whole-genome sequencing to control antimicrobial resistance*. Trends Genet, 2014. **30**(9): p. 401-7.
219. Harris, S.R., et al., *Whole-genome sequencing for analysis of an outbreak of methicillin-resistant Staphylococcus aureus: a descriptive study*. Lancet Infect Dis, 2013. **13**(2): p. 130-6.
220. Grad, Y.H., et al., *Genomic epidemiology of Neisseria gonorrhoeae with reduced susceptibility to cefixime in the USA: a retrospective observational study*. Lancet Infect Dis, 2014. **14**(3): p. 220-6.
221. Tritt, A., et al., *An integrated pipeline for de novo assembly of microbial genomes*. PLoS One, 2012. **7**(9): p. e42304.
222. Faison, W.J., et al., *Whole genome single-nucleotide variation profile-based phylogenetic tree building methods for analysis of viral, bacterial and human genomes*. Genomics, 2014. **104**(1): p. 1-7.

223. Lee, T.H., et al., *SNPhylo: a pipeline to construct a phylogenetic tree from huge SNP data*. BMC Genomics, 2014. **15**: p. 162.
224. Leekitcharoenphon, P., et al., *snpTree--a web-server to identify and construct SNP trees from whole genome sequence data*. BMC Genomics, 2012. **13 Suppl 7**: p. S6.
225. Grad, Y.H., et al., *Genomic epidemiology of the Escherichia coli O104:H4 outbreaks in Europe, 2011*. Proc Natl Acad Sci U S A, 2012. **109**(8): p. 3065-70.
226. Raz, N., et al., *Genome-wide SNP-genotyping array to study the evolution of the human pathogen Vibrio vulnificus biotype 3*. PLoS One, 2014. **9**(12): p. e114576.
227. Kurtz, S., et al., *Versatile and open software for comparing large genomes*. Genome Biol, 2004. **5**(2): p. R12.
228. Krzywinski, M., et al., *Circos: an information aesthetic for comparative genomics*. Genome Res, 2009. **19**(9): p. 1639-45.
229. Aziz, R.K., et al., *The RAST Server: rapid annotations using subsystems technology*. BMC Genomics, 2008. **9**: p. 75.
230. Meyer, F., R. Overbeek, and A. Rodriguez, *FIGfams: yet another set of protein families*. Nucleic Acids Res, 2009. **37**(20): p. 6643-54.
231. Pukatzki, S., et al., *Identification of a conserved bacterial protein secretion system in Vibrio cholerae using the Dictyostelium host model system*. Proc Natl Acad Sci U S A, 2006. **103**(5): p. 1528-33.
232. Mougous, J.D., et al., *Threonine phosphorylation post-translationally regulates protein secretion in Pseudomonas aeruginosa*. Nat Cell Biol, 2007. **9**(7): p. 797-803.
233. Schell, M.A., et al., *Type VI secretion is a major virulence determinant in Burkholderia mallei*. Mol Microbiol, 2007. **64**(6): p. 1466-85.
234. Murdoch, S.L., et al., *The opportunistic pathogen Serratia marcescens utilizes type VI secretion to target bacterial competitors*. J Bacteriol, 2011. **193**(21): p. 6057-69.
235. Lertpiriyapong, K., et al., *Campylobacter jejuni type VI secretion system: roles in adaptation to deoxycholic acid, host cell adherence, invasion, and in vivo colonization*. PLoS One, 2012. **7**(8): p. e42842.
236. Bingle, L.E., C.M. Bailey, and M.J. Pallen, *Type VI secretion: a beginner's guide*. Curr Opin Microbiol, 2008. **11**(1): p. 3-8.
237. Coulthurst, S.J., *The Type VI secretion system - a widespread and versatile cell targeting system*. Res Microbiol, 2013. **164**(6): p. 640-54.
238. Filloux, A., *The rise of the Type VI secretion system*. F1000Prime Rep, 2013. **5**: p. 52.
239. Miyata, S.T., et al., *The Vibrio Cholerae Type VI Secretion System: Evaluating its Role in the Human Disease Cholera*. Front Microbiol, 2010. **1**: p. 117.
240. Zaluga, J., et al., *Comparative genome analysis of pathogenic and non-pathogenic Clavibacter strains reveals adaptations to their lifestyle*. BMC Genomics, 2014. **15**: p. 392.
241. Ho, B.T., T.G. Dong, and J.J. Mekalanos, *A View to a Kill: The Bacterial Type VI Secretion System*. Cell Host Microbe, 2014. **15**(1): p. 9-21.
242. Hood, R.D., et al., *A type VI secretion system of Pseudomonas aeruginosa targets a toxin to bacteria*. Cell Host Microbe, 2010. **7**(1): p. 25-37.

243. Ishikawa, T., et al., *Pathoadaptive conditional regulation of the type VI secretion system in Vibrio cholerae O1 strains*. Infect Immun, 2012. **80**(2): p. 575-84.
244. Jani, A.J. and P.A. Cotter, *Type VI secretion: not just for pathogenesis anymore*. Cell Host Microbe, 2010. **8**(1): p. 2-6.
245. MacIntyre, D.L., et al., *The Vibrio cholerae type VI secretion system displays antimicrobial properties*. Proc Natl Acad Sci U S A, 2010. **107**(45): p. 19520-4.
246. Russell, A.B., et al., *Type VI secretion delivers bacteriolytic effectors to target cells*. Nature, 2011. **475**(7356): p. 343-7.
247. Russell, A.B., S.B. Peterson, and J.D. Mougous, *Type VI secretion system effectors: poisons with a purpose*. Nat Rev Microbiol, 2014. **12**(2): p. 137-48.
248. Schwarz, S., et al., *Burkholderia type VI secretion systems have distinct roles in eukaryotic and bacterial cell interactions*. PLoS Pathog, 2010. **6**(8): p. e1001068.
249. Williams, S.G., et al., *Vibrio cholerae Hcp, a secreted protein coregulated with HlyA*. Infect Immun, 1996. **64**(1): p. 283-9.
250. Wang, J., et al., *A novel serine/threonine protein kinase homologue of Pseudomonas aeruginosa is specifically inducible within the host infection site and is required for full virulence in neutropenic mice*. J Bacteriol, 1998. **180**(24): p. 6764-8.
251. Folkesson, A., S. Lofdahl, and S. Normark, *The Salmonella enterica subspecies I specific centisome 7 genomic island encodes novel protein families present in bacteria living in close contact with eukaryotic cells*. Res Microbiol, 2002. **153**(8): p. 537-45.
252. Parsons, D.A. and F. Heffron, *sciS, an icmF homolog in Salmonella enterica serovar Typhimurium, limits intracellular replication and decreases virulence*. Infect Immun, 2005. **73**(7): p. 4338-45.
253. Bladergroen, M.R., K. Badelt, and H.P. Spink, *Infection-blocking genes of a symbiotic Rhizobium leguminosarum strain that are involved in temperature-dependent protein secretion*. Mol Plant Microbe Interact, 2003. **16**(1): p. 53-64.
254. Salomon, D., et al., *Vibrio parahaemolyticus type VI secretion system 1 is activated in marine conditions to target bacteria, and is differentially regulated from system 2*. PLoS One, 2013. **8**(4): p. e61086.
255. Boyer, F., et al., *Dissecting the bacterial type VI secretion system by a genome wide in silico analysis: what can be learned from available microbial genomic resources?* BMC Genomics, 2009. **10**: p. 104.
256. Zoued, A., et al., *Architecture and assembly of the Type VI secretion system*. Biochim Biophys Acta, 2014. **1843**(8): p. 1664-73.
257. Broms, J.E., et al., *A functional VipA-VipB interaction is required for the type VI secretion system activity of Vibrio cholerae O1 strain A1552*. BMC Microbiol, 2013. **13**: p. 96.
258. Brunet, Y.R., et al., *Type VI secretion and bacteriophage tail tubes share a common assembly pathway*. EMBO Rep, 2014. **15**(3): p. 315-21.
259. Basler, M., et al., *Type VI secretion requires a dynamic contractile phage tail-like structure*. Nature, 2012. **483**(7388): p. 182-6.
260. Hachani, A., et al., *The VgrG proteins are "a la carte" delivery systems for bacterial type VI effectors*. J Biol Chem, 2014. **289**(25): p. 17872-84.
261. Silverman, J.M., et al., *Structure and regulation of the type VI secretion system*. Annu Rev Microbiol, 2012. **66**: p. 453-72.

262. Durand, E., et al., *Structural characterization and oligomerization of the TssL protein, a component shared by bacterial type VI and type IVb secretion systems*. J Biol Chem, 2012. **287**(17): p. 14157-68.
263. Ma, L., et al., *Expression of the type VI secretion system 1 component Hcp1 is indirectly repressed by OpaR in Vibrio parahaemolyticus*. ScientificWorldJournal, 2012. **2012**: p. 982140.
264. Pell, L.G., et al., *The phage lambda major tail protein structure reveals a common evolution for long-tailed phages and the type VI bacterial secretion system*. Proc Natl Acad Sci U S A, 2009. **106**(11): p. 4160-5.
265. Leiman, P.G., et al., *Type VI secretion apparatus and phage tail-associated protein complexes share a common evolutionary origin*. Proc Natl Acad Sci U S A, 2009. **106**(11): p. 4154-9.
266. Mougous, J.D., et al., *A virulence locus of Pseudomonas aeruginosa encodes a protein secretion apparatus*. Science, 2006. **312**(5779): p. 1526-30.
267. Silverman, J.M., et al., *Haemolysin coregulated protein is an exported receptor and chaperone of type VI secretion substrates*. Mol Cell, 2013. **51**(5): p. 584-93.
268. Shneider, M.M., et al., *PAAR-repeat proteins sharpen and diversify the type VI secretion system spike*. Nature, 2013. **500**(7462): p. 350-3.
269. Ma, A.T., et al., *Translocation of a Vibrio cholerae type VI secretion effector requires bacterial endocytosis by host cells*. Cell Host Microbe, 2009. **5**(3): p. 234-43.
270. Pukatzki, S., et al., *Type VI secretion system translocates a phage tail spike-like protein into target cells where it cross-links actin*. Proc Natl Acad Sci U S A, 2007. **104**(39): p. 15508-13.
271. Kube, S., et al., *Structure of the VipA/B type VI secretion complex suggests a contraction-state-specific recycling mechanism*. Cell Rep, 2014. **8**(1): p. 20-30.
272. Segal, G., M. Feldman, and T. Zusman, *The Icm/Dot type-IV secretion systems of Legionella pneumophila and Coxiella burnetii*. FEMS Microbiol Rev, 2005. **29**(1): p. 65-81.
273. Felisberto-Rodrigues, C., et al., *Towards a structural comprehension of bacterial type VI secretion systems: characterization of the TssJ-TssM complex of an Escherichia coli pathovar*. PLoS Pathog, 2011. **7**(11): p. e1002386.
274. Ma, A.T. and J.J. Mekalanos, *In vivo actin cross-linking induced by Vibrio cholerae type VI secretion system is associated with intestinal inflammation*. Proc Natl Acad Sci U S A, 2010. **107**(9): p. 4365-70.
275. Ma, L.S., F. Narberhaus, and E.M. Lai, *IcmF family protein TssM exhibits ATPase activity and energizes type VI secretion*. J Biol Chem, 2012. **287**(19): p. 15610-21.
276. Ma, L.S., J.S. Lin, and E.M. Lai, *An IcmF family protein, ImpLM, is an integral inner membrane protein interacting with ImpKL, and its walker a motif is required for type VI secretion system-mediated Hcp secretion in Agrobacterium tumefaciens*. J Bacteriol, 2009. **191**(13): p. 4316-29.
277. Aschtgen, M.S., M.S. Thomas, and E. Cascales, *Anchoring the type VI secretion system to the peptidoglycan: TssL, TagL, TagP... what else?* Virulence, 2010. **1**(6): p. 535-40.

278. Zoued, A., et al., *TssK is a trimeric cytoplasmic protein interacting with components of both phage-like and membrane anchoring complexes of the type VI secretion system*. J Biol Chem, 2013. **288**(38): p. 27031-41.
279. Miyata, S.T., et al., *Vibrio cholerae requires the type VI secretion system virulence factor VasX to kill Dictyostelium discoideum*. Infect Immun, 2011. **79**(7): p. 2941-9.
280. Shalom, G., J.G. Shaw, and M.S. Thomas, *In vivo expression technology identifies a type VI secretion system locus in Burkholderia pseudomallei that is induced upon invasion of macrophages*. Microbiology, 2007. **153**(Pt 8): p. 2689-99.
281. Burtneck, M.N., et al., *The cluster 1 type VI secretion system is a major virulence determinant in Burkholderia pseudomallei*. Infect Immun, 2011. **79**(4): p. 1512-25.
282. Schwarz, S., et al., *VgrG-5 is a Burkholderia type VI secretion system-exported protein required for multinucleated giant cell formation and virulence*. Infect Immun, 2014. **82**(4): p. 1445-52.
283. English, G., et al., *New secreted toxins and immunity proteins encoded within the Type VI secretion system gene cluster of Serratia marcescens*. Mol Microbiol, 2012. **86**(4): p. 921-36.
284. Fritsch, M.J., et al., *Proteomic Identification of Novel Secreted Antibacterial Toxins of the Serratia marcescens Type VI Secretion System*. Mol Cell Proteomics, 2013. **12**(10): p. 2735-49.
285. Durand, E., et al., *VgrG, Tae, Tle, and beyond: the versatile arsenal of Type VI secretion effectors*. Trends Microbiol, 2014. **22**(9): p. 498-507.
286. Russell, A.B., et al., *A widespread bacterial type VI secretion effector superfamily identified using a heuristic approach*. Cell Host Microbe, 2012. **11**(5): p. 538-49.
287. Whitney, J.C., et al., *Identification, structure, and function of a novel type VI secretion peptidoglycan glycoside hydrolase effector-immunity pair*. J Biol Chem, 2013. **288**(37): p. 26616-24.
288. Unterweger, D., et al., *The Vibrio cholerae type VI secretion system employs diverse effector modules for intraspecific competition*. Nat Commun, 2014. **5**: p. 3549.
289. Russell, A.B., et al., *Diverse type VI secretion phospholipases are functionally plastic antibacterial effectors*. Nature, 2013. **496**(7446): p. 508-12.
290. Dong, T.G., et al., *Identification of T6SS-dependent effector and immunity proteins by Tn-seq in Vibrio cholerae*. Proc Natl Acad Sci U S A, 2013. **110**(7): p. 2623-8.
291. Koskiniemi, S., et al., *Rhs proteins from diverse bacteria mediate intercellular competition*. Proc Natl Acad Sci U S A, 2013. **110**(17): p. 7032-7.
292. Lesic, B., et al., *Quorum sensing differentially regulates Pseudomonas aeruginosa type VI secretion locus I and homologous loci II and III, which are required for pathogenesis*. Microbiology, 2009. **155**(Pt 9): p. 2845-55.
293. Ishikawa, T., et al., *Quorum sensing regulation of the two hcp alleles in Vibrio cholerae O1 strains*. PLoS One, 2009. **4**(8): p. e6734.
294. Wu, C.F., et al., *Acid-induced type VI secretion system is regulated by ExoR-ChvG/ChvI signaling cascade in Agrobacterium tumefaciens*. PLoS Pathog, 2012. **8**(9): p. e1002938.

295. Unterweger, D., et al., *Constitutive type VI secretion system expression gives Vibrio cholerae intra- and interspecific competitive advantages*. PLoS One, 2012. **7**(10): p. e48320.
296. Wu, H.Y., et al., *Secretome analysis uncovers an Hcp-family protein secreted via a type VI secretion system in Agrobacterium tumefaciens*. J Bacteriol, 2008. **190**(8): p. 2841-50.
297. Basler, M. and J.J. Mekalanos, *Type 6 secretion dynamics within and between bacterial cells*. Science, 2012. **337**(6096): p. 815.
298. Basler, M., B.T. Ho, and J.J. Mekalanos, *Tit-for-tat: type VI secretion system counterattack during bacterial cell-cell interactions*. Cell, 2013. **152**(4): p. 884-94.
299. LeRoux, M., et al., *Quantitative single-cell characterization of bacterial interactions reveals type VI secretion is a double-edged sword*. Proc Natl Acad Sci U S A, 2012. **109**(48): p. 19804-9.
300. Suarez, G., et al., *A type VI secretion system effector protein, VgrG1, from Aeromonas hydrophila that induces host cell toxicity by ADP ribosylation of actin*. J Bacteriol, 2010. **192**(1): p. 155-68.
301. Carruthers, M.D., et al., *Acinetobacter baumannii utilizes a type VI secretion system for bacterial competition*. PLoS One, 2013. **8**(3): p. e59388.
302. Hensel, M. and D.W. Holden, *Molecular genetic approaches for the study of virulence in both pathogenic bacteria and fungi*. Microbiology, 1996. **142 (Pt 5)**: p. 1049-58.
303. Milton, D.L., et al., *Flagellin A is essential for the virulence of Vibrio anguillarum*. J Bacteriol, 1996. **178**(5): p. 1310-9.
304. Shao, C.P., et al., *Regulation of cytotoxicity by quorum-sensing signaling in Vibrio vulnificus is mediated by SmcR, a repressor of hlyU*. J Bacteriol, 2011. **193**(10): p. 2557-65.
305. Tan, W., et al., *Molecular characterization of vulnibactin biosynthesis in Vibrio vulnificus indicates the existence of an alternative siderophore*. Front Microbiol, 2014. **5**: p. 1.
306. Alice, A.F., H. Naka, and J.H. Crosa, *Global gene expression as a function of the iron status of the bacterial cell: influence of differentially expressed genes in the virulence of the human pathogen Vibrio vulnificus*. Infect Immun, 2008. **76**(9): p. 4019-37.
307. Carver, T., et al., *Artemis and ACT: viewing, annotating and comparing sequences stored in a relational database*. Bioinformatics, 2008. **24**(23): p. 2672-6.
308. Chou, S., et al., *Structure of a peptidoglycan amidase effector targeted to Gram-negative bacteria by the type VI secretion system*. Cell Rep, 2012. **1**(6): p. 656-64.
309. Jiang, F., et al., *A Pseudomonas aeruginosa type VI secretion phospholipase D effector targets both prokaryotic and eukaryotic cells*. Cell Host Microbe, 2014. **15**(5): p. 600-10.
310. Zhang, W., et al., *Modulation of a thermoregulated type VI secretion system by AHL-dependent quorum sensing in Yersinia pseudotuberculosis*. Arch Microbiol, 2011. **193**(5): p. 351-63.
311. Miyata, S.T., et al., *Dual expression profile of type VI secretion system immunity genes protects pandemic Vibrio cholerae*. PLoS Pathog, 2013. **9**(12): p. e1003752.

312. Hsu, F., S. Schwarz, and J.D. Mougous, *TagR promotes PpkA-catalysed type VI secretion activation in Pseudomonas aeruginosa*. Mol Microbiol, 2009. **72**(5): p. 1111-25.
313. Silverman, J.M., et al., *Separate inputs modulate phosphorylation-dependent and -independent type VI secretion activation*. Mol Microbiol, 2011. **82**(5): p. 1277-90.
314. de Pace, F., et al., *Characterization of lcmF of the type VI secretion system in an avian pathogenic Escherichia coli (APEC) strain*. Microbiology, 2011. **157**(Pt 10): p. 2954-62.
315. Hachani, A., N.S. Lossi, and A. Filloux, *A visual assay to monitor T6SS-mediated bacterial competition*. J Vis Exp, 2013(73): p. e50103.
316. Hachani, A., et al., *Type VI secretion system in Pseudomonas aeruginosa: secretion and multimerization of VgrG proteins*. J Biol Chem, 2011. **286**(14): p. 12317-27.
317. Decoin, V., et al., *A type VI secretion system is involved in Pseudomonas fluorescens bacterial competition*. PLoS One, 2014. **9**(2): p. e89411.
318. Lu, X., et al., *Identification of genetic bases of vibrio fluvialis species-specific biochemical pathways and potential virulence factors by comparative genomic analysis*. Appl Environ Microbiol, 2014. **80**(6): p. 2029-37.
319. Ramamurthy, T., et al., *Vibrio fluvialis: an emerging human pathogen*. Front Microbiol, 2014. **5**: p. 91.
320. Kelly, M.T. and E.M. Stroh, *Occurrence of Vibrionaceae in natural and cultivated oyster populations in the Pacific Northwest*. Diagn Microbiol Infect Dis, 1988. **9**(1): p. 1-5.
321. Garcia Cortes, V. and F. Antillon, *[Isolation of enteropathogenic Vibrio in bivalves and mud from the Nicoya Gulf, Costa Rica]*. Rev Biol Trop, 1990. **38**(2B): p. 437-40.
322. Long, R.A., et al., *Antagonistic interactions among marine bacteria impede the proliferation of Vibrio cholerae*. Appl Environ Microbiol, 2005. **71**(12): p. 8531-6.
323. Hibbing, M.E., et al., *Bacterial competition: surviving and thriving in the microbial jungle*. Nat Rev Microbiol, 2010. **8**(1): p. 15-25.
324. Cho, H., T. Uehara, and T.G. Bernhardt, *Beta-lactam antibiotics induce a lethal malfunctioning of the bacterial cell wall synthesis machinery*. Cell, 2014. **159**(6): p. 1300-11.
325. Bangen K, H.N., Louie A, Mei G and Trewartha J, *The effects of Incubation with Ampicilin and Tetracycline on the Expression of the bla and tetA genes of pBR322*. Journal of Experimental, Microbiology and Immunology 2004. **5**: p. 23-28.
326. Jones, C., et al., *Subinhibitory concentration of kanamycin induces the Pseudomonas aeruginosa type VI secretion system*. PLoS One, 2013. **8**(11): p. e81132.
327. Vidal, J.E. and F. Navarro-Garcia, *EspC translocation into epithelial cells by enteropathogenic Escherichia coli requires a concerted participation of type V and III secretion systems*. Cell Microbiol, 2008. **10**(10): p. 1975-86.
328. Shao, C.P. and L.I. Hor, *Metalloprotease is not essential for Vibrio vulnificus virulence in mice*. Infect Immun, 2000. **68**(6): p. 3569-73.

Appendix

Appendix A1: Statistical 2-way ANOVA analysis of *V. vulnificus* growth curve data. The OD growth curves carried out for the 10 *V. vulnificus* strains were analysed using a 2-way ANOVA followed by a post-hoc Tukey test using GraphPad 6. Highlighted in yellow are the strains which demonstrated a statistical significance, shown in red and green is whether the strain was clinical or environmental respectively. The “Summary” column gives an indication of significance which is denoted with an asterisk(s) and “ns” denotes a non-significant difference between the strains. The corresponding P-value for the significance is shown in the last column entitled, “Adjusted P-Value”. The “Row” corresponds to the Time (hours), where Row1 = 0 hours, Row2 = 2hours, Row3 =4 hours and Row4 = 6 hours.

Within each row, compare columns
(simple effects within rows)

Number of families	4
Number of comparisons per family	45
Alpha	0.05

Tukey's multiple comparisons test	Mean Diff.	95% CI of diff.	Significant?	Summary	Adjusted P Value
Row 1					
ORL-1506 vs. S3-16	0.0	-1.925 to 1.925	No	ns	> 0.9999
ORL-1506 vs. 106-2A	0.0	-1.925 to 1.925	No	ns	> 0.9999
ORL-1506 vs. NSV-5830	0.0	-1.925 to 1.925	No	ns	> 0.9999
ORL-1506 vs. S2-22	0.0	-1.925 to 1.925	No	ns	> 0.9999
ORL-1506 vs. DAL-79040	0.0	-1.925 to 1.925	No	ns	> 0.9999
ORL-1506 vs. 99-743	0.0	-1.925 to 1.925	No	ns	> 0.9999
ORL-1506 vs. DAL-79087	0.0	-1.925 to 1.925	No	ns	> 0.9999
ORL-1506 vs. ATL-9824	0.0	-1.925 to 1.925	No	ns	> 0.9999
ORL-1506 vs. 99-796	0.0	-1.925 to 1.925	No	ns	> 0.9999
S3-16 vs. 106-2A	0.0	-1.925 to 1.925	No	ns	> 0.9999
S3-16 vs. NSV-5830	0.0	-1.925 to 1.925	No	ns	> 0.9999
S3-16 vs. S2-22	0.0	-1.925 to 1.925	No	ns	> 0.9999
S3-16 vs. DAL-79040	0.0	-1.925 to 1.925	No	ns	> 0.9999
S3-16 vs. 99-743	0.0	-1.925 to 1.925	No	ns	> 0.9999
S3-16 vs. DAL-79087	0.0	-1.925 to 1.925	No	ns	> 0.9999

S3-16 vs. ATL-9824	0.0	-1.925 to 1.925	No	ns	> 0.9999
S3-16 vs. 99-796	0.0	-1.925 to 1.925	No	ns	> 0.9999
106-2A vs. NSV-5830	0.0	-1.925 to 1.925	No	ns	> 0.9999
106-2A vs. S2-22	0.0	-1.925 to 1.925	No	ns	> 0.9999
106-2A vs. DAL-79040	0.0	-1.925 to 1.925	No	ns	> 0.9999
106-2A vs. 99-743	0.0	-1.925 to 1.925	No	ns	> 0.9999
106-2A vs. DAL-79087	0.0	-1.925 to 1.925	No	ns	> 0.9999
106-2A vs. ATL-9824	0.0	-1.925 to 1.925	No	ns	> 0.9999
106-2A vs. 99-796	0.0	-1.925 to 1.925	No	ns	> 0.9999
NSV-5830 vs. S2-22	0.0	-1.925 to 1.925	No	ns	> 0.9999
NSV-5830 vs. DAL-79040	0.0	-1.925 to 1.925	No	ns	> 0.9999
NSV-5830 vs. 99-743	0.0	-1.925 to 1.925	No	ns	> 0.9999
NSV-5830 vs. DAL-79087	0.0	-1.925 to 1.925	No	ns	> 0.9999
NSV-5830 vs. ATL-9824	0.0	-1.925 to 1.925	No	ns	> 0.9999
NSV-5830 vs. 99-796	0.0	-1.925 to 1.925	No	ns	> 0.9999
S2-22 vs. DAL-79040	0.0	-1.925 to 1.925	No	ns	> 0.9999
S2-22 vs. 99-743	0.0	-1.925 to 1.925	No	ns	> 0.9999
S2-22 vs. DAL-79087	0.0	-1.925 to 1.925	No	ns	> 0.9999
S2-22 vs. ATL-9824	0.0	-1.925 to 1.925	No	ns	> 0.9999
S2-22 vs. 99-796	0.0	-1.925 to 1.925	No	ns	> 0.9999
DAL-79040 vs. 99-743	0.0	-1.925 to 1.925	No	ns	> 0.9999
DAL-79040 vs. DAL-79087	0.0	-1.925 to 1.925	No	ns	> 0.9999
DAL-79040 vs. ATL-9824	0.0	-1.925 to 1.925	No	ns	> 0.9999
DAL-79040 vs. 99-796	0.0	-1.925 to 1.925	No	ns	> 0.9999
99-743 vs. DAL-79087	0.0	-1.925 to 1.925	No	ns	> 0.9999
99-743 vs. ATL-9824	0.0	-1.925 to 1.925	No	ns	> 0.9999
99-743 vs. 99-796	0.0	-1.925 to 1.925	No	ns	> 0.9999
DAL-79087 vs. ATL-9824	0.0	-1.925 to 1.925	No	ns	> 0.9999
DAL-79087 vs. 99-796	0.0	-1.925 to 1.925	No	ns	> 0.9999
ATL-9824 vs. 99-796	0.0	-1.925 to 1.925	No	ns	> 0.9999
Row 2					
ORL-1506 vs. S3-16	0.5970	-1.328 to 2.522	No	ns	0.9909
ORL-1506 vs. 106-2A	0.4913	-1.434 to 2.417	No	ns	0.9979
ORL-1506 vs. NSV-5830	0.3137	-1.612 to 2.239	No	ns	> 0.9999

ORL-1506 vs. S2-22	-0.4590	-2.384 to 1.466	No	ns	0.9987
ORL-1506 vs. DAL-79040	0.3410	-1.584 to 2.266	No	ns	0.9999
ORL-1506 vs. 99-743	0.4810	-1.444 to 2.406	No	ns	0.9982
ORL-1506 vs. DAL-79087	0.4843	-1.441 to 2.410	No	ns	0.9981
ORL-1506 vs. ATL-9824	0.5310	-1.394 to 2.456	No	ns	0.9961
ORL-1506 vs. 99-796	0.7510	-1.174 to 2.676	No	ns	0.9576
S3-16 vs. 106-2A	-0.1057	-2.031 to 1.820	No	ns	> 0.9999
S3-16 vs. NSV-5830	-0.2833	-2.209 to 1.642	No	ns	> 0.9999
S3-16 vs. S2-22	-1.056	-2.981 to 0.8695	No	ns	0.7425
S3-16 vs. DAL-79040	-0.2560	-2.181 to 1.669	No	ns	> 0.9999
S3-16 vs. 99-743	-0.1160	-2.041 to 1.809	No	ns	> 0.9999
S3-16 vs. DAL-79087	-0.1127	-2.038 to 1.813	No	ns	> 0.9999
S3-16 vs. ATL-9824	-0.06600	-1.991 to 1.859	No	ns	> 0.9999
S3-16 vs. 99-796	0.1540	-1.771 to 2.079	No	ns	> 0.9999
106-2A vs. NSV-5830	-0.1777	-2.103 to 1.748	No	ns	> 0.9999
106-2A vs. S2-22	-0.9503	-2.876 to 0.9752	No	ns	0.8412
106-2A vs. DAL-79040	-0.1503	-2.076 to 1.775	No	ns	> 0.9999
106-2A vs. 99-743	-0.01033	-1.936 to 1.915	No	ns	> 0.9999
106-2A vs. DAL-79087	-0.007000	-1.932 to 1.918	No	ns	> 0.9999
106-2A vs. ATL-9824	0.03967	-1.886 to 1.965	No	ns	> 0.9999
106-2A vs. 99-796	0.2597	-1.666 to 2.185	No	ns	> 0.9999
NSV-5830 vs. S2-22	-0.7727	-2.698 to 1.153	No	ns	0.9494
NSV-5830 vs. DAL-79040	0.02733	-1.898 to 1.953	No	ns	> 0.9999
NSV-5830 vs. 99-743	0.1673	-1.758 to 2.093	No	ns	> 0.9999
NSV-5830 vs. DAL-79087	0.1707	-1.755 to 2.096	No	ns	> 0.9999
NSV-5830 vs. ATL-9824	0.2173	-1.708 to 2.143	No	ns	> 0.9999
NSV-5830 vs. 99-796	0.4373	-1.488 to 2.363	No	ns	0.9991
S2-22 vs. DAL-79040	0.8000	-1.125 to 2.725	No	ns	0.9377
S2-22 vs. 99-743	0.9400	-0.9855 to 2.865	No	ns	0.8496
S2-22 vs. DAL-79087	0.9433	-0.9822 to 2.869	No	ns	0.8469
S2-22 vs. ATL-9824	0.9900	-0.9355 to 2.915	No	ns	0.8068
S2-22 vs. 99-796	1.210	-0.7155 to 3.135	No	ns	0.5706
DAL-79040 vs. 99-743	0.1400	-1.785 to 2.065	No	ns	> 0.9999
DAL-79040 vs. DAL-79087	0.1433	-1.782 to 2.069	No	ns	> 0.9999
DAL-79040 vs. ATL-9824	0.1900	-1.735 to 2.115	No	ns	> 0.9999

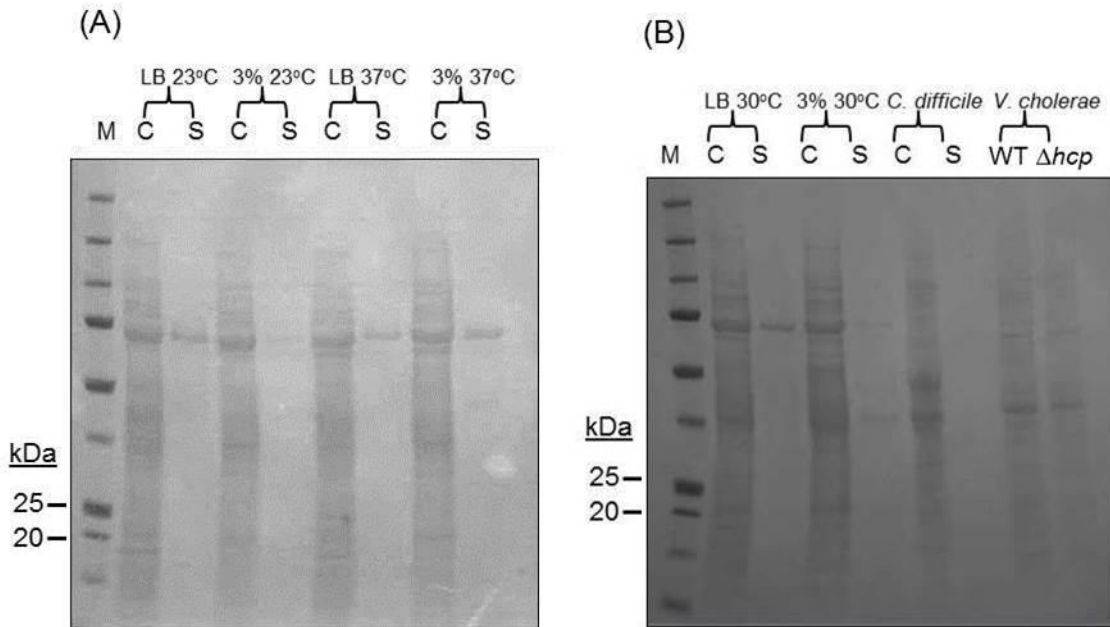
DAL-79040 vs. 99-796	0.4100	-1.515 to 2.335	No	ns	0.9995
99-743 vs. DAL-79087	0.003333	-1.922 to 1.929	No	ns	> 0.9999
99-743 vs. ATL-9824	0.05000	-1.875 to 1.975	No	ns	> 0.9999
99-743 vs. 99-796	0.2700	-1.655 to 2.195	No	ns	> 0.9999
DAL-79087 vs. ATL-9824	0.04667	-1.879 to 1.972	No	ns	> 0.9999
DAL-79087 vs. 99-796	0.2667	-1.659 to 2.192	No	ns	> 0.9999
ATL-9824 vs. 99-796	0.2200	-1.705 to 2.145	No	ns	> 0.9999
Row 3					
ORL-1506 vs. S3-16	0.6427	-1.283 to 2.568	No	ns	0.9847
ORL-1506 vs. 106-2A	0.8767	-1.049 to 2.802	No	ns	0.8954
ORL-1506 vs. NSV-5830	-0.2000	-2.125 to 1.725	No	ns	> 0.9999
ORL-1506 vs. S2-22	-0.2117	-2.137 to 1.714	No	ns	> 0.9999
ORL-1506 vs. DAL-79040	-1.078	-3.004 to 0.8472	No	ns	0.7190
ORL-1506 vs. 99-743	-1.778	-3.704 to 0.1472	No	ns	0.0952
ORL-1506 vs. DAL-79087	-2.045	-3.970 to -0.1195	Yes	*	0.0283
ORL-1506 vs. ATL-9824	-1.878	-3.804 to 0.04716	No	ns	0.0619
ORL-1506 vs. 99-796	-1.045	-2.970 to 0.8805	No	ns	0.7537
S3-16 vs. 106-2A	0.2340	-1.691 to 2.159	No	ns	> 0.9999
S3-16 vs. NSV-5830	-0.8427	-2.768 to 1.083	No	ns	0.9159
S3-16 vs. S2-22	-0.8543	-2.780 to 1.071	No	ns	0.9092
S3-16 vs. DAL-79040	-1.721	-3.646 to 0.2045	No	ns	0.1202
S3-16 vs. 99-743	-2.421	-4.346 to -0.4955	Yes	**	0.0038
S3-16 vs. DAL-79087	-2.688	-4.613 to -0.7622	Yes	***	0.0008
S3-16 vs. ATL-9824	-2.521	-4.446 to -0.5955	Yes	**	0.0021
S3-16 vs. 99-796	-1.688	-3.613 to 0.2378	No	ns	0.1370
106-2A vs. NSV-5830	-1.077	-3.002 to 0.8488	No	ns	0.7208
106-2A vs. S2-22	-1.088	-3.014 to 0.8372	No	ns	0.7083
106-2A vs. DAL-79040	-1.955	-3.880 to -0.02950	Yes	*	0.0436
106-2A vs. 99-743	-2.655	-4.580 to -0.7295	Yes	***	0.0010
106-2A vs. DAL-79087	-2.922	-4.847 to -0.9962	Yes	***	0.0002
106-2A vs. ATL-9824	-2.755	-4.680 to -0.8295	Yes	***	0.0005
106-2A vs. 99-796	-1.922	-3.847 to 0.003829	No	ns	0.0509
NSV-5830 vs. S2-22	-0.01167	-1.937 to 1.914	No	ns	> 0.9999
NSV-5830 vs. DAL-79040	-0.8783	-2.804 to 1.047	No	ns	0.8943

NSV-5830 vs. 99-743	-1.578	-3.504 to 0.3472	No	ns	0.2048
NSV-5830 vs. DAL-79087	-1.845	-3.770 to 0.08050	No	ns	0.0717
NSV-5830 vs. ATL-9824	-1.678	-3.604 to 0.2472	No	ns	0.1420
NSV-5830 vs. 99-796	-0.8450	-2.770 to 1.080	No	ns	0.9146
S2-22 vs. DAL-79040	-0.8667	-2.792 to 1.059	No	ns	0.9017
S2-22 vs. 99-743	-1.567	-3.492 to 0.3588	No	ns	0.2133
S2-22 vs. DAL-79087	-1.833	-3.759 to 0.09216	No	ns	0.0754
S2-22 vs. ATL-9824	-1.667	-3.592 to 0.2588	No	ns	0.1485
S2-22 vs. 99-796	-0.8333	-2.759 to 1.092	No	ns	0.9211
DAL-79040 vs. 99-743	-0.7000	-2.625 to 1.225	No	ns	0.9729
DAL-79040 vs. DAL-79087	-0.9667	-2.892 to 0.9588	No	ns	0.8274
DAL-79040 vs. ATL-9824	-0.8000	-2.725 to 1.125	No	ns	0.9377
DAL-79040 vs. 99-796	0.03333	-1.892 to 1.959	No	ns	> 0.9999
99-743 vs. DAL-79087	-0.2667	-2.192 to 1.659	No	ns	> 0.9999
99-743 vs. ATL-9824	-0.1000	-2.025 to 1.825	No	ns	> 0.9999
99-743 vs. 99-796	0.7333	-1.192 to 2.659	No	ns	0.9634
DAL-79087 vs. ATL-9824	0.1667	-1.759 to 2.092	No	ns	> 0.9999
DAL-79087 vs. 99-796	1.000	-0.9255 to 2.925	No	ns	0.7976
ATL-9824 vs. 99-796	0.8333	-1.092 to 2.759	No	ns	0.9211
Row 4					
ORL-1506 vs. S3-16	0.06333	-1.862 to 1.989	No	ns	> 0.9999
ORL-1506 vs. 106-2A	0.8777	-1.048 to 2.803	No	ns	0.8947
ORL-1506 vs. NSV-5830	-0.6700	-2.595 to 1.255	No	ns	0.9797
ORL-1506 vs. S2-22	-1.943	-3.868 to -0.01717	Yes	*	0.0462
ORL-1506 vs. DAL-79040	-2.543	-4.468 to -0.6172	Yes	**	0.0019
ORL-1506 vs. 99-743	-3.143	-5.068 to -1.217	Yes	****	< 0.0001
ORL-1506 vs. DAL-79087	-2.709	-4.635 to -0.7838	Yes	***	0.0007
ORL-1506 vs. ATL-9824	-3.243	-5.168 to -1.317	Yes	****	< 0.0001
ORL-1506 vs. 99-796	-3.043	-4.968 to -1.117	Yes	****	< 0.0001
S3-16 vs. 106-2A	0.8143	-1.111 to 2.740	No	ns	0.9309
S3-16 vs. NSV-5830	-0.7333	-2.659 to 1.192	No	ns	0.9634
S3-16 vs. S2-22	-2.006	-3.931 to -0.08050	Yes	*	0.0343
S3-16 vs. DAL-79040	-2.606	-4.531 to -0.6805	Yes	**	0.0013
S3-16 vs. 99-743	-3.206	-5.131 to -1.281	Yes	****	< 0.0001

S3-16 vs. DAL-79087	-2.773	-4.698 to -0.8472	Yes	***	0.0005
S3-16 vs. ATL-9824	-3.306	-5.231 to -1.381	Yes	****	< 0.0001
S3-16 vs. 99-796	-3.106	-5.031 to -1.181	Yes	****	< 0.0001
106-2A vs. NSV-5830	-1.548	-3.473 to 0.3778	No	ns	0.2276
106-2A vs. S2-22	-2.820	-4.746 to -0.8948	Yes	***	0.0003
106-2A vs. DAL-79040	-3.420	-5.346 to -1.495	Yes	****	< 0.0001
106-2A vs. 99-743	-4.020	-5.946 to -2.095	Yes	****	< 0.0001
106-2A vs. DAL-79087	-3.587	-5.512 to -1.662	Yes	****	< 0.0001
106-2A vs. ATL-9824	-4.120	-6.046 to -2.195	Yes	****	< 0.0001
106-2A vs. 99-796	-3.920	-5.846 to -1.995	Yes	****	< 0.0001
NSV-5830 vs. S2-22	-1.273	-3.198 to 0.6528	No	ns	0.4982
NSV-5830 vs. DAL-79040	-1.873	-3.798 to 0.05283	No	ns	0.0635
NSV-5830 vs. 99-743	-2.473	-4.398 to -0.5472	Yes	**	0.0028
NSV-5830 vs. DAL-79087	-2.039	-3.965 to -0.1138	Yes	*	0.0291
NSV-5830 vs. ATL-9824	-2.573	-4.498 to -0.6472	Yes	**	0.0016
NSV-5830 vs. 99-796	-2.373	-4.298 to -0.4472	Yes	**	0.0050
S2-22 vs. DAL-79040	-0.6000	-2.525 to 1.325	No	ns	0.9906
S2-22 vs. 99-743	-1.200	-3.125 to 0.7255	No	ns	0.5822
S2-22 vs. DAL-79087	-0.7667	-2.692 to 1.159	No	ns	0.9518
S2-22 vs. ATL-9824	-1.300	-3.225 to 0.6255	No	ns	0.4672
S2-22 vs. 99-796	-1.100	-3.025 to 0.8255	No	ns	0.6956
DAL-79040 vs. 99-743	-0.6000	-2.525 to 1.325	No	ns	0.9906
DAL-79040 vs. DAL-79087	-0.1667	-2.092 to 1.759	No	ns	> 0.9999
DAL-79040 vs. ATL-9824	-0.7000	-2.625 to 1.225	No	ns	0.9729
DAL-79040 vs. 99-796	-0.5000	-2.425 to 1.425	No	ns	0.9976
99-743 vs. DAL-79087	0.4333	-1.492 to 2.359	No	ns	0.9992
99-743 vs. ATL-9824	-0.1000	-2.025 to 1.825	No	ns	> 0.9999
99-743 vs. 99-796	0.1000	-1.825 to 2.025	No	ns	> 0.9999
DAL-79087 vs. ATL-9824	-0.5333	-2.459 to 1.392	No	ns	0.9960
DAL-79087 vs. 99-796	-0.3333	-2.259 to 1.592	No	ns	> 0.9999
ATL-9824 vs. 99-796	0.2000	-1.725 to 2.125	No	ns	> 0.9999

Appendix A2: Ponceau S stain for Western blot images demonstrating expression and secretion of Hcp.

(A) *V. vulnificus* cells lysate (C) and culture filtrates (S) from cells grown at 23°C and 30°C in LB with and without 3% NaCl. (B) Cell lysate (C) and supernatant (S) from *V. vulnificus* cells grown as 30°C in LB and LB supplemented with 3% NaCl. *V. cholerae* V52 cell lysate run as a positive control (*V. cholerae* WT). Negative controls provided by *V. cholerae* $\Delta hcp1\Delta hcp2$ (*V. cholerae* Δhcp), and *C. difficile*. Protein samples loaded equalled 14 μ g of protein/lane. Protein marker is represented with (M). Indicated above each lane are the temperature and media conditions.



Appendix A3: Gene sequence of *icmF* gene from *V. vulnificus* 106-2A T6SS1. The sequence below shows the gene sequence encoding for *icmF* including the flanking genes, *tssA* from T6SS1 of *V. vulnificus* 106-2A.

GGAGTCGAGATGGAAATAACCAATATCGTCAGTGCATTTCCAAACCTGT
TACCAATGACAATCCAATTGGAGAGCGATTGGTCGATCACCCGCTGTTTG
ATTTCAATTGAAGAGCAAATGATGAAAGTTGGATCACTTTCTCATGCTACG
GTGCAGTGGGAAGAGGTTGAGCATAGTACGATTAAGTTACTTAGCGAGCA
AAGTAAAGACATCAAGCTATTGGTTTATCTGCTTCAATGCTTGCATAACC
AAATTACCCCTTTGCGCTTCATTA CTCTTTTTTAGTGATGAGCGAGTTT
ATCGAGCAGTATTGGAATGAGTCTTACCCTGCACCAGGTGCTCGTGGCAA
CCTACCTAGGCGCAAGTATTTTAGTCAGATGACACAACGTTTTAGTACGG
TTGTTGATAAGTTTGATTTTTGCCATCTTGACGCAGCTGATCGTCAAGCG
TTGCAAGCAGCTGTTGGGGAATGGAACTTGTAATCGAAAAGCAGGGGCT
GTTATCAGATTTAGTTGAATCAATAGCGGTCCGTATCGAAGCGGAGATTC
AACGTGCAGAAAAGCAGCAGTCATCGGTT CAGAACGTAGAACAATGACG
CCAAGCATGCCAGCAACGACTCCTAGTTCCAGTATTGTAGCTGACCACTC
TAGCGATAAAGCAGCAAAGCAGACACTACTCAAAGTTGCTGATTTTTTAG
CTGAGCAAGATTTTGAATACCACTATCTATTCGGTTACGGCGTTTTGCA
GTATGGGGCAGTATTACTTCTCTTCCGGATCATAACCCTGATGGTCAAAC
TCTACTAAGAAGTATGCAAGCAGATCGTGTCAAAGATTACCAAGCGCAAC
TGCGTCATGCAGATTTAGCACTATGGCGGAAAGTGAACAAAGCTTAACG
ATGTCTCCGTA CTGGTTTGAAGGTCAGTGGATGAGCTACACCATTGCCCA
GCAACTTGGGAAAAGTGATTGGTCTGAGGCCATTGCAGAAGAGACACAAT
CCTTCTTACATCGTCTACCTTCATTGTTTGACCTCAAATTC AAAGATGGA
GACCCTTTTGTGAGCGAATCAGTTAAAGAGTGGTTAGCCACTATCGGACA
AAAGGAATCATCCTCTGTACAAGCAATAGAGGGAGGTTGGCAAGAAAAAC
GAAAAGTCGCATTCCA ACTTGCTAAGGAAGGAGGAATTGCTGTGGCACTT
TCCATGCTGAACGATGGATTAGTTGGAGCAGTAGAACCACGTGACAAGTT
T TACTGGAGATTATTATCAGCTGATTTGTTACGTGCGAATCATCTTGATG
CGATGGCTGGTGAACAGTACCAA ACTTTGCTCGAGCAGGCGACGACAATG
TCAGTGCCTGAGTGGGAGCCAAGCTTAATTGAACAAATTCAAAGATATAC
AACGTCAGAGTAAACAAGGACACAATTCATGTGGAAATTCATTGTCCGAA

TAGTAAAGCGGCTCAAACCCACAGTGGTCGCTGCATTACCAATTTTGCTA
TTCCTACGTTTCATATTGTTGAACGTCGCCATTTGGTGGGCAGGCCCTG
GTTAGAATTCGCCGGTTATAAACCTTTGGAGTCTATTGTGGCTCGAGTTG
TGCGGAGTAGCTTATTTACTCTCAGTTGTCTAGCCATTTGGGGCATTGG
CAATGGCGAAAACCTGCAAACCTTTTCGAGCGGAACAAAAACGTGAAGACCA
GTTACGTCAAGACCCGATAAAAGTGTATGAAGAAAGACAAGAAGTTGAGT
TGAATCAGGTCATGAACAACATGAAGCAGAACCTGAACAAACACAACCTAC
TTATACGCGTTACCATGGTACTTAGTATTGGGGTTAGAAAACGCAGGAAA
AACCAGCTTAATCAACCGTTCAGGACAAAATTTGTTTTTCTTCAGTAA
TGCGAGCGTCGGGTCAAAAAAGTGAAAATCCGTATTCATTTGATTGGTGG
ATTGGTGACGAATCTGTGTTAATTGACCCTGATGGTGAGTTATTAACCCA
AGGTAATCGAAGTGAAGACAACAACGGGGCAATGGAACGTCGTTTATGGT
TACATTTTGTAGATTGGCTTGACCGTACGCGGAGTAGGCGTCCCCTTAAT
GGAATAGTACTAGCTCTCGATGTTTCCCACCTTGCAACGGCTACGGCATC
CGAGCGTAAAGCTTATGCTAGTTTACTGCGTGCTCGTTTACGAGAAGTGA
TGGAGACACTATCGACTCGTTTACCAGTCTATATTGCTCTAACTAACTC
GATCTTCTTCATGGTTTTGACCCCTTCTTTAAGCACTACACTAAAAGTCA
GAGAGAAGAGGTGTTAGGTTTACATTCTCAATGGATTCGTTAGATAACC
TTGATTCATGGTTAGATGAATTTGCAGAGGAATATGCACAATTTGTTGAA
CGGATGAATCGAATGCTACCACATGCAGTAGCAATGCCGATGACGTTGGA
AGAGCGAAACGCGATTTATAGTTTTACTCGGCAGCTATTTGGCCTAAAAG
ATATTCTTCAGCAGTTTTTCAAAGAAGCGTTGGAGAGTGATCAGTTTTCT
ACTTCTGCCTTGGTGAGGGGAGCGTACTTTACTTCTGTTTATCAGCAAGG
CGTTCCTACAAATGCCTTTGATGATGCAGCTTCACGTCGTTATAGTCTCT
CACACGCGATTAATACTGCGCAGAGAGCGAAAACTCAACCGTCTATTTT
ACACAGAAATTGTTTACGCACATAATTTATCCAGAAGCAGGTTTGGCTTC
GGATAACTTTTCGTGTTGCAAGAAATAAACGTCGTTTAATTGGACTTTCT
TCATTGCATGTACAATTGCAACATTACTTTTGGCGGGAACCTGGCATCGT
AGTTATATTAACAATGTGCAACATGCCGATGCAGTATTAGAAAAAGTAAA
CCAGTATAAAGAGCAGTTTTTCGAGCAATCGCAATCTTGCCTCTCAGAAAG
ACGTACTAGAACCGCTGAATAAGATTCGTGAAGCGACTCTAGAATTTGGT

TTCTTTAGAGATAAGCCGAAATATGTTTCAGATTTTGGTCTTTACCAAGG
GCATACCATTGGCCCTAAAGTTGAAGAAACCTACCTCAATTTACTTGAAA
ACCGTTTTTTGCCCTTACTCATGGCCGATGTGGTAGTGGCTTTAAATCAA
GCCGAGAGTGATGAGGAGAAGCTTGCGGTCCTTCGTGTCTATCGAATGTT
GGTAGATAAAAGTGGTCGATACCAAGATTACGTGATGGATTATTTGCTA
AGTATTGGCAGATGTCTTTTTCGGGTCAACGCAAACTCAAGAGGAATTA
CTAGGGCACTTGGATTATGCGATGCGTCATACCGATTTAACCGCAGATCG
TCTAAACGATGATAAAGGGGCTGAAAAGGTTATGCGTCCATACGATAAAG
TGATCGCGAAAGCCAGGTTGAGTTGAGTTCAATGCCAAACGATCAGCGT
GTCTACAGAAACCTTAAGCTGAGTGCGCAAACGGTTCTAGGTCCTCCAGT
GAATCTTAGAAGCTTGATTGGTCCGGTTTTTGATGTCGTTTTTGAAGAAC
GGGTAAGTGAATAGCAAGAATTTGTATATTCCTCAAATGTTAACCAAACGT
GGGTTTGATGACTATTTTATGCCGCAGTCTGAATCAGTTTCCGAGTTGGC
TTTGATTGATAGCTGGGTATTGGGTCAAAGTAAAACGGCACAATTTAGTG
AAGCTGACAAACAGGCACTGCGCGACAAAATACGAGATCTCTACGTCGCT
GATTATACAAACACATGGCGCTCAGCACTGAACGAGATAGATGTTAAGTA
TTTTAATGATATCAATGATGCAGTTATGGTGTTAGAGAACATCACGAGTA
ATCTCGAACCAATGCAACGCTTACTTCGTA CTCTAGAGGATAATACGCAA
CTGTATAGCGCGTTACCTAAAGACGAAGCTGCAATCAAAGAATTGCTGAA
AAATCCAAAGTACAAAGTGGCTTCTATGATAGAAACACCATTTGCTGAAC
TTAACAGTATGCTCCAGTCTGCTGACAGTAAGCCAGCATAACATGACAGAA
GTGCTCGCATCGGTTGATGAGTTAAAGAGTTATCTAAAATCGATCCAAGA
TGCGCCGGATGTTGGCATGGCTGCATTAGATGCGACCAAAGCGCGAGTAA
AACTAGTCAACGCGGATCCTATTTATACATTAAGCGCGTCTCATCTGGG
TTACCTAAACCACTGGATACAATGATGACGAAAATTGCAGATGAGAGCTG
GTATGTTGTTAAACAAGAAGCGATCAAGCATCTTGAAGTGCGCTGGGCTG
AAGACGTTTATGACACGTTCCAAAGTAAATTAGCAGGACGTTATCCATTT
AATTCTGCTTCCAATAAAGATGTTTCCTTGGAAGATTTTGAACCTTTCTT
TGCGCCTAATGGTACGCTGGATAACTTTTATAATCATCAGTTAAAGATGT
TTATTGAAGAGAATATAACTGTTTCAGCAGATGACTCTACGCAATCAATT
GTCCGTAAAGAGGTACTAGAGCAGATTGAACAAGCACAAAAAATTCGAGA

AGCATTCTTTAATCGTAAAGGTATCTTAGATGTTAGTTTCTCCGTCGAAC
CGCTTAGTCTGAGTAACAACAAACGGCGGAGTGTATTGAATGTGACGGT
CAGTTTTTGGCTTATAGCCATGGACAGCGTGAAAATGTTGAATTGATTTG
GCCAAATACTCTACGTGATTCCGCTGTTTCTAAAGTCACGTTGGTACCGA
CTCAAAGCAACATGTGCGCCACGCAGTATACAGATACAAGGGCCTTGGGCA
TTCTTTTCGATTGTTAGATGAAGGAGATGTGGTTGCGGCTAGTCAGACGTC
AGTAGATTTTAAGTTCATAGTTGATGGTGGTGAAATGATCTACAGAATTA
ACTCAGAAGCGGATGCAAATCCTTTTACTGAACGTCTTTTCAAGTCATTC
AAACTGTCTAAAACCTTTTATTAATTGTTATCAGAGCGAGATTCTCGCTC
TATTCCTTTAGGAAGAAGTCGCGATGTCTAATGTAATTTTCATTGACAAT
CTTTGTTATCGGTTAACCTCAGATTGCAAGAAATTAGAGGGTTAGAACC
TTACTTTAAAATTCGAGAAGAAATAAACCGCCGCTTCAATCCTATTGTAG
GTGGTACGGATTGGCAGTGTGTAAGAGCAATGTGAACTACTCGCTTTT
CATCAAGGAATGGATTTCTTGGTATGTGGCTACTATGCGGTAGCTTGCCT
AAAACTCAGGGCTTATCTGGTTACGCTAAAGGTATGGAATTAATGAGTG
CTAGCCTTGCTAATCAAGGTGAATGTGATGTCAAAGTGCCAAAATACGT
AAAGAGATTCTAGATTGGGTGAATGCACGTGTCGTACATGAATTGAAAAC
GCTCAAACCTAATTATGAATCATTGAGAGAGCTTTATCGTGCCGAGCGTT
ATTGTGAGCGTCTACATCAGTTATTTGAGTACCAGCAAACCGAGTACAAA
GTTGATTTTGAGGGCGTCGGTTTTGCACTGTTTGAGCATATTGACAGGAT
CGAAACTCATTATCACAGTTTGCTTAAAAACAGGAGAAAAATCAACTTC
CCGAGCTCAAGTTATGGCAAAGACATTATGGTCTGGCAATGCTTGGTGGGA
TTGGGTATTGTAATAGGTCTAATTGGCGGATATTGGGTGTGGCCTTGGTT
ACATACCACACCGTATGCAGCTCCACAAATTGTAACAACGCTAAATGACG
AAACAAAATCTCACTCTTTGATCGCTGAATCATCTCAAGCTGAACGACTT
CGTTGGCAAATACTCTTATTCCACTTTATCGCTCTACTCTAGAGCAAAA
TTTATCAGCTCCTTTTAATGCCTCAAACAACAGGCCAACAGCCATCTTA
TATTGCTGAAAAAACTGTACCCTAAGGATGAGCGAGTTACTACTCTTAGC
CAAGAGTTCAGTCAGAAGCAACAAATTGCGTTGGAACAAACGGAAATGTT
TGTTAGCAAATTTAGTGAAATAAGGACCAAATGGCCAATATTGCGCTGC
TTGCAAAAAAGGGCAGATGGAAGGAACTGGAAAAACAAACCAAATCGCTC

GAAGATTTTGCAGTGAGCCTGTCACCGATTTATGGCAGGGTTGATTATGT
GCAAGGCTTAATTCGGCAAGGTGACATTTCTAGCGCAGAGAAAGAGCTAT
CAATTCTTCAACAAAGACTAGATAGTTTGAGCTGGAAAATTGTTGAACTG
GAACTGAGTATCCGCAATAAATCGAAACAGCAGTAACCAC

Appendix A4: *icmF* gene sequence from *V. vulnificus* 106-2A T6SS2. The gene sequence below encodes for *icmF* and flanking genes from *V. vulnificus* 106-2A T6SS2.

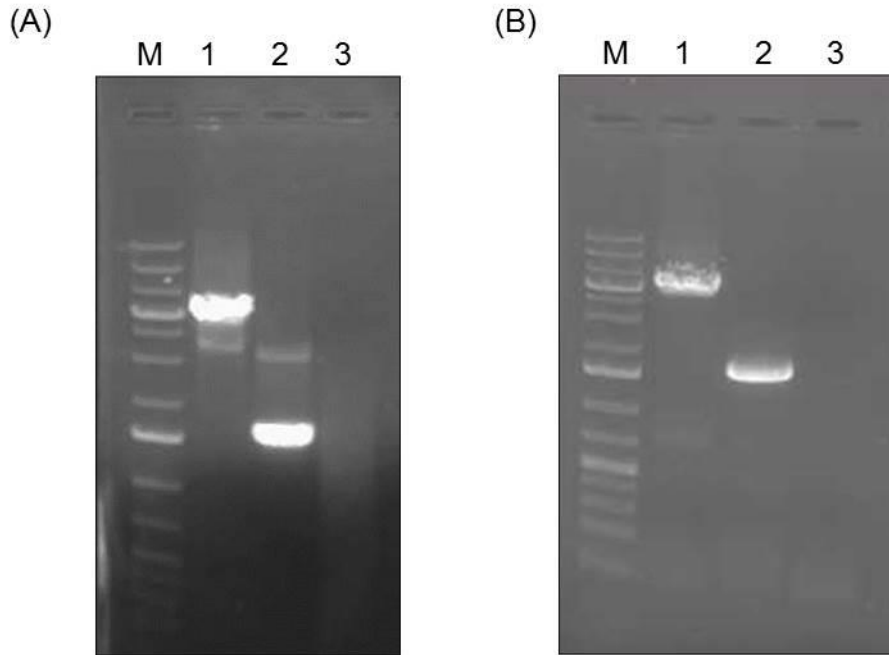
TAAGTGAAGCTATGGACGAAACGATTGTAAAACCAACCCCTGGGCGTAAA
AAAGCACCGCAGTCGACACCTGTTGCATCGCTTGAAAGCGATAACACGGT
TCTCTTTACGCAAAATAGTAAAGAAACGCGTGAAACGAGTATCATCGCGT
TTGGCAATAACGTA CTGCTGGCAGAAGCGAATGTCATTGTTTCCTTGCTT
GGCCAAATTAGAGCGACGGCCACGCACAGTGATGTCAAACAGTTACGTGA
AGCATTGTGCAAAAAATGCGTGACTATGAAAACCGGTTGAGATTACAAG
GCGCAAATAGCAAGCAGATCGATATCGCACGCTACTGTTTATGTAGTGCT
ATCGATGAAGCCGTCCTAAATACCGAATGGGGAAGTCAATCCGTTTGGGG
ACACA ACTCGTTATTGTGACATTCTATTCCAATACTCAAGGCGGTGAGC
AGTTCTTCATACATCTCGATGAAAGCCTTGCCGAACCCAATAAGCACTTA
GATCTGCTAGAAGTCATGTATATCTGCATGAGCTTAGGTTTTTTGGGGCA
ATTTGAGTTTCGAGAAAATGGAATCGAGCAACATCGTTCCTTAAAAAACC
GCGTAATGGATGTCCTTAAATCGCACGGTCGGGACTACAGTCCTTCACTC
AACGATGATGCGTTAGCCAAAGTATTGGTTGGTGAGCAGATCGCAGAAAA
AGCACCATTGTGGGTTGTTTTATCAATTACCGCGGCTGTGTTAGTCAGTG
TGTACATGTACTTAAGTTATAGCCTAAACGAAAAATCCGATCAGACCTTT
AGTCAGTTAATGAACTTAGTGCCGAGCAAAGAGATAGAGAACCAGAGTGC
GGATTATATTTTCGTCTCTTGCCGTAGCAAATCAAATCCAACGCTCGTTGG
CAACGGAAATAGAAATGGGTTTGCTAAAAGTCGATGCATTACCCGATAGA
GTGCGTATTACTTTTCAGTCCAATGATCTGTTTGAATCGGGCAGTGCGGA
GCTTGTGCGCATATATTCCCTGTGGTTTCGAAAGTGGCCAGAGCACTCG
AGGCGACCAATGGAAAAATATTGGTTGTCGGACATACCGATAATAACCCC
ATTTTTACCAGTAAATTCCCTTCTAACTGGCATTATCTCTCGCCAGAGC

GACAGCGCTAACCGATCGCTTAGCATCAGCAGGCAAATTGAGTGGGCGTG
TCATTCCGGAAGGAATGGGAGATGCGAGACCTTTGGTATCAAATGAAACC
GCAGAAGGAAAAAGCATCAACCGTAGAGTCGAAATCGATCTCCTAGTTCA
AACCCAATCAAAAATGGATGCAAACAATGGCAAAGATTAAACGTTTATTG
GGGCAAAAATGGCTGATTAGCTTGATCGGGCTTGGGGCAATTTCTATTTT
TATTTGGTTTGTTCGGACCATTGATCGCGATAGCAGGCATAGAGCCACTGA
AATCTGACTTTAACCGTTTGTGGTTATTGTGGTTTTAGTCTTCATTTGG
GGCGTGACGAATGTTGTCCGTCAACAGAAGGAGCGAAAGGAACAAGATGA
AAGCATCCAAAGCCTATTAGAGGTGGATGCCCTGACCGATAAAGAAGCGG
CGGCAGAAATAGACGTCATGCGCGAAAGAATTGAGAAGGCGATTCAAGTC
GTGACGAAAGGTGGAAGCGTAAGAGTCATCTCTACGAGTTGCCTTGGTA
TGTACTIONTTGGTCCTCCTGGAACAGGTAAAACGACGGCATTAAAAGAAT
CGGGTCTCGAGTTTCCTCTATCAGATTCAATGGGTGTTGACTCGGTTTCT
GGTATTGGCGGTACGAGAAATTGTGATTGGTGGTTTACCAATAAAGCGGT
GTTGATTGATACGGCTGGCCGATACACCACGCAAGACAGCCAAGCTCATG
TCGATTCAAAGCATGGTATGGATTCTTAGGCTTATTGAAGCAATACCGT
AAACAGCGTCCTATTAATGGTGCGATTGTTACCGTCAGCATCGCAAGTAT
GCTCACACAAACTCGCACCGAACGAGGCATGCATGCAAGAGCGATAAAAA
ATCGGCTACAAGAACTGAAAAATCAATTGGGTATGCAGTTCCCAATCTAC
GTTGTGTTGACTAAGGCTGATCTCATTGCTGGTTTTAGTGAGTTTTTTAC
GGAAGTACCAAGGAAGAGCGTGAGCAGTTATTAGGTTTTATGTTTCCAC
CTTCAACAGAAGACGAGCGAGGCGTCATCTCTCTATTTAACAAAGAGTTT
CATGACTTACTGGAGAGACTTGATCGCCGCATGATGCAAAGGCTTGAAC
GGAGCATGACCTTGACAAACGATCTTTAATTTTTGAATTTCCAAAACAAT
TGCGTTGTCTTCAAGCGAATCTAGACGAGTTTCTGAACGACATTTTTGCC
CAAAACAAGTTTGAAGAATCTTCAATGATTCGCGGCGTCTTTATTGTGAG
TTCATTGCAAGAAGGCACGCCGGTTGATCGTATTATGTCTGAAACATCCC
AAGGGCTGGGGTTGGGCAAACCTCTACTGCGGTTAAGTTCCAAAGAATCA

AGCAGCTATTTTGTAAAAAAGTGTGTTGAAAACGTCATCTTTAAAGAACA
GTTTTTAGGGACGGTCAATCGTCATCATCAAAGCAAAGTGGCTGGATTC
GAAAAGGCGTCTACTGCTCGTGCATGGCACTGTCTGGGGCTGCGATCACA
CTGTGGATGATGAGTTATCAGTGGAAACAATCAACTCATTGATGAAACGGA
TCGTCAAGTGAAGTGAATGACTTACTTGCTAAGTCTGGTCTGGACT
TCGAAAACGACTTGATCCCCTCGATAAACATTCTCAATCACATCATGCGT
TTCCCTATGGGTATAGACAGCAAGATGACGAGAGAGATCGTGTGACATC
GTTTGGTTTTTTCAAGGTGAAAAAATTGGCCAATCAGCGAAGAGTGCTT
ATCACCAAGCACTGACAAATTACTATTCATCCTATGTTGAATCGGTA
CTCAGTGAATGAAGAACAATGAACAACACCGAGAATATTTGTACGAAAC
ACTCAAACATATTTGATGCTTTTCAACGATGATAAATTTGAGCGTGAAC
ATGTTCTTGGTTGGTTCAATTATTTCTTTGAAAGGCAGTATCCCGGCGAA
TTGAATGAAGAGTTAAGAGAGCAACTCTACGCTCATACCGAAAACTTTTT
GTCGCAGGCAGACAGAGGCTTATATATCAACAACGATTCAGTAACCGCTG
CCAGATTGGTTCTAACAGAAATGTCGTTGTCGGAAAGGGCTTACCAAAGA
ATGAAACTGCAGTTCCTTAAAAGTCATGTGCCTTCATTCCGTTAACGGA
CGTTCTAGGGGCTAGGGGAGTTGAGCAGTTTGAGCGAAAAAGTGGCAAGC
CATTATCGATGGGGATTTCCGGTTTCTACACGTACAACGGTTTCCATAGC
ATCTTCCAATTGCAACTGGGTGCGTATGGTAAAAGCCTTGATGGAAGAAAA
CTGGGTGTATGGGGATGAGATTGACGCCAAAACATCGACAATGATCTCG
CTTTGCAAGGTGTGAGAGAGCGCTACTATCGTGACTATGTCTATGAATGG
AAGACACTGCTCAATGATATCCAACCTCAAAGCGGCACCCAGTTTGAACT
AAGTTTAGAGCAGAGTATGACATTAGCGGGCTCTGAGCGACCAATTGAAT
CGCTGCTTAAAGCGGTACAAAAGAGGTGGCATTAAACGAAAATTTGCTA
AGCAACAACGAAAAGCGGCAGCAGAAGTCGCTGGTAAAGTTGCCAAAGT
AAAATTTTCAAATACGGCGGACAACTTGATTTATATCGTCCGGAAGAGG
GCAATACGTTTGATATTGCGCTTCTGGAAAAGAAGTGGAAGCCGAGTTT
GACGATCTTGTTAGGATGACAGACCAAGACTTTGACGATATTCATCTCGC

ACTGAGCGGTTTAAAAAGTTATTTGGCCGATCTCTCTAGCTCAGGAAATA
ATCAGAAAGTCGCCTACAAGAGCATCTTAAATGGCACCGTGACAGGAGAA
GTTGCCGCGTCAATTGAACATGCTAAACAGCTTTTACCCGCTCCGTTTAA
CAACTGGCTAGGTGAACTTTCCGAGGAATCGGTCAAGTTAGCGGAAAAAG
GATCGCGATCTCACCTTAATACGCTATGGGTAAACAAGGTTCTTAAACCT
TATGAGCGCAGCATCAAAGGCAGGTATCCGTTTGAGCCAAGAGCGAAAAC
AGAAGTGACGTTAAAGGACTTCAGTCGATTCTTTGGCTACGGCGGAACAC
TTGATGCGTTCTTTGTGAATACTTGGAACCGTTTGTGATACGTGCGAGA
AGTGTGTGGCGCTTCGAGAAGGAAATCGGTGTCAGTCAAGAAACCCTCGC
CGTATTTCAACGCGCAGATCGCATCCGACAATCGTTTTTTCGAACTCGACA
ATACACTAAAAGTCGATTTTGCAATGAAACCGATATACCTCGACCAACAT
ATAACCAGTTTTGTACTGGAAGTCGGGGGGCAGAATCTTGCATACCGACA
TGGGCCGGCAAGAGTAAAAATCTGTCTTGGCCAGCTAAGCGTTCAGCGA
CAAGAGTGGTCTTCACACCACCTGATTGATTGTTGAAATTGCTTATACC
TATGAGGGCGAATGGGGCATTTTTAAGTTGCTTGATCAATCTCTGAAAGC
AAGGCCGCAATCTCGCAAAGACAATATCGTCATGATTGATTTGAAAGGCA
ACAAAGTTCAACTGGAATTGATTCCTAAAAGTACGATGAACCCATTTTGG
TCGAGTGATATGGAGAGTTTCCGATGTCCGCAAACGCTATAACACCAAGT
TGGGGCTTTATAGGCAAATTCCTGCGAAAGGGGATTTTATCAAGCAAGA
CTTGCCGAAACCTTTTGC GGATCTTTTCCACGACTGGCAGCAGGCGATTA
TCGCCGTTAGCAAAGAACAGCTACAGGAAACATGGCAAAGCCATTTTCTA
AATGCGCCAATTTGGCATTTCGCATTGGACAGTGGTGTAAACCAATGACGC
CACGATCATCGGAACGATGATTCCTAGCGTAGATGCCGCTGGACGGTACT
TCTTTTTTGCATTAGCCAGGCCCGTTCTTGGTGATGCCGTGAGCTATTGG
AGCTGTCGAGATTGGGCCAACGAATCGCAAGAGCTGGCGTTAACCGTGCT
GGACGACCATTTTACCTTCGACGTTTGGAGTCAGAATCTACAGTCCGGTA
CAGAGTTAATTAACGCTATTTCCGGCAGAAACGTTACCGGTTTCCAAAAG
AAACTGAGCGGAGAAAACCTCTTTATTAAGGAACATACAGAAACCGATGT

GATGAGTTTGCTCTCTCATGTTGTACGACAGCAGTTCCTAAGCCGTGCT
ACTGGTGGACGGATGGTAATGATGCCATCGAGCCGATGATGCTCGTCATG
GATGGTTTACCTCAAATTGGCAAATTTGCCGCAATGTTGGATGGGCAATG
GCAGAAATGGAATTGGTAACGGTGATCGAATGAGTTG



Appendix A5: Gel electrophoresis image of PCR to confirm an *icmF* mutant in *V. vulnificus* 106-2A T6SS1 and *V. vulnificus* 106-2A T6SS2. (A) PCR bands generated when using the MutScreen forward and reverse primers for the *icmF* gene in T6SS1. Lane 1, wild-type *icmF* gene, 4622bps; lane 2, mutated *icmF* gene, 1555bps; lane 3, negative control (B) PCR bands generated when using the MutScreen forward and reverse primers for the *icmF* gene of T6SS2. Lane 1, wild-type *icmF* gene, 4802 bps; lane 2, mutated *icmF* gene, 1573bps; lane 3, negative control. Lane M contains the Fermentas 1kb plus ladder in both images (A) and (B).

Appendix A6: Statistical two-way ANOVA analysis of data from *V. vulnificus* 106-2A, 99-743, Δ T6SS1 mutant, Δ T6SS2 mutant and *V. fluvialis* NCTC 11327 grown in LB at 30°C. The OD growth curves carried out for the strains, *V. vulnificus* 106-2A, 99-743, Δ T6SS1 mutant, Δ T6SS2 mutant and *V. fluvialis* NCTC 11327 were analysed using a two-way ANOVA followed by a post-hoc Tukey test using GraphPad 6. Highlighted in yellow are the strains which demonstrated a statistical significance. The “Summary” column gives an indication of significance which is denoted with an asterisk(s) and “ns” denotes a non-significant difference between the strains at the designated time point. The corresponding P-value for the significance is shown in the last column entitled, “Adjusted P-Value”. The “Row” corresponds to the Time (hours), where Row1 = 0 hours, Row2 = 2hours, Row3 =4 hours and Row4 = 6 hours, Row5 = 8 hours and Row6 = 24 hours.

Within each row, compare columns
(simple effects within rows)

Number of families	6
Number of comparisons per family	10
Alpha	0.05

Tukey's multiple comparisons test	Mean Diff.	95% CI of diff.	Significant?	Summary	Adjusted P Value
Row 1					
106-2A WT vs. 106-2A:lcmF1 mutant	0.0	-1.229 to 1.229	No	ns	> 0.9999
106-2A WT vs. 106-2A:lcmF2 mutant	0.0	-1.229 to 1.229	No	ns	> 0.9999
106-2A WT vs. 99-743	0.0	-1.229 to 1.229	No	ns	> 0.9999
106-2A WT vs. <i>V.fluvialis</i>	0.0	-1.229 to 1.229	No	ns	> 0.9999
106-2A:lcmF1 mutant vs. 106-2A:lcmF2 mutant	0.0	-1.229 to 1.229	No	ns	> 0.9999
106-2A:lcmF1 mutant vs. 99-743	0.0	-1.229 to 1.229	No	ns	> 0.9999
106-2A:lcmF1 mutant vs. <i>V.fluvialis</i>	0.0	-1.229 to 1.229	No	ns	> 0.9999
106-2A:lcmF2 mutant vs. 99-743	0.0	-1.229 to 1.229	No	ns	> 0.9999
106-2A:lcmF2 mutant vs. <i>V.fluvialis</i>	0.0	-1.229 to 1.229	No	ns	> 0.9999
99-743 vs. <i>V.fluvialis</i>	0.0	-1.229 to 1.229	No	ns	> 0.9999
Row 2					
106-2A WT vs. 106-2A:lcmF1 mutant	0.01000	-1.219 to 1.239	No	ns	> 0.9999

106-2A WT vs. 106-2A:lcmF2 mutant	-0.04333	-1.272 to 1.186	No	ns	> 0.9999
106-2A WT vs. 99-743	-0.006667	-1.236 to 1.222	No	ns	> 0.9999
106-2A WT vs. V.fluvialis	-0.8333	-2.062 to 0.3957	No	ns	0.3249
106-2A:lcmF1 mutant vs. 106-2A:lcmF2 mutant	-0.05333	-1.282 to 1.176	No	ns	> 0.9999
106-2A:lcmF1 mutant vs. 99-743	-0.01667	-1.246 to 1.212	No	ns	> 0.9999
106-2A:lcmF1 mutant vs. V.fluvialis	-0.8433	-2.072 to 0.3857	No	ns	0.3131
106-2A:lcmF2 mutant vs. 99-743	0.03667	-1.192 to 1.266	No	ns	> 0.9999
106-2A:lcmF2 mutant vs. V.fluvialis	-0.7900	-2.019 to 0.4390	No	ns	0.3788
99-743 vs. V.fluvialis	-0.8267	-2.056 to 0.4024	No	ns	0.3329

Row 3

106-2A WT vs. 106-2A:lcmF1 mutant	-0.06667	-1.296 to 1.162	No	ns	0.9999
106-2A WT vs. 106-2A:lcmF2 mutant	-0.06667	-1.296 to 1.162	No	ns	0.9999
106-2A WT vs. 99-743	-0.3667	-1.596 to 0.8624	No	ns	0.9173
106-2A WT vs. V.fluvialis	-2.500	-3.729 to -1.271	Yes	****	< 0.0001
106-2A:lcmF1 mutant vs. 106-2A:lcmF2 mutant	-7.947e-008	-1.229 to 1.229	No	ns	> 0.9999
106-2A:lcmF1 mutant vs. 99-743	-0.3000	-1.529 to 0.9290	No	ns	0.9587
106-2A:lcmF1 mutant vs. V.fluvialis	-2.433	-3.662 to -1.204	Yes	****	< 0.0001
106-2A:lcmF2 mutant vs. 99-743	-0.3000	-1.529 to 0.9290	No	ns	0.9587
106-2A:lcmF2 mutant vs. V.fluvialis	-2.433	-3.662 to -1.204	Yes	****	< 0.0001
99-743 vs. V.fluvialis	-2.133	-3.362 to -0.9043	Yes	****	< 0.0001

Row 4

106-2A WT vs. 106-2A:lcmF1 mutant	0.03333	-1.196 to 1.262	No	ns	> 0.9999
106-2A WT vs. 106-2A:lcmF2 mutant	0.03333	-1.196 to 1.262	No	ns	> 0.9999

106-2A WT vs. 99-743	0.1333	-1.096 to 1.362	No	ns	0.9981
106-2A WT vs. <i>V.fluvialis</i>	-2.200	-3.429 to -0.9710	Yes	****	< 0.0001
106-2A:lcmF1 mutant vs. 106-2A:lcmF2 mutant	0.0	-1.229 to 1.229	No	ns	> 0.9999
106-2A:lcmF1 mutant vs. 99-743	0.1000	-1.129 to 1.329	No	ns	0.9994
106-2A:lcmF1 mutant vs. <i>V.fluvialis</i>	-2.233	-3.462 to -1.004	Yes	****	< 0.0001
106-2A:lcmF2 mutant vs. 99-743	0.1000	-1.129 to 1.329	No	ns	0.9994
106-2A:lcmF2 mutant vs. <i>V.fluvialis</i>	-2.233	-3.462 to -1.004	Yes	****	< 0.0001
99-743 vs. <i>V.fluvialis</i>	-2.333	-3.562 to -1.104	Yes	****	< 0.0001

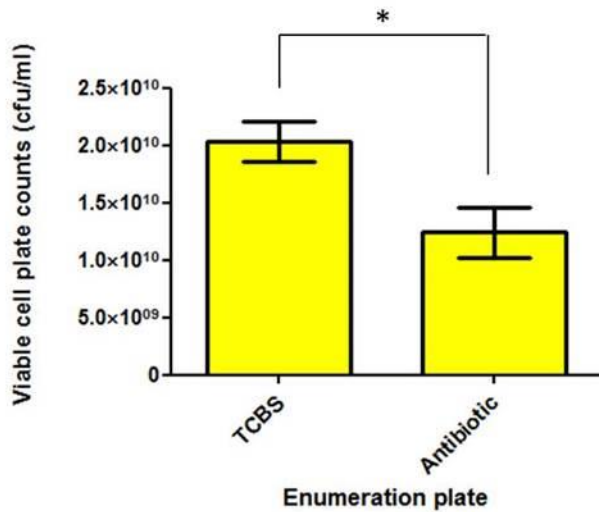
Row 5

106-2A WT vs. 106-2A:lcmF1 mutant	0.03333	-1.196 to 1.262	No	ns	> 0.9999
106-2A WT vs. 106-2A:lcmF2 mutant	0.06667	-1.162 to 1.296	No	ns	0.9999
106-2A WT vs. 99-743	2.133	0.9043 to 3.362	Yes	****	< 0.0001
106-2A WT vs. <i>V.fluvialis</i>	0.5333	-0.6957 to 1.762	No	ns	0.7396
106-2A:lcmF1 mutant vs. 106-2A:lcmF2 mutant	0.03333	-1.196 to 1.262	No	ns	> 0.9999
106-2A:lcmF1 mutant vs. 99-743	2.100	0.8710 to 3.329	Yes	***	0.0001
106-2A:lcmF1 mutant vs. <i>V.fluvialis</i>	0.5000	-0.7290 to 1.729	No	ns	0.7824
106-2A:lcmF2 mutant vs. 99-743	2.067	0.8376 to 3.296	Yes	***	0.0001
106-2A:lcmF2 mutant vs. <i>V.fluvialis</i>	0.4667	-0.7624 to 1.696	No	ns	0.8221
99-743 vs. <i>V.fluvialis</i>	-1.600	-2.829 to -0.3710	Yes	**	0.0047

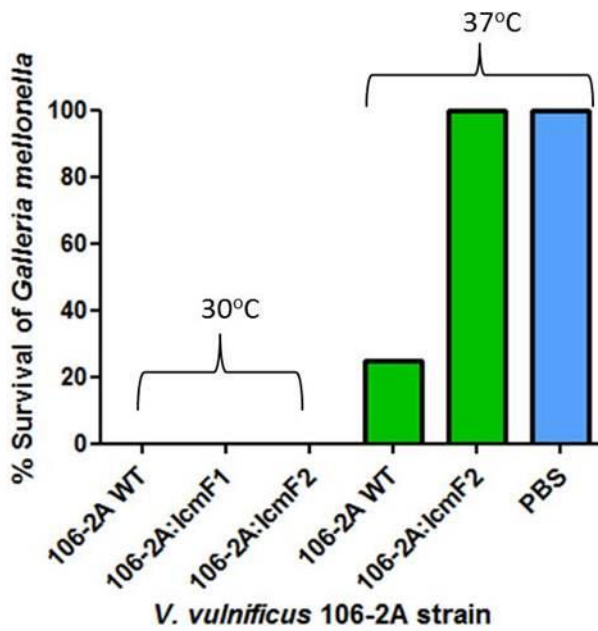
Row 6

106-2A WT vs. 106-2A:lcmF1 mutant	0.1667	-1.062 to 1.396	No	ns	0.9954
106-2A WT vs. 106-2A:lcmF2 mutant	0.2000	-1.029 to 1.429	No	ns	0.9907
106-2A WT vs. 99-743	0.5333	-0.6957 to 1.762	No	ns	0.7396
106-2A WT vs. <i>V.fluvialis</i>	-0.7667	-1.996 to 0.4624	No	ns	0.4094

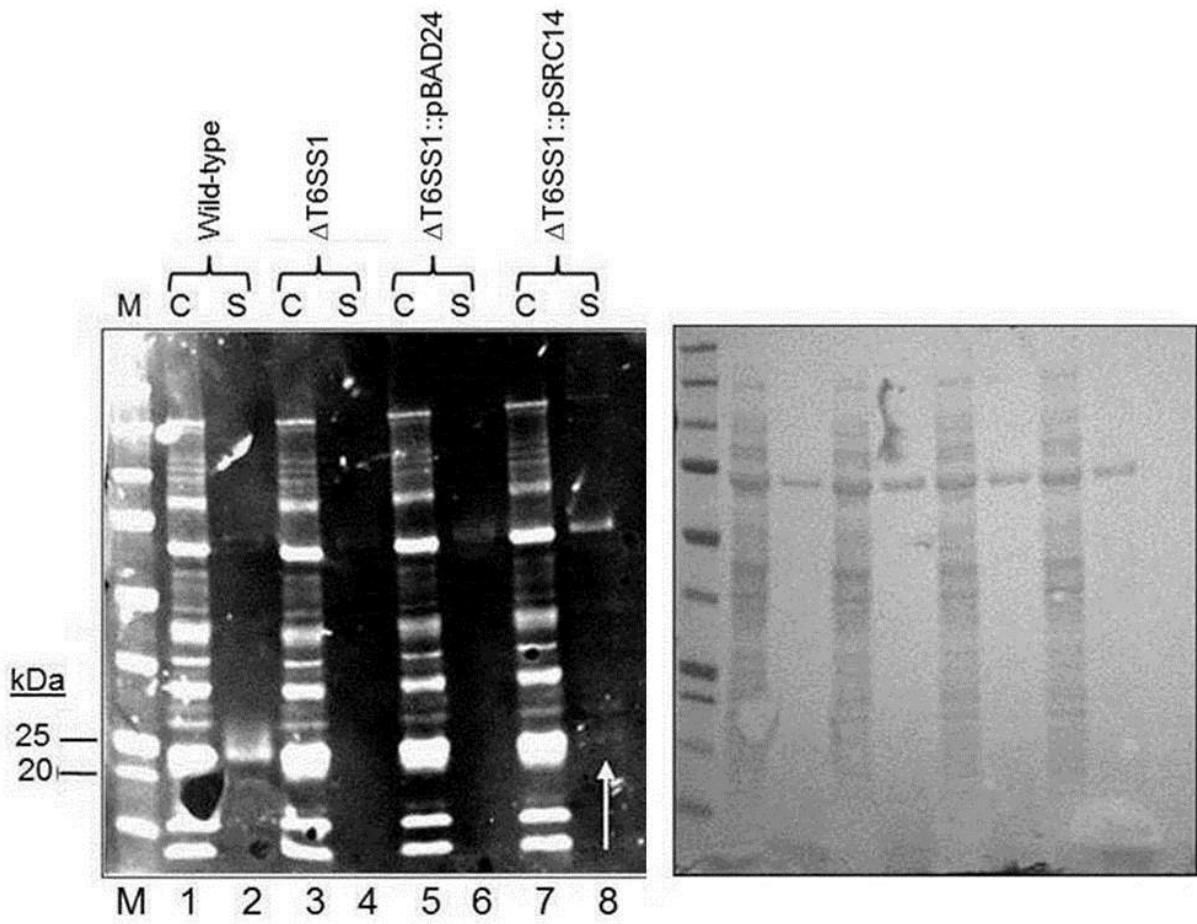
106-2A:lcmF1 mutant vs. 106-2A:lcmF2 mutant	0.03333	-1.196 to 1.262	No	ns	> 0.9999
106-2A:lcmF1 mutant vs. 99-743	0.3667	-0.8624 to 1.596	No	ns	0.9173
106-2A:lcmF1 mutant vs. <i>V.fluvialis</i>	-0.9333	-2.162 to 0.2957	No	ns	0.2188
106-2A:lcmF2 mutant vs. 99-743	0.3333	-0.8957 to 1.562	No	ns	0.9402
106-2A:lcmF2 mutant vs. <i>V.fluvialis</i>	-0.9667	-2.196 to 0.2624	No	ns	0.1894
99-743 vs. <i>V.fluvialis</i>	-1.300	-2.529 to -.07096	Yes	*	0.0331



Appendix A7: Stability of the plasmid pBHR-RFP in *V. fluvialis*. Stability tests demonstrate that pBHR-RFP is not stable in *V. fluvialis* during a 5 hour co-culture assay when no antibiotic selection pressure is present. Experiments were performed three times in triplicate, error bars show standard error of the mean. Statistics were performed using the unpaired 2-way Student's t-test, * $P < 0.05$.



Appendix A8: Preliminary challenge of *G. mellonella* with *V. vulnificus* 106-2A wild-type Δ T6SS1 and Δ T6SS2 mutants. The graph demonstrates the % survival of *G. mellonella* following a challenge with either *V. vulnificus* 106-2A wild-type indicated by "106-2A WT" or the T6SS1 or T6SS2 mutants indicated by "106-2A:lcmF1" and "106-2A:lcmF2" respectively. *G. mellonella* were challenged with 10⁵ cfu/ml of each strain which had been grown to mid-log phase at either 37°C or 30°C. Following inoculation *G. mellonella* were incubated at their respective temperature either 30°C or 37°C for 24 hours. Following incubation the survival of *G. mellonella* from each was assessed. The preliminary experiment suggested that the T6SS2 mutant was attenuated when incubated at 37°C. PBS negative control shown in blue. The results shown are from 1 experiment where n=5.



Appendix A9: Western blot using anti-Hcp antibody to detect Hcp secretion in 106-2A Δ T6SS1::pSRC14. *V. vulnificus* cells lysate (C) and culture filtrates (S) from cells grown at 30°C in LB supplemented with 0.1% arabinose. Hcp detection ~23 kDa, Hcp detection in Δ T6SS1::pSRC14 is indicated with a white arrow. Protein marker is represented with (M).